

10-31-2013

# Synthesis of environmentally-friendly polyurethane dispersions based on soybean oil- derived polyols and their applications in advanced water-based and uv-cure coatings

Senthikumar Rengasamy

Follow this and additional works at: <http://commons.emich.edu/theses>

 Part of the [Polymer Chemistry Commons](#)

---

## Recommended Citation

Rengasamy, Senthikumar, "Synthesis of environmentally-friendly polyurethane dispersions based on soybean oil- derived polyols and their applications in advanced water-based and uv-cure coatings" (2013). *Master's Theses and Doctoral Dissertations*. 554.  
<http://commons.emich.edu/theses/554>

This Open Access Dissertation is brought to you for free and open access by the Master's Theses, and Doctoral Dissertations, and Graduate Capstone Projects at DigitalCommons@EMU. It has been accepted for inclusion in Master's Theses and Doctoral Dissertations by an authorized administrator of DigitalCommons@EMU. For more information, please contact [lib-ir@emich.edu](mailto:lib-ir@emich.edu).

**Synthesis of Environmentally-Friendly Polyurethane Dispersions Based on Soybean Oil-Derived Polyols and their Applications in Advanced Water-Based and UV-cure Coatings**

by

Senthilkumar Rengasamy

Dissertation

Submitted to the College of Technology

Eastern Michigan University

in partial fulfillment of the requirements for the degree of

DOCTOR OF PHILOSOPHY

Technology

Concentration in Polymers and Coatings

Dissertation Committee:

Dr. Vijay Mannari, Chair

Dr. Jamil Baghdachi

Dr. Subhas Ghosh

Dr. Donald Snyder

October 31, 2013

Ypsilanti, Michigan

**Dedication**

**All to My Family**

## ACKNOWLEDGEMENTS

I would like to thank my Chair, Professor Vijay Mannari, for his guidance and invaluable advice throughout my graduate career. As a baccalaureate from polymer engineering, I encountered many difficulties to understand the basic chemistry of coatings and their application. It is he who has truly helped me to build my basic research and chemistry knowledge in the polymers and coating field. I also would like to thank my academic advisor, Prof. Jamil Baghdachi, for his guidance in adhesion and cure chemistry of coatings. My committee members also significantly influenced the direction of my research. And I thank my committee members for their advice and help: Prof. Donald Snyder and Pro. Subhas Ghosh. Thanks also to all of the staff, who have made my time in graduate school go more smoothly and enjoyably: Tracy Rush Byers and Julia Wells. I would also like to convey especial thanks to Dr. Christopher Kluse, without whom Six Sigma methodology chapter would not have been successfully completed. I also acknowledge the funding source USDA for financial support under Cooperative State Research Education, and extension Services (CSREES) through Grant award no. 2009-38303-05085.

I would also like to thank my cohorts: Billy Whisnant and James Banefield for their encouragement in building my presentation skills. Thanks also to the graduate students and postdocs from Coatings Research Institute: Dr. Vivek Arjunan Vasantha, Dr. Chintan Patel, Jigar Patel, and Erica Scrinzi.

Thanks to all of my friends outside of the labs: Dr. Raghuraman Govindan, Beatrice Benhamida, Jetson Gospel, Arun Dhamodaran, Nishant Kumaran, Jayraj Ramachandran, and Guru Anbarasan. Thanks especially to Himaja Ramayanam, who is basking in her 21<sup>st</sup> birthday. Hima thanks for letting me join your ultimate family and for having so much fun with me and for

not letting me take myself too seriously. Thanks especially to your mom Sujatha Allu for the delicious food and her support towards my PhD career.

I greatly appreciate and dedicate my entire research work to my family for their tremendous support and encouragement throughout my life. It is my parents, who did not even complete elementary school, who made me realize the importance of education in my young age and encouraged me to pursue my dreams with their unlimited love and financial support. My brother Santhosh Kumar, who always fought with me for small things and in the end, always gives up for me. Brother you made my childhood so enjoyable.

I cannot imagine my life without my beautiful wife Renu who painted my life with so much color and fun. She not only made me a better person, but also made me finish my project with her selfless love, support, motivation and encouragement throughout the years.

# **Synthesis of Environmentally-Friendly Polyurethane Dispersions Based on Soybean Oil-Derived Polyols and their Applications in Advanced Water-Based and UV-cure Coatings**

## **Abstract**

Polyurethane dispersions (PUD) have established themselves as most versatile polymeric binder in coating, adhesive, sealant, and elastomer industries. Like any other polymers, PUDs also have certain limitations, such as hydrolytic stability, water resistance, and oil resistance. In order to develop these properties, two different polyol families were synthesized. The first polyol can be used in ambient curable systems, and the second can be utilized in ultraviolet radiation cure coatings. For ambient curable systems polyether chemistry based soy-polyol was developed from epoxidized soy fatty acid methyl ester (ESFAME). The cationic ring opening of oxirane oxygen groups from ESFAME resulted in polyol with average hydroxyl number 88 mgKOH/g and number average molecular weight 1517.

The indigenous soy-polyol was used as soft segment polymeric chain backbone of aqueous PUD. The PUDs with varying soft segment to hard segment ratios were developed and characterized for film properties, surface properties, chemical resistance, and thermal properties. The PUD (55% bio content) with reasonable aforementioned properties was utilized for further developmental work, where hydrophobicity and oleophobicity of the coatings were improved to meet the goal of the project. Siliconated (Si) and fluorinated (F) polyol was utilized with indigenous soy-polyol, and 7 different polyurethane polymeric chains were fabricated with varying Si and F concentration. The topographical morphologies of these PUDs were monitored with AFM, and the hydrophobicity was monitored with contact angle instrument. All other basic film properties, water and oil resistance properties were thoroughly discussed. Also, the PUDs

were self-crosslinked with carbodiimide and excellent water resistance and oil resistance coatings were achieved from this research.

For ultraviolet curable coatings, novel hydroxylated acrylic epoxidized soybean oil was synthesized from commercially available epoxidized soybean oil (ESO). It was characterized for viscosity, hydroxyl number, iodine number, molecular weight, FT-IR, and NMR studies. The UV-cured coating films were designed from this indigenous acrylated ESO (AESO) and they were tested for pencil hardness, pendulum hardness, impact resistance, adhesion strength, and thermal properties. In order to further improve the mechanical properties, AESO was used in dual curable coatings. The developed instant radiation curable and ambient curable coatings resulted in excellent chemical resistance, optimum mechanical and thermal properties. The advantage of hydroxyl groups of AESO was taken to develop 9 different UV-curable PUDs. The coating properties were characterized based on constant crosslink density, increasing crosslink density. Once again, topographical studies were conducted with AFM, and contact angle studies were used to determine the UV-PUDs water resistance.

## Table of Contents

Chapter 1: Introduction	1
1.1 Dissertation Overview	1
1.2 Problem Statement	2
1.3 Goals of this Research Work	2
1.4 Dissertation Layout	3
1.5 Reference	4
Chapter 2: Review of the Literature	5
2.1 Polyurethane Dispersions	5
2.1.1 Effect of Soft Segment of PUD	7
2.1.2 Effect of Hard Segment of PUD	7
2.1.3 Anionic Polyurethane Dispersion	8
2.1.4 Cationic Polyurethane Dispersion	9
2.1.5 UV-Curable Polyurethane Dispersion	10
2.2 Polyurethanes from Bio Renewable Materials	13
2.3 Hydrophobic Polyurethanes	19
2.3.1 Surface Requirements for Hydrophobicity	20
2.3.2 Design of Surface Fluorinated / Siliconated Systems	23
2.4 Methodology to Reduce Waste in Production Process	25
2.5 References	26
Chapter 3: Development of Soybean Oil-based Polyols and Their Application in Urethane and Melamine Coatings	37
3.1 Abstract	37
3.2 Introduction	38
3.3 Experimental	39
3.3.1 Raw Materials	39
3.3.2 Synthesis of ESO based Phosphate Ester Polyol: (ESO – Polyol)	39
3.3.3 Synthesis of Epoxidized Monoglyceride: (EMG)	40
3.3.4 Synthesis of EMG based Phosphate Ester Polyol: (EMG Polyol)	42
3.3.5 Synthesis of EMG based Phthalic Acid Ester Polyol: (EMG – PEP)	43
3.4 Results and Discussion	45
3.4.1 Characterization Polyol	45
3.4.2 <sup>1</sup> H NMR Characterization	46
3.4.3 FT-IR Characterization	49
3.4.4 Urethane and Melamine Cured Film Properties	51
3.5 Conclusion	53
3.6 References	54



Chapter 4: An Application of Six Sigma Methodology to Reduce Waste in Synthesis of Environmental Friendly Green Polyurethane Dispersion.....	56
4.1 Abstract.....	56
4.2 Introduction.....	57
4.3 Problem Statement and It’s Significance.....	58
4.3.1 Define Phase.....	59
4.3.2 Measure Phase.....	62
4.3.2.1 Addition Time.....	62
4.3.2.2 Pre-Polymer Exposure Time.....	62
4.3.2.3 The Output (% of gelled particles).....	63
4.3.3 Analyze Phase (Data Analysis).....	64
4.3.4 Improve Phase.....	65
4.3.5 Control Phase.....	68
4.4 Conclusion.....	72
4.5 Acknowledgements.....	72
4.6 References.....	73
4.7 Appendix.....	75
Chapter 5: Synthesis of Soy-based Polyether Polyol and its Application in Aqueous Polyurethane Dispersions.....	76
5.1 Abstract.....	76
5.2 Introduction.....	77
5.3 Experimental.....	79
5.3.1 Raw Materials.....	79
5.3.2 Synthesis of Soy - Polyol.....	80
5.3.3 Synthesis of Soy based Aqueous Polyurethane Dispersions.....	81
5.4 Results and Discussion.....	84
5.4.1 Characterization of Soy – Polyol.....	84
5.4.2 Film Properties of PUD.....	85
5.4.3 Effect of Soy – Polyol content on Hydrophobicity.....	86
5.4.4 Nano-indentation Test.....	90
5.5 Conclusion.....	92
5.6 Acknowledgements.....	92
5.7 References.....	93
Chapter 6: Hydrophobic and Oil-Resistant Coatings based on Advanced Green Polyurethane Dispersions.....	95

6.1 Abstract	95
6.2 Introduction	96
6.3 Experimental	97
6.3.1 Raw Materials	97
6.3.2 Standard Testing Methods	98
6.3.3 Synthesis of Soy - Polyol	98
6.3.4 Synthesis of Green (bio)- PUD	99
6.3.5 Synthesis of Hydrophobically modified Bio - PUDs	101
6.4 Results and Discussion	104
6.4.1 Characterization of Soy - Polyol	104
6.4.2 Characterization of Bio-PUDs and their Film Properties	105
6.4.3 Hydrophobic and Water Resistance Characteristics of Bio - PUDs	106
6.4.4 Characterization of PUD Film Properties	107
6.4.5 Self – Crosslinking of PUD	112
6.4.6 Contact Angle Measurements	113
6.4.5 Hydrophobic and Oleophobic Properties	117
6.5 Conclusion	120
6.6 Acknowledgements	120
6.7 References	121

Chapter 7: Development of Soy-based UV-curable Acrylate Oligomers and Study of their Film Properties.	125
7.1 Abstract	125
7.2 Introduction	126
7.3 Experimental	128
7.3.1 Raw Materials	128
7.3.2 Synthesis of Acrylated ESO (AESO) and Acrylated EME (AEME)	128
7.3.3 Methods of Characterization	129
7.3.4 Coating Compositions and Testing	129
7.4 Results and Discussion	130
7.4.1 Synthesis of AESO and AEME	130
7.4.2 Characteristics of ESO, EME and their Corresponding Acrylated Oligomers	133
7.4.3 <sup>1</sup> H NMR characterization of AESO and AEME	134
7.4.4 FT-IR Spectra Characterization of Initial and Acrylated Products	136
7.4.5 Thermal Analysis	138
7.4.6 Coating Compositions and Cured Film Properties	141
7.4.7 Dual Cure Acrylic Urethane Coating Film Properties	144
7.5 Conclusion	148
7.6 Acknowledgements	149
7.7 References	149

Chapter 8: UV-curable PUDs based on Sustainable Acrylated Polyol: Study of their Hydrophobic and Oleophobic Properties.....	152
8.1 Abstract.....	152
8.2 Introduction.....	153
8.3 Experimental.....	156
8.3.1 Raw Materials.....	156
8.3.2 Methods of Characterization.....	156
8.3.3 Synthesis of Soy-based Acrylic Polyol.....	157
8.3.4 Synthesis of Silylated and Fluorinated UV-PUDs.....	159
8.4 Results and Discussion.....	163
8.4.1 Design of UV-PUDs.....	163
8.4.2 Synthesis of Acrylated Epoxidized Soybean Oil (AESO).....	164
8.4.3 Average Particle Size and Stability of UV-PUDs.....	167
8.4.4 Cured Film Properties.....	168
8.4.5 Contact Angle.....	171
8.4.6 Hydrophobic & Oleophobic Properties based on Swelling Ratio of Solvents.....	172
8.5 Conclusion.....	177
8.6 Acknowledgements.....	178
8.7 References.....	178
Chapter 9: Overall Conclusions and Recommendations.....	181

<b>Table</b>	<b>List of Tables</b>	<b>Page</b>
1.1	Mind map of topics covered in each chapter.....	3
2.1	Fatty acid distributions in various plant oils.....	14
2.2	List of some successfully developed route to synthesis polyol from epoxidized vegetable oil.....	18
3.1	Bio-Polyol Characteristics.....	45
3.2	<sup>1</sup> H NMR Characteristics peaks of ESO polyol.....	47
3.3	<sup>1</sup> H NMR Characteristics peaks of EMG phosphate ester polyol .....	48
3.4	<sup>1</sup> H NMR Characteristics peaks of phthalic acid based polyester Polyol.....	49
3.5	Cured Film Properties: (Urethane).....	51
3.6	Cured Film Properties: (Melamine).....	52
4.1	Project Charter.....	61
4.2	Yield with respect to addition time and exposure time.....	63
4.3	Calculation for Regression Line Equation.....	67
4.4	Calculation for Durbin – Watson Statistic.....	68
4.5	55% Bio-PUD batch sheet.....	69
5.1	Composition of PUDs.....	82
5.2	Film properties of PUDs.....	86
5.3	Characteristics of PUD and their films.....	88
5.4	Surface Mechanical Properties of PUD films.....	91
6.1	Composition of Green PUDs.....	100
6.2	Composition of Hydrophobic PUDs.....	103
6.3	Characteristics of Bio PUDs and Their Film Properties.....	104
6.4	Mechanical Properties of uncross-linked Film Properties.....	109
6.5	Mechanical Properties of Self Cross-linked PUD Film Properties.....	113
6.6	Contact angle of uncross-linked PUD and their respective % Content of Siloxane and Fluorine.....	116
7.1	Characteristics of ESO, EME and their corresponding acrylated oligomers.....	133
7.2	<sup>1</sup> H NMR Spectral data of AESO and AEME.....	135
7.3	FTIR absorption peaks of ESO and AESO.....	136
7.4	FTIR Spectra for EME and AEME.....	138
7.5	Composition and coating properties of UV-curable AESO and AEME.....	141
7.6	Coating formulation and dual cured film properties of acrylic urethane coatings.....	146
7.7	Interpretation of DMA Curve.....	148
8.1	UV-PUD Compositions in millimoles.....	160
8.2	Characteristics of UV-PUD Compositions.....	161
8.3	Characteristics of ESO and AESO.....	165
8.4	Characteristics of UV-PUDs and their Cured Film Properties.....	166
8.5	Average Contact Angle UV-PUDs.....	172
8.6	Water and n-Octane Absorption (%) of UV-PUDs.....	174

<b>Figure</b>	<b>List of Figures</b>	<b>Page</b>
1.1	Schematic representation of project layout. ....	4
2.1	Schematic representation of coulombic PUD particles. ....	6
2.2	Schematic representation of PUD architecture.....	6
2.3	Schematic representation of a) cationic and b) anionic PU in water.....	10
2.4	Schematic representation of a) non-crosslinked and b) crosslinked film.....	11
2.5	Schematic representation of end capped UV-PUD.....	12
2.6	Triglyceride molecule of natural oil.....	13
2.7	General Synthetic route of water dispersible polyol.....	15
2.8	Various synthetic routes of bio-polyols.....	17
2.9	a) Low energy hydrophobic surface (>90°). b) Low energy hydrophobic surface (>90°)	21
2.10	Wenzel and Cassie-Baxter transitional state.....	22
3.1	Triglyceride molecule of natural oil.....	39
3.2	Reaction scheme for synthesis of phosphate ester polyol based on ESO.....	41
3.3	Synthesis of epoxidized monoglyceride.....	42
3.4	Synthesis phosphate ester polyol from epoxidized monoglyceride.....	43
3.5	Schematic representation of synthesis of phthalic acid based polyester polyol.....	44
3.6	<sup>1</sup> H NMR of ESO – Polyol.....	46
3.7	<sup>1</sup> H NMR of EMG phosphate ester polyol.....	47
3.8	<sup>1</sup> H NMR of phthalic acid based polyester Polyol.....	48
3.9	FT-IR Characteristics of ESO polyol.....	48
3.10	FT-IR Characteristics of EMG Polyol.....	50
3.11	FT-IR characteristics of phthalic acid based polyester polyol.....	50
4.1	Five Phases of Six Sigma.....	59
4.2	Yield (%) with respect to Addition Time (AT) & Exposure Time (ET).....	64
4.3	Pareto chart for vital defect analysis of cured coating films.....	65
4.4	Scatter plot of addition time vs. yield and exposure time vs. yield.....	66
4.5	Process control flow chart of 55% Bio- PUD.....	70
4.6	Comparison of existing and previous problem frequency of basic film properties.....	71
4.7	Comparison of existing and previous average yields of 55% Bio-PUD synthesis process.....	71
5.1	Schematic reaction scheme for synthesis of soy-polyol.....	80
5.2	Schematic reaction scheme for synthesis of Bio PUD.....	83
5.3	FT-IR Characterization of ESFAME & Soy – Polyol.....	84
5.4	DSC thermogram showing Tgs for PUDs.....	88
5.5	Effect of soy-polyol content on water-contact angle and dispersion particle size.....	89
5.6	Water Resistance Test (1) PUD-1 (2) PUD-2 and (3) PUD-3 after immersion.....	90
5.7	Nano-indentation test –indentation curves for PUDs.....	91
6.1	Schematic reaction scheme for synthesis of soy-polyol.....	99
6.2	Cationic ring-opening polymerization of epoxy compound.....	99
6.3	Schematic reaction scheme for synthesis of Bio PUD.....	101
6.4	Schematic representation of hydrophobic PUDs with three different polyol polymeric chain backbone.....	102
6.5	FTIR Characterization of ESFAME & Soy – Polyol.....	104

6.6	Water immersion test of Bio-PUD samples.....	106
6.7	Water resistance test of Bio-PUD samples by 24 hours water immersion of steel panels in tap water.....	107
6.8	Three dimensional AFM 10 X 10 $\mu\text{m}$ images for hydrophobic PUDs obtained by tapping method.....	110
6.9	Two dimensional AFM 10 X 10 $\mu\text{m}$ changing phase morphology images for hydrophobic PUDs obtained by tapping method.....	111
6.10	Schematic reaction of formation of N-Acyl Urea.....	112
6.11	Effect of % Siloxane Content on Water Contact Angle.....	116
6.12	Solvent absorption of Bio-PUD and Crosslinked Bio-PUD % Values represents the % improvement in water and oil resistance after crosslinking.....	117
6.13	Solvent absorption of bio-PUD and crosslinked bio-PUD based on % Siloxane content.....	119
7.1	Competing reactions of oxirane compounds with alcohol in presence of strong acid yielding (1a) beta hydroxyl ether and (1b) polyether oligomers.....	132
7.2	Synthetic scheme for acrylated ESO in presence of strong acid catalyst.....	132
7.3	Synthetic scheme for acrylated EME in presence of strong acid catalyst.....	133
7.4	Proton NMR Spectra of a) AESO, b) AEME.....	134
7.5	FTIR Spectra of ESO and AESO.....	136
7.6	FTIR Spectra of EME and AEME.....	137
7.7	TGA thermogram of AESO & AEME.....	139
7.8	DSC thermogram of AESO & AEME.....	140
7.9	Effect of %Bio – Content of UV-Cured Film Properties. Results of all properties normalized to 0-16 scale.....	143
7.10	Schematic representation of dual cure acrylic polymer.....	144
7.11	Acrylic Urethane Dual Cure Film Properties.....	147
7.12	Dynamic Mechanical Analysis of Dual Cure Coating Films.....	147
8.1	A simplified synthetic scheme for acrylated ESO (Oligomeric product not shown).....	158
8.2	General reaction scheme for synthesis of Silylated sand fluorinated UV-PUDs.....	162
8.3	Average Particle Size of UV-PUDs.....	165
8.4	Water and Hexadecane Contact Angle of UV-PUDs.....	175
8.5	Solvent absorption of UV-PUDs.....	176
8.6	% Solvent absorption compared to control UV-PUD.....	176

## Chapter 1: Introduction

### 1.1 Dissertation Overview

The use of paints and coatings can be traced back to the prehistoric era when these materials were derived from naturally available resources and primarily used for improving aesthetics of the surfaces. In today's industrialized world, coatings are sophisticated materials that are used not only for aesthetic reasons but also to provide protection for the underlying substrate and in many instances other special properties. A simple organic coating can protect metals from corrosion and wood from bacterial and fungal attack. Ever since industrialization, paint and coating industries have been using various types of synthetic polymeric materials to make efficient protective coatings. Among them, polyurethanes (PUs) are one of the most versatile polymeric materials due to their excellent chemical, solvent, and abrasion resistance, as well as outstanding hardness and toughness combined with low temperature flexibility.<sup>1</sup> These high performance properties have established PU materials as preferred binder for myriads of applications. From consumer products to engineering applications, PU materials can be seen in the form of coatings, adhesives, sealants, elastomers and foams. However, many of the conventional commercial PUs contain organic solvents and sometime free monomeric isocyanates that are harmful to environment and human health.<sup>2-3</sup> Stringent environmental regulations regarding volatile organic compounds (VOC) have started replacing commercial PUs with aqueous polyurethane dispersions (PUDs) with water as primary volatile carrier.

In general, conventional PUs are hydrophobic in nature and require hydrophilic modification in order to obtain their stable aqueous dispersions. Due to these hydrophilic groups, aqueous PUDs suffer from poor water resistance properties. Also, most of the commercially available PUDs are derived from fast depleting petrochemical-based raw materials

– mainly the polyols, and isocyanate compounds, making them unsustainable for future developments. Polyols are major components of PUDs and developing polyols from renewable resources such as agro-based materials (green chemistry) will not only resolve the impending scarcity for petrochemical resources but will also reduce their carbon footprint. This research is undertaken with a view to develop value-added polyurethane products from vegetable oils, more specifically from soybean oil, which is produced in abundance within the United States of America.

### **1.2 Problem Statement:**

After it became necessary to use green chemistry, many researchers have developed environmentally-friendly low carbon impact bio-renewable polyols from vegetable oils and have demonstrated their applications in PUD chemistry. However, there is still a need to improve the water and oil resistance of coatings based on PUDs without affecting their high performance.

This research is aimed at the design and development of renewable soybean oil-based polyols using principles of green chemistry and engineering. The applications of these polyols in synthesis of environmentally-friendly polyurethane dispersions for high performance and water and oil-resistant coatings will be investigated. . This research also aims to optimize PUD processing method to increase the yield and consistency of the PUDs.

### **1.3 Goals of this Research Work:**

1. Synthesis of soybean oil-based polyols suitable for synthesis of PUD (Bio-PUD) and for performance of their coatings.
2. Development of suitable process for synthesis of PUDs that is reproducible and has high yield.



- Development of thermoplastic and thermoset types of bio-PUDs with silicone and fluorine compounds in their polymeric chain backbone, and study of their film properties.

#### 1.4 Dissertation Layout:

The dissertation is written in a way that each chapter can be read on its own, without having to read the other chapters. Each chapter after literature review (Chapter 2) has an abstract, introduction, experimental (except Chapter 3), results and discussions (except Chapter 3), conclusion and reference. Except Chapter 2, rest of the chapters have been published or under review in leading journals. So, some topics may overlap, although this has been kept to a minimum. The following Table 1.1 shows a mind map of relevance of each chapter.

Table 1.1: Mind map of topics covered in each chapter

Layout	Topic	Chapter
Research Design: 1A	Synthesis of soybean oil-based polyols	3,5
	Synthesis of soybean oil-based PUDs (bio-PUDs)	5,6
	Synthesis of bio-PUDs with excellent water resistance and oil resistance properties	6
Research Design: 1B	To perform design of experiment (DOE) based on Six Sigma tools and develop and optimize the PUD processing methods that results in high yield and consistency.	4
Research Design: 2	Synthesis of acrylated polyols and their application in 100% solids UV-curable coatings	7
	Synthesis of acrylated polyol based UV-PUDs with excellent water resistance and oil resistance properties	8

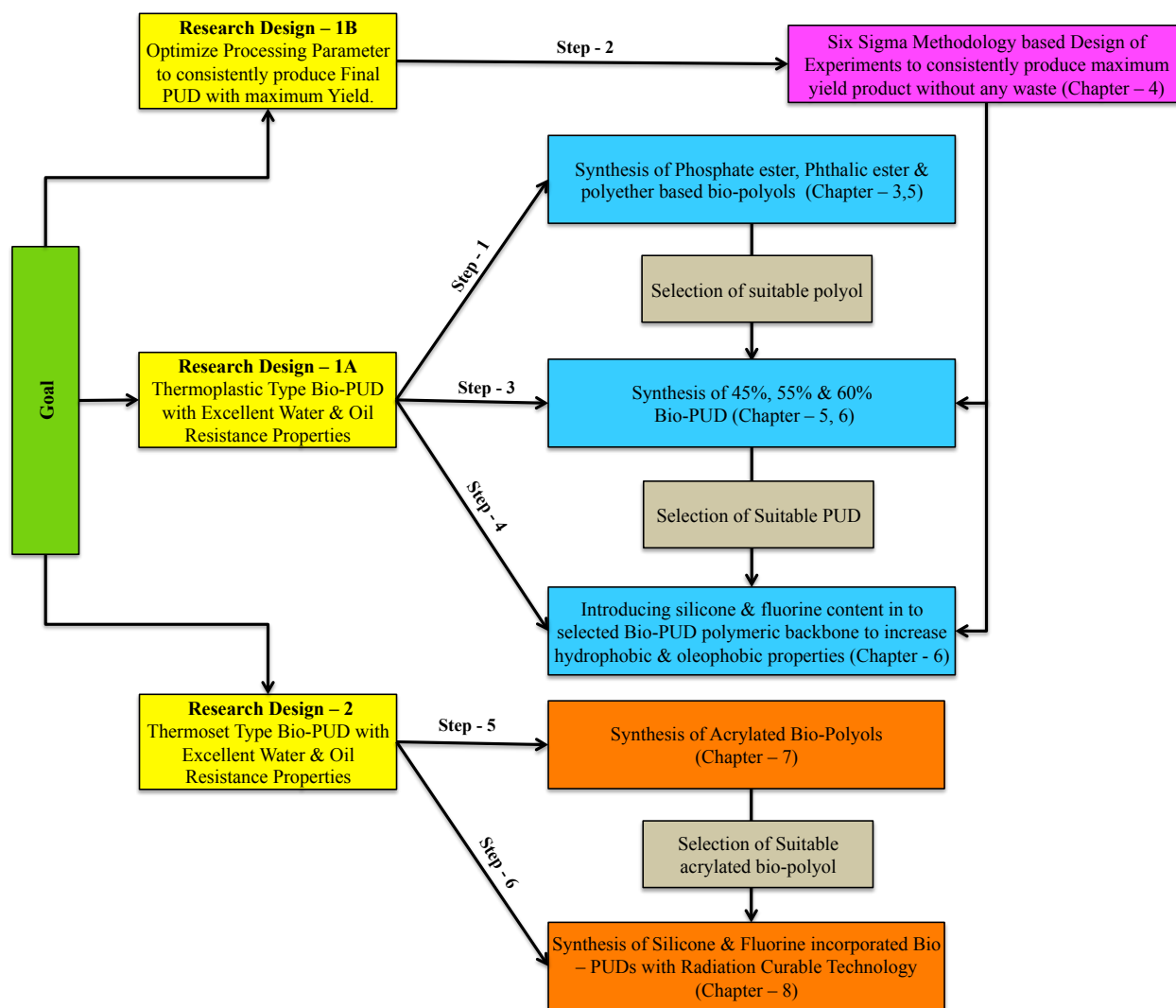


Figure 1.1: Schematic representation of Project Layout

### 1.5 Reference:

1. Saimani, S., Palanisamy, A., Ummadisetty, V., & Radhakrishnan, G. *Colloid. Polym. Sci.* 283, (2004), 209 – 218.
2. Li. P., Shen, Y., Yang, X., & Li, G. *J. Polym. Res.* 19, (2012), 1-10.
3. Lu, Y., & Larock, R.C. *Prog. Org. Coat.* 69, (2010), 31-37.

## Chapter 2: Review of the Literature

### 2.1 Polyurethane Dispersions

Polyurethanes (PUs) are one of the most versatile polymeric materials with variety of applications in both industrial and architectural sector. Topology of PU can be easily tailored using commercially available polyols, isocyanates and chain extenders. This has enabled PU to gain wide range of physical, chemical, electrical and thermal properties that can be useful in construction materials,<sup>1</sup> pharmaceuticals,<sup>2</sup> packaging,<sup>3</sup> textiles,<sup>4</sup> paper,<sup>5</sup> leather<sup>6</sup> and sports goods<sup>7,8</sup> in the form of coatings, adhesives, sealants, elastomers, fibers and foams. However, fossil feedstocks based solvents used in PU formulations raised environmental concerns. To reduce volatile organic compound (VOC) emission and to meet Environmental Protection Agency's (EPA) stringent regulations; water borne polyurethane dispersions (PUDs) have established themselves as preferred binder materials for coatings, adhesives, sealants, elastomers, fibers and foams. The PUD based polymeric material offers the freedom to develop unique and broad-ranging portfolio of characteristics including superior hardness, toughness, low temperature flexibility, abrasion resistance and good adhesion.<sup>9-14</sup> The water borne PUDs are binary colloidal systems in which PU matrix particles are dispersed in continuous aqueous phase.<sup>15-17</sup> Their ability to form uniform film at low temperature even with aqueous phase make PUDs more environmental friendly.

Depending on the type of ionomers introduced into polymeric chain backbone; PUDs can be classified as anionic,<sup>18</sup> cationic<sup>19</sup> and zwitterionic.<sup>20</sup> These ionomers acts as internal emulsifier or self-emulsifiers and makes PU particles to be stable in water media for extended period of time.<sup>9,10,14,21</sup> These ionomers are electrically charged particles that try to aggregate via coulombic forces.<sup>22,23,24</sup> The interaction between the coulombic particles in polymeric matrix

strengthen intermolecular forces and result in physical crosslinking. This ion dipole interaction phenomenon plays a significant role in PUD's moduli and adhesion strength.<sup>22-28</sup> However, the ionomer properties depend on the degree of neutralization and content of ionic component.<sup>17</sup>

Figure 2.1 represents the coulombic particle aggregation of PUD particles.

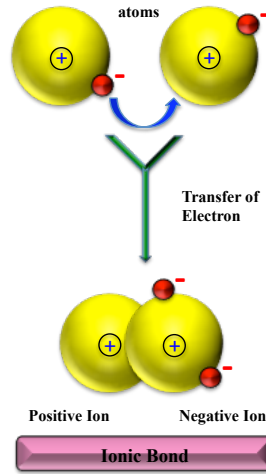


Figure 2.1: Schematic representation of coulombic PUD particles

PUDs are segmented polymeric chains involving soft segments (SS) and hard segments (HS). A typical polyurethane chain comprises polymeric diol, diisocyanate, ionic group and chain extender. These units are linked together by urethane /urea linkages. Figure 2.2 represents the schematic structure of PUD architecture.

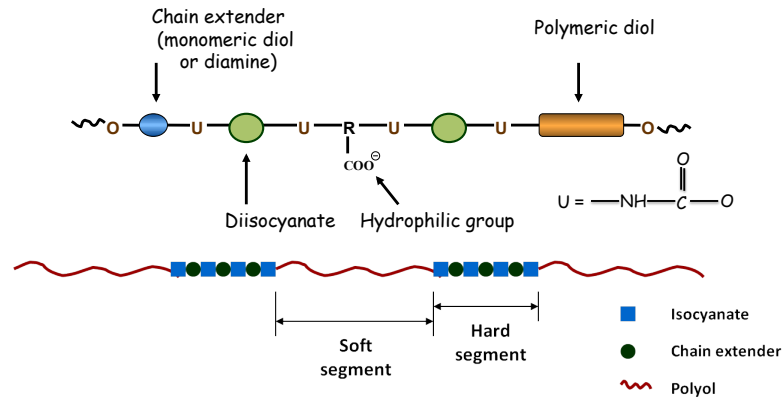


Figure 2.2: Schematic representation of PUD architecture

### **2.1.1 Effect of Soft Segment on PUD**

Soft segments comprise a large part of PUD chains and contribute significantly to properties, performance and to their cost with respect to molecular weight distribution and chemical composition of polyol (polyether polyol, polyester polyol and acrylic polyol) used in synthesis. For instance, M.S. Yen et al.<sup>29</sup> reported modifying the chemical composition of soft segment with ether based PUD gained higher contact angle and surface tension than ester based PUD. In the case of thermal studies within the given series of compounds, soft segment glass transition temperature ( $T_g$ ) is indirectly proportional to soft segment length where as melting point temperature ( $T_m$ ) of soft segment is directly proportional to its soft segment length.<sup>29</sup> Increase in pre-polymer Mw at constant functionality increases the degree of phase separation between soft and hard segment and make them thermodynamically incompatible due to the higher Flory-Huggins interaction parameter.<sup>17,30,31</sup> However, as per S.M. Cakic et al.<sup>32</sup> not only Mw but also both chemical structure of polyols and degree of oxygen content in soft segment play significant role in thermal properties of PUD. M.S. Yen et al.<sup>29</sup> also claimed increasing the molecular weight (Mw) of soft segment increased both surface tension and contact angle between PUD and nylon fabric. This research was backed by W.K. Lee and H.D. Kim et al.<sup>33</sup> who increased the water resistance by increasing Mw of polydimethyl siloxane (PDMS) soft segment with fixed mole % of PDMS content. Like  $T_g$ , increasing the pre-polymer Mw would also affect mechanical properties such as tensile strength<sup>33</sup> and pencil hardness.<sup>34</sup>

### **2.1.2 Effect of Hard Segment on PUD**

Hard segment comprises ionic groups, diisocyanates, chain extenders and end-capping agents. Once again the chemical composition, length, distribution and functionality type plays a vital role in PUD morphology, thermal properties, chemical resistance, water resistance, and also in mechanical properties. Restricted movement imposed at hard segment domains and at phase

boundaries alter the  $T_g$  of soft segment.<sup>17,35</sup> The mechanical properties can be tailored by changing the morphology of PUD through hard segment length.<sup>17,36,37</sup> Increase in hard segment length changes the domain from interconnecting to isolated hard domains.<sup>37</sup> K.V.S.N. Raju et al.<sup>17</sup> claims that three dimensional hydrogen bonding at hard segment domain aids strong hard domain cohesion. Also the crystallites and ordered structures of hydrogen bonding between the urethane/urethane groups and urethane/ester groups correlate the water resistance properties.<sup>37</sup> Type of neutralizing compound can affect the hard segment characteristics. For example, anionic PUD prepared by H.D. Kim et al.<sup>38</sup> explains the role of neutralizing agents effect on hard segment properties. Kim's anionic PUD (model compound) was chain extended with 1,4 butane diamine (BDA), ethylene diamine (EDA), hydrazine monohydrate (HD) and neutralized with triethyl amine (TEA) or  $\text{NH}_4\text{OH}/\text{Cu}(\text{OH})_2$ . The PUDs neutralized with TEA increased the hard segment  $T_g$ , the degree of thermodynamic incompatibility, tensile strength and modulus in the order of  $\text{BDA} > \text{EDA} > \text{HD}$  whereas the PUD neutralized with  $\text{NH}_4\text{OH}/\text{Cu}(\text{OH})_2$  increased the aforementioned characteristics in the order of  $\text{HD} > \text{EDA} > \text{BDA}$ . Ionomer type can also affect PUD properties. In general cationic-based hard segment exhibit superior water resistance, better antibacterial,<sup>16</sup> anti-microbial properties<sup>11</sup> and excellent adhesion on anionic substrate such as textile paper and glass<sup>39</sup> than the much discussed anionic hard segment based PUD.

### **2.1.3 Anionic Polyurethane Dispersion**

Anionic PUDs are widely used and much discussed PU family both in industries and academic society. Dimethylol Propionic Acid (DMPA) is generally used as an anionic domain to influence the stable dispersion of PU particles in water medium. These anions interact with their counter ions (positively charged particles from neutralizer such as TEA) and stabilize the dispersions. The ion-dipole interaction between ionomers and dispersing media results in the

formation of solvation sheath<sup>19</sup> that relies on content of ionic component and the degree of neutralization of ionomer properties.<sup>17</sup> The degree of ionization of pre-polymer decides the particle size, dispersion stability and water resistance of cured PU film. Hydrophilic nature of anionic moiety is easily attracted by water and forms finer PUD particles. The interference of electric double layer  $\{-\text{COO}^-\text{HN}^+(\text{C}_2\text{H}_5)\}$  repulsive forces of different PU particles' aids the stabilization mechanism.<sup>40-4</sup> Curing the hydrophilic ionic domain attached to polymeric backbone makes the PU film vulnerable to water. Therefore to get better coating performance, amount of DMPA used in pre-polymer stage should be optimized. Restricting the movement of anionic moiety to surface of coating can improve the water resistance. This can be done by either crosslinking the DMPA with aziridine or carbodiimide compounds<sup>43</sup> or increasing degree of phase separation of soft and hard segment domain by introducing PDMS<sup>44-46</sup> or fluorine<sup>47,48</sup> molecules either in pre-polymer or hard segment of PUD.

#### **2.1.4 Cationic PUD**

As shown in Figure 2.3, unlike anionic PUDs, cationic PUDs have hydrophobic ionic domains ( $\text{OH}^-$ ) in pre-polymer backbone and hydrophilic domains ( $^+\text{NHR}_2$ ) at hard segment. The polymeric chain of PU can self-organize to micelles when dispersed in water.<sup>49</sup> The repulsive forces of the electric double layer make the PU particles stable in aqueous phase.<sup>40-42</sup> The hydrophilic groups in the micelles are on the particle surface whereas the hydrophobic groups are crimped into the particles. The electrostatic forces formed around the micelles undergo Brownian motion due to hydrogen bonds between hydrophilic groups and water molecules and the particles surrounded by water molecules. This solvation sheath phenomena repels the intermicelle aggregation.<sup>17</sup>

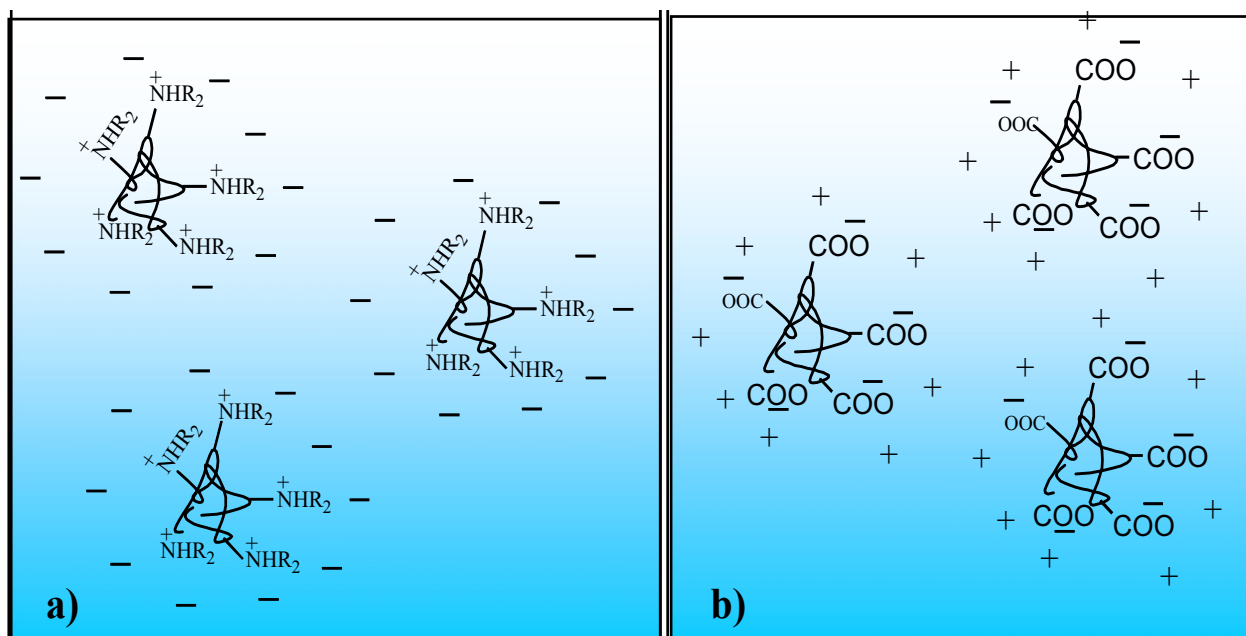


Figure 2.3: Schematic representation of a) cationic and b) anionic PU in water<sup>50</sup>

### 2.1.5 UV-Curable PUD:

UV-curable PUDs, also called UV-PUDs are fast growing advanced systems that combine benefits of both water-borne systems and UV-cure systems. The specific benefits are low or zero VOC, no need for reactive diluents, reduced oxygen inhibition and ready to handle before UV cure.<sup>51</sup> Since water is used as continuous phase, the viscosity is not an issue. Absence of reactive diluents makes UV-PUD technology more environmentally friendly. Overspray can be recycled and matted finish can be easily obtained.<sup>52</sup> Due to the aforementioned distinct advantages, the UV-PUD technology has steadily extended its applications in to many industrial coating .<sup>34,53</sup> For instance, moisture curing of urethane segments and UV curing of unsaturation moieties can benefit to coat complex three dimensional objects. The UV-PUDs exhibits excellent resistant to chemicals,<sup>52,54</sup> water,<sup>52,55</sup> mar<sup>56,57</sup> and weathering.<sup>52,58,59</sup> Incident radiation upon unsaturation groups present in pre-polymer, hard segment or in both pre-polymer and hard



segment results in three-dimensional network as shown in Figure 2.4. The conventional UV-cure systems where reactive diluents are used generally suffer from volume shrinkage. As Mequanint. K et al.<sup>60</sup> explained, the shrinkage is caused by conversion of non-bonding distances between the monomers that are converted to shorter bonding distances in polymers. The shrinkage develops internal stresses in the coating film due to which the film can be easily delaminated from underlying substrate over a period of time or even with minimal external forces. UV-PUD provides better flexibility due to low UV-crosslink density between polymeric chains compared to conventional 100% UV-cure polymers. Since crosslink density of the film is low, the average MW between crosslinks is higher due to presence of long urethane chains in UV-PUD that results in tack-free film before irradiation.<sup>51,61</sup> These characteristics make UV-PUD more suitable to furniture and floor applications where handling of tack-free film become more useful during irradiation process.

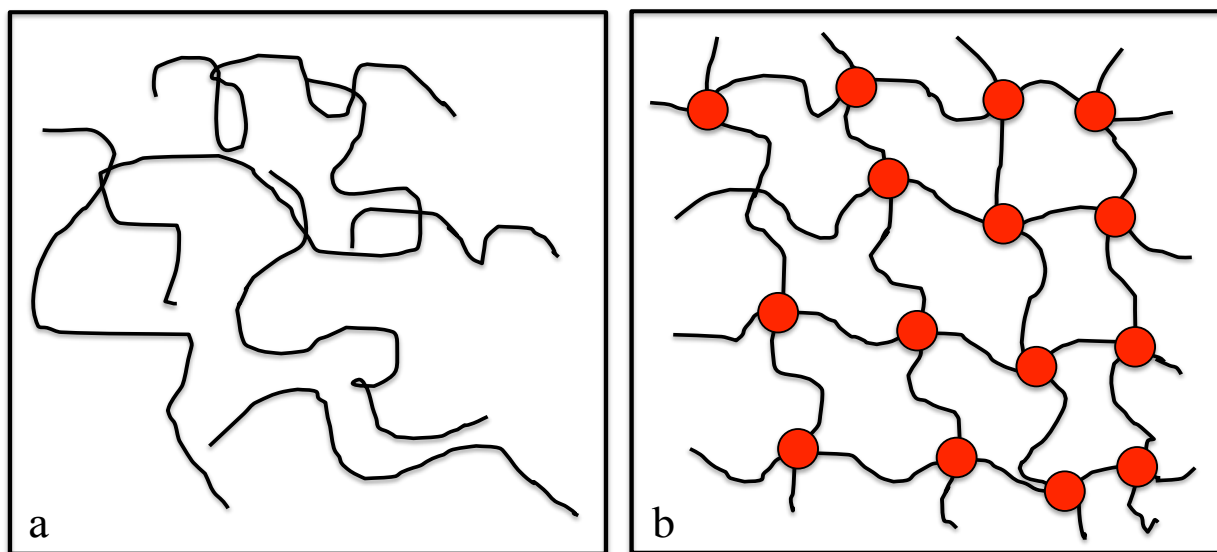


Figure 2.4: Schematic representation of a) non-crosslinked and b) crosslinked film

A generalized reaction scheme for synthesis of UV-PUD is shown in Figure 2.5.

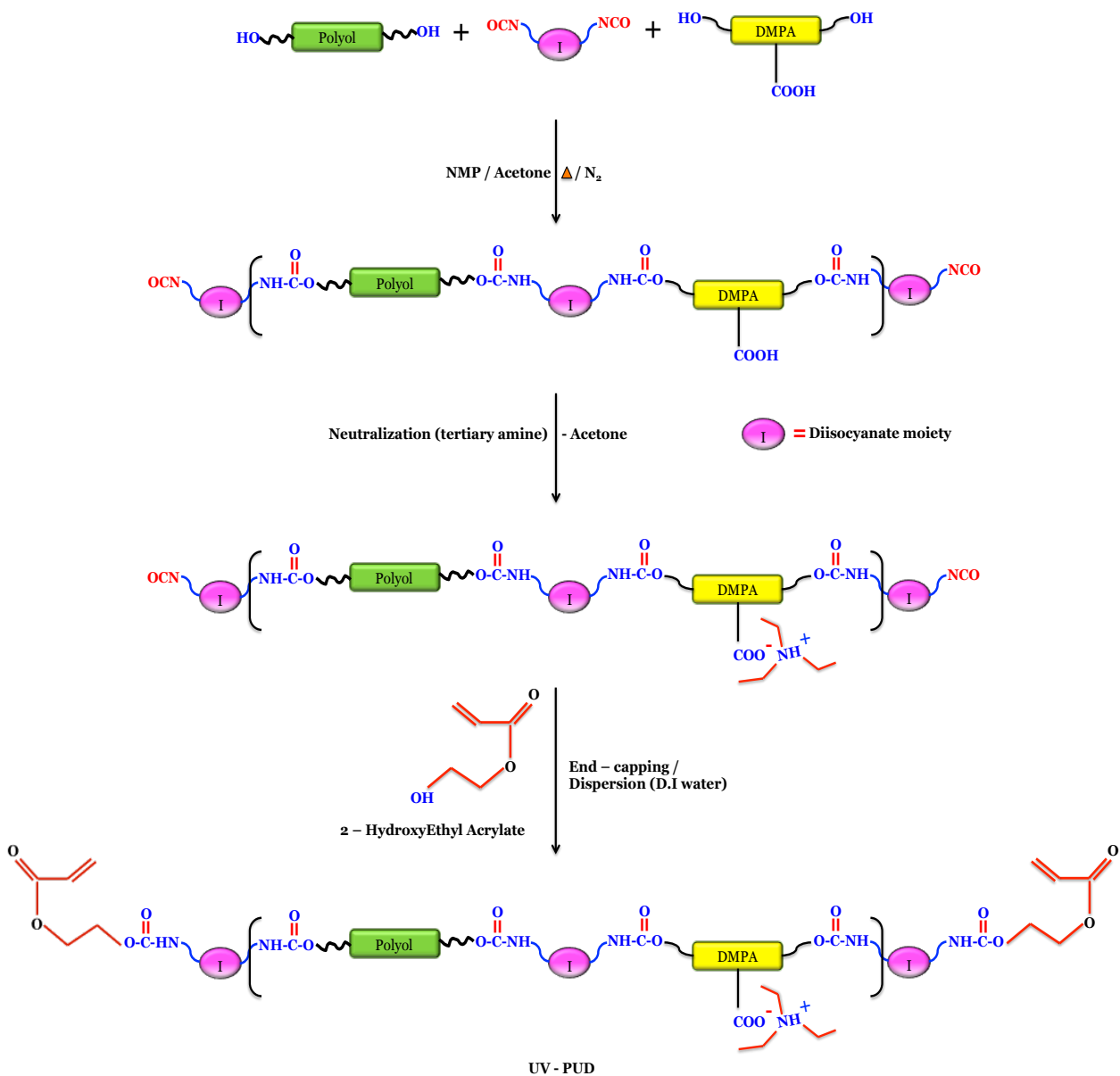


Figure 2.5: Schematic representation of end capped UV-PUD

## 2.2 Polyurethanes from Bio Renewable Materials

As discussed, aqueous PUDs present many advantages over conventional solvent based PUDs. However, like polyethylene, polypropylene, polyesters, polyethers and poly (vinyl chlorides), raw materials required to synthesis PUDs are also derived from fossil feedstocks, which are predicted to deplete within 8 decades.<sup>62</sup> In an age of increasing oil prices, scarcity of fossil feedstocks, environmental concerns and global warming, a transition from petroleum based raw materials to environmentally friendly renewable agro based materials are much needed.<sup>51,62-64</sup> The unique combination of chemical structure, functionality and reactivity combined with low toxicity and inherent biodegradability makes vegetable oils an excellent resource for deriving sustainable polymers.<sup>51,65-68</sup> Therefore, researchers around the world are showing much interest in developing environmentally friendly and economically viable polymeric materials from renewable feedstocks. Wide variety of vegetable oil based polymers such as epoxy resins,<sup>69-71</sup> alkyd resins, vinyl polymers,<sup>62,72-75</sup> polyanhydrides,<sup>76</sup> acrylic polymers,<sup>77-80</sup> hybrid latexes<sup>81</sup> and PUs<sup>62,70,76,82,83,85,86</sup> have been developed successfully. Narine et al.<sup>89</sup> developed linear terminal diisocyanates from oleic acid via Curtius rearrangement and used it making PUD. Plants and animals are great source for natural oils, which can be found in abundance around the world.<sup>90</sup>

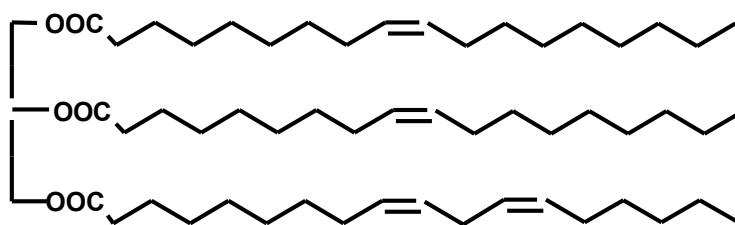


Figure 2.6: Triglyceride molecule of natural oil

Most common oils contain fatty acids with 14 to 22 carbons in length and 0 to 3 double bonds per fatty acid.<sup>75</sup> The fatty acid distribution in several common oils are found in Table 2.1.<sup>90-93</sup>

Table 2.1: Fatty acid distributions in various plant oils

Fatty Acid	#C: #DB	Soybean	Soybean High Oleic	Canola	Corn	Cottonseed	Linseed	Olive	Palm	Rapeseed	Castor	Peanut	Sunflower	Sunflower High Oleic
Myristic	14:0	0.1	0.0	0.1	0.1	0.7	0.0	0.0	1.0	0.10	0.00	0.10	0.10	0.00
Myristoleic	14:1	0.0	0.0	0.0	0.0	0.0	0.0	0.0	0.0	0.00	0.00	0.00	0.00	0.00
Palmitic	16:0	11.0	6.4	4.1	10.9	21.6	5.5	13.7	44.4	3.00	2.00	11.10	7.00	3.70
Palmitoleic	16:1	0.1	0.1	0.3	0.2	0.6	0.0	1.2	0.2	0.20	0.00	0.20	0.10	0.10
Margaric	17:0	0.0	0.0	0.1	0.1	0.1	0.0	0.0	0.1	0.00	0.00	0.00	0.00	0.00
Margaroleic	17:1	0.0	0.0	0.0	0.0	0.1	0.0	0.0	0.0	0.00	0.00	0.00	0.00	0.00
Stearic	18:0	4.0	3.1	1.8	2.0	2.6	3.5	2.5	4.1	1.00	1.00	2.40	4.50	5.40
Oleic	18:1	23.4	82.6	60.9	25.4	18.6	19.1	71.1	39.3	13.20	7.00	46.70	18.70	81.30
Linoleic	18:2	53.2	2.3	21.0	59.6	54.4	15.3	10.0	10.0	13.20	3.00	32.00	67.50	9.00
Linolenic	18:3	7.8	3.7	8.8	1.2	0.7	56.6	0.6	0.4	9.00	0.00	0.00	0.80	0.00
Arachidic	20:0	0.3	0.2	0.7	0.4	0.3	0.0	0.9	0.3	0.50	0.00	1.30	0.40	0.40
Gadoleic	20:1	0.0	0.4	1.0	0.0	0.0	0.0	0.0	0.0	9.00	0.00	1.60	0.10	0.00
Eicosadienoic	20:2	0.0	0.0	0.0	0.0	0.0	0.0	0.0	0.0	0.70	0.00	0.00	0.00	0.00
Behenic	22:0	0.1	0.3	0.3	0.1	0.2	0.0	0.0	0.1	0.50	0.00	2.90	0.70	0.10
Erucic	22:1	0.0	0.1	0.7	0.0	0.0	0.0	0.0	0.0	49.20	0.00	0.00	0.00	0.00
Lignoceric	24:0	0.0	0.0	0.2	0.0	0.0	0.0	0.0	0.0	1.20	0.00	1.50	0.00	0.00
Iodine Value		123-139	-	100-115	118-128	98-118	>177	76-88	50-55	100-115	81-91	84-100	125-140	81-91
Average #DB/triglyceride		4.6	3.0	3.9	4.5	3.9	6.6	2.8	1.8	3.8	2.7	-	4.7	-

# C = Number of Carbons

# DB = Number of Double Bonds

Castor oil contains 87% of OH-bearing ricinoleic acid

Some oil composition may not add to 100% due to the presence of minor fatty acids

Except castor oil and lesquerella oil, all other natural oils need to be chemically modified to introduce hydroxyl groups in their unsaturated sites.<sup>16</sup> These oils are predominantly made up of triglycerides as shown in Figure 2.6. This can be accomplished by hydroformylation,

followed by hydrogenation;<sup>94</sup> epoxidation, followed by oxirane opening;<sup>65</sup> ozonolysis, followed by hydrogenation<sup>62,68,95</sup> and microbial conversion.<sup>96</sup> Following Figure 2.7 shows the general synthetic route to develop water dispersible polyol which is followed in ongoing research of Professor Mannari's research group from Eastern Michigan University.

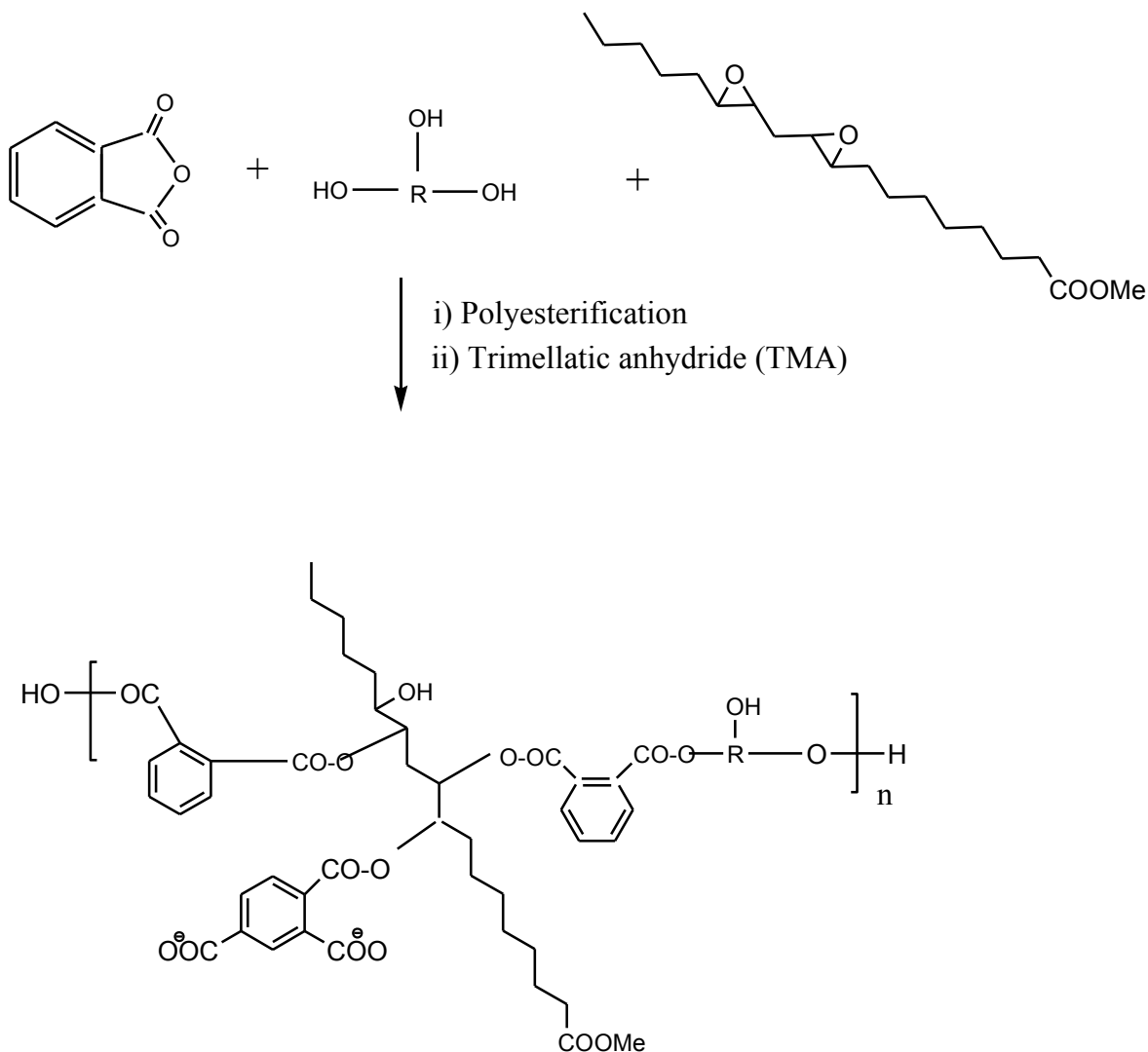


Figure 2.7: General Synthetic route of water dispersible polyol

Petrovic et al. extensively studied the use of various types of soybean oil based polyols to synthesize PUs, depends on structure of triglyceride used,<sup>62,66</sup> type of isocyanate group<sup>62,97</sup> and degree of cross-linking.<sup>87</sup> Lligadas et al.<sup>98-100</sup> cationically polymerized epoxidized methyl oleate

and introduced hydroxyl groups at carboxylate sites. The developed soy polyol was used to make PU plastics that exhibit excellent chemical resistance, physical properties, thermal stability and enhanced hydrolytic stability due to the presence of hydrophobic triglyceride in PU polymeric chain backbone.<sup>68,94,99,100</sup> Larock et al. synthesized methylated soy polyol that varies in functionality from 2.4 to as high as 4.0 and developed series of polyurethane dispersions out of them.<sup>62,81,92,101-103</sup> Larock also showed a synthesis route to develop acrylic PU emulsion from soybean oil based agro derivatives. Wool et al.<sup>90,92</sup> synthesized different monomers from triglyceride oils and successfully used them to develop structural engineering composite. Following Figure 2.8 is the synthetic route of Wool's bio-polymers that were patented in US patent 6,121,398. Ahmad et al.<sup>91</sup> utilized linum usitatissimum seed oil (LO) and its derivatives to develop plain acrylic and grafted epoxy PUs. The LO is epoxidated and hydroxylated using hydrogen peroxide and acetic acid. The developed epoxy material was modified with acrylonitrile and methylmethacrylate in the presence of benzoyl peroxide to synthesize acrylic grafted epoxy polyols, which were later, reacted with isocyanates to get acrylic grafted epoxy polyurethanes. Recently, Lligadas et al.<sup>104</sup> described the way to develop fire resistance polymeric materials from agrochemicals. Hydrosilylation of methyl 10-undecenoate with phenyl tris(dimethylsiloxy)silane followed by a reduction of carboxylate group was used to obtain a silicon containing polyol with terminal primary hydroxyl groups. Later silicon-containing polyol was reacted with vegetable oil based polyol and reacted with 4,4'-methylenebis(phenyl isocyanate) to derive fire resistance hard or rubber like PU plastic. Some of the successfully developed route to synthesis polyol from epoxidized vegetable oil is shown in Table 2.2.

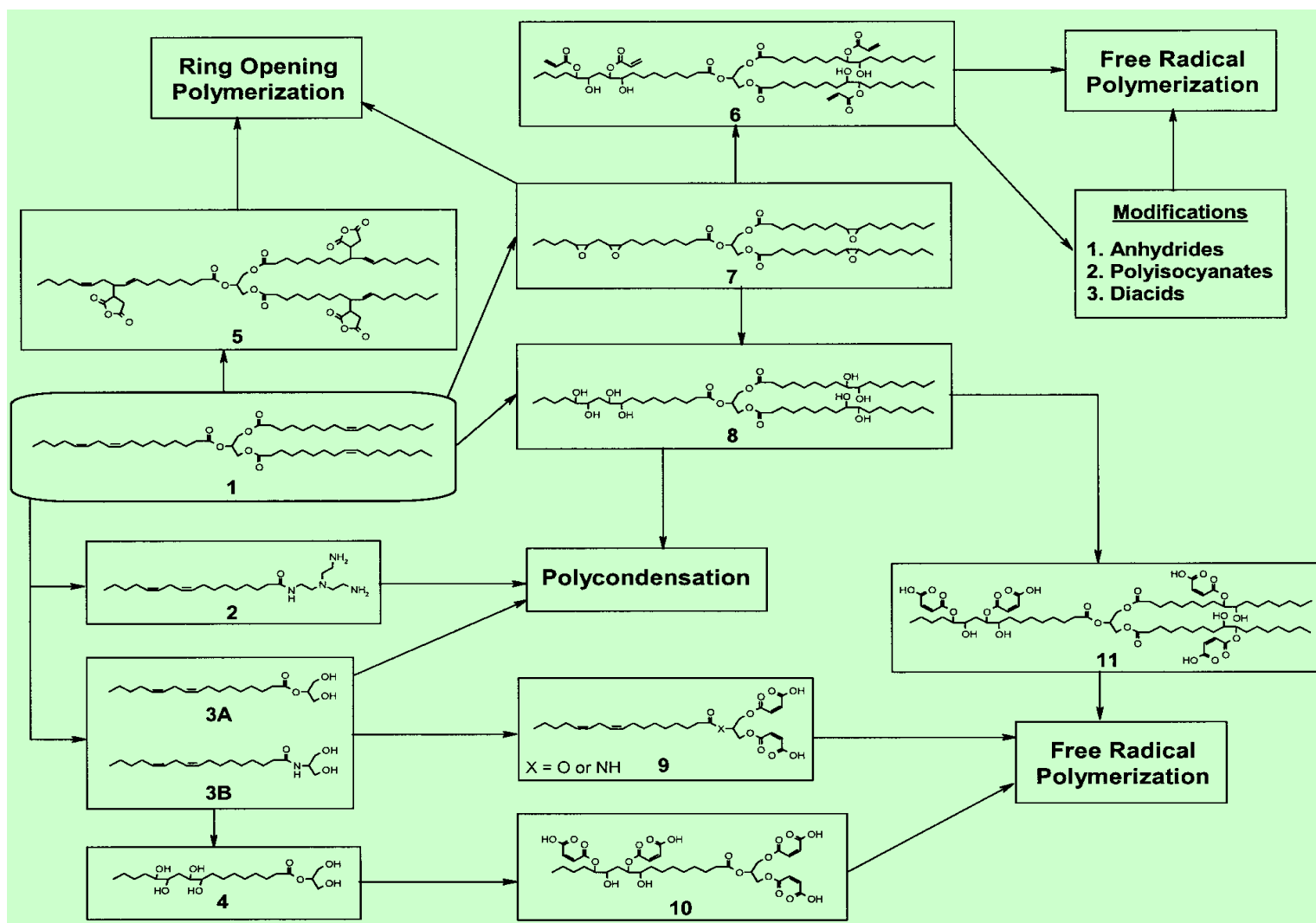
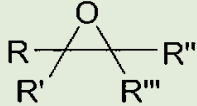
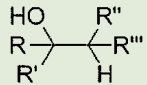
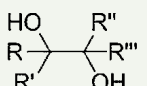
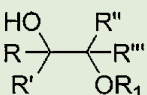
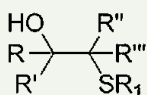
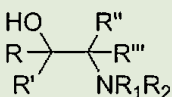
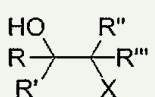
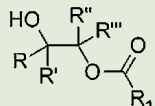
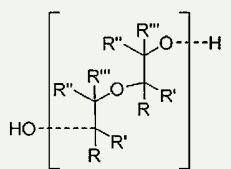


Figure 2.8: Various synthetic routes of bio-polymers<sup>90,92</sup>

Table 2.2: List of some successfully developed route to synthesis polyol from epoxidized vegetable oil

Epoxidized Natural Oil	Reactant	Product	Reference
	H <sub>2</sub>		69, 132
	H <sub>2</sub> O		69, 106 - 111
	HOR <sub>1</sub>		112 - 122
	HSR <sub>1</sub>		69, 123
	HNR <sub>1</sub> R <sub>2</sub>		105, 124, 125
	HX, X=Cl,Br		69, 126, 127
	HOC(O)R <sub>1</sub>		65, 69, 128, 129 - 131
	Polymerization		69, 135



## 2.3 Hydrophobic Polyurethanes

The distinctive advantage of PUDs is their ability to form coherent film and to control the microphase morphology by controlling degree of phase separation between hard and soft segment in polymer chain.<sup>136</sup> The PUDs have freedom to alter their hard and soft segment ratio that results in optimum mechanical properties such as high abrasion, good toughness, low temperature flexibility, excellent adhesion strength, durability, low VOC and so on. However some properties of both agrochemical and petroleum based aqueous PUDs must be further improved. Such properties are water resistance,<sup>137</sup> hydrophobicity,<sup>138,139</sup> oleophobicity,<sup>138,140</sup> cleanability<sup>48</sup> and weather resistance.<sup>141,142</sup>

Several methods are available to improve the hydrophobicity of coatings. For example electrospinning process, lithography, templates, sublimation, vapor deposition<sup>143-148</sup> laser irradiation, plasma,<sup>149-155</sup> etching etc. Fan. J. et al.<sup>143</sup> utilized electrospinning machine used to produce nano-fibers and sprayed polyvinylidene fluoride (PVDF) and silicone on coatings' surface. McCarthy et al.<sup>156</sup> prepared silicon surfaces by photolithography and hydrophobized using silanization reagents whereas Natali<sup>157</sup> et al used nanoimprint lithography and chemical etching process. Mazur et al.<sup>158</sup> irradiated the silicon wafers with femtosecond laser pulses and then coated the surface with fluoralkylsilane molecules. Xu et al.,<sup>159</sup> Jiang et al.,<sup>160</sup> and Bormashenko et al.,<sup>161</sup> followed the template process and densely packed the poly (vinyl alcohol), poly (acrylonitrile) and PVDF respectively. Their nano-fiber like densely packed polymer surface produced superhydrophobic surfaces. Watanabe et al.<sup>162,163</sup> successfully synthesized coatings with excellent self-cleaning properties utilizing sublimation material such as aluminum acetylacetonate and subsequent coating of (fluoroalkyl)silane. Though aforementioned methodologies derive excellent hydrophobic properties; to commercialize the

coatings for vast area of application is more challenging due to the cost and requirement of special equipments to carry out such coatings. Besides some of the methodologies may not be useful for all the materials. So, an alternate approach of introducing hydrophobic chemicals into the PU surface is necessary. This can be done by surface chemistry modification of PU polymeric chain backbone with fluorine or silicon compounds. For example, reacting hydroxylated fluorine or silicone group with diisocyanates reduce the surface energy of entire PU film. This approach may not produce superhydrophobic coatings but it improves the water resistance, oil resistance and thermal stability of aqueous PUDs. Besides superhydrophobic coatings suffer from poor adhesive properties which make the coatings to be useful in limited area of applications such as optical industry. Moderately improving the hydrophobic characteristics of PUDs make them to be useful in wide range of application from industrial to architecture and from house coatings to automotive coatings.

### 2.3.1 Surface Requirements for Hydrophobicity

The hydrophobicity is directly related to contact angle of water that represents the adhesion of water drop on the surface. Less strongly the surface holds the water droplet, the more hydrophobicity. As shown in Figure 2.9 and explained by Young Laplace, theoretical contact of liquid to substrate arises from the consideration of thermodynamic equilibrium between liquid (L), Solid (S) and Vapor (V). Thus tallying up capillary forces acting on the line of contact equates to zero (equation 1).

$$\gamma_{SG} - \gamma_{SL} - \gamma_{LG} \cos \theta_c = 0 \quad (1)$$

Where  $\gamma_{SG}$  = solid – gas interfacial energy  
 $\gamma_{SL}$  = solid – liquid interfacial energy  
 $\gamma_{LG}$  = liquid – gas interfacial energy  
 $\theta_c$  = equilibrium contact angle

From equation 1 the energy of solid surface (in atmospheric gas medium) can be characterized by balancing the force between the liquid-gas surface tension and the interfacial tension between liquid drop and surface that are established through the contact angle. The following Young-Dupre's equation explains the work of adhesion related to contact angle of liquid to substrate in gas medium. It explains the total free energy change corresponds to interfacial energy.

$$\gamma(1 + \cos\theta) = \Delta W_{SLG} \quad (2)$$

Where

$\Delta W_{SLG}$  = solid – liquid adhesion energy per unit area (gas medium)

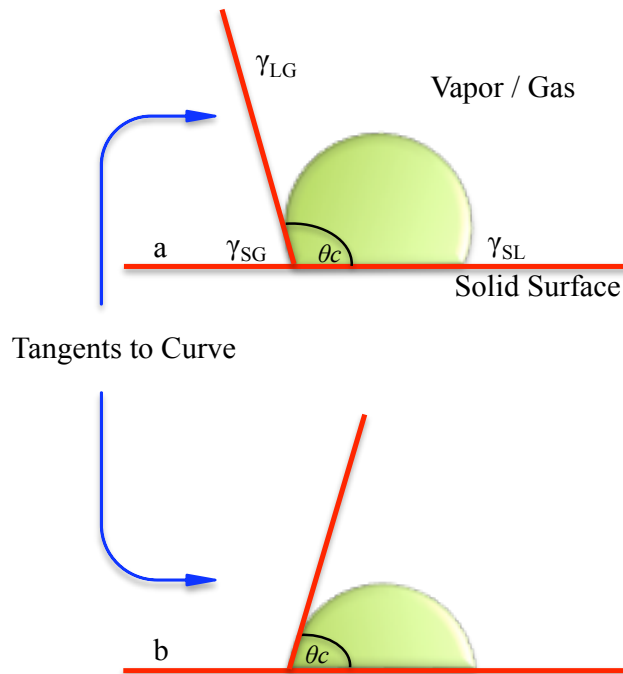


Figure 2.9: a) Low energy hydrophobic surface ( $>90^\circ$ ) b) High energy hydrophilic surface ( $<90^\circ$ )

It can be understood from equation 2 that decreasing the  $\cos\theta$  value can minimize the work of adhesion of solid to liquid. This can be achieved by lowering the surface energy (hydrophobic) of solid substrate. In recent years, many researchers have been systematically

attempting to investigate the Cassie-Baxter and Wenzel transitional states of hydrophobic surfaces shown in Figure 2.10.

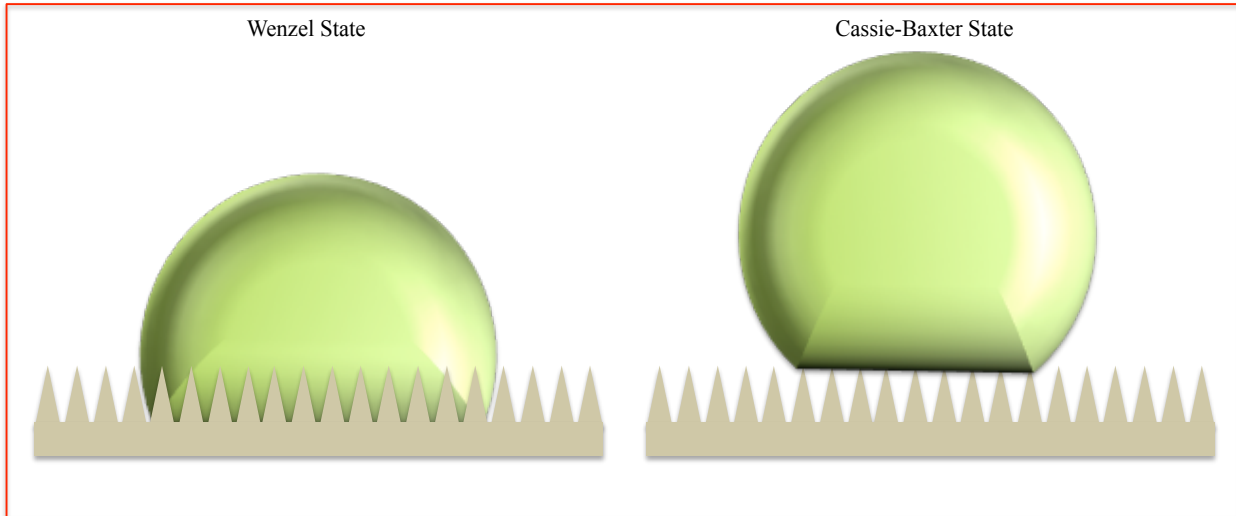


Figure 2.10: Wenzel and Cassie-Baxter transitional state

In Wenzel state, liquid droplet covers more surface area by filling the voids below the drop. When the contact angle is greater than  $90^\circ$ , Wenzel derived the apparent contact angle formula ( $\theta^a$ ) as roughness ( $r$ ) multiplied by contact angle. In this state hydrophobicity and the repellency of the surface is directly proportional to roughness factor.

$$\cos\theta^a = r(\cos\theta) \quad (3)$$

In Cassie-Baxter state, the liquid droplets rest upon the asperities due to which the voids below the liquid droplets are filled with gas instead of liquid. This state covers less surface area than the area covered by same volume of liquid drop used in Wenzel state. To adjust the reduction in surface area, Cassie used the factor  $\phi_s$ .

$$\cos\theta^a = \phi_s (\cos\theta + 1) - 1 \quad (4)$$

However many researchers started enquiring the credibility of Wenzel's and Cassie's phenomenon of wettability of surface. McCarthy. T.J and Gao. L<sup>164</sup> experimental data proves liquid drops' contact lines not contact areas are important in determining wettability or

repellency. McCarthy's research findings claim Wenzel's and Cassie's equations respectively 3 and 4 can be authenticated only to the extent that the structure of contact area reflects the ground state energies of contact lines and the transition states between them. The US Patent 6976585 given to Extrand C.W claims three phase line dictates the contact angle not the liquid-solid interface below the liquid drop.<sup>165-167</sup> Also Edward Bormashenko's presentation at 2008 Contact Angle symposium describes a Cassie impregnated regime in which the Cassie state the voids under the liquid drops are fully or partially filled with liquid.<sup>168</sup>

### **2.3.2 Design of Surface Fluorinated / Siliconated Systems**

Most widely used organosilanes to modify the surface of the coatings have minimum one organic substituent and three hydrolysable substituents such as trialkoxysilane compounds. Upon curing the trialkoxy groups hydrolyze to form silanol containing species which covalently bonds with hydroxyl groups of substrate.<sup>169,170</sup> Recently Arkles et al. described the organic substitution of organosilane, extent of surface coverage, residual unreacted groups from both silane in surface distribution and orientation of silane on the surface plays significant role in hydrophobic characteristics of the coated surface. Moreover the free energy transfer of hydrocarbon molecules from aqueous phase to homogenous hydrocarbon phase could be the reason for hydrophobicity. Minimizing the Van der Waals contact forces between liquid to surface can exhibit good hydrophobic coatings. Thus sterically closed structures are most suitable for the development of hydrophobic coatings.<sup>170</sup> The organosilanes react with hydroxyl groups and eliminate the hydrogen bonding effect and shields the polar surfaces (water absorbing sites) by creating non-polar interphase. Also increasing the alkyl chain lengths attached with organosilane compounds could increase the hydrophobicity of coatings.<sup>170,171</sup>

Anton's research systematically attempts to study the significance of amount of fluorine

used in coating formulation. A relatively small amount of fluorine is enough to exhibit excellent hydrophobic property. Optimizing the fluorine amount could control both the surface and bulk property of coatings.<sup>173</sup> To successfully achieve only the surface property of fluorine researchers derived the following design rules to successfully achieve only the surface properties like water resistance and oil resistance of fluorine.

- 1) The formulation should contain closely packed CF<sub>3</sub> terminated fluoroalkyl groups rather than loosely packed CF<sub>2</sub> groups. This creates the surface energy of coatings as less as 10 dynes/cm.<sup>172,174-176</sup>
- 2) To express surface properties all the fluoroalkyl groups must be in the surface of the coatings also they should be attached to surface.<sup>173</sup>
- 3) In order to cover entire surface of coatings, the fluoroalkyl groups should be in continuous phase rather in separate phase, which might result in hazy coatings. Sometime higher levels of fluorine used in coating formulation might phase separate from hydrocarbon portion of the polymer. Thus the phase separated and light refracted fluorochemical groups exhibit haze in the film.<sup>172</sup>

Therefore to achieve acceptable surface properties; low surface tension molecules should be used in coatings, so that thermodynamic driving forces<sup>172,177</sup> can occupy the gas-liquid interface.<sup>175</sup> Kinetically migrating the fluoroalkyl groups to the surface and providing the mechanism for migrated molecules attached with surface can result in excellent hydrophobicity and oleophobicity coatings.<sup>172</sup>

## **2.4 Methodology to Reduce Waste in Production Process**

The chemistry behind polyurethane development is a theoretically known mechanism but manufacturing PUD is not as easy as making two component polyurethane coating systems

where component A (polyol) and component B (isocyanate) is mixed together at the time of application. A typical PUD manufacturing process involves; (a) preparation of pre-polymer; (b) neutralization; and (c) chain extension in aqueous dispersion. This multistep process is not only time consuming (3 – 8 hours) but also produce considerable amount of waste that often results in low yield. So, there is a need to derive production methodology through which the PUD manufacturing process can be carefully monitored and waste can be significantly reduced.

For the past 2 decades, the Six Sigma business strategy has become a popular quality improvement methodology. Its ultimate goal is customer satisfaction and profit by reducing process variation and errors in any unit of the organization. Sigma is the term used to represent variation around the process mean.<sup>178-179</sup> Six Sigma can be readily applied to manufacturing and service industries where product quality and consistency are key product drivers.<sup>180-181</sup>

Many multinational industries believe in KAIZEN and hence adopted the Six Sigma methodology to provide quality products with minimum waste while increasing profits.<sup>178,182-183</sup> Six Sigma has been wide spread among many industries after its success in Motorola, General Electric and other organizations such as Citi bank, Sony and Allied Signal who all applied the Six Sigma strategy to their business process and reaped the benefits.<sup>178,182</sup> So, the fact-based decision-making aspect of the Six Sigma methodology will be utilized in this research work to determine the root cause of waste that may be generated during PUD manufacturing process.<sup>184-</sup>

190

## 2.5 References

1. Xiang, X.J., Qian, J.W., Yang, W.Y., Fang, M.H., & Qian, X.Q. (2006). *J. APP. Polym. Sci.* 100, 4333-4337.
2. Bouchemal, K., Braincon, S., Perrier, E., Fessi, H., Bonnet, I., & Zydowicz, N. (2004). *International Journal of Pharmaceutics.* 269, 89-100.
3. Chiu, H.T., Chang, C.Y., Pan, H.W., Chiang, T.Y., Kuo, M.T., & Wang, Y.H. (2012). *J. Polym. Res.* 19, 1-12.
4. Giraud, S., Bourbigot, S., Rochery, M., Vroman, I., Tighzert, L., Delobel, R., & Poutch, F. (2005). *Polymer Degradation and Stability.* 88, 106-113.
5. Kallio, T., Kekkonen, J., & Stenius, P. (2004). *The Journal of Adhesion.* 80, 933-969.
6. Li, P.Z., Shen, Y.D., Yang, X.W., & Li, G.H. (2010). *Journal of The Society of Leather Technologists and Chemists.* 94, 240-247.
7. McDowell, M., & Ciocco, M.V. (2005). *Br. J. Sports. Med.* 39, 223-225.
8. Burbank, S.D., & Smith, L.V. (2012). *Proceedings of the Institution of Mechanical Engineers Part P- Journal of Sports Engineering and Technology.* 226, 77-85.
9. Buruiana, T., Melinte, V., Buruiana, E.C., & Mihai, A. (2009). *Polym. Int.* 58, 1181-1189.
10. Xin, H., Shen, Y.D., & Li, X.R. (2011). *Polym.Bull.* 67, 1849-1863.
11. Sundar, S., Vijayalakshmi, N., Gupta, S., Rajaram, R., & Radhakrishnan, G. (2006). *Prog. In. Org. Coat.* 56, 178-184.
12. Yen, M.S., Tsai, H.C., & Hong, P.D. (2006). *J. APP. Polym. Sci.* 100, 2963-2974.
13. Li, X., Fei, G., & Wang, H. *J. APP. Polym. Sci.* 100, (2006), 40 – 46.
14. Saimani, S., Palanisamy, A., Ummadisetty, V., & Radhakrishnan, G. *Colloid. Polym. Sci.* 283, (2004), 209 – 218.
15. Li, P., Shen, Y., Yang, X., & Li, G. *J. Polym. Res.* 19, (2012), 1-10.
16. Lu, Y., & Larock, R.C. *Prog. Org. Coat.* 69, (2010), 31-37.
17. Chattopadhyay, D.K., & Raju, K.V.S.N. *Prog. Polym. Sci.* 32, (2007), 352 – 418.



18. Subramani, S., Lee, J.M., Cheong, I.W., & Kim, J.H. *J. App. Polym. Sci.* 98, (2005), 620 – 631.
19. Gurunathan, T., Rao, R.K.C., Narayan, R., & Raju, K.V.S.N. 76, (2013), 639 – 647.
20. Zhang, Q., Zhu, D., Su, F., Xie, Y., Ma, Z.M., & Shen, J. *Journal of Biomedical Materials Research Part A. 100A*, (2012), 1868 – 1876.
21. Delucchi, M., Trombetta, T., Ricotti, R., Cerisola, G., & Turri, S. *J. Appl. Electrochem.* 39, (2009), 2107 – 2113.
22. Liminana, M.A.P., Ais, A.F., Palau, A.M.T., Barcelo, A.C.O., & Martinez, J.M.M. *International Journal of Adhesion & Adhesives.* 25, (2005), 507 – 517.
23. Bakshi, H., Yeganeh, H., Ataei, S.M., Shokrgozar, M.A., Yari, A., & Eslami, S.N.S. *Material Science and Engineering.* 33, (2013), 153 – 164.
24. Capek, I. *Advances in Colloid and Interface Science, 118*, (2005), 73 – 112.
25. McGee, D.E. *U.S. Patent. No. 2003/0207121.*
26. Wilson, J.M. *European Patent No. 0420662 A3.*
27. Hsu, S.L., Xiao, H.X., Szmant, H.H. & Frisch, K.C. *J. APP. Polym. Sci.* 29, (2003), 2467 – 2479.
28. Malavasic, T., Cernilec, N., Mirceva, A., & Osredkar, U. *International Journal of Adhesion and Adhesives.* 12, (1992), 38 – 42.
29. Yen, M.S., Tsai, H.C., & Hong, P.D. *J. App. Polym. Sci.* 105, (2007), 1391 – 1399.
30. Stanford, J.L., Still, R.H., & Wilkinson, A.N. *Polymer.* 44, (2003), 3985 – 3994.
31. Petrovic, Z., & Javni, I. *Journal of Polymer Science Part B: Polymer Physics.* 27, (1989), 545 – 560.
32. Cakic, S.M., Ristic, I.S., Cincovic, M.M., & Spirkova, M. *International Journal of Adhesion & Adhesives.* 41, (2013), 132 – 139.
33. Rahman, M.M., Hasneen, A., Kim, H.D., & Lee, W.K. *J. App. Polym. Sci.* 125, (2012), 88 – 96.
34. Ahn, B.U., Lee, S.K., Lee, S.K., Park, J.H., & Kim, B.K. *Prog. Org. Coat.* 62, (2008), 258 – 264.

35. Chang, S.L., Yu, T.L., Huang, C.C., Chen, W.C., Linliu, K., & Lin, T.L. *Polymer*. 39, (1998), 3479 – 3489.
36. Bengston, B., Feger, C., Macknight, W.J., & Schneider, N.S. *Polymer*. 26, (1985), 895 – 900.
37. Yang, Y.D., Hu, C.P., & Ying, S.K. *Journal of Polymer Science: Part A: Polymer Chemistry*. 43, (2005), 2606 – 2614.
38. Kwak, Y.S., Park, S.W., & Kim, H.D. *Colloid. Polym. Sci.* 281, (2003), 957 – 963.
39. Xin, H., Shen, Y., & Li, X. *Colloids and Surfaces A: Physicochem. Eng. Aspects*. 384, (2001), 205 – 211.
40. Chen, G.N., & Chen, K.N. *J. Appl. Polym. Sci.* 63, (1997), 1609 – 1623.
41. Nanda, A.K., & Wicks, D.A. *Polymer*. 47, (2006), 1805 – 1811.
42. Manvi, G.N., & Jagtap, R.N. *Journal of Dispersion Science and Technology*. 31, (2010), 1376 – 1382.
43. Coogan, R.G. *Prog. Org. Coat.* 32, (1997), 51 – 63.
44. Zhang, M., Wu, Y., Wu, H., & Zhang, Q. *J. Polym. Res.* 19, (2012), 9807 – 9816.
45. Hwang, H.D., & Kim, H.J. *Reactive & Functional Polymers*. 71, (2011), 655 – 665.
46. Rahman, M.M., Chun, H.H., & Park, H. *JCT. Research*. 8, (2011), 389 – 399.
47. Krol, B., Krol, P., Pikus, S., Chmielarz, P., & Skrzypiec, K. *Colloid. Polym. Sci.* 288, (2010), 1255 – 1269.
48. Manvi, G.N., Singh, A.R., Jagtap, R.N., & Kothari, D.C. *Prog. Org. Coat.* 75, (2012), 139 – 146.
49. Zhu, Y., & Sun, D.X. *J. Appl. Polym. Sci.* 92, (2004), 2013 – 2016.
50. Narayan, R., Chattopadhyay, D.K., Sreedhar, B., Raju, K.V.S.N., Mallikarjuna, N.N., & Aminabhavi, T.M. *J. Appl. Polym. Sci.* 99, (2006), 368 – 380.
51. Rengasamy, S., Patel, J., & Mannari, V. *European Coating Journal*. 4, (2011), 125 – 129.
52. Williams, T.C., Callen, K., Gambino, C.A & Dvorchak, M. 39<sup>th</sup> *Waterborne Symposium, Sponsored by the School of Polymers and High Performance Materials, The University of Southern Mississippi, February 13- 17, 2012 in New Orleans, L.A.*

53. Decker, C., Masson, F., & Schwalm, R. *Macromol. Mater. Eng.* 288, (2003), 17 – 28.
54. Bai, C., Zhang, X., & Dai, J. *Prog. Org. Coat.* 60, (2007), 63 – 68.
55. Zhang, T., Wu, W., Wang, X., & Mu, Y. *Prog. Org. Coat.* 68, (2010), 201 – 207.
56. Hwang, H., Moon, J., Choi, J.H., Kim, H.J., Kim, S.D., & Park, J.C. *Journal of Industrial and Engineering Chemistry.* 15, (2009), 381 – 387.
57. Lee, S.H., & Kim, D.S. *Polym. Adv. Technol.* 23, (2012), 414 – 417.
58. Decker, C., & Lorinczova, I. *JCT. Research.* 1, (2004), 247 – 256.
59. Wang, X., Hu, Y., Song, L., Xing, W., Lu, H., Lv, P., & Jie, G. *J. Polym. Res.* 18, (2011), 721 – 729.
60. Mequanint, K., & Sanderson, R.D. *Macromol. Symp.* 193, (2003), 169 – 185.
61. Liu, T., Pan, X., Wu, Y., Zhang, T., Zheng, Z., Ding, X., & Peng, Y. *J. Polym. Res.* 19, (2012), 9741 – 9748.
62. Lu, Y., & Larock, R.C. *Biomacromolecules.* 9, (2008), 3332 – 3340.
63. Meier, M.A.R., Metzger, J.O., Schubert, U.S. *Chem. Soc. Rev.* 36, (2007), 1788 – 1802.
64. Williams, C.K., & Hillyer, M.A. *Polym. Rev.*, 48, 2008, 1 – 10.
65. Guo, A., Cho, Y., & Petrovic, Z.S. *Journal of Polymer Science, Part A: Polymer Chemistry.* 38, (2000), 3900 – 3910.
66. Petrovic, Z.S., Guo, A., & Zhang, W. *Journal of Polymer Science, Part A: Polymer Chemistry.* 38, (2000), 4062 – 4069.
67. Lligadas, G. *Biomacromolecules*, 8, (2007), 686 – 692.
68. Kong, X.H. & Narine, S.S. *Biomacromolecules*, 8, 2007, 2203 – 2209.
69. Caollol, S., Desroches, M., Boutevin, G., Loubat, C., Auvergne, R., & Boutevin, B. *Eur. J. Lipid. Sci. Technol.* 114, (2012), 1447 – 1459.
70. Monteavaro, L.L., Silva, E.O.D., Costa, A.P.O., Samios, D., Gerbase, A.E., & Petzhold, C.L. *JAOCs.* 82, (2005), 365 – 371.
71. Xia, Y., Lu, Y., & Larock, R.C. *Polymer.* 51 (2010), 53 – 61.

72. Li, R., & Larock, R.C. *Biomacromolecules*. 4, (2003), 1018 – 1025.
73. Andjelkovic, D.D., Valverde, M., Henna, P., Li, F., & Larock, R.C. *Polymer*. 46, (2005), 9674 – 9685.
74. LaScala, J.J., & Wool, R.P. *Polymer*. 46, (2005), 61 – 69.
75. Khot, S.N., LaScala, J.J., Can, C., Morye, S.S., Williams, G.I., Palmese, G.R., Ku, S.H., & Wool, R.P. *J. Appl. Polym. Sci.* 82, (2001), 703 – 723.
76. Jain, J.P., Sokolsky, M., Kumar, N., & Domb, A.J. *Polym. Rev.* 48, (2008), 156 – 191.
77. Sharmin, E., Ashraf, S.M., & Ahmad, S. *Eur. J. Lipid. Sci. Technol.* 109, (2007), 134 – 146.
78. Lu, J., & Wool, R.P. *J. Appl. Polym. Sci.* 99, (2006), 2481 – 2488.
79. Behra, D., & Banthia, A.K. *J. Appl. Polym. Sci.* 109, (2008), 2583 – 2590.
80. Rengasamy, S., & Mannari, V. *Prog. Org. Coat.* 76, (2013), 78 – 85.
81. Lu, Y., & Larock, R.C. *Biomacromolecule*. 8, (2007), 3108 – 3114.
82. Zhong, N., & Yuan, Q. *J. Appl. Polym. Sci.* 128, (2013), 460 – 469.
83. Lozada, Z., Suppes, G.J., Tu, Y.C., & Hsieh, F.H. *J. Appl. Polym. Sci.* 113, (2009), 2552 – 2560.
84. Ni, B., Yang, L., Wang, C., Wang, L., & Finlow, D.E. *J. Therm. Anal. Calorim.* 100, (2010), 239 – 246.
85. Sharmin, E., Ashraf, S.M., & Ahmad, S. *International Journal of Biological Macromolecules*. 40, (2007), 407 – 422.
86. Wang, C., Yang, L., Ni, B., & Wang, L. *J. Appl. Polym. Sci.* 112, (2009), 1122 – 1127.
87. Petrovic, Z.S., Yang, L., Zlatanic, A., Zhang, W., & Javni, I. *J. Appl. Polym. Sci.* 105, (2007), 2717 – 2727.
88. Jiang, X., Li, J., Ding, M., Tan, H., Ling, Q., Zhong, Y., & Fu, Q. *European Polymer Journal*. 43, (2007), 1838 – 1846.
89. Hojabri, L., Kong, X., & Narine, S.S. *Biomacromolecules*. 10, (2009), 884 – 891.
90. Khot, S.N., LaScala, J.J., Can, E., Shantaram, S.M., George, I.W., Palmese, G.R., Kusefoglu, S.H., & Wool, R.P. *J. Appl. Polym. Sci.* 82, (2001), 703 – 723.

91. Petrovic, Z.S. *Polymer Reviews*. 48, (2008), 109 – 155.
92. Kusefoglu, S., Palmese, G., Khot, S., & Wool, R.P. *World Intellectual Property Organisation. International Publication Number: WO 99/21900*. (1999).
93. Lu, Y., & Larock, R.C. *ChemSusChem*. 2, (2009), 136 – 147.
94. Z.S., Guo, A., Javni, I., Cvetkovic, I., & Hong, D.P. *Polym. Int.* 57, (2008), 275 – 281.
95. Petrovic, Z.S., Zhang, W., & Javni, I. *Biomacromolecules*. 6, (2005), 713 – 719.
96. Huo, C.T. *Adv. Appl. Microbiol.* 41, (1995), 1 – 23.
97. Javni, I., Zhang, W., & Petrovic, Z.S. *J. Appl. Polym. Sci.* 88, (2003), 2912 – 2916.
98. Lligadas, G., Ronda, J.C., Galia, M., Biermann, U., & Metzger, J.O. *Journal of Applied Polymer Science: Part A: Polymer Chemistry*. 44, (2006), 634 – 645.
99. Lligadas, G., Ronda, J.C., Galia, M., & Cadiz, V. *Biomacromolecules*. 8, (2007), 686 – 692.
100. Lligadas, G., Ronda, J.C., Galia, M., & Cadiz, V. *Biomacromolecules*, 8, (2007) 1858 – 1864.
101. Lu, Y., Tighzert, L., Dole, P., & Erre, D. *Polymer*. 46, (2005), 9863 – 9870.
102. Lu, Y., Tighzert, L., Berzin, F., & Rondot, S. *Carbohydrate Polymers*. 61, (2005), 174 – 182.
103. Lu, Y., & Larock, R.C. *J. Appl. Polym. Sci.* 119, (2011), 3305 – 3314.
104. Lligadas, G., Ronda, J.C., Galia, M., & Cadiz, V. *Biomacromolecules*. 7, (2006), 2420 – 2426.
105. Zhao, H., Herrington, R., Driguez, F. *WO Patent 008675A1*, 2010.
106. Campanella, A., Bonnaillie, L., & Wool, R.P. *J. Appl. Polym. Sci.* 112, (2009), 2567 – 2578.
107. Desroches, M., Escouvois, M., Auvergne, R., Caillol, S., & Boutevin, B. *Polym. Rev.* 52, (2012), 38 – 79.
108. Dwan., J.P.L., Mohanty, A.K., Misra, M., Drzal, L.T., & Kazemizadeh, M. *J. Mater. Sci.* 39, (2004), 1887 – 1890.

109. Erhan, S.Z., Adhvaryu, A., & Liu, Z. *US Patent 6583302*, (2003).
110. Sharma, B., Adhvaryu, A., Liu, Z., & Erhan, S. *J. Am. Oil. Chem. Soc.* 83, (2006), 129 – 136.
111. Wang, L., & Wang, T. *J. Am. Oil. Chem. Soc.* 84, (2007), 1149 – 1159.
112. Adhvaryu, A., Liu, Z., & Erhan, S.Z. *Ind. Crops. Prod.* 21, (2005), 113 – 119.
113. Geiger, E.J., Becker, N.M., & Armbruster, L.A. *WO Patent 094227*, 2006.
114. Meffert, A., & Kluth, H. *US Patent 4886893*, (1989).
115. Shani, A. *Ind. Eng. Chem. Prod. Res. Dev.* 22, (1983), 121- 123.
116. Cheong, M.Y., Ooi, T.L., Ahmad, S., Yunus, W.M.Z.W., & Kuang, D. *J. Appl. Polym. Sci.* 111, (2009), 2353 – 2361.
117. Dai, H., Yang, L., Lin, B., Wang, C., & Shi, G. *J. Am. Oil. Chem. Soc.* 86, (2009), 261 – 267.
118. Choi, S.W., Wan, S.D., Don Lim, Y., Gi Jeong, Y., Mollah, I., Heon, P., Tae, W. H., & Whan, G.K. *J. Appl. Polym. Sci.* 121, (2011), 764 – 769.
119. Palaskar, D.V., Boyer, A., Cloutet, E., Le Menins, J.F., Gadenne, B., Alfos, C., Farcet, C., & Cramail, H. *J. Polym. Sci. Part A: Polymer Chemistry.* 50, (2012), 1766 – 1782.
120. Hu, Y.H., Gao, Y., Wang, D.N., Hu, C.P., Zu, S., Vanoveloop, L., & Randall, D. *J. Appl. Polym. Sci.* 84, (2002), 591 – 597.
121. Zlatanovic, A., Lava, C., Zhang, W., & Petrovic, Z.S. *J. Polym. Sci. Part B: Polymer Physics.* 42, (2004), 809 – 819.
122. Chasar, D., & Hughes, W. *WO Patent 029182 A1*, (2003).
123. Lathi, P.S., & Mattiasson, B. *Appl. Catal. B: Environ.* 69, (2007), 207 – 212.
124. Dahlke, B., Hellbardt, S., Paetow, M., & Zech, W. *J. Am. Oil. Chem. Soc.* 72, (1995), 349 – 353.
125. Lu, Y., & Larock, R. *ChemSusChem.* 3, (2009), 329 – 333.
126. Sharma, B.K., Adhvaryu, A., & Erhan, S.Z. *J. Agri. Food. Chem.* 54, (2006), 9866 – 9872.

127. Biswas, A., Adhvaryu, A., Gordon, S.H., Erhan, S.Z., & Willett, J.L. *J. Agri. Food. Chem.* 53, (2005), 9485 – 9490.
128. Lee, C., Ooi, T., Chuah, C., & Ahmad, S. *J. Am. Oil. Chem. Soc.* 84, (2007), 945-952.
129. Scholnick, F., Saggese, E., Wrigley, A., & Riser, G. *J. Am. Oil. Chem. Soc.* 47, (1970), 180 – 182.
130. Kiatsimkul, P.P., Suppes, G.J., Hsieh, F.H., Lozada, Z., & Tu, Y.C. *Ind. Crops. Prod.* 27, (2008), 257 – 264.
131. Campanella, A., Rustoy, E., Baldessari, A., & Baltanas, M.A. *Bioresour. Technol.* 101, (2009), 245 – 254.
132. Pelletier, H., Belgacem, N., Gandini, A. *J. Appl. Polym. Sci.* 99, (2006), 3218 – 3221.
133. Doll, K.M., Sharma, B.K., & Erhan, S.Z. *Ind. Eng. Chem. Res.* 46, (2007), 3513 - 3519.
134. Moser, B., Sharma, B., Doll, K., & Erhan, S. *J. Am. Oil. Chem. Soc.* 84, (2007), 675 – 680.
135. Miao, S., Zhang, S., Su, S., & Wang, P. *J. Polym. Sci. Part B: Polymer Chemistry.* 48, (2010), 243 – 250.
136. Athawale, V.D., & Kulkarni, M.A. *Prog. Org. Coat.* 65, (2009), 392 – 400.
137. Tian, H., Wang, Y., Zhang, L., Quan, C., & Zhang, X. *Ind. Crops. Prod.* 32, (2010), 13 – 20.
138. Bai, C.Y., Zhang, X.Y., Dai, J.B., & Zhang, C.Y. *Prog. Org. Coat.* 59, (2007), 331 – 336.
139. Rabea, A.M., Mohseni, M., Mirabedini, S.M., & Tabatabaei, M.H. *Applied Surface Science.* 258, (2012), 4391 – 4396.
140. Liu, K., Tian, Y., & Jian, L. *Progress in Materials Science.* 58, (2013), 503 – 564.
141. Mirabedini, S.M., Sabzi, M., Zohuriaan, J., Atai, M., & Behzadnasab, M. *Applied Surface Science.* 257, (2011), 4196 – 4203.
142. Decker, C., Masson, F., & Schwalm, R. *Polymer Degradation and Stability.* 83, (2004), 309 – 320.
143. Sarkar, M.K., Bal, K., He, F., & Fan, J. *Applied Surface Science.* 257, (2011), 7003 – 7009.

144. Lau, K.K.S., Bico, J., Teo, K.B.K., Chhowalla, M., Amaratunga, G.A.J., Milne, W.I., McKinley, G.H., & Gleason, K.K. *Nano Letters*. 3, (2003), 1701 – 1705.
145. Wu, Y., Sugimura, H., Inoue, Y., & Takai, O. *Chem. Vap. Deposition*. 8, (2002), 47 – 50.
146. Wu, Y., Bekke, M., Inoue, Y., Sugimura, H., Kitaguchi, H., Liu, C., & Takai, O. *Thin Solid Films*. 457, (2004), 122 – 127.
147. Tavana, H., Amirfazli, A., & Neumann, A.W. *Langmuir*. 22, (2006), 5556 – 5559.
148. Wu, Y., Bekke, M., Inoue, Y., Sugimura, H., Takai, O., Kato, H., Murai, S., & Oda, H. *Thin Solid Films*. 407, (2002), 45 – 49.
149. Zhang, J., France, P., Radomyselskiy, A., Datta, S., Zhao, J., & Ooij, W. *J. Appl. Polym. Sci.* 88 (2003) 1473–1481.
150. Kim, S.H., Kim, J.H., Kang, B.K., & Uhm, H.S. *Langmuir* 21 (2005) 12213–12217.
151. Yang, J.X., Wen, X.F., Pi, P.H., Zheng, D.F., Cheng, J. & Yang, Z.R. *J. Mol. Catal. B: Enzyme*. (2007), 91 – 96.
152. Balu, B., Breedveld, V., & Hess, D.W. *Langmuir*. 24, (2008), 4785–4790.
153. Youngblood, J.P., & McCarthy, T.J. *Macromolecules*. 32, (1999), 6800–6806.
154. Yang, S.H., Liu, C.H., Hsu, W.T., & Chen, H. *Surf. Coat. Technol.* 203, (2009), 1379 – 1383.
155. Song, W., Veiga, D.D., Custodio, C.A., Mano, J.F. *Adv.Mater.* 21, (2009), 1830–1834.
156. Oner, D., & McCarthy, T.J. *Langmuir*. 16, (2000), 7777 – 7782.
157. Pozzato, A., Zilio, S.D., Fois, G., Vendramin, D., Mistura, G., Belotti, M., Chen, Y., & Natali, M. *Microelectronic Engineering*. 83, (2006), 884 – 888.
158. Baladacchini, T., Carey, J.E., Zhou, M., & Mazur, E. *Langmuir*. 22, (2006), 4917 – 4919.
159. Feng, L., Song, Y., Zhai, J., Liu, B., Xu, J., Jiang, L., & Zhu, D. *Angew. Chem. Int. Ed.* 42, (2003), 800 – 802.
160. Feng, L., Li, S., Li, H., Zhai, J., Song, Y., Jiang, L., & Zhu, D. *Angew. Chem. Int. Ed.* 41, (2002), 1222 – 1223.



161. Bormashenko, E., Stein, T., Whyman, G., Bormashenko, Y., & Pogreb, R. *Langmuir*. 22, (2006), 9982 – 9985.
162. Nakajima, A., Fujishima, A., Hashimoto, K., & Watanabe, T. *Adv. Mater.* 11, (1999), 1365 – 1368.
163. Nakajima, A., Fujishima, A., Hashimoto, K., & Watanabe, T. Takai, K., Yamauchi, G., & Fujishima, A. *Langmuir*. 16, (2000), 7044 – 7047.
164. Gao, L., & McCarthy, T.J. *Langmuir*. 23, (2007), 3762 – 3765.
165. Extrand, C.W. *US Patent 6976585 B2*, (2005).
166. Extrand, C.W. *Langmuir*. 19, (2003), 3793 – 3796.
167. Extrand, C.W. *Langmuir*. 21, (2005), 11546 – 11546.
168. Bormashenko, E. Study of the Cassie-Wenzel Wetting Transition Using Vibrated Drops. *Contact Angle Symposium*. (2008).
169. Arkles, B., Pan, Y., & Kim, Y.M. *Silanes and Other Coupling Agents*. 5. (2009), 51–64.
170. Fadeev, A.Y., & McCarthy, T.J. *Langmuir*. 16, (2000), 7268 – 7274.
171. Menger, F.M., & Chlebowski, M.E. *Langmuir*. 21, (2005), 2689 – 2695.
172. Anton, D. *Adv. Mater.* 10, (1998), 1197 – 1205.
173. Thomas, R.R., Anton, D.R., Graham, W.F., Darmon, M.J., Sauer, B.B., Stika, K.M., & Swartzfager, D.G. *Macromolecules*, 30, (1997), 2883 – 2890.
174. Soliveri, G., Annunziata, R., Ardizzone, S., Cappelletti, G., & Meroni, D. *J. Phys. Chem. C*. 116, (2012), 26405 – 26413.
175. Coulson, S.R., Woodward, I.S., & Badyal, J.P.S., Brewer, S.A., & Willis, C. *Chem. Mater.* 12, (2000), 2031 – 2038.
176. Graham, P.D., Joint, I., Nevell, T.G., Smith, J.R., Stone, M., & Tsibouklis, J. *Biofouling*. 16, (2000), 289 – 299.
177. Ming, W., Laven, J., & Linde, R.V.D. *Macromolecules*. 33, (2000), 6886 – 6891.
178. Banuelas, R., Antony, J., & Brace, M. *Qual. Reliab. Engng. Int.* 21, (2005) 553 – 570.

179. Linderman , K., Schroeder, R., Zaheer, S., Choo, A. *Journal of Operations Management*, 2, (2003) 193–203.
180. Kling, M.B.B.T.J., & Haney, M.B.B.C.N. *Abstracts of Papers of American Chemical Society*, 241, (2011).
181. Koban, M.E. *Journal of Coating Technology*, (2004) 28 – 33.
182. Antony, J., & Banuelas, R. *Manufacturing Engineering*, 8, (2001), 119–121.
183. Henderson, K., & Evans, J. *Benchmarking and International Journal*, 7, (2000), 260-281
184. Chang, S., Yen, D., Chou, C.C., Wu, C.H., & Lee, H.P. *Total Quality Management*. 23, (2012), 291-308.
185. Mast, J.D., & Lokkerbol, J. *Int. J. Production Economics*. 139, (2012), 604 - 614.
186. Aksoy, B., & Orbak, A.Y. *Qual. Reliab. Engng. Int.* 25, (2009), 495-512.
187. Heuvel, J.V., Does, R.j.M.M., & Vermaat, M.B. *Qual. Reliab. Engng. Int.* 20, (2004), 419-426.
188. Plecko, A., Herzog, V.N., & Polajnar, A. *Advances in Production Engineering & Management*. 4, (2009), 243-254.
189. Mohan, R.R., Thiruppathi, K., Venkatraman, R., & Raghuraman, S. *Journal of Applied Sciences*. 12, (2012), 985-991.
190. Gijo, E.V., Scaria, J., & Antony, J. *Qual. Reliab. Engng. Int.* 27, (2011), 1221-1234.

## **Chapter 3: Development of Soybean Oil-based Polyols and their Applications in Urethane and Melamine-Cured Thermoset Coatings**

### **3.1 Abstract:**

Polyols are versatile and increasingly important resins for thermoset coatings, adhesives, sealants and foam applications. Bio-based polyols have emerged as environmentally friendly and sustainable alternative to petrochemical based ones due to their renewability, lower carbon footprint and often lower cost. Novel family of vegetable oil-based polyols has been derived from epoxidized soybean oil with broad range of chemical structures and hydroxyl contents. This research focuses on design of unique polyol architectures and use of novel synthetic approaches for deriving these polyols and demonstration of their potential application in polyurethane and melamine-cured thermoset coatings. The chemical structure of these polyols and their functionality primarily dictate performance properties and their end-use applications. The successfully synthesized polyols have been characterized with NMR and FT-IR spectra for qualitative confirmation of functional groups. Epoxidized soybean oil has also been characterized and compared with other polyols.

### 3.2 Introduction:

Polyols are indispensable components of polyurethanes that are finding increasingly important applications in such diverse products as plastics, foams, coatings, composites, and adhesives, among others. Most of the commercially available conventional polyols are petrochemical-based and are available in wide range of chemistries, morphologies, functionalities viscosities, and cost. Due to their dependence on petroleum, these polyols are not very sustainable. Bio-based materials are increasingly used in meeting the present-day demands of developing sustainable products and processes. Vegetable oils are triglycerides and are excellent agro-based resources for development of polyols for aforementioned applications. Vegetable oils are composed of fatty acid triglycerides of variety of types as shown in Figure 3.1. Depending upon their end-use applications, polyols are required to meet such demanding requirements as functionality, reactivity, compatibility, hydrolytic stability, surface tension, rheology, to name a few. The unique combination of chemical structure, functionality and reactivity combined with low toxicity and inherent biodegradability makes vegetable oils an excellent resource for deriving sustainable polymers.<sup>1-14</sup>

A variety of soybean oil derived polyols, frequently referred in literature as soy-polyols, prepared from different synthetic routes, have been reported in the literature.<sup>15-26</sup> Polyurethanes prepared from these soy-polyols, replacing petro-based polyols show interesting performance properties besides their high bio-renewable contents.<sup>15-26</sup> Soy-polyols for use in polyurethane dispersions (PUD) require unique set of properties and hydroxyl functionality. Except castor oil and lesquerella oil with naturally occurring hydroxyl groups all other natural oils need to be chemically modified to introduce hydroxyl groups at their unsaturated sites.<sup>27</sup> This can be

accomplished by hydroformylation, followed by hydrogenation,<sup>28</sup> epoxidation, followed by oxirane opening,<sup>1</sup> ozonolysis, followed by hydrogenation<sup>4,22,29</sup> and microbial conversion.<sup>30</sup>

Epoxidized Soybean Oil (ESO), a commercial bio-based product has been used for decades as plasticizer and stabilizer for polyvinyl chloride (PVC), a commodity plastic. ESO offers unique chemical structure and functionality that allows design and development of a wide range of polyols. This chapter presents our research efforts on development of a range of polyols useful for coatings and allied applications. In the present work, ESO and their derivatives have been used as starting materials in polyol synthesis. Synthetic routes to derive a range of polyols with controlled chemical structures, types and number of functional groups, hydroxyl equivalent weight, viscosity and their potential applications are studied.

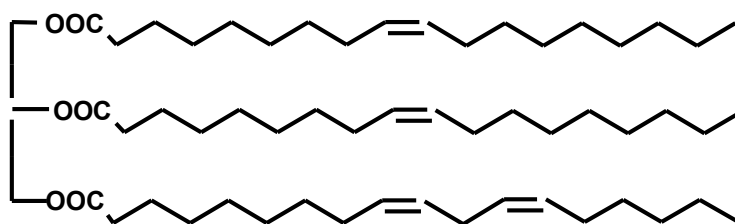


Figure 3.1: Triglyceride molecule of natural oil

### 3.3 Experimental:

#### 3.3.1 Raw Materials:

Vikoflex 7170 – Epoxidized Soybean Oil (ESO) was procured from Arkema Inc., USA and used without purification. Phosphoric Acid, calcium oxide (CaO), phthalic acid and tertiary butanol was obtained from Sigma Aldrich, USA and used as received.

#### 3.3.2 Synthesis of ESO based Phosphate Ester Polyol: (ESO – Polyol)

Epoxidized soybean oil (100.0g / 0.1 mole) and tertiary butanol (90.0g) was added in a three-neck flask equipped with mechanical stirrer, temperature controller, heating mantle, additional funnel and water condenser. Acid solution was prepared by mixing phosphoric acid

(4.5g / 0.0459 moles) with 10g of tertiary butanol and 10.0g of DI-water. The prepared acid solution was slowly added from an additional funnel into the three neck flask maintained at 80° C for about 45 minutes. The progress of reaction was monitored by % oxirane oxygen content (%OOC) and acid value of the reaction mixture at a regular interval. Reaction was continued until the %OOC of ESO drops from 7% to less than 0.3%. Rotary vacuum evaporator was used to remove solvent and other volatiles. The final product was stored in glass bottle in a desiccator. Figure 3.2(a) shows simplified reaction scheme for synthesis of phosphate-ester polyol from ESO. Figure 3.2(b) shows the reaction of oxirane oxygen groups with another oxirane oxygen group.

### **3.3.3 Synthesis of Epoxidized Soybean oil Monoglyceride: (EMG)**

One mole of ESO (1000.0g) was taken in three-neck flask equipped with addition funnel, mechanical stirrer, and temperature controller. Reaction was carried out at 145°C in presence of nitrogen gas and at this temperature 1.9 mole (174.8g) glycerol was slowly added from an addition funnel within 5 minutes. The CaO (0.2% based on ESO weight) was used as catalyst. The reaction was continued at 145°C for 3 hours and then the %OOC was determined to study the loss of oxirane oxygen content during reaction. The unreacted excess glycerol was removed by centrifuge method. A waxy like final product (EMG) was obtained which was characterized for %OOC, hydroxyl number and viscosity. The Figure 3.3 shows the schematic representation of synthesis of EMG.

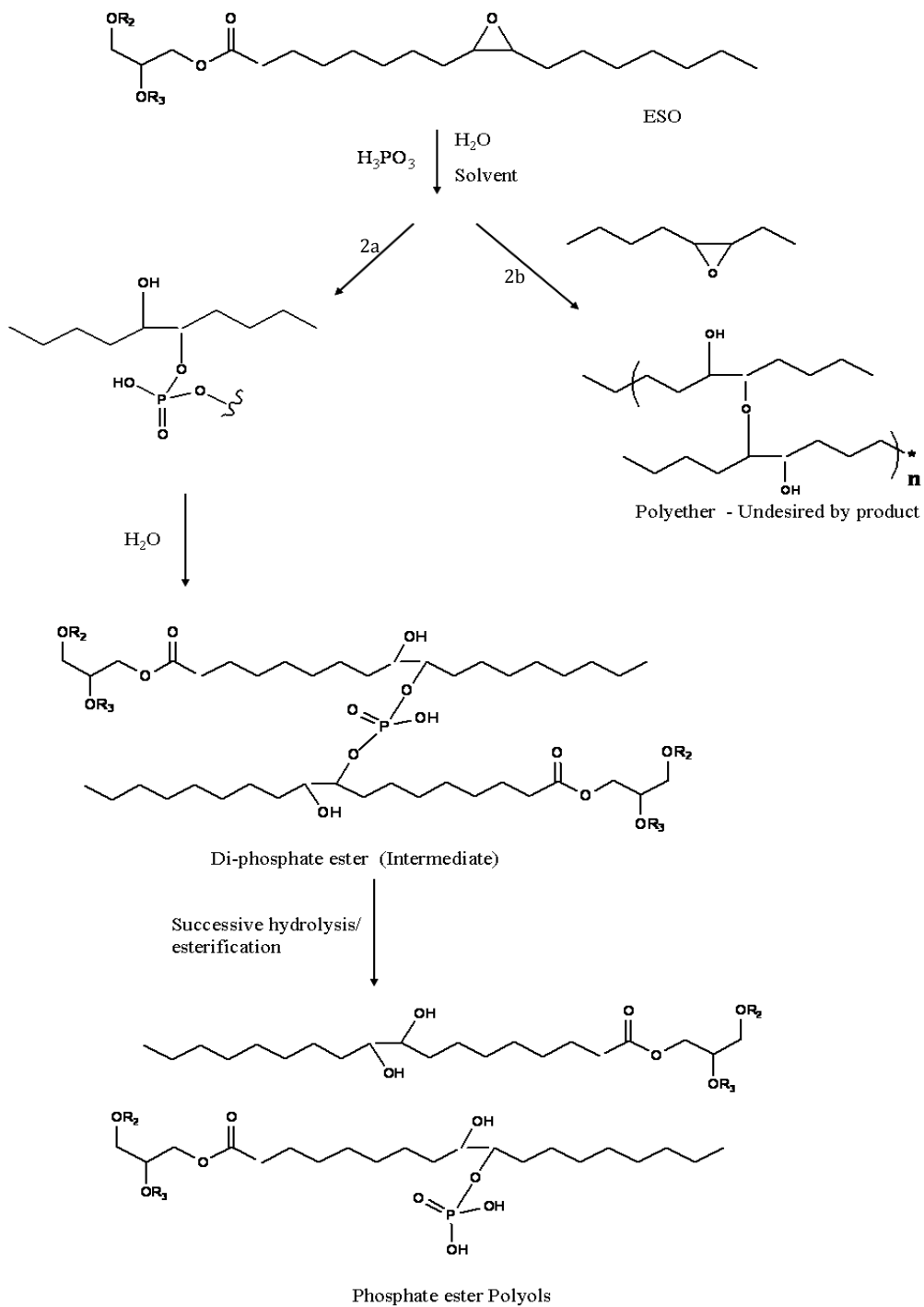


Figure -3.2: Reaction scheme for synthesis of phosphate ester polyol based on ESO

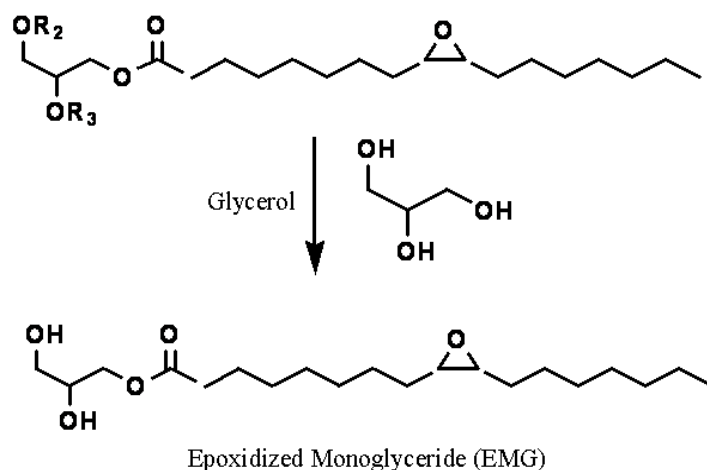


Figure 3.3: Synthesis of epoxidized monoglyceride

### 3.3.4 Synthesis of EMG based Phosphate Ester Polyol: (EMG Polyol)

EMG (100g / 0.2649 moles) and tertiary butanol (90g) was taken in three-neck flask connected to mechanical stirrer, temperature controller, heating mantle, additional funnel and a water condenser. Phosphoric acid, (3.9984g / 0.0408 mole) was placed in a beaker and mixed with DI water (10g) and tertiary butanol (10g). Similar to ESO polyol synthesis, in this reaction also EMG and tertiary butanol was taken as 1:1 weight ratio. Only 90% of tertiary butanol was added in to the three-neck flask and rest of the amount was used to prepare acid solution. The prepared solution in the beaker was placed into an addition funnel and added slowly into the three neck flask at 80° C for about 30 – 45 minutes. Reaction was continued until %OOC of ESO dropped from 7.0% to less than 0.3%, which took about 3 hrs. Rotary vacuum evaporator was used to remove solvent and other volatiles from the product. The final phosphate ester polyol was characterized for its % OCC, viscosity and hydroxyl numbers. The Figure 3.4 shows the schematic representation of EMG based phosphate ester polyol.



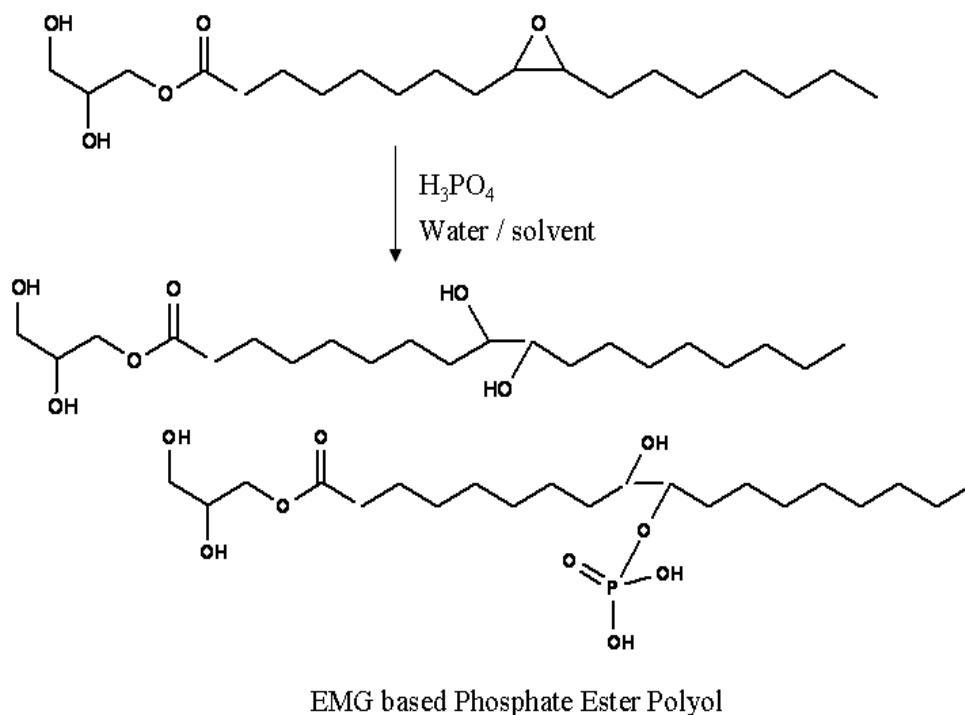


Figure 3.4: Synthesis phosphate ester polyol from epoxidized monoglyceride

### 3.3.5 Synthesis of EMG based Phthalic Acid Ester Polyol: (EMG – PEP)

The phthalic acid ester based polyol was successfully synthesized from EMG and phthalic acid in the presence of tertiary butanol. In the three neck flask, EMG (100g / 0.2649 moles) and 50g of tertiary butanol was added and the reaction kettle was connected with water condenser, temperature controller, heating mantle and nitrogen inlet / outlet. The reaction mixtures were heated to 80° C and at this temperature the addition of phthalic acid was started. The phthalic acid (18g / 0.1084 mole) was divided as three equal parts and added one part at a time as 15 minutes interval. The part-by-part addition of phthalic acid was followed to control the exothermic reaction and maintain the reaction temperature with in 80° C. After the addition of acid, the reaction was carried out at this temperature until desired % OOC values (less than 0.3%) was achieved. Once the desired % OOC value was achieved, the solvent was removed from the final product using rotary vacuum evaporator. The final product was characterized for

its viscosity and hydroxyl numbers. The Figure 3.5 shows the schematic representation of phthalic ester based polyol.

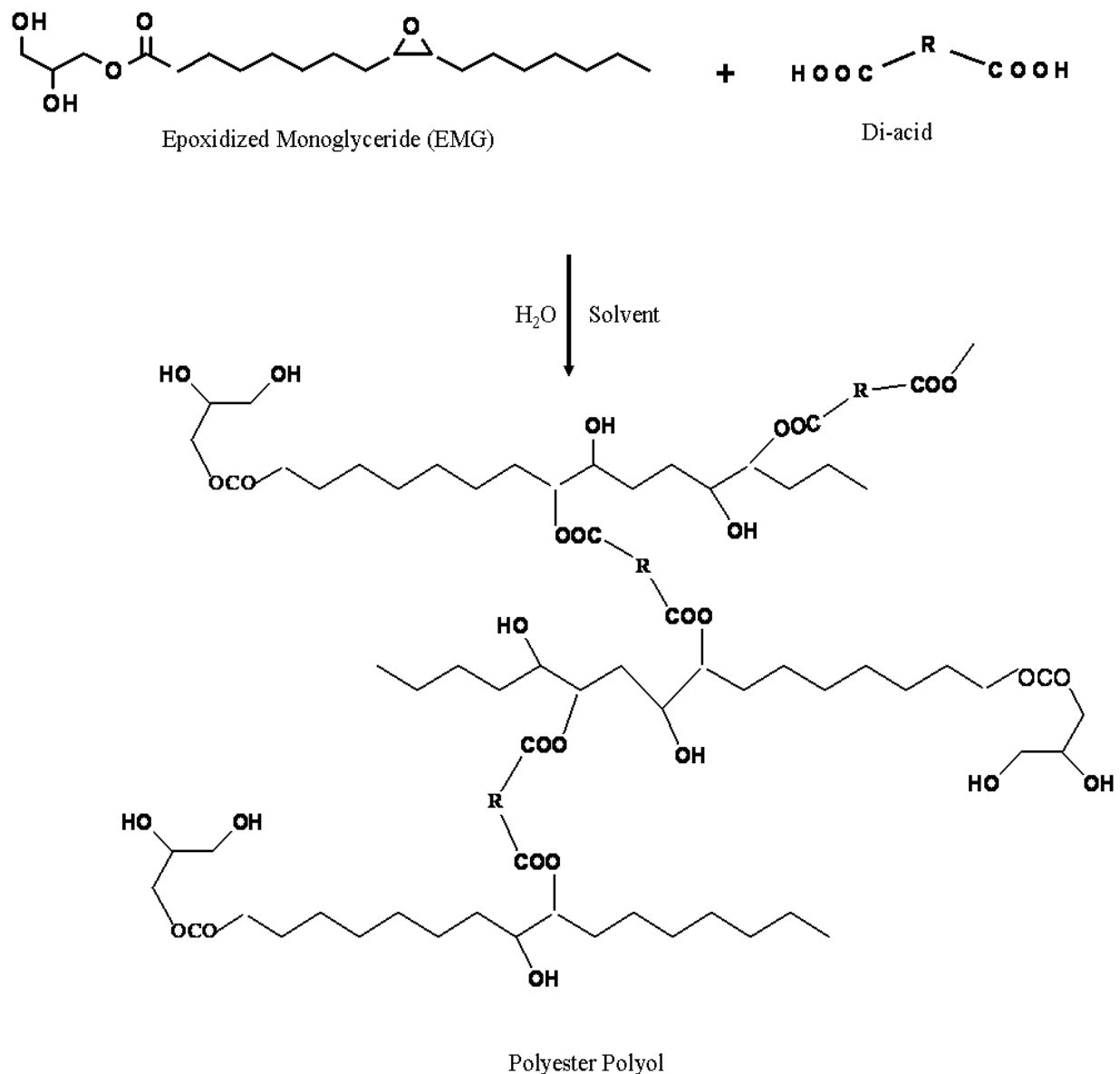


Figure 3.5: Schematic representation of synthesis of phthalic acid based polyester polyol

### 3.4 Results and Discussion:

#### 3.4.1 Characterization of Polyols.

Acid catalyzed addition of nucleophile to oxirane group has been extensively studied and reported in the literature.<sup>31</sup> Under the conditions of reaction two competing reactions are known to take place, (a) esterification by addition of phosphoric acid to the oxirane group to form phosphate ester product, and (b) reaction of oxirane group with another oxirane (carbocation) to form an ether linkage. As shown in Figure 3.2a, phosphoric acid reacts with oxirane oxygen groups of ESO and protonate them. The protonated epoxides form electrophilic site, which will be attacked by available nucleophilic compound phosphoric acid to produce diphosphate ester intermediate. The nucleus-seeking agent further attacks carbon of carbonyl groups of diphosphate ester and results in the final product phosphate ester polyol. S<sub>N</sub>2 mechanism is also possible if one alcohol chain act as nucleophile and protonated alcohol chain acts as substrate. As shown in Figure 3.2b, the protonated oxirane oxygen groups might react with each other and also forms oligomeric ethers. Similar kind of reaction can also be observed in epoxidized monoglyceride based phosphate ester polyol and phthalic ester polyol.

Table 3.1: Bio-Polyol Characteristics

<b>Bio-Polyol Types</b>	<b>%OOC</b>	<b>Acid Value (mgs KOH/g)</b>	<b>Viscosity @ 25° C</b>	<b>Hydroxyl Value (mgs KOH/g)</b>
ESO Polyol	0.2	4.3	1100	165
EMG Polyol	0.12	4.1	1385	373
EMG - PEP	0.3	4.45	1200	389

The Table 3.1 represents the characterization of the bio-polyols. The table proves that nucleophilic attack on electrophilic site results in newly formed hydroxyl groups.

### 3.4.2 $^1\text{H}$ NMR Characterization:

Spectroscopic characterization of ESO, EMG and EMG – PEP polyols have been carried out using  $^1\text{H}$  NMR and the spectra are shown in Figures 3.6, 3.7 and 3.8. Also, the characteristic peaks are summarized in Tables 3.2, 3.3 and 3.4. For every hydroxyl groups appears at epoxy moieties, the corresponding peak appears at 3.6 to 3.76 ppm. The difference between EMG – PEP polyol with ESO and EMG polyols can be observed from the peaks obtained at 7.0 to 7.6 ppm. These peaks represents the aromatic protons of phthalic ester fragment of polyester of EMG – PEP polyol.

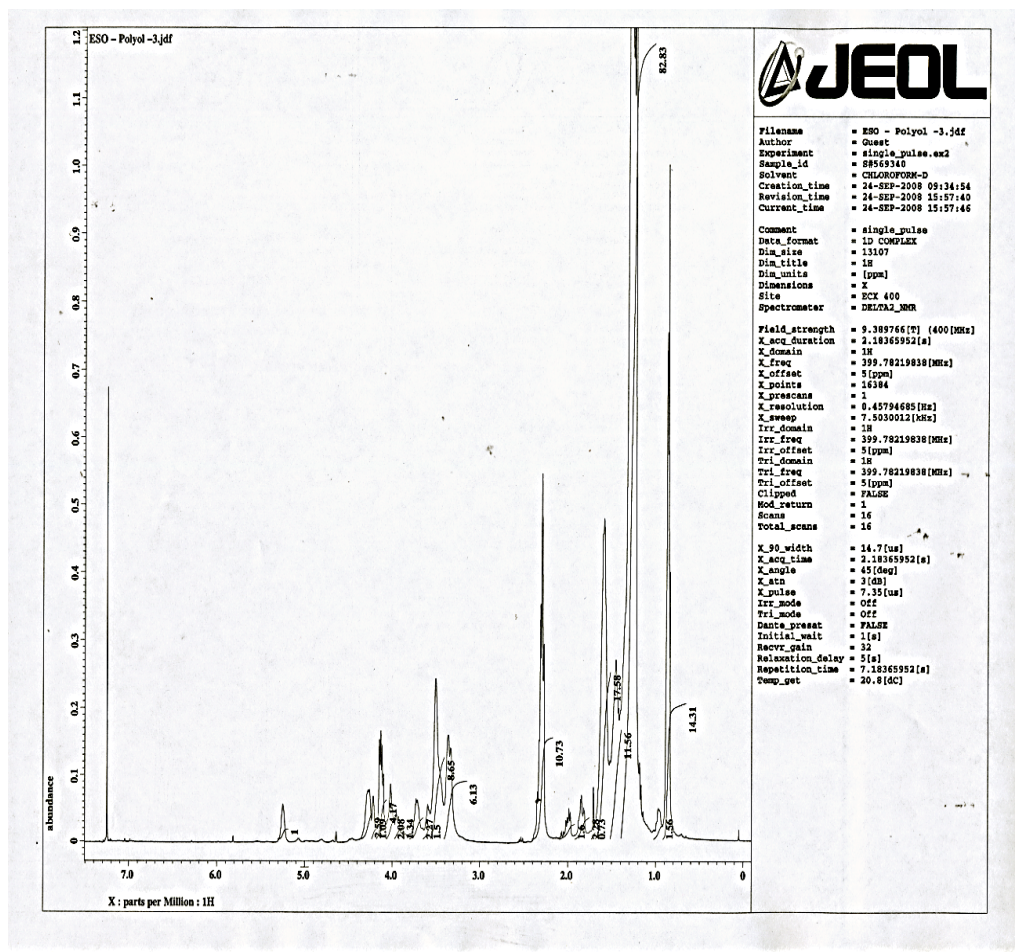


Figure 3.6:  $^1\text{H}$  NMR of ESO – Polyol

Table 3.2: <sup>1</sup>H NMR Characteristics peaks of ESO polyol

<sup>1</sup> H NMR Spectra (Signal Peak – PPM)	ESO Polyol
0.90	CH <sub>3</sub> (terminal group)
1.20 – 1.40	CH <sub>2</sub> (aliphatic backbone)
2.25 – 2.35	CH <sub>2</sub> - C = O
3.68 – 3.76	CH – OH (low field region)
3.98 – 4.30	Triglycerols (or) glyceryl carbons

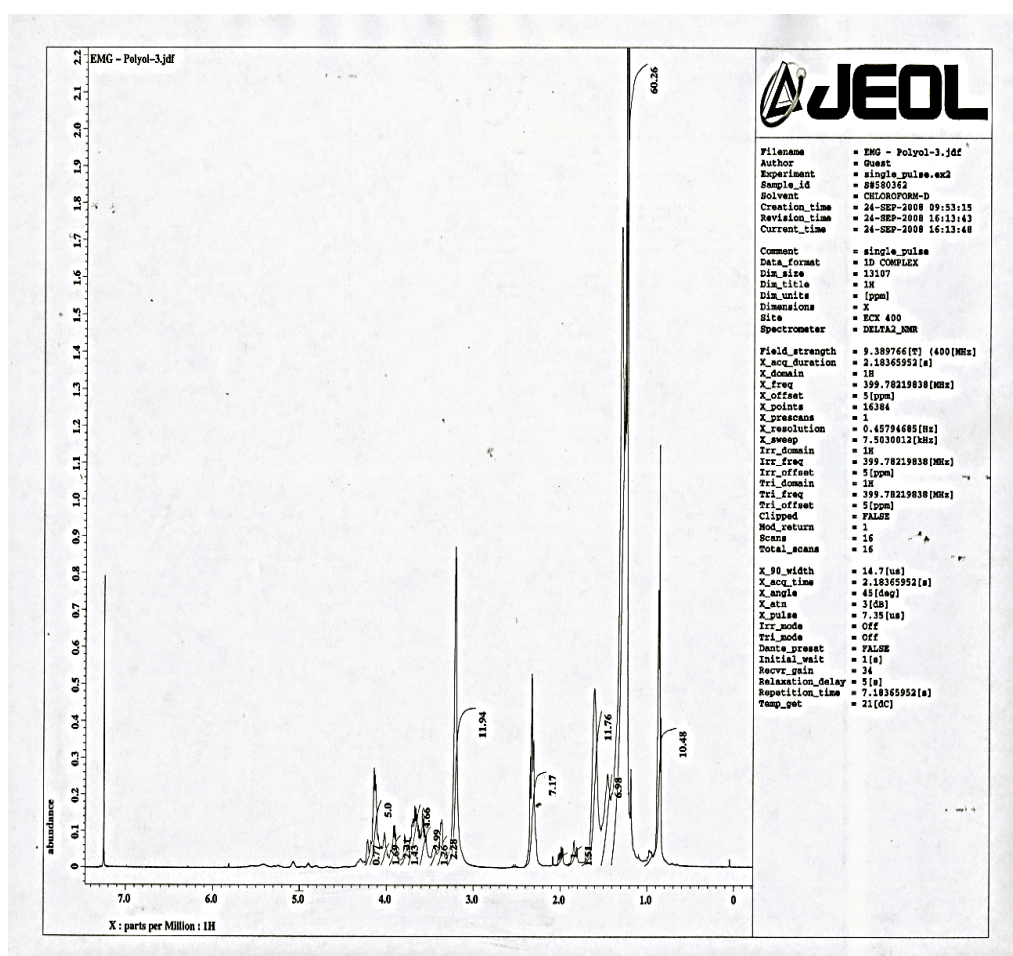


Figure 3.7: <sup>1</sup>H NMR of EMG phosphate ester polyol

Table 3.3: <sup>1</sup>H NMR Characteristics peaks of EMG phosphate ester polyol

<sup>1</sup> H NMR Spectra (Signal Peak – PPM)	EMG – Polyol
0.90	CH <sub>3</sub> (terminal group)
1.20 – 1.40	CH <sub>2</sub> (aliphatic backbone)
1.44 – 1.66	CH <sub>2</sub> (aliphatic backbone)
2.28 – 2.38	CH <sub>2</sub> - C = O
3.60 – 3.70	OH groups
3.90 – 4.22	Triglycerols / glyceryl carbon

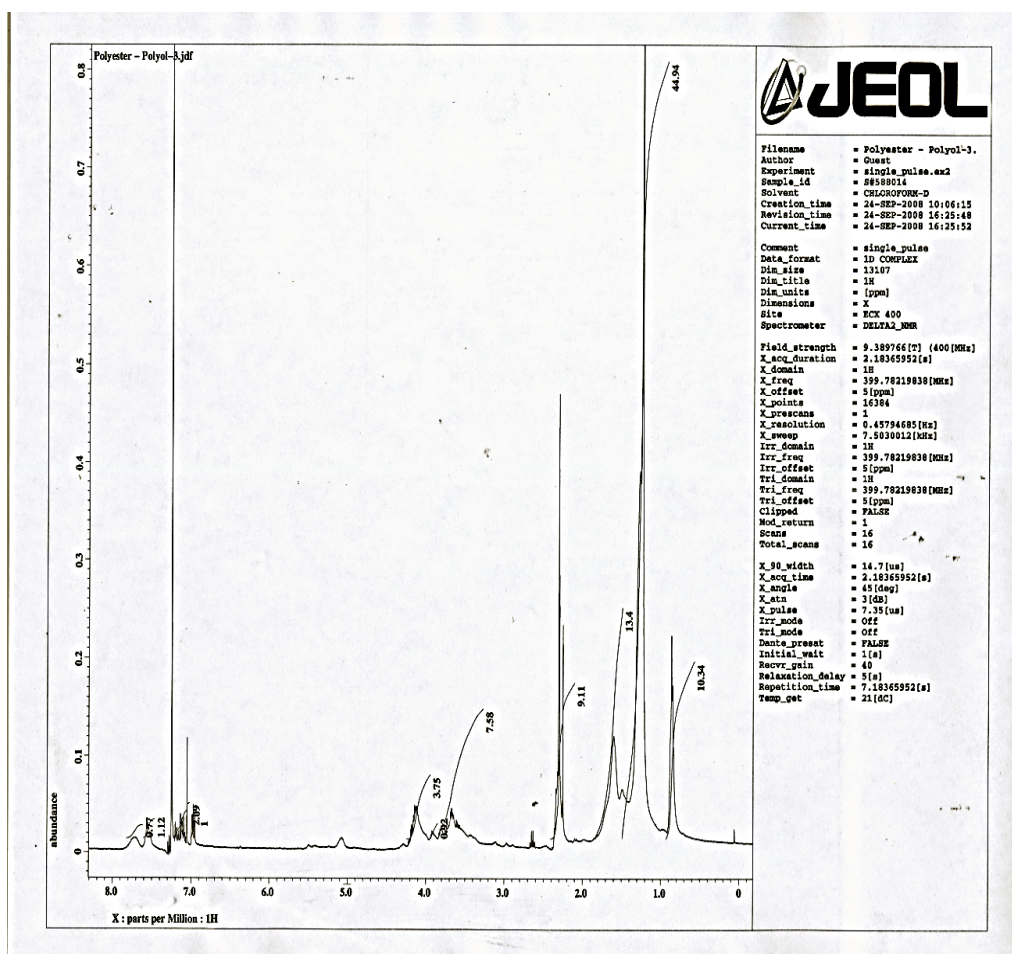


Figure 3.8: <sup>1</sup>H NMR of phthalic acid based polyester Polyol

Table 3.4: <sup>1</sup>H NMR Characteristics peaks of phthalic acid based polyester Polyol

<sup>1</sup> H NMR Spectra (Signal Peak – PPM)	Polyester Polyol
0.88	CH <sub>3</sub> (terminal group)
1.20 – 1.60	CH <sub>2</sub> (aliphatic backbone)
2.25 – 2.50	Methyl group at phenyl ring
3.60 – 3.72	CH – OH (low field region)
4.20 – 4.32	CH <sub>2</sub> - C = O (low field region)
7.0 – 7.60	Low field region contains aromatic protons or phthalic ester fragment of polyester

### 3.4.3 FT-IR Characterization:

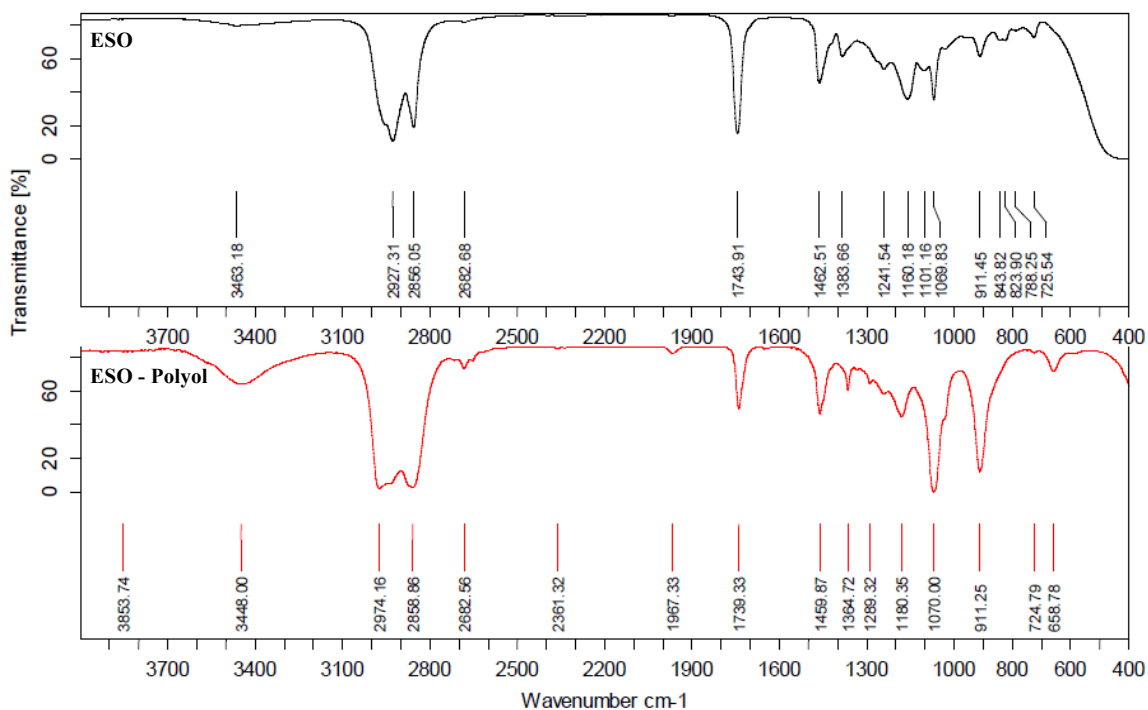


Figure 3.9: FT-IR Characteristics of ESO polyol

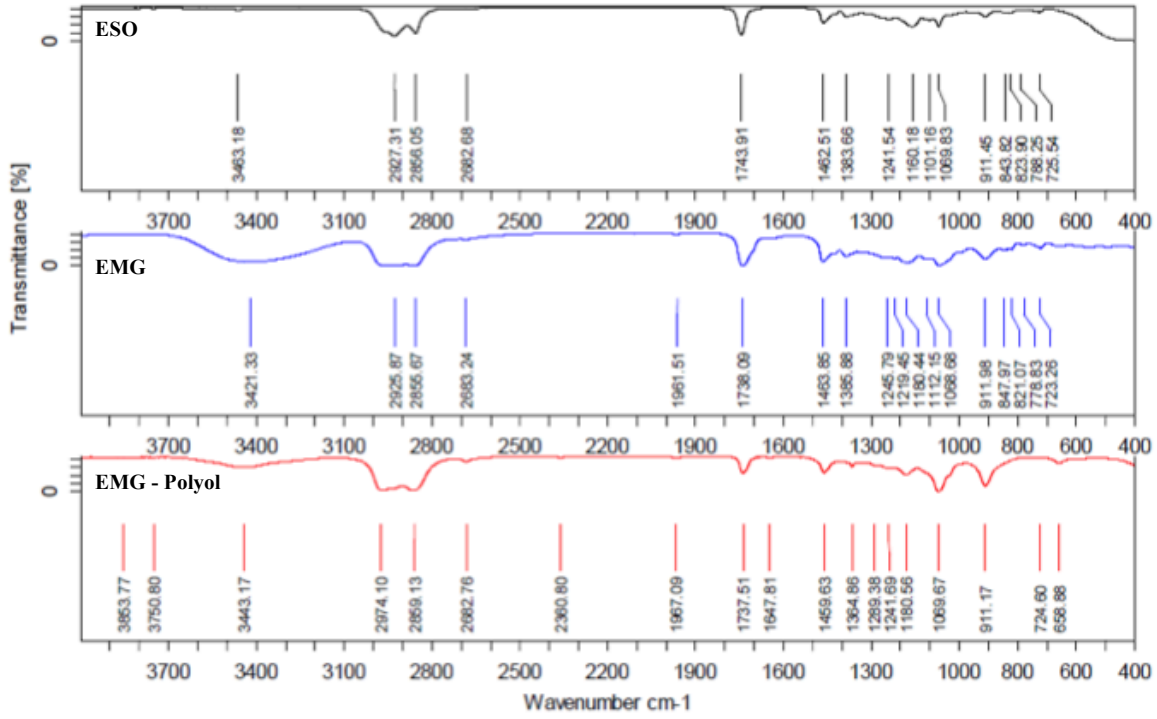


Figure 3.10: FT-IR Characteristics of EMG Polyol

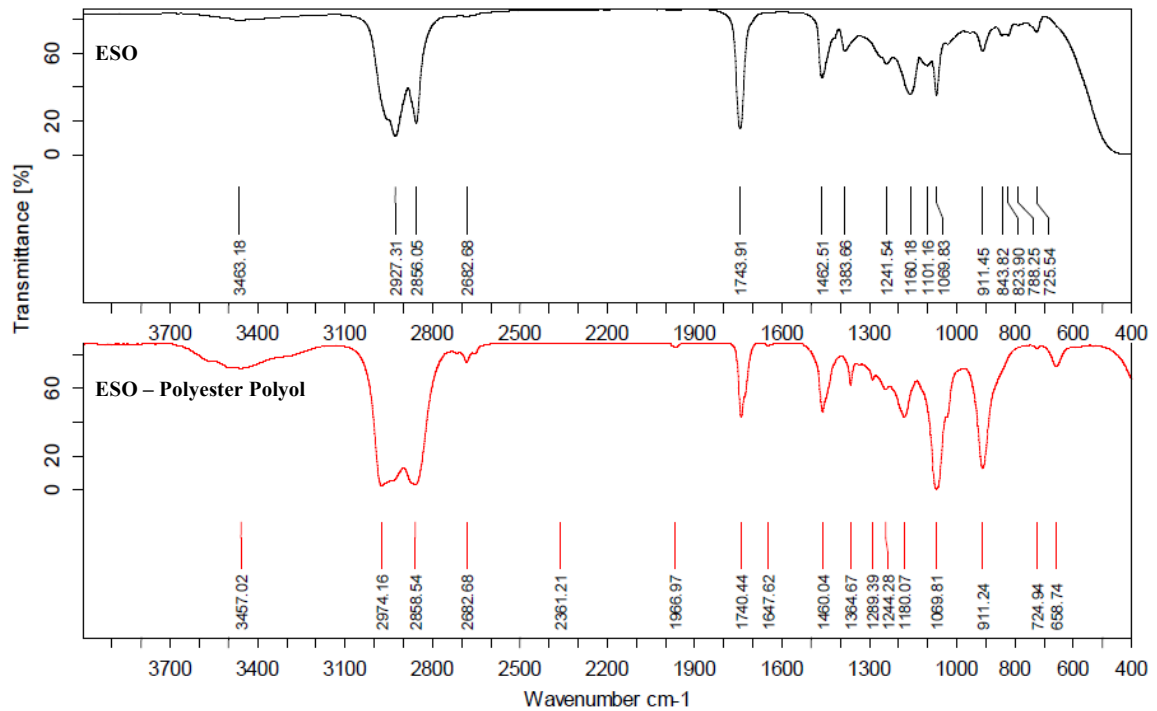


Figure 3.11: FT-IR characteristics of phthalic acid based polyester polyol



Typical FT-IR spectra of ESO and its corresponding hydroxylated derivatives are shown in Figures 3.9, 3.10 and 3.11. The oxirane (C-O-C) groups in ESO and EMG can be clearly observed from the absorption peaks at  $824\text{cm}^{-1}$  and  $844\text{cm}^{-1}$ . The oxirane groups and enhancement of peak at  $3421\text{cm}^{-1}$  corresponding to OH groups from EMG proves that not only the epoxy groups are surviving during synthesis but also glycerides are attached to end of the polymer chain. The disappearance of oxirane groups from ESO polyol, EMG polyol and Polyester polyol proves that newly formed hydroxyl groups at  $3400\text{cm}^{-1}$  are result of ring opening of oxirane groups. The FT-IR analysis corroborates very well with chemical characteristics of the products determined (epoxy value, hydroxyl number). This also concludes that the epoxide groups are reacted with acid in the presence of nucleophilic agent, resulting in the formation of an ether group and  $-\text{OH}$  group, as proposed in the above reaction schemes.

#### 3.4.4 Urethane and Melamine-Cured Film Properties:

Table 3.5: Cured Film Properties: (Urethane)

<b>Composition</b>		<b>ESO –Polyol</b>	<b>EMG - Polyol</b>	<b>EMG - PEP</b>
Polyol		10.00g	10.00g	10.00g
Desmodur N75BA		15.46g	6.84g	6.56g
Desmodur N75BA used as 1: 1 equivalent weight ratio to OH groups				
<b>Film Properties</b>				
Pencil Hardness		2H	HB	HB
Koenig Hardness		73.2	36.4	29.4
Impact Resistance lbs.inches	Direct	160	160	160
	Reverse	160	160	160
MEK double rub		50	225	100
Cross-cut adhesion		5B	5B	5B
Dry Film Thickness		1.5mil	1.5mil	1.5mil

Polyol and hexamethylene diisocyanate (Desmodur N75BA) was thoroughly mixed with 0.01% of dibutyl tindilaurate (DBTDL) and applied on the steel panel using automatic applicator. After one week curing at room temperature panels were tested for basic film properties. The Table 3.5 shows, among all three 100% bio polyol based coatings the surface hardness is better in ESO polyol based coatings where as the required automotive standard chemical resistance is achieved in EMG phosphoric acid based polyol coating.

Table 3.6: Melamine (Cymel 303) Cured Film Properties

<b>Formulation OH / Melamine Wt. ratio</b>	<b>Pencil Hardness</b>	<b>Koenig Hardness (Seconds)</b>	<b>Impact Resistance (Direct/ Reverse lbs.inches</b>	<b>MEK Double Rub</b>	<b>Cross – Cut Adhesion</b>	<b>Dry Film Thickness (mil)</b>
<b>ESO - Polyol</b>						
60/40	3H	143	28/4	75	2B	1.5
70/30	3H	126	40/4	25FAILS	3B	1.5
80/20	2H	84	40/12	25FAILS	4B	1.5
90/10	H	28	60/20	25FAILS	5B	1.5
<b>EMG - Polyol</b>						
60/40	4H	205	10/0	600	2B	1.5
70/30	4H	191	40/0	500	3B	1.5
80/20	HB	32	120/20	25	5B	1.5
90/10	HB	15	140/30	25	5B	1.5
<b>EMG - PEP</b>						
60/40	3H	186	30/0	250	2B	1.5
70/30	3H	174	30/0	350	3B	1.5
80/20	2H	156	70/6	200	3B	1.5
90/10	HB	104	140/10	75	5B	1.5

The various film properties obtained from series of melamine-based coatings (Table 3.6) prove that bio-based polyols can be utilized in numerous coating applications. Based on requirement the final film properties can be formulated either with isocyanates or melamine.

### **3.5 Conclusion:**

A range of polyols has been synthesized from soybean oil derivative – ESO. The results of our investigation show that it is possible to prepare polyols from oxirane derivatives of soybean oil under controlled reaction conditions. However, due to competing oxirane-oxirane reactions under acid catalyzed conditions, some of the oxirane groups do not yield –OH groups but form polyether derivatives. While this is undesirable, it is difficult to control and suppress this reaction and hence the resulting polyols almost always have polyether structure present.

Further, it has been demonstrated that it is possible to carry out transesterification reaction of ESO with glycerol without affecting oxirane groups. This allows incorporation of additional hydroxyl groups and related modifications before ring-opening reaction. The polyols prepared by transesterification followed ring-opening esterification/etherification have been characterized for various properties. The study also demonstrates usefulness of these polyols as components of thermoset coatings. Two series of coatings – polyurethane and melamine-cured thermosets have been prepared and their properties indicate their usefulness for a variety of end-use coating applications.

### 3.6 References:

1. Guo, A., Cho, Y., & Petrovic, Z.S. *Journal of Polymer Science, Part A: Polymer Chemistry*. **2000**, *38*, 3900 – 3910.
2. Petrovic, Z.S., Guo, A., & Zhang, W. *Journal of Polymer Science, Part A: Polymer Chemistry*. **2000**, *38*, 4062 – 4069.
3. Lligadas, G. *Biomacromolecules*. **2007**, *8*, 686 – 692.
4. Kong, X.H. & Narine, S.S. *Biomacromolecules*. **2007**, *8*, 2203 – 2209.
5. Zlatanic, A., Petrovic, Z.S., & Dusek, K. *Biomacromolecules* **2002**, *3*, 1048–1056.
6. Zlatanic, A., Lava, C., Zhang, W., & Petrovic Z.S. *Journal of Polymer Science, Part B: Polymer Physics*. **2004**, *42*, 809–19.
7. Petrovic, Z.S., Cevallos, M.J, Javni, I., Schaefer, D.W., & Justice, R. *Journal of Polymer Science, Part B: Polymer Physics*. **2005**, *43*, 3178–3190.
8. Javni, I., Zhang, W., Petrovic, Z.S. *Journal of Applied Polymer Science*. **2003**, *88*, 2912 – 2916.
9. Javni, I., Petrovic, Z.S., Guo, A., & Fuller, R. *Journal of Applied Polymer Science*. **2000**, *77*, 1723 – 1734.
10. Javni, I., Petrovic, Z.S., Zhang, W., Guo, A. *58th Annual technical conference – society of plastics engineers*. **2000**. *3*, 3732–3736.
11. Guo, A., Zhang, W., & Petrovic, Z.S. *Journal of Materials Science*. **2006**, *41*, 4914–4920.
12. Guo, A., Javni, I., & Petrovic, Z. *Journal of Applied Polymer Science*. **2000**, *77*, 467–473.
13. Guo, A., Demydov, D., Zhang, W., & Petrovic, Z.S. *Journal of Polymers and the Environment* **2002**, *10*, 49–52.
14. Petrovic, Z.S., Zhang, W., & Javni, I. *Biomacromolecules* **2005**, *6*, 713–719.
15. Lligadas, G.; Ronda, J.C.; Galia, M.; Biermann, U.; Metzger, J.O. *J. Polym. Sci. Part A: Poly. Chem.* **2006**, *44*, 634-645.
16. Hojabri, L.; Kong, X.; Narine, S.S. *Biomacromolecules*. **2009**, *10*, 884-891.
17. Dumont, M.J.; Kong, X.; Narine, S.S. *J. App. Polym. Sci.* **2010**, *117*, 3196-3203.
18. Rengasamy, S.; Mannari, V. *Prog. Org. Coat.* **2013**, *76*, 78-85.

19. Lligadas, G.; Ronda, J.C.; Galia, M.; & Cadiz, V. *Biomacromolecules*, **2007**, *8*, 686 – 692.
20. Lligadas, G.; Ronda, J.C.; Galia, M.; & Cadiz, V. *Biomacromolecules*, **2007**, *8*, 1858 – 1864.
21. Lu, Y., & Larock, R.C. *Biomacromolecules*. **2007**, *8*, 3108 – 3114.
22. Lu, Y., & Larock, R.C. *J. Appl. Polym. Sci.* **2008**, *9*, 3332 - 3340.
23. Khot. S.N., Lascala, J.J., Can, E., Shantaram, S., Williams, G.I., Palmese, G.R., Kusefoglu, S.H., & Wool, R.P. *J. App. Polym. Sci.* **2001**, *82*, 703 – 723.
24. Sharmin, E., Ashraf, S.M., & Ahmad, S. *Eur. J. Lipid. Sci. Technol.* **2007**, *109*, 134 – 146.
25. Petrovic, Z.S., Guo, A., Javni, I., Cvetkovic, I., & Hong, D.P. *Polym. Int.* **2008**, *57*, 275 – 281.
26. Javni, I., Zhang, W., & Petrovic, Z.S. *J. Appl. Polym. Sci.* **2003**, *88*, 2913 – 2916.
27. Lu, Y., & Larock, R.C. *Prog. Org. Coat.* **2010**, *69*, 31-37.
28. Z.S., Guo, A., Javni, I., Cvetkovic, I., & Hong, D.P. *Polym. Int.* **2008**, *57*, 275 – 281.
29. Petrovic, Z.S., Zhang, W., & Javni, I. *Biomacromolecules*. **2005**, *6*, 713 – 719.
30. Huo, C.T. *Adv. Appl. Microbiol.* **1995**, *41*, 1 – 23.
31. Guo, Y., Hardesty, J.H., Mannari, V.M., & Massingill, J.L. *J. Am. Oil. Chem. Soc.* **2007**, *84*, 929 – 935.

**Chapter 4: An Application of Six Sigma Methodology to Reduce Waste in Synthesis of  
Environmental Friendly Green Polyurethane Dispersion**

**Senthilkumar Rengasamy, Christopher Kluse, Vijay Mannari**

*This chapter is accepted for publication in Six Sigma Forum Magazine (2013).*

**4.1 Abstract:**

Six Sigma methodology has been widely used as a business improvement tool that promotes continuous improvement for manufacturing industries by focusing on reduction of process variability and waste minimization. This article presents a case study conducted at the Coating Research Institute (CRI) of Eastern Michigan University illustrating how the CRI effectively applied Six Sigma to reduce the waste in synthesis of bio-based PUD. In summary this study demonstrates how the Six Sigma methodology was used to reduce waste during bio-based PUD synthesis. The Six Sigma implementation resulted in a significant reduction in waste and improved the average yield from 78.9% to 98.05%.

## 4.2 Introduction:

For the past 2 decades the Six Sigma business strategy has become a popular quality improvement methodology. Its ultimate goal is customer satisfaction and profit by reducing process variation and errors in any unit of the organization. Sigma is the term used to represent variation around the process mean.<sup>1-2</sup> Six Sigma can be readily applied to manufacturing and service industries where product quality and consistency are key product drivers.<sup>3-4</sup>

Many multinational industries believe in KAIZEN and hence adopted the Six Sigma methodology to provide quality products with minimum waste while increasing profits.<sup>1,5-6</sup> Six Sigma has been wide spread among many industries after its success in Motorola, General Electric and other organizations such as Citi bank, Sony and Allied Signal who all applied the Six Sigma strategy to their business process and reaped the benefits.<sup>1,5</sup>

This case study deals with the reduction of waste in the form of gelled (chunks) polyurethane dispersion (PUD) particles in the synthesis and development of bio-based PUDs in Coating Research Institute (CRI) at Eastern Michigan University, USA. The CRI is an active academic research and development lab that deals with the coating materials required for automobile and architectural applications.

PUDs present many advantages over the conventional solvent-borne polyurethanes. These advantages include but are not limited to low viscosity at high molecular weight, absence of hazardous free-isocyanate compounds in the final product, and faster drying time. Typical thermoplastic PUDs are dispersions of high molecular weight segmented polyurethanes that form films by physical drying. These systems have become very popular in the architectural and automobile coating fields due to their ability to form coatings with desirable properties under ambient conditions while utilizing water as the solvent during the manufacturing process. Since

water (green material) does not have a hazardous impact on the global environment, aqueous PUDs are preferable over petrochemical based solvent borne polyurethanes. To make green + green PUDs, the author has utilized bio-based renewable materials as a reagent to produce aqueous PUD. Even though the chemistry behind PUD development is a theoretically known mechanism, manufacturing PUD is not as easy as making two component polyurethane coating system where component A (polyol) and component B (isocyanate) will be mixed together at the time of application. A typical PUD manufacturing process involves; (a) preparation of pre-polymer; (b) neutralization; and (c) chain extension in aqueous dispersion. This multistep process carried out at the CRI is time consuming (5 – 8 hours) and often results in low yield. The waste is in the form of gelled particles (useless chunks). These chunks/gelled particles have been observed only during the chain extension step in aqueous media. In the past, many attempts were made to eliminate waste using different methodologies, however these attempts were unsuccessful. Since the problem was unclear, the fact-based decision-making aspect of the Six Sigma methodology was recommended to determine root cause of the waste.<sup>7-13</sup>

#### **4.3 Problem Statement and It's Significance:**

The factor(s) that affect yield and produce gelled particles (waste) during manufacturing of polyurethane dispersion (PUD) are unknown. The gelled particles not only affect the yield of the final product but also significantly affect the stability (shelf life) of the product. Polyurethane dispersions are polyurethane/polyurea polymer particles dispersed in water. These nano or micro-sized particles coalesce upon exposure to moisture or high temperature and form a tack free film. Good coalescence improves cured film properties; in order to achieve good coalescence, the distribution of PUD particles size must be finer. The gelation problem disturbs finer particle size distribution and results in poor coalescence. Since the quality of the PUD has



been compromised, the coating made from these products results in poor performance of the coating film and includes defects such as poor appearance, low solvent resistance, delamination of film from its coated substrate. As shown in Figure 4.1, five phases of the DMAIC were applied to reduce waste and optimize the manufacturing parameters.

Define : Define the problem

Measure: Map out current process

Analyze: Identify cause of the problem

Improve: Implement and verify the solution

Control : Maintain the solution

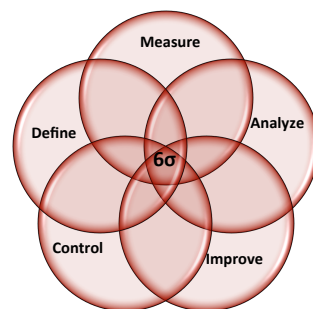


Figure 4.1: Five Phases of Six Sigma

#### 4.3.1 Define Phase:

The initial phase of Six Sigma methodology is the “define” phase where the scope and goals of the improvement project are defined in terms of customer requirements.<sup>1,14-17</sup> This phase normally defines the SS team members, the problem and significance, the impact of the problem and the current status of the problem. The SS team members will demonstrate a business case and set the goal of the project.<sup>18</sup> The problem significance and required resources needed to support the project are determined in this stage. The team selected for this project consisted of the process owner (black belt), a senior manager as the Project Champion and a senior engineer as the planning manager.

Development of Polyurethane Dispersions (PUDs) from renewable resources is one of the important projects that were undertaken by CRI resulting from the financial support of a USDA grant under Cooperative State Research, Education, and Extension Service (CSREES) program. Formation of gelled particles during processing of PUD often results in low yield and forces the R&D team to re-develop the product over and over for multiple characterizations and

testing. This is not an efficient process. Additionally, this gelled particle results in poor quality of the final coating film. Approximate cost is \$500-750/month including chemical waste and disposal from the CRI. The gelation problem not only increases the waste but also increases the viscosity of the entire coating system, which demands more solvent and leads to low solid content. The primary concern is appearance of gelled particles during manufacturing or storage of bio-based PUD. This problem reduced the amount of final product's yield and created undesirable coating properties in applied steel panels. The problem was first noticed in the final stage of manufacturing of bio-PUD. Standard filter paper was used to filter the gelled particles before applying the PUD on a clean cold rolled steel panel. Once again gelled particles were observed on the entire steel panel. The SS team concluded that three factors influenced the gelled particles after filtration. These are; a) the polyurethane/polyurea polymers are susceptible to moisture therefore during filtration the moisture might be entered into the polyurethane dispersion and; b) further crosslinking occurred with the polyurethane/polyurea particles during storage; and c) the nano size gelled particles accumulated together and formed large particles during storage. In order to prove the SS team's conclusion, gelled particles were observed in the airtight glass jar in which PUD was filtered and stored for observation. Erroneous data (film appearance) were observed when a small amount of the sample was periodically (once in two days) withdrawn from the airtight glass jar and applied on steel panels for further coating film characterization. It was observed that coating films, when applied immediately after filtration, showed no gelled particles and the films applied 2 or 3 days after initial filtration showed more gelled particles. Creating an inert atmosphere during storage might remove the moisture and eliminate the crosslinking problem, however this is a temporary solution. Furthermore, constantly keeping the product under inert atmosphere is not economically viable. Additionally,

it is important to eliminate the gelation problem to increase the percent yield. Although the process of making PUD from renewable resources is chemically viable, increase in waste during manufacturing process not only increases cost of the product but also has an adverse environmental impact due to isocyanate based waste which will discourage researchers to develop PUD from renewable resources. The Table 4.1 is the project charter developed by the team:

Table 4.1: Project Charter

<b>Title</b>	Using DMAIC to reduce waste and improve quality in the synthesis of environmentally friendly green polyurethane dispersion.
<b>Problem Concept</b>	Many factors can affect the final yield when processing Polyurethane Dispersions. Additionally, factors that affect yield can also affect final product quality. Identification of the significant factors can increase quality and final yield.
<b>Project Objective</b>	The objective of this project is to significantly increase the final yield during PUD production while simultaneously improving final product quality. Current the yield is ranging from 25% to 85% while the quality is not acceptable for commercializing the product.
<b>Business Case</b>	Development of Polyurethane Dispersions (PUD's) from renewable resources is one of the important projects at the CRI funded by a grant from the USDA under the CSREES program. Improving yield and overall quality will lead to a cost savings of \$500 per month for each increase in yield percentage. Additionally, an increase in batch yeild will further encourage the development of green PUDs.
<b>Scope</b>	The project will be conducted at the Coatings Research Institue at Eastern Michingan University. Lab quantity batch producitn will be utilized to idenfity the critical facotrs when synthesizing PUD's. Results can be directly applied to mass batch produciton.

### **4.3.2 Measure Phase:**

The measure phase consists of defining and validating the measurement system. The measure phase focuses on how to effectively measure the critical parameters. The SS team listed the vital inputs and outputs of PUD manufacturing beginning with charging the raw materials into the reaction kettle to the final product stored in the airtight glass jar. The raw materials used for this research methodology were freshly procured from suppliers and used for all the 19 experiments. The stoichiometric amount of chemicals used for polyol, diisocyanate, hydrophilic groups, neutralizing agent, chain extender and solvents were held constant throughout all 19 experiments. Additionally, as showed in Table 4.5, the reaction temperature, reaction time and stirring speed were maintained constant throughout all 19 experiments. The experimental inputs that varied from batch to batch are addition time of chain extender and the exposure time of pre-polymer to moisture.

#### ***4.3.2.1 Addition Time:***

Addition time is the time taken by the operator to add the chain extender into the pre-polymer mixture. A calibrated stopwatch was started at the moment the first drop of chain extender was added to the pre-polymer and stopped at the moment the last drop of chain extender was mixed into the pre-polymer. The time was recorded in the laboratory notebook.

#### ***4.3.2.2 Pre-Polymer Exposure Time:***

Exposure time is the time that the pre-polymer is exposed to moisture until the time when final product is formed. Exposure time starts the moment nitrogen flow is stopped into the pre-polymer and ends at the moment final product are stored in the airtight glass jar. Exposure time includes the transition time where the pre-polymer is only exposed to atmospheric air and dispersion time in high-speed disperser where the pre-polymer is exposed both to moisture and

water. Similar to addition time a calibrated stopwatch and laboratory notebook were used to measure and record the time.

**4.3.2.3 The Output (% of gelled particles):**

The goal of this project is to minimize or eliminate the gelled particles from PUD and increase the yield. Therefore the output was measured in the form amount (%) gelled particles collected at the end of the process. A calibrated analytical balance was used to measure the generated gelled particles in each batch. The weight (gram) measurement values were recorded in laboratory notebook. Waste measurement in grams were converted to % using the equation  $\{(x-y)/x\} * 100$ , where x = total weight of pre-polymer including chain extender + water and y = final weight of the product having no gelled particles.) To assure measurement system reproducibility, the same operator, calibrated stopwatch, and calibrated balance were used to measure time and weight for all 19 experiments.

Table 4.2: Yield with respect to addition time and exposure time

Experiment #	Addition Time (AT) Minutes	Exposure Time (ET) Minutes	% Yield = 100 - Waste
1	1.000	38.000	63.000
2	0.500	40.000	25.000
3	1.500	40.000	64.000
4	4.000	37.000	88.000
5	4.000	40.000	83.000
6	2.000	35.000	73.000
7	2.500	38.000	68.000
8	2.500	40.000	61.000
9	3.250	40.000	88.000
10	3.000	39.000	88.000
11	3.000	45.000	81.000
12	5.000	40.000	85.000
13	5.000	43.000	78.000
14	5.500	40.000	85.000
15	6.000	40.000	82.000
16	5.000	38.000	94.000
17	4.500	37.000	97.000
18	4.500	36.000	98.000
19	4.000	36.000	98.000

### 4.3.3 Analyze Phase: (Data Analysis)

The Analyze phase leads to improvement solutions and sustained control. This phase determined the significant contributors to the output by analyzing the variation using Statgraphics software.

As mentioned earlier, it was observed that the two inputs, which varied from batch to batch, are addition time of chain extender and the exposure time. Figure 4.2 represents the percent yield with respect to varying addition time and exposure time. A percent yield of 97 and above is considered as an acceptable yield. The 3% loss is related to loss of solvent (acetone) during chain extension and water dispersion process. Due to its volatile properties, the acetone evaporates at room temperature. Loosing acetone at this stage would not affect viscosity of the pre-polymer because of addition of water in the chain extension step. Evaporation of acetone was confirmed by determination of solid content of respective batches. The Pareto chart identifies the critical issues related to percent yield. The Pareto chart for basic film properties and its corresponding critical issues are shown in Figure 4.3.

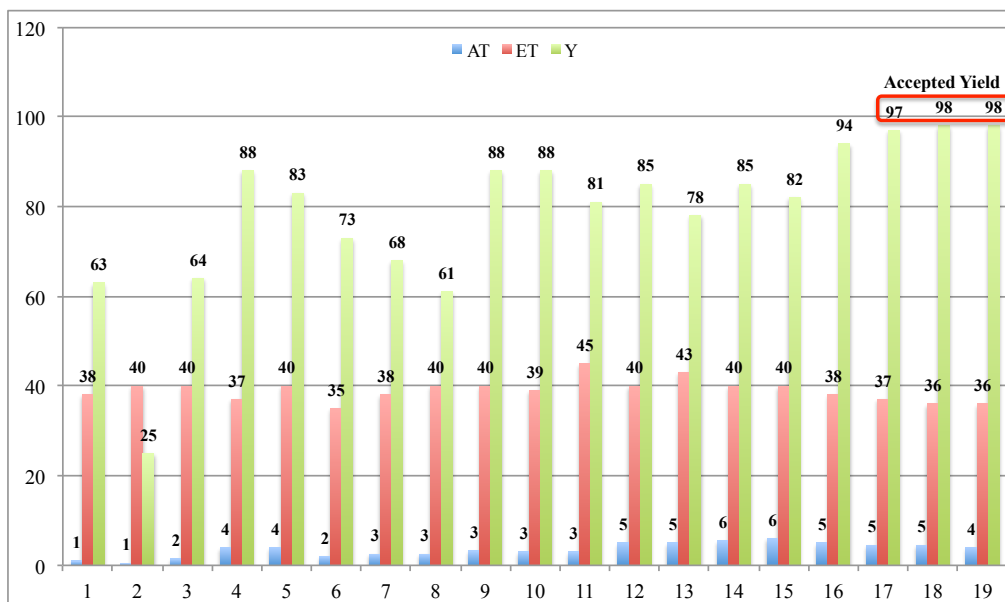


Figure 4.2: Yield (%) with respect to Addition Time (AT) & Exposure Time (ET)

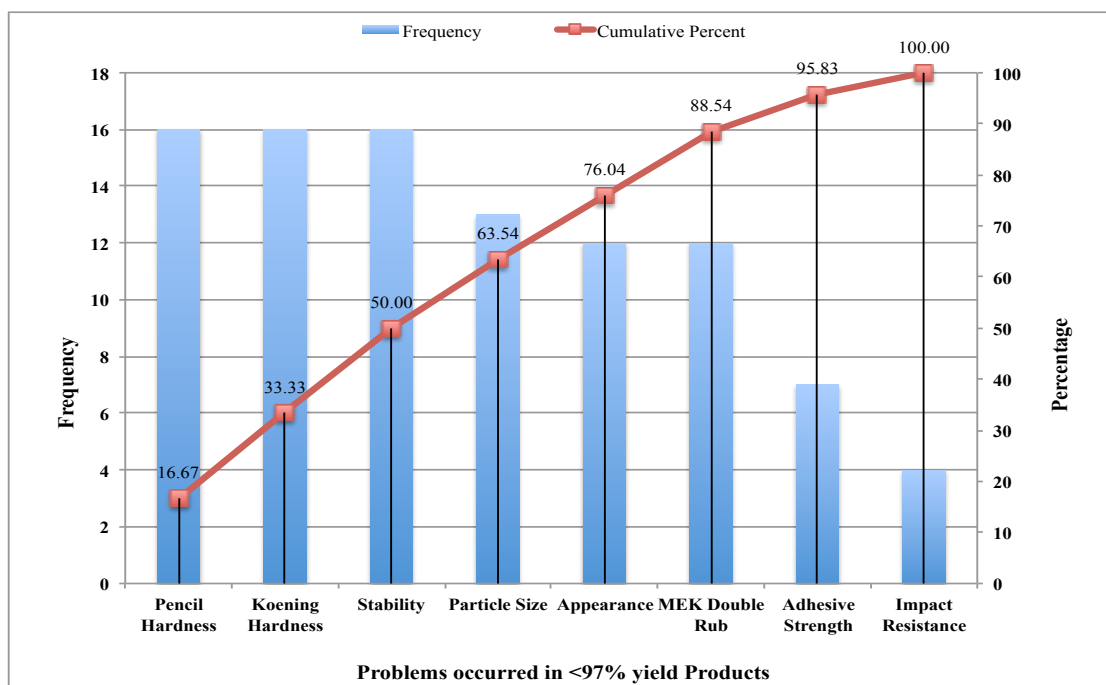


Figure 4.3: Pareto chart for vital defect analysis of cured coating films

#### 4.3.4 Improve Phase:

Scatterplot and correlation coefficient studies were conducted to determine the relationship between chain extender addition time and pre-polymer exposure time to yield. As shown in Figure 4.4, the linear regression line drawn through the points of the scatterplot and calculated correlation values ( $r$ ) indicates that there is a relationship between addition time of chain extender to yield and the exposure time of pre-polymer to yield. The  $r$ -value 0.7436 represents the strong positive correlation of addition time on % yield. It can be concluded that increasing addition time increases % yield. The two-tailed  $P$  value calculated from this positive  $r$ -value equal to 0.0003. By conventional criteria, this difference is considered to be statistically significant. The obtained negative correlation coefficient value ( $r = -0.2409$ ) for exposure time reveals that increasing the pre-polymer exposure time to moisture decreases product yield. However, the calculated  $P$  value 0.3205 suggests the negative correlation of exposure time to yield is not statistically significant. Since moisture varies day to day, the effect of moisture to

pre-polymer is also varies. Thus no statistical significance found in the data. The coefficient of determination ( $r^2$ ) values for addition time to % yield and exposure time to % yield suggests 55.29% variation in % yield can be explained by the variation in addition time of chain extender and only 5.80% variation in % yield can be explained by the variation in pre-polymer exposure time to moisture. The flyer at 25 % yield belongs to run # 2, which involves superfast reaction of pre-polymer to chain extender in a given addition time of chain extender and exposure time of pre-polymer. Since the reaction rate is too high, this particular batch resulted in very low yield.

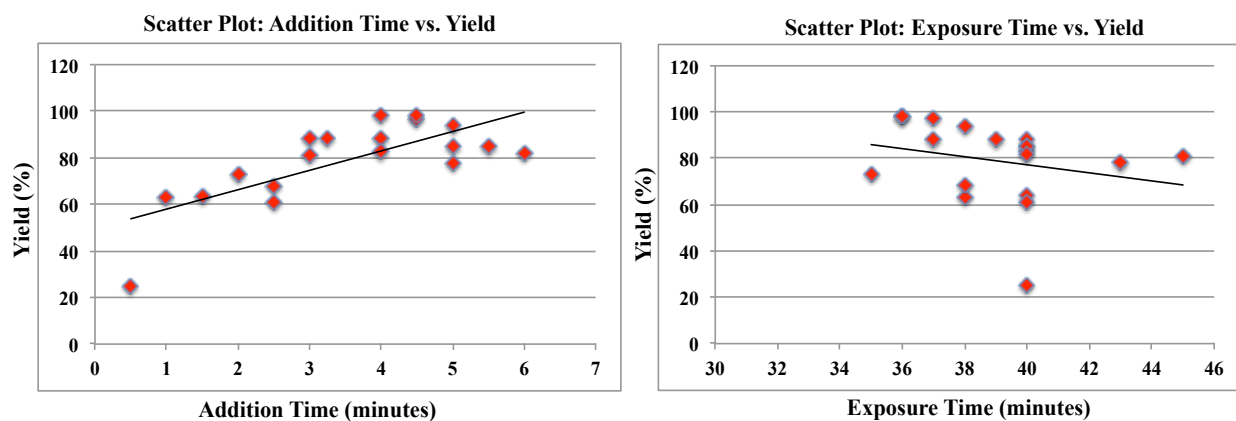


Figure 4.4: Scatter plot of addition time vs. yield and exposure time vs. yield

Since percent yield strongly depends on addition time and exposure time, analysis of variance (ANOVA) and regression models were developed to determine the best model, which fits the above data (Table 4.2) and can increase the percent yield of the product.

In Table 4.2,  $R^2$  is the proportions of variance in yield (Y) accounted for by addition time (AT) and exposure time (ET). Therefore calculated  $R^2$  statistics indicates that the independent variables AT and ET accounted for 63.1% of the total variance of the dependent variable yield. Therefore 63.1% of the change in yield can be explained by the change in the 2 independent variables (AT and ET) adjusted for sample size based on result of regression equation. Therefore the analysis is Significant.



Durbin – Watson test can be used to identify whether the calculated multiple regression residuals from Table 4.3 is independent or not. The selected model has 2 independent variables or regressors (k) with the sample size 19. To use Durbin – Watson’s table, the sample size (n) was cross-referenced against number of regressors, excluding the constant from the count of the number of regressors. The upper ( $d_U$ ) and lower ( $d_L$ ) critical values corresponding to  $k=2$ ,  $n=19$  with  $\alpha=0.05$  was cross-referenced as  $d_L = 1.074$  and  $d_U = 1.536$ . Since  $d$  (1.597) is greater than  $d_U$  there is no significant autocorrelation detected at 95% confidence. Table 4.4 represents the Durbin – Watson’s statistical calculation.

Table 4.3: Calculation for Regression Line Equation

Experiment #	AT	ET	Y	AT.Y	ET.Y	AT.ET	AT^2	ET^2	Y^2	Predicted Values	Residuals
1	1.000	38.000	63.000	63.000	2394.000	38.000	1.000	1444.000	3969.000	59.726	3.274
2	0.500	40.000	25.000	12.500	1000.000	20.000	0.250	1600.000	625.000	51.404	-26.404
3	1.500	40.000	64.000	96.000	2560.000	60.000	2.250	1600.000	4096.000	59.886	4.114
4	4.000	37.000	88.000	352.000	3256.000	148.000	16.000	1369.000	7744.000	87.213	0.787
5	4.000	40.000	83.000	332.000	3320.000	160.000	16.000	1600.000	6889.000	81.091	1.909
6	2.000	35.000	73.000	146.000	2555.000	70.000	4.000	1225.000	5329.000	74.331	-1.331
7	2.500	38.000	68.000	170.000	2584.000	95.000	6.250	1444.000	4624.000	72.449	-4.449
8	2.500	40.000	61.000	152.500	2440.000	100.000	6.250	1600.000	3721.000	68.368	-7.368
9	3.250	40.000	88.000	286.000	3520.000	130.000	10.563	1600.000	7744.000	74.729	13.271
10	3.000	39.000	88.000	264.000	3432.000	117.000	9.000	1521.000	7744.000	74.650	13.350
11	3.000	45.000	81.000	243.000	3645.000	135.000	9.000	2025.000	6561.000	62.404	18.596
12	5.000	40.000	85.000	425.000	3400.000	200.000	25.000	1600.000	7225.000	89.573	-4.573
13	5.000	43.000	78.000	390.000	3354.000	215.000	25.000	1849.000	6084.000	83.450	-5.450
14	5.500	40.000	85.000	467.500	3400.000	220.000	30.250	1600.000	7225.000	93.814	-8.814
15	6.000	40.000	82.000	492.000	3280.000	240.000	36.000	1600.000	6724.000	98.055	-16.055
16	5.000	38.000	94.000	470.000	3572.000	190.000	25.000	1444.000	8836.000	93.654	0.346
17	4.500	37.000	97.000	436.500	3589.000	166.500	20.250	1369.000	9409.000	91.454	5.546
18	4.500	36.000	98.000	441.000	3528.000	162.000	20.250	1296.000	9604.000	93.495	4.505
19	4.000	36.000	98.000	392.000	3528.000	144.000	16.000	1296.000	9604.000	89.254	8.746
<b>Sum</b>	66.750	742.000	1499.000	5631.000	58357.000	2610.500	278.313	29082.000	123757.000		
<b>N</b>	19.000	19.000	19.000	19.000	19.000	19.000	19.000	19.000	19.000		
<b>Mean</b>	3.513	39.053	78.895	296.368	3071.421	137.395	14.648	1530.632	6513.526		
<b>STD</b>	1.560	2.415	17.470	151.942	664.370	62.381	10.465	191.866	2340.130		
<b>Variance</b>	2.434	5.830	305.211	23086.357	441387.368	3891.405	109.515	36812.579	5476206.930		
<b><math>\Sigma at^2</math></b>	43.809		<b><math>\Sigma at.y</math></b>	364.776		<b><math>b_1</math></b>	8.482		<b>SSreg</b>	3467.304	
<b><math>\Sigma et^2</math></b>	104.947		<b><math>\Sigma et.y</math></b>	-182.895		<b><math>b_2</math></b>	-2.041		<b>SSres</b>	2026.485	
<b><math>\Sigma y^2</math></b>	5493.789		<b><math>\Sigma at.et</math></b>	3.737		<b>a</b>	128.797		<b>R<sup>2</sup></b>	0.631	
<b>Regression Equation: Yield = 128.797+8.482*Addition Time - 2.041*Exposure Time</b>											

Table 4.4: Calculation for Durbin – Watson Statistic

i	AT <sub>i</sub>	ET <sub>i</sub>	Residuals (e <sub>i</sub> )	e <sup>2</sup> <sub>i</sub>	(e <sub>i</sub> - e <sup>2</sup> <sub>i-1</sub> ) <sup>2</sup>
1	1.000	38.000	3.274	10.717	
2	0.500	40.000	-26.404	697.151	880.740
3	1.500	40.000	4.114	16.928	931.347
4	4.000	37.000	0.787	0.619	11.073
5	4.000	40.000	1.909	3.645	1.260
6	2.000	35.000	-1.331	1.772	10.499
7	2.500	38.000	-4.449	19.797	9.724
8	2.500	40.000	-7.368	54.282	8.516
9	3.250	40.000	13.271	176.115	425.947
10	3.000	39.000	13.350	178.235	0.006
11	3.000	45.000	18.596	345.799	27.512
12	5.000	40.000	-4.573	20.910	536.773
13	5.000	43.000	-5.450	29.704	0.770
14	5.500	40.000	-8.814	77.682	11.314
15	6.000	40.000	-16.055	257.754	52.432
16	5.000	38.000	0.346	0.119	268.969
17	4.500	37.000	5.546	30.755	27.041
18	4.500	36.000	4.505	20.294	1.083
19	4.000	36.000	8.746	76.490	17.986
			<b>Sum (Σ)</b>	2018.766	3222.996
			<b>d</b>	1.597	

#### 4.3.5 Control Phase:

After identifying the root cause and possible solutions to reduce variation and improve yield, the team proceeded to the control phase. The objective of this phase is to implement the ongoing measures and actions to sustain the improvement by monitoring, standardizing, documenting and integrating the new process on a daily basis.<sup>19</sup> The success of the Six Sigma project depends on the sustainability of the process improvements identified during the improve phase. Standardization of the improved methods and the introduction of monitoring mechanisms are the key factors for the sustainability. Since isocyanates are susceptible to moisture, the reaction time and addition of chain extender are key factors for the maximum yield of the PUD

synthesis; therefore awareness has been created among all the operators and supervisors involved in this project. The revised process flow and operator instructions are shown below in Table 4.5 and Figure 4.5.

Table 4.5: 55% Bio-PUD batch sheet

Raw Material	Amount (g)	Reaction Temperature & Time	Mixing Speed (RPM)
<b>Stage 1:</b>			
Soy - Polyol	165.0009	110 deg C 20 minutes	500
1,4 Butane Diol	3.1186		
DMPA	20.901		
NMP	35.8698		
<b>Stage 2:</b>			
DBTDL Solution	0.5	80 deg C 95 minutes	500
IPDI	102.656		
<b>Stage 3:</b>			
Acetone	35.8698	55 deg C 30 minutes	800
TEA	15.7538		
<b>Stage 4:</b>			
DI Water	266	25 to 30 deg C 30 minutes after addition of EDA Solution	5000
EDA Solution (EDA+DI Water)	88.8302 (8.3235+80.5067)		
DI Water	266		
<b>Total</b>	<b>1000.5001</b>		

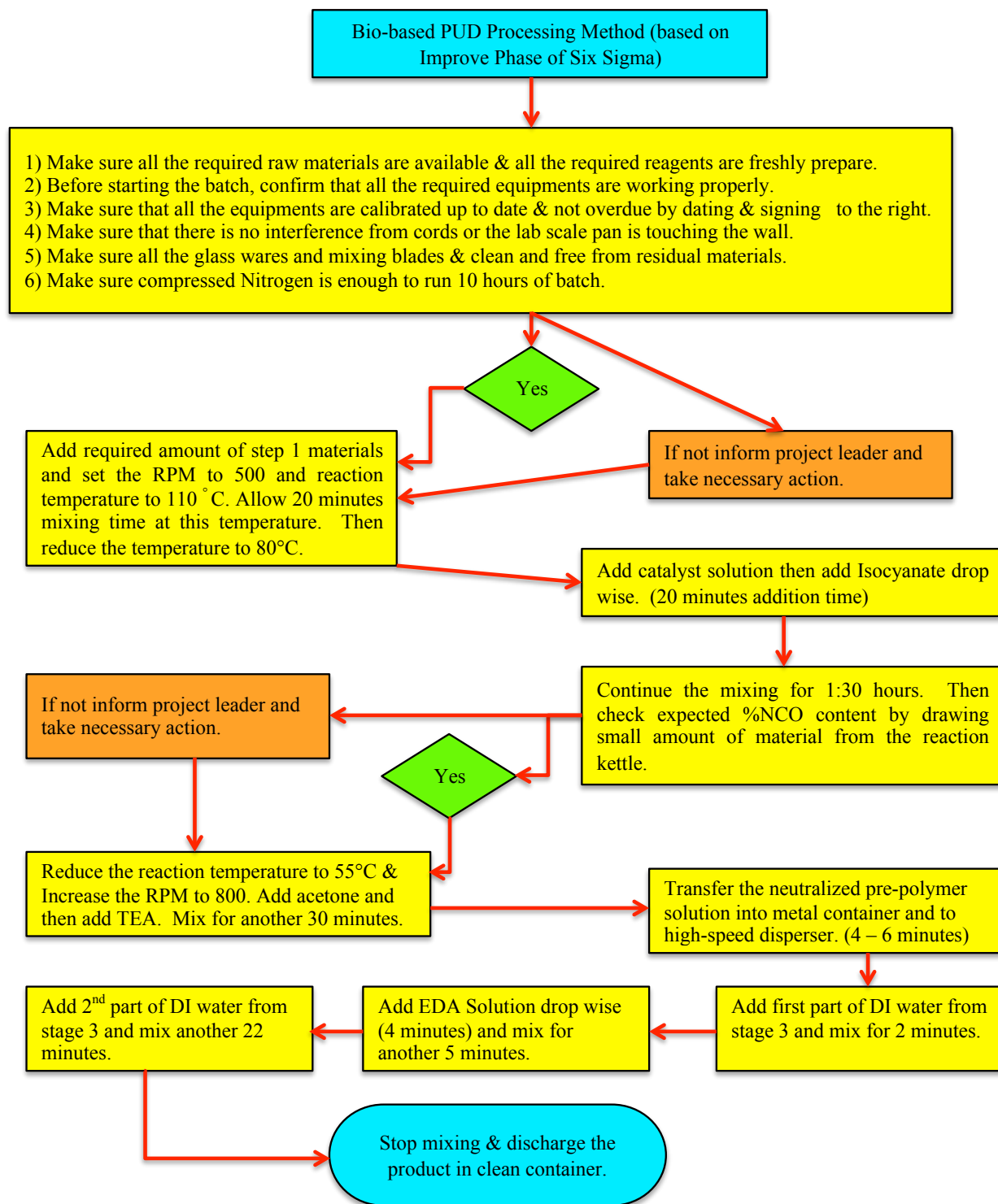


Figure 4.5: Process control flow chart of 55% Bio- PUD

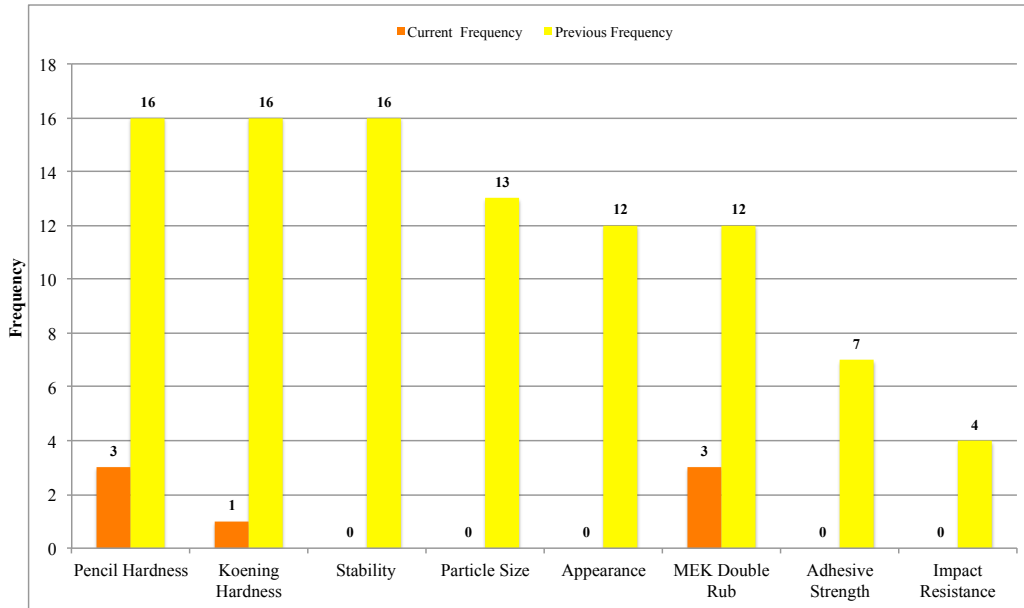


Figure 4.6: Comparison of existing and previous problem frequency of basic film properties

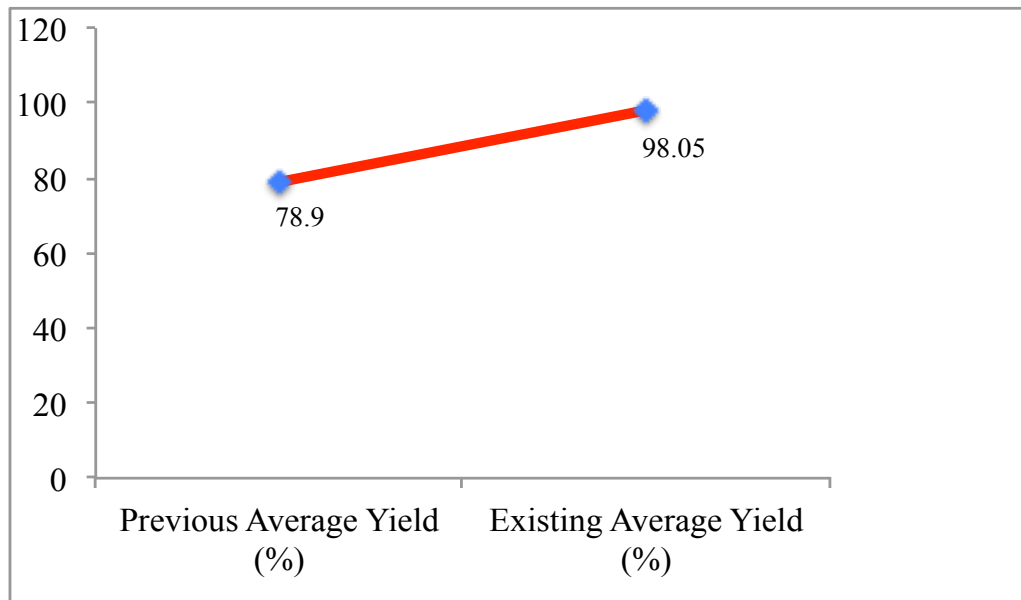


Figure 4.7: Comparison of existing and previous average yield of 55% Bio-PUD synthesis process

From Figure 4.6 and 4.7, it can be understood that average yield is increased from 78.9% to 98.05% after implementing the regression analysis based process control flow chart. Also all the batches exhibit no significant variation basic film properties.

#### **4.4 Conclusion:**

This paper illustrated effective use of Six Sigma to reduce waste in development of bio-PUD. The project showed the step-by-step application of Six Sigma methodology for reducing waste. It elaborates how the project was selected, important of project, necessity to address problems, impact of problems and how to control the problems effectively. The potential impact of chain extender addition time and pre-polymer exposure time on percent yield was identified using DMAIC methodology. The scatterplot indicated 63.1% of variability in the yield significantly depended on these key factors. The team followed the five phases of DMAIC and as a result the average yield improved from 78.9% to 98.05%.

The research showed that Six Sigma could be utilized within the coatings industry, particularly in the synthesis discipline.

#### **4.5 Acknowledgement:**

The research work is part of the PhD thesis belongs to Senthilkumar Rengasamy. Authors sincerely acknowledge USDA for financial support under Cooperative State Research Education, and extension Services (CSREES) through Grant award no. 2009-38303-05085. We would also like to express the deepest appreciation to Arkema Inc., Bayer MaterialScience LLC and Geo Specialty Chemicals for providing raw materials respectively ESFAME, IPDI, and DMPA.

#### 4.6 References:

1. Banuelas, R., Antony, J., & Brace, M. (2005). An Application of Six Sigma to Reduce Waste. *Qual. Reliab. Engng. Int.* 21, 553 – 570.
2. Linderman, K., Schroeder, R., Zaheer, S., Choo, A. (2003). Six Sigma: A goal-theoretic perspective. *Journal of Operations Management*, 2, 193–203.
3. Kling, M.B.T.J., & Haney, M.B.C.N. (2011). Six Sigma & problem solving at Dow Chemical. *Abstracts of Papers of American Chemical Society*, 241.
4. Koban, M.E. (2004). Using Six Sigma Tools to Evaluate Pigment Dispersant Demand Performance. *Journal of Coating Technology*, 28 – 33.
5. Antony, J., & Banuelas, R. (2001). Six Sigma a business strategy for manufacturing organisations. *Manufacturing Engineering*, 8, 119–121.
6. Henderson, K., & Evans, J. (2000). Successful implementation of Six Sigma: Benchmarking General Electric Company. *Benchmarking and International Journal*, 7, 260–281.
7. Chang, S., Yen, D., Chou, C.C., Wu, C.H., & Lee, H.P. (2012). Applying Six Sigma to the management and improvement of production planning procedure's performance. *Total Quality Management*. 23 (3), 291-308.
8. Mast, J.D., & Lokkerbol, J. (2012). An analysis of the Six Sigma DMAIC method from the perspective of problem solving. *Int. J. Production Economics*. 139, 604-614.
9. Aksoy, B., & Orbak, A.Y. (2009). Reducing the quantity of reworked parts in a robotic arc welding process. *Qual. Reliab. Engng. Int.* 25, 495-512.
10. Heuvel, J.V., Does, R.j.M.M., & Vermaat, M.B. (2004). Six Sigma in a Dutch hospital: Does it work in the nursing. *Qual. Reliab. Engng. Int.* 20, 419-426.

11. Plecko, A., Herzog, V.N., & Polajnar, A. (2009). An application of Six Sigma in manufacturing company. *Advances in Production Engineering & Management*. 4 (4), 243-254.
12. Mohan, R.R., Thirupathi, K., Venkatraman, R., & Raghuraman, S. (2012). Quality improvement through first pass yield using statistical process control approach. *Journal of Applied Sciences*. 12 (10), 985-991.
13. Gijo, E.V., Scaria, J., & Antony, J. (2011). An application of Six Sigma methodology to reduce defects of a grinding process. *Qual. Reliab. Engng. Int.* 27, 1221-1234.
14. Kaushik, P., & Khanduja, D. (2009). Application of Six Sigma DMAIC methodology in thermal power plants: A case study. *Total Quality Management*, 20 (2), 197 – 207.
15. Breyfogle III, F. (2003). Implementing Six Sigma: Smarter Solutions Using Statistical Methods, *Second Edition*. Hoboken, New Jersey: John Wiley.
16. Pande, P., Neuman, R., & Cavanagh, R. (2002). The Six Sigma Way: TEAM FIELDBOOK. An Implementation Guide for Process Improvement Teams. *New York: McGraw-Hill*.
17. Harry, M., & Schroeder, R. (2000). Six Sigma: The Breakthrough Management Strategy Revolutionizing the World's Top Corporations, *First Edition*, *New York:*
18. Vinodh, S., Gautham, S.G., & Ramiya, A.R. (2011). Implementing lean sigma framework in an Indian automotive valves manufacturing organisation: a case study. *Production Planning & Control*. 22 (7), 708-722.
19. Pande, P., Neuman, R., & Cavanagh, R. (2000). The Six Sigma Way: How GE, Motorola and other top companies are honing their performance. *New York: McGraw-Hill*.



## 4.7 Appendix

1) The correlation coefficient was calculated using following formula.

$\text{Correlation (r)} = S_{xy} / \{S_{xx}S_{yy}\}^{1/2}$
<p>Where <math>S_{xy} = (\sum xy) - (\sum x \sum y / n)</math></p> <p><math>S_{xx} = (\sum x^2) - (\sum x)^2 / n</math></p> <p><math>S_{yy} = (\sum y^2) - (\sum y)^2 / n</math></p> <p>x = Addition time , y = Exposure time and n = total number of samples.</p>

2) Formula used in Table 4.3

$\Sigma at^2 = \Sigma AT^2 - \frac{(\Sigma AT)^2}{N}$	$\Sigma y^2 = \Sigma Y^2 - \frac{(\Sigma Y)^2}{N}$	$\Sigma et.y = \Sigma ET.Y - \frac{(\Sigma ET * \Sigma Y)}{N}$
$\Sigma et^2 = \Sigma ET^2 - \frac{(\Sigma ET)^2}{N}$	$\Sigma at.y = \Sigma AT.Y - \frac{(\Sigma AT * \Sigma Y)}{N}$	$\Sigma at.et = \Sigma AT.ET - \frac{(\Sigma AT * \Sigma ET)}{N}$
<b>Regression Equation :</b>		
$Y' = a + b_1 AT + b_2 ET$		
$b_1 = \frac{(\Sigma et^2 * \Sigma at.y - \Sigma at.et * \Sigma et.y)}{(\Sigma at^2 * \Sigma et^2 - \Sigma at.et)}$	$a = \bar{Y} - b_1 \bar{AT} - b_2 \bar{ET}$	$R^2 = \frac{SS_{reg}}{\Sigma y^2}$
$b_2 = \frac{(\Sigma at^2 * \Sigma et.y - \Sigma at.et * \Sigma at.y)}{(\Sigma at^2 * \Sigma et^2 - \Sigma at.et)}$	$SS_{reg} = b_1 \Sigma at.y + b_2 \Sigma et.y$	
	$SS_{res} = \Sigma y^2 - SS_{reg}$	

3) Formula used in Table 4.4

$\text{Durbin - Watson Statistic} = d = \frac{\sum_{i=2}^{i=14} (e_i - e_{i-1})^2}{\sum_{i=1}^{i=20} e_t^2}$
--

## **Chapter 5: Synthesis of Soy based Polyether Polyol and its Application in Aqueous Polyurethane Dispersions**

**Senthilkumar Rengasamy, Vijay Mannari**

*This chapter is published in European Coating Journal, (2013), 03, 80-85*

### **5.1 Abstract:**

A novel soy-polyol has been derived from epoxidized soybean oil fatty acid methyl ester by a single-step low energy intensive process. A series of aqueous polyurethane dispersions (PUDs) have been prepared using soy-polyol as soft-segment and using conventional prepolymer process. PUDs were also prepared using conventional polyester diol and its blend with soy-polyol to investigate their compatibility and effect of dry film properties. Besides physical and mechanical properties, the cured films are also characterized for their hydrophobicity and water-resistance. Besides high bio-based contents, the superior water resistance and hydrophobic nature of these novel PUDs provide a useful insight into the potential commercial applications of soy-polyol as component in environmentally- friendly and sustainable coatings for many end-use applications.

## 5.2 Introduction:

In the recent years, aqueous Polyurethane Dispersions (PUDs) have established themselves as one of the most important binder systems for such applications as coatings, adhesives, sealants and elastomers (CASE).<sup>1-5</sup> Their increasing acceptance, both in architectural and industrial coatings is mainly driven by their low volatile organic content (VOC) that allows formulations of environmentally compliant coatings combined with excellent performance properties of polyurethane for myriads of applications. Polyurethanes are segmented polymers comprising of alternating sequences of soft segments and hard segments, which constitute a microphase separation structure.<sup>6</sup> PUDs present many advantages over conventional solvent borne polyurethanes, including low viscosity at high molecular weight, absence of hazardous free-isocyanate compounds, faster drying time, beside others.<sup>7</sup> The typical thermoplastic PUDs are dispersions of high molecular weight segmented polyurethanes that essentially form films by physical drying. Such systems have become very popular in architectural coating field due to their ability to form coatings with desirable properties under ambient conditions. Despite being thermoplastic in nature, the segmented polyurethane structure provides excellent mechanical and chemical resistance properties due to strong hydrogen bonding through urethane groups and their high molecular weight, making them preferred candidates for a number of high performance industrial applications.

PUDs, like most other contemporary coating binders, are generally based on fast depleting petrochemical feedstock.<sup>8-10</sup> Vegetable oils are agro-based renewable materials available at relatively low cost. The unique combination of their chemical structure, functionality and reactivity combined with low toxicity and inherent biodegradability makes them excellent resource for deriving sustainable polymers.<sup>11-13</sup> There have been many studies that demonstrate

use of vegetable oils in modifying polyurethanes.<sup>14-17</sup> One of the most attractive performance benefits of using vegetable oil-based polyols in water-borne system is excellent water resistance of their films and enhanced hydrolytic stability – the key requirements of resins for waterborne applications.<sup>18</sup> Therefore, it seems prudent to explore the use of vegetable oils in modifying PUDs for their commercial exploitation.

There are number of chemistries available to prepare vegetable oil based polyol that can produce polyols with varying type and amount of –OH content, functionality, viscosity and chemical structure.<sup>19-25</sup> We carefully looked at the requirements of such polyols from the standpoint of their suitability as components (soft segment) of PUDs and performance needs of their end products. Among the key desirable attributes identified are: (a) low viscosity, (b) functionality of ~ 2, (c) high hydrophobicity, and (d) high bio-based content. Polyols with low viscosity allows for low viscosity pre-polymer, which turn produces aqueous dispersions with lower particle size and hence stability. Lower viscosity of pre-polymer is also desirable since it would need less organic solvent for efficient processing.<sup>26-27</sup> Polyols with functionality ~2 are most suitable since they allow attainment of high molecular weight without cross-linking during the chain extension step. PUDs are expected to have good hydrolytic stability and must resist hydrolysis during storage. Also, their films must have adequate water-resistance for general durability. Polyols with greater hydrophobicity are known to produce coatings with better water resistance and hydrolytic stability.<sup>18</sup> For sustainable development, high bio-based content is highly desirable of polyols since they make up significant part of PUDs. We designed soy-polyol in keeping with all of the above criteria and selected synthetic procedure that requires simple and low energy intensive steps. Cationic ring-opening polymerization of ESFAME using a super-acid catalyst  $\text{HBF}_4$  was thought to be an appropriate synthetic route.<sup>27-29</sup>

In the present study, we have designed and developed a novel hyper-branched soy-polyol with controlled chemical structure, molecular weight and functionality, for use as soft segments of thermoplastic PUDs. Our primary goal is to derive high performance PUDs without a significant change in processing steps and to achieve bio-base content of 52 - 58% in PUD soft segment. The study also explores the potential of blending bio-base polyol with conventional petro-based polyester. A soy-polyol, (polyether polyol type), with controlled molecular weight and functionality, has been synthesized from epoxidized soy fatty acid methyl ester (ESFAME). A series of PUDs has been prepared containing up to 58% bio-based content. For comparison, a conventional PUD based on polyester-diol has also been prepared with comparable soft segment / hard segment ratio. PUDs, based on a blend of polyester-diol and soy-polyol is also prepared to investigate their compatibility and to study their performance. Besides basic physical and mechanical properties, coatings are evaluated for their hydrophobicity, by measuring water contact-angle of coating surfaces and corrosion resistance properties of their films on steel panels.

## **5.3 Experimental**

### **5.3.1 Raw Materials**

Epoxidized Soy Fatty Acid Methyl Ester (ESFAME) was procured from Arkema (Vikoflex-7010, % oxirane content = 7), and used without any purification. Dimethylolproprionic acid was procured from Perstorp (Bis-MPA). Isophorone diisocyanate (IPDI), ethylenediamine (EDA), triethylamine (TEA), 48% fluoroboric acid in water, N-Methyl-2-pyrrolidone (NMP), acetone and dibutyl tin dilaurate (DBTDL) were purchased from Sigma Aldrich, USA.

### 5.3.2 Synthesis of Soy – Polyol

250 g of ESFAME was placed into a 500 ml, 3-neck reaction flask attached with a mechanical stirrer, a pressure equalized dropping funnel, an inlet for dry nitrogen gas, and a thermometer probe. A 48% aqueous solution of fluoboric acid ( $\text{HBF}_4$ ), 1.49% by weight of ESFAME, was placed into a pressure equalized dropping funnel. Reaction flask was heated to  $40^\circ\text{C}$  and  $\text{HBF}_4$  solution was added slowly for 10-20 min. under gentle stirring, maintaining reaction temperature below  $70^\circ\text{C}$ . After the addition of  $\text{HBF}_4$  solution, the reaction was continued for 3 hours at  $40^\circ\text{C} \pm 3^\circ\text{C}$ , and the sample of reaction mixture was drawn and tested for %oxirane oxygen content (%OOC) as per ASTM D – 1652-04. Reaction was continued until %OOC dropped below 0.2%. Product was characterized for viscosity, Acid number and hydroxyl number (ASTM D 4274-05) and stored in air-tight glass jar. The product, soy-polyol was used for preparation of PUDs without further purification. Figure 5.1 shows simplified schematic reaction scheme for synthesis of soy-polyol from ESFAME.

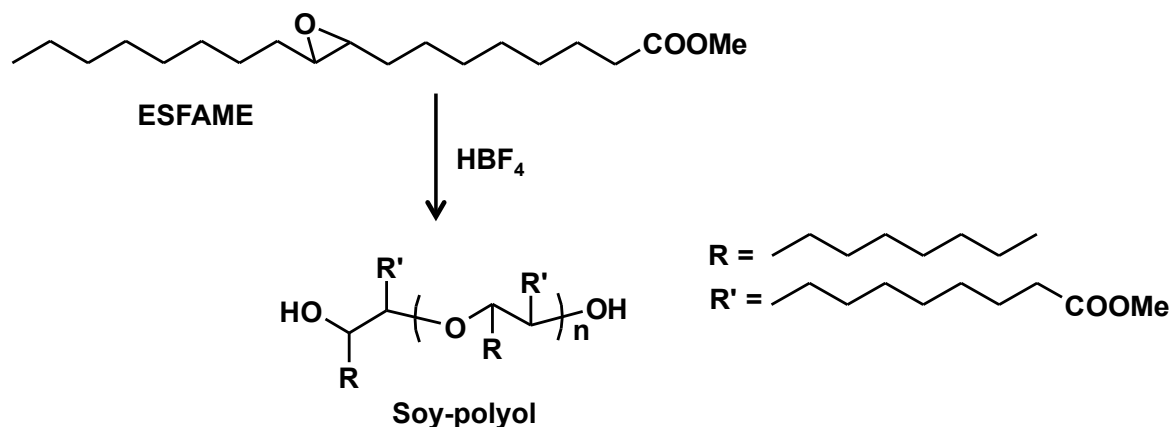


Figure 5.1: Schematic reaction scheme for synthesis of soy-polyol

### 5.3.3 Synthesis of Soy based Aqueous Polyurethane Dispersions

Into a 500 ml, 3-neck reaction flask attached with a mechanical stirrer, water-condenser, and nitrogen gas inlet / outlet, was placed dimethylolpropionic acid, soy-polyol, (standard polyester polyol where required), NMP (5% by wt. of final PUD). Reaction mixture was pre-mixed at 100°C under inert atmosphere for 10-15 minutes, until all DMPA was dissolved. Reaction temperature was then brought to 70°C at which point IPDI was added slowly from pressure equalized dropping funnel, for 10-15 minutes. DBTDL about 0.01% of pre-polymer amount was added into the reaction kettle before the addition of IPDI. Acetone (5% based on pre-polymer weight) was used to control the viscosity of pre-polymer. Reaction was continued until desired % isocyanate content (%NCO) was achieved. A sample of reaction mixture was drawn at each 30 minutes interval and tested for %NCO (ASTM D 2572-97 method). When desired %NCO was reached, reaction mixture was cooled to 50°C and then calculated amount of TEA (neutralizer) was added (degree of neutralization ~ 90%) and the mixture was stirred for 30 minutes. After neutralization of pre-polymer the heating was discontinued and the reaction mixture was brought to room temperature and transferred to 1000 ml plastic beaker.

The mixture was stirred under a high-speed disc disperser at 15000 rpm (Dispermat). D.I water containing ethylene diamine (chain extender) was added slowly for 4 minutes in a thin stream directed at the center of the impeller blade. When addition of water was completed, stirring was continued for additional 30 minutes. The white opalescent product was then transferred into a rotary vacuum evaporator and acetone was removed under vacuum at 40-45°C. When acetone removal was completed product was cooled to room temperature and stored in a glass jar. Figure 5.2 shows a simplified general reaction scheme for preparation of PUD based on soy-polyol.

As shown in Table 5.1, four polyurethane dispersions were prepared using a modified isocyanate pre-polymer process. PUD-1 is based on soy-polyol as the sole soft segment. PUD-2 is based solely on a standard commercial polyester-diol (OH# =230 mgs of KOH). PUD-3 used a combination (50% by weight each) of soy-polyol and std. polyester diol. PUD-1, PUD-2, and PUD-3 were prepared by keeping NCO/OH equivalent ratio of 1.5 for their isocyanate pre-polymers. PUD-4 is based solely on soy-polyol but it used NCO/OH of 1.25 for its pre-polymer to incorporate much higher amount of soft segment (and less chain extension). NMP solvent was used (at ~5% by wt. of final PUD) to facilitate processing. Acetone was also used to reduce solution viscosity of pre-polymers prior to their dispersion. All PUDs were formulated such that the acid number of their pre-polymers was 30 mgs of KOH/g. TEA was used as neutralizing amine and degree of neutralization of 100% was used for all the PUDs. All the PUDs so obtained were opaque to translucent dispersions and did not show any instability on accelerated storage test (incubation test for 6 weeks at 60°C).

Table 5.1: Composition of PUDs

<b>Identity</b>	<b>Polyol Type</b>	<b>Prepolymer NCO/OH mole ratio</b>	<b>Soft Segment (% by wt.)</b>	<b>Hard Segment (% by wt.)</b>
PUD-1	Soy-polyol	1.5	52.5	47.5
PUD-2	Std.Polyester diol	1.5	38.8	61.2
PUD-3	Soy-polyol+Polyesterdiol	1.5	43.9	56.1
PUD-4	Soy-polyol (low chain extender)	1.25	58.2	41.9



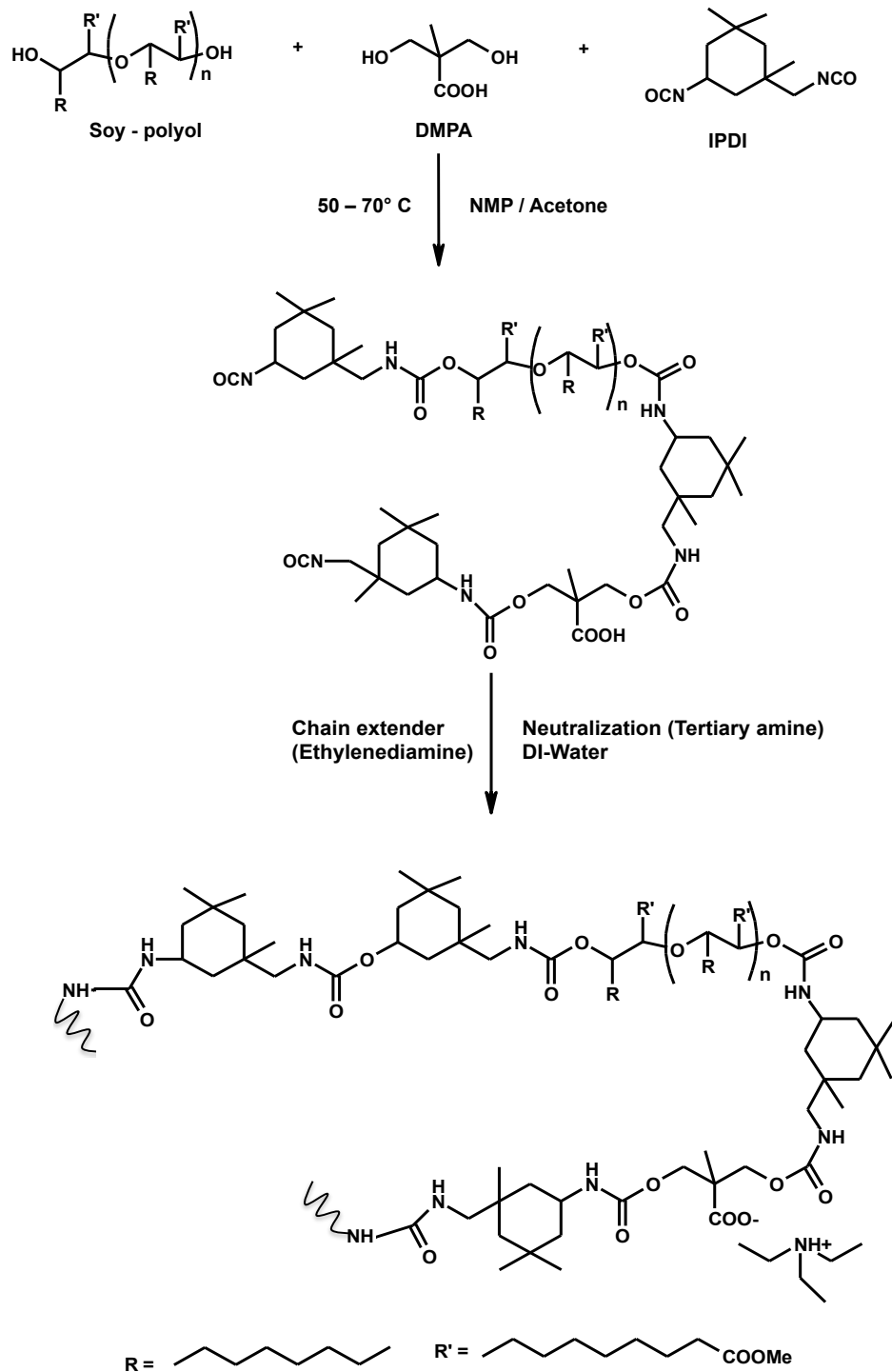


Figure 5.2: Schematic reaction scheme for synthesis of Bio PUD

## 5.4 Results and Discussion

### 5.4.1 Characterization of Soy-Polyol

The oligomerization reaction was monitored by following % oxirane content as well as by FTIR spectroscopy, which showed a decrease in the absorption centered at  $836\text{ cm}^{-1}$ , corresponding to an oxirane ring, and finally disappeared. An increase in the absorption at  $1088\text{ cm}^{-1}$  (C-O-C ether) and in the broad band around  $3400\text{ -}3500\text{ cm}^{-1}$  (O-H hydroxyl group) was also noticed. This indicated that oxirane ring opening took place to form ether linkages and formation of hydroxyl groups. Figure 5.3 presents FT-IR spectrum for soy-polyol. The resulted soy-polyol was clear, yellow, viscous oil, having –OH number 88 (mgs of KOH per g), viscosity 6200 cPs (at  $25^\circ\text{C}$ ), hydroxyl equivalent wt. of 637.5 g. The number average molecular weight of polyol was 1517 g/mole (GPC) with polydispersity index of 6.04.

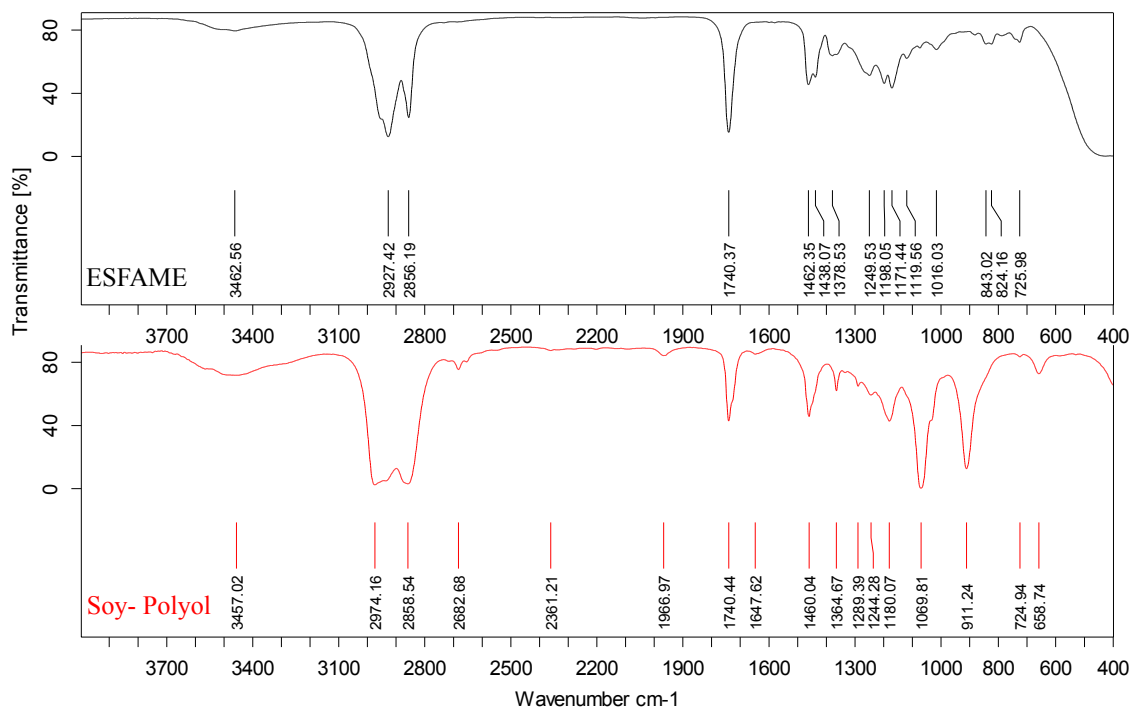


Figure 5.3: FT-IR Characterization of ESFAME & Soy – Polyol

#### 5.4.2 Film properties of PUDs:

Table 5.2 shows film properties of PUDs casted on steel panels. All properties were tested after 168 hours of drying under ambient conditions. Comparison of film properties PUD-1 (Soy-polyol) and PUD-2 (polyester polyol) shows significant difference in their pendulum hardness, and impact resistance properties. The PUD-2 has higher impact resistance and greater pendulum hardness, due to the short chain polyester structure (hard structure) as soft segment. The lower impact resistance and pendulum hardness of PUD based on soy-polyol (PUD-1) might be due to the longer flexible polyether chains in the soft segment. Also, the % hard segment in PUD-2 is higher than that of PUD-1, contributing to the hardness of the former. PUD-3, containing a blend of soy-polyol and polyester diol, has comparable properties with that of PUD-1 but with slightly improved toughness, perhaps due to stronger polar inter-chain interactions in polyester. The glass transition temperature  $T_g$ , measured by DSC, of PUD-3 (20.3 °C), that is intermediate to that for PUD-1 (18.5°C) and PUD-2 (23.68°C), indicating good compatibility of soy-polyol and polyester diol. The  $T_g$  results appear to be consistent with the results of pendulum hardness as well as hardness measured by nano-indentation test. Comparison of films of PUD-1 and PUD-2 indicates that relatively rigid polyester segment is responsible for higher  $T_g$ , and hence hardness and impact resistance compared to, much flexible soy-polyol (polyether) segment. This observation is consistent with flexible structure of hyper-branched soy-polyol and presence of C-O-C linkages. PUD-4 is based on soy-polyol and has significantly higher (58.2%) soft segment content compared to PUD-1. As one would expect, pendulum hardness and pencil hardness of its film is much poorer compared to PUD-1. Significantly lower  $T_g$  of PUD-4 is consistent with its other film properties. Lower numbers for both direct and reverse impact can also be explained based on their very low  $T_g$  among other factors such as reduced hydrogen

bonding, which could not resist to rapid deformation to load greater than 90 lbs. inch. DSC thermogram showing Tg of all PUD films is shown in Figure 5.4. Adhesion of all the films is generally good, which is characteristic feature of polyurethane coatings.

Table 5.2: Film properties of PUDs

Identity	PUD-1	PUD-2	PUD-3	PUD-4
Description Based on Soft Segment	Soy-polyol	Std.Polyester diol	Soy-polyol + Polyester diol	Soy-polyol (low chain extender)
Pendulum Hardness	106 (97)	196 (154)	101 (73)	43 (35)
Pencil Hardness	2H	2H	2H	3B
Impact Resistance (lbs.inch)				
Direct	120	160	140	90
Reverse	120	140	120	80
Cross-cut Adhesion	5B	5B	4B	5B
Tg (by DSC) °C	18.5	23.6	20.3	-28.6

### 5.4.3 Effect of soy-polyol content on hydrophobicity:

Soy-polyol, due to its chemical structure comprising of non-polar aliphatic fatty acid chains and presence of C-O-C ether linkages is expected contribute hydrophobic character to PUD films. Water-contact angle measurement is a good measure of surface hydrophobicity of coatings. PUD films with varying soy-polyol content were characterized for static water-contact angle measurements. Table 5.3 shows water-contact angles (averages of 5 results with accuracy of  $\pm 1^\circ$ ) of all PUD films. The results clearly show that for PUD-1 through PUD-3, as soy-polyol content in the film increases, surface hydrophobicity of their films increases as indicated by increase in their water-contact angles. For PUD-4, however, despite much higher soy-polyol content its water-contact angle is comparable to that of PUD-1. This indicates that there exists a maximum hydrophobicity achievable at a critical amount of soy- polyol, above which no further increase is observed. Hydrophobicity of polymer is also known to influence the average particle

size of their aqueous dispersion.<sup>15</sup> As shown in Table 5.3, and graphically in Figure 5.5, for PUD-1 through PUD-3, as soy-polyol content increases the particle size of their dispersion increases. Thus, there appears to be a good correlation between hydrophobicity of polymer and particle size of their dispersion. PUD-4 however shows much lower particle size despite its higher soy-polyol content. This can be attributed to its lower molecular weight, because of lower amount of chain extender amine content, resulting from NCO/OH =1.25 of its pre-polymer compared to that of 1.5 for PUD-1 through PUD-3.

PUD films were also subjected to water-resistance test. The results of water resistance test clearly corroborate with hydrophobicity of the films. Water-resistance test was performed in accordance with ASTM-D 870-02. The prepared coating samples were immersed in water for 24hrs followed by visual rating. The results of water resistance and acid-resistance tests are reported in Table 5.3. Figure 5.5 presents photographic images of films of PUD-1 through PUD-3, water-contact angle and average particle size. As can be seen in Figure 5.6, PUD-1 based on soy-polyol show excellent water resistance properties compared to PUD-2 films that is based on polyesters. As expected, PUD-3 shows moderate water resistance. Poor performance of PUD-2 can be attributed to the presence of significant number of hydrolysable ester groups, and lower hydrophobicity of their films. Acid resistant of coating was evaluated by using 10% sulphuric acid solution. Several drops of about 50 $\mu$ l of 10% sulphuric acid solution were placed along the length of the panel. Then the uncovered acid drops were observed after 5 hours. The rating was assigned according to the nature of failure of cured coating film.

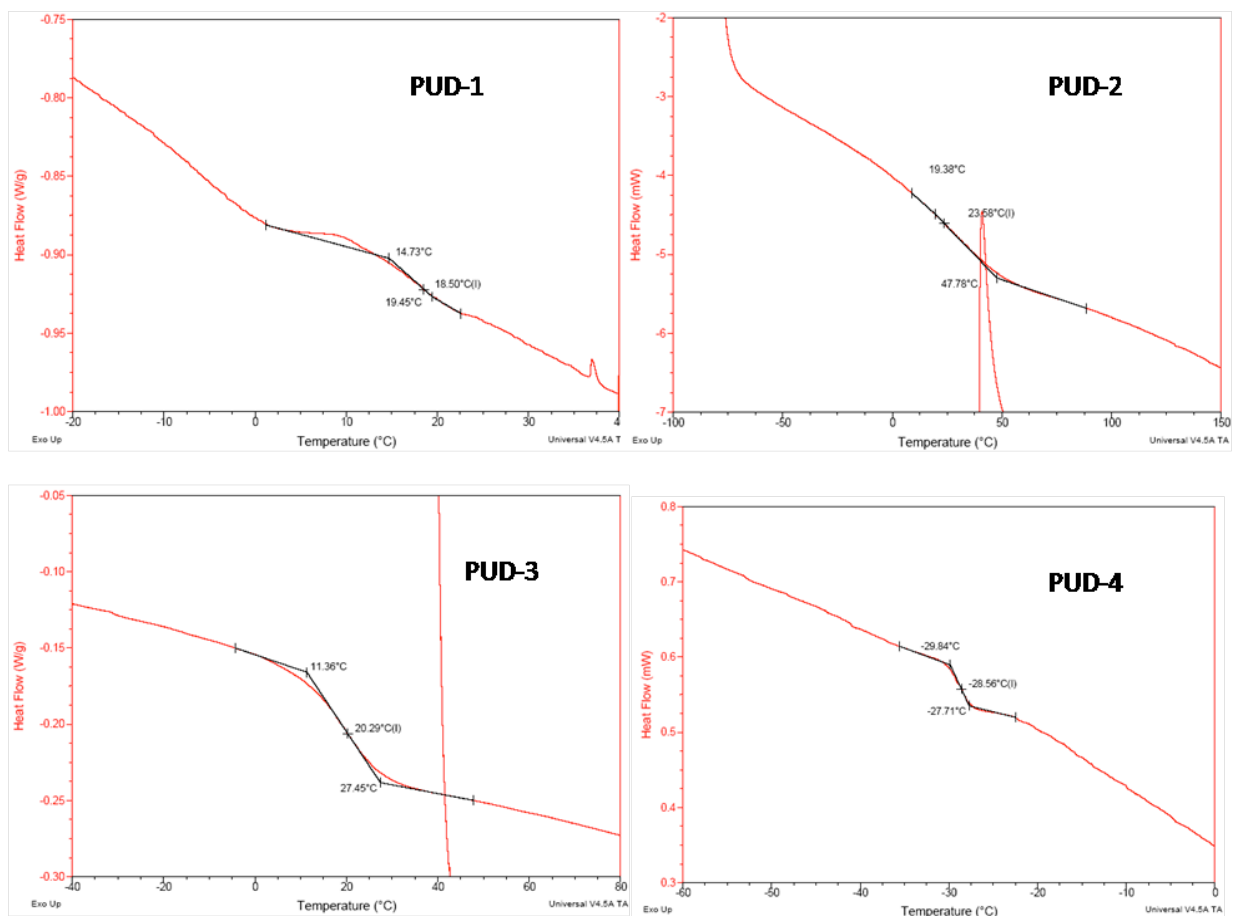


Figure 5.4: DSC thermograms showing Tgs for PUDs

Table 5.3: Characteristics of PUD and their films

Identity	Polyol Type	Soy-polyol Content (% by weight)	Water Contact Angle (degree)	Particle size (nm)	Water resistance	Acid resistance
PUD-1	Soy-polyol	52.5	84	194.4	5	4
PUD-2	Std.Polyester diol	0	78	24.5	0	4
PUD-3	Soy-polyol+Polyesterdio	22	80	33.7	3	4
PUD-4	Soy-polyol (low chain extender)	58.2	83	79.5	3	4

\*test ratings on 0=5 scale, 5 - unaffected, 4 - slight color change, 3 - moderated blushing & color change, 2 - complete color change, 1 - completecolor change & blushing, 0 - complete failure

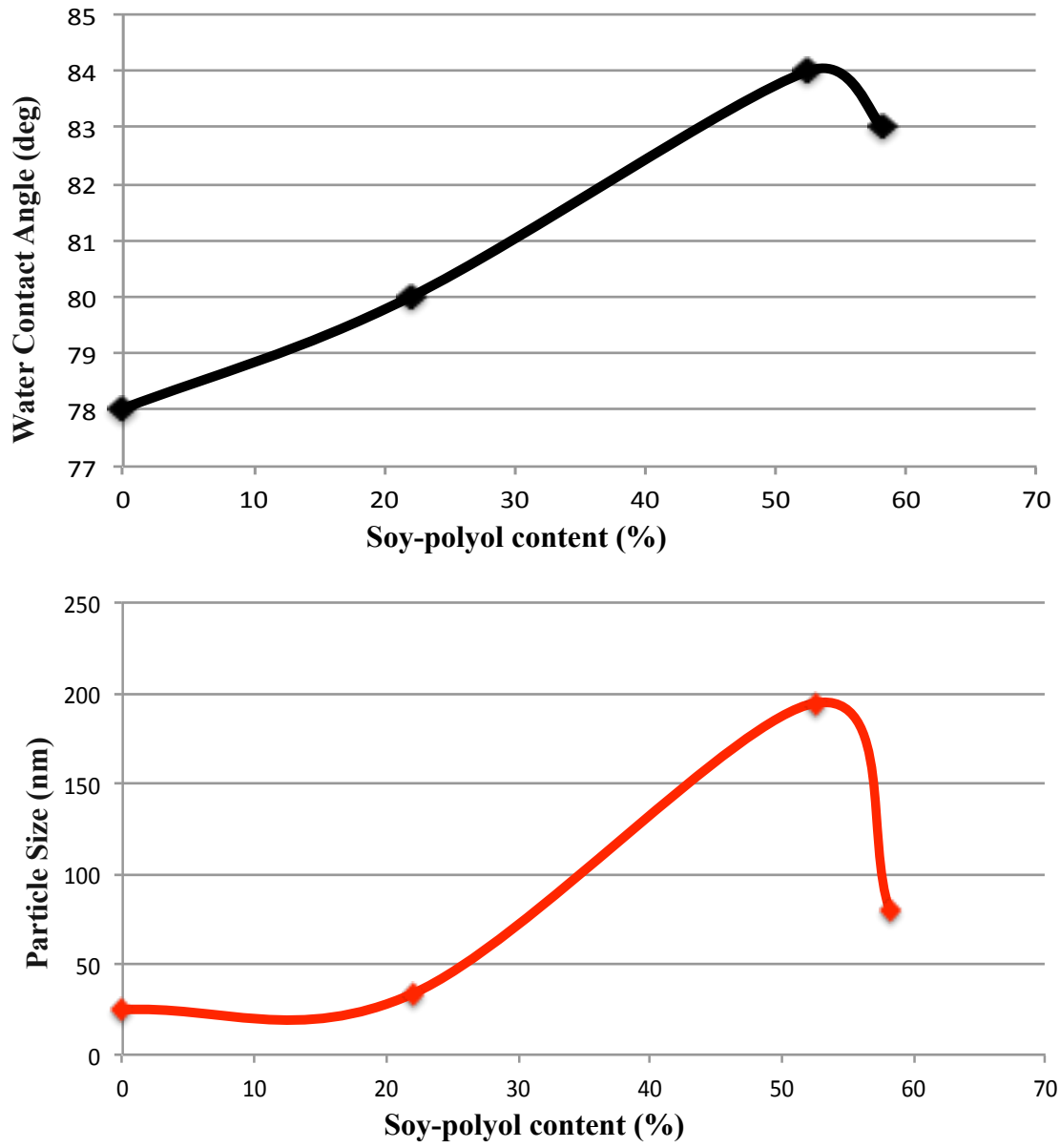


Figure 5.5: Effect of soy-polyol content on water-contact angle and dispersion particle size.

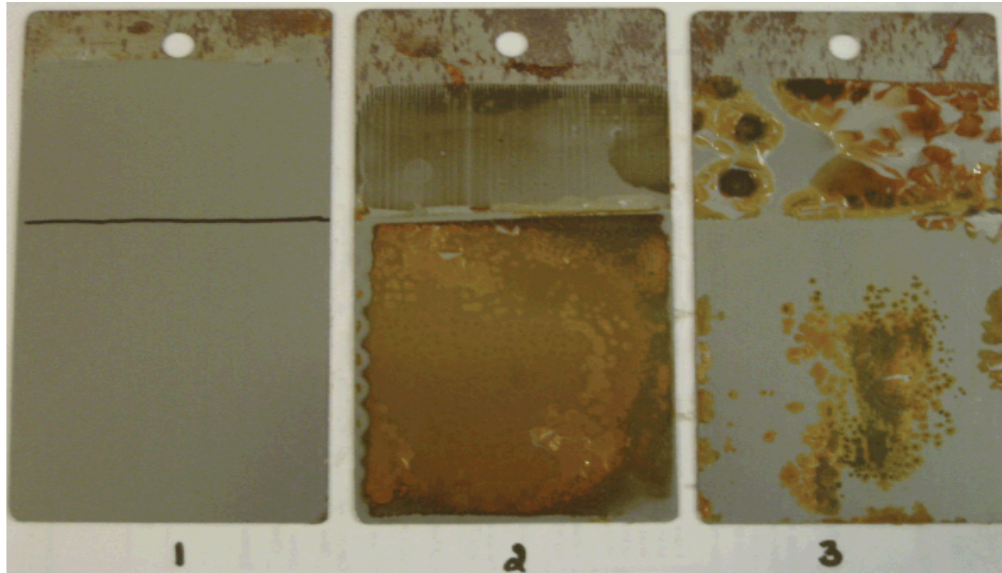


Figure 5.6: Water Resistance Test (1) PUD-1 (2) PUD-2 and (3) PUD-3 after immersion

#### 5.4.4 Nano-indentation test

The surface mechanical properties (modulus and hardness) of the PUD films have been studied by nano-indentation test and the obtained results were shown in Table 5.4. In this test, a nano-indenter tip indents the surface with a predetermined load, *i.e.* to a predetermined depth, in 15 seconds, hold at the load for 30 seconds to observe visco-creep, if any, and then unload in 15 seconds. Based on the indentation curve, the hardness and elastic modulus can be calculated. For all samples, a sufficient load was gradually applied to reach penetration depth of 2000 nm, and the corresponding modulus and hardness were calculated. Table 5.4 shows results of nano-indentation study and Figure 5.7 shows indentation curves for each PUD sample. For all four samples, the difference in maximum load can be clearly observed when reaching the same depth of 2000 nm.

In PUDs containing NCO/OH mole ratio 1.5 (PUD-1 - PUD-3), hardness increases with decreasing soft segment of PUD backbone. This might be due to the amount of tough urethane-



urea linkages presence in the PUD chemical structure. PUD-2 with only short chain rigid polyester as soft segment has high modulus and hardness. It is interesting to note that PUD-4 shows high modulus and hardness compared to PUD-1, despite higher soft segment content.

Table 5.4: Surface Mechanical Properties of PUD films

Identity	Polyol Type	Prepolymer NCO/OH mole ratio	Soft Segment (% by wt.)	Modulus (Gpa)	Hardness (Mpa)
PUD-1	Soy-polyol	1.5	52.5	0.911	36.2
PUD-2	Std.Polyester diol	1.5	38.8	4.44	238.6
PUD-3	Soy-polyol+Polyesterdiol	1.5	43.9	1.048	34.4
PUD-4	Soy-polyol (low chain extender)	1.25	58.2	1.526	62.5

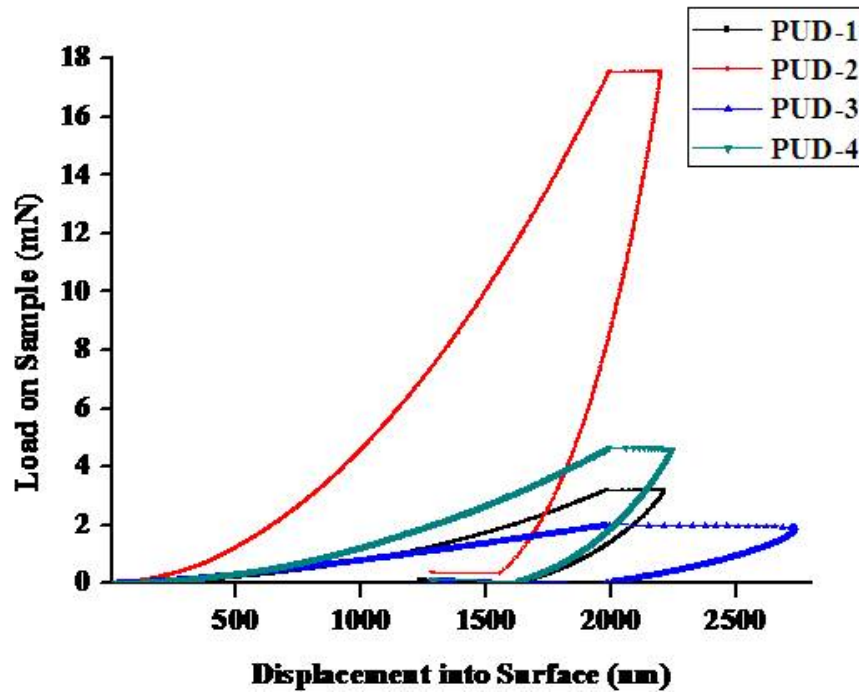


Figure 5.7: Nano-indentation test –indentation curves for PUDs

## **5.5 Conclusion:**

This study demonstrates a sustainable technology for utilization of bio-based resources for development of advanced polymeric coating materials with >50% bio-based content. The study shows that it is possible to synthesize polymeric polyol with controlled functionality and molecular weight, from ESFAME. Such soy-polyols are suitable as primary components in formulation of aqueous polyurethane dispersions for coating applications. PUDs based on soy-polyol demonstrate some very unique and desirable properties, such as the hydrophobicity of their films, with a number of potential applications. Further, it is possible to customize performance properties of PUDs using a combination of soy-polyol and commercially available polyesters polyols, for a broad range of potential commercial applications.

## **5.6 Acknowledgement:**

This research was funded by USDA Cooperative State Research Education, and extension Services (CSREES) through grant award no. 2009-38303-05085 to Prof. Mannari. Authors wish to thank Arkema Inc. for providing VIKOFLEX-7010, the key raw materials for this study. We also thank Mr. Sen Song, PhD candidate at Coatings Research Institute for his assistance with nano-indentation tests.

## 5.7 References:

1. Zhang, L. Jeon, H. K.; Malsam, J.; Herrington, R.; Macosko, C. W. *Polymer* 2007, 48, 6656–6667.
2. Liaw, D.-J.; Lin, S.-P.; Liaw, B.-Y. *J. Polym. Sci., Part A: Polym. Chem.* 1999, 37, 1331–1339.
3. Liaw, D.-J.; Huang, C.-C.; Liaw, B.-Y. *Polymer* 1998, 39, 3529–3535.
4. Liaw, D.-J. *J. Appl. Polym. Sci.* 1997, 66, 1251–1265.
5. Baron, A.; Rodriguez-Hernandez, J.; Papon, E. *Macromol. Chem. Phys.* 2005, 206, 2381–2389.
6. Wei, X.; Yu, X. *J. Appl Polym Sci Part B: Polym Phys* 1997, 35, 225.
7. Lee, S. Y.; Lee, J. S.; Kim, B. K. *Polym. Int.* 1997, 42, 67–76.
8. Chiellini, E.; Cinelli, P.; Corti, A. Graziani, M., Fornasiero, P., Eds.; CRC Press: Boca Raton, FL, 2007; pp 63-112.
9. Meier, M. A. R.; Metzger, J. O.; Schubert, U. S. *Chem. Soc. ReV.* 2007, 36, 1788–1802.
10. Williams, C. K.; Hillmyer, M. A. *Polym. ReV.* 2008, 48, 1–10. (1.)
11. M. Eissen, J.O. Metzger, E. Schmidt, and U. Schneidewind, *Angew. Chem. Int. Ed.*, 41, 414 (2002).
12. U. Biermann, W. Friedt, S. Lang, W. Luhs, G. Machmuller, J.O. Metzger, M.R. Klaas, H.J. Schafer, and M.P. Schneider, *Angew. Chem. Int. Ed.*, 39, 2206 (2000).
13. H. Baumann, M. Buhler, H. Fochem, F. Hirsinger, H. Zoebelein, and J. Falbe, *Angew, Chem. Int. Ed. Engl.*, 27, 41 (1988).
14. Guo, A.; Cho, Y.; Petrovic', Z. S. *J. Polym. Sci., Part A: Polym. Chem.* 2000, 38, 3900–3910.

- 15 Petrovic', Z. S.; Guo, A.; Zhang, W. *J. Polym. Sci., Part A: Polym.Chem.* 2000, 38, 4062–4069.
- 16 Lligadas, G.; Ronda, J. C.; Galia', M.; Ca'diz, V. *Biomacromolecules* 2007, 8, 686–692.
- 17 Kong, X. H.; Narine, S. S. *Biomacromolecules* 2007, 8, 2203–2209.
- 18 Suresh Subramanian, Bedri Erdem, Jeff Anderson, Jihui Guo, Mike Kaufman, and Jeff Schneider, Third International Coating wood ACSeries Conference, Sept. 2009 .
- 19 Petrovic', Z. S.; Guo, A.; Javni, I.; Cvetkovic', I.; Hong, D. P. *Polym. Int.* 2008, 57, 275–281.
- 20 Petrovic', Z. S.; Zhang, W.; Javni, I. *Biomacromolecules* 2005, 6, 713–719.
- 21 Hou, C. T. *Adv. Appl. Microbiol.* 1995, 41, 1–23.
- 22 Petrovic', Z.S., *Polymer Reviews* (2008), 48(1), 109-155.
- 23 Lu, Youngshang, and Larock, R.C., *Biomacromolecules* 2008, 9, 3332-3340
- 24 Lligadas, G.; Ronda, J. C.; Galia', M.; U. Biermann, Metzger, J.O., *Journal of Polymer Science: Part A: Polymer Chemistry*, Vol. 44, 634–645 (2006)
- 25 Bernquist H, James,D., Ekvall,K.,Wennerberg, P., and Sörensen, K., *RadTech Europe -2007*
- 26 Nanda AK, Wicks DA, Madbouly SA, Otaigbe JU. *Macromolecules* 2006; 39:7037.
- 27 Nanda AK, Wicks DA. *Polymer* 2006; 47, 1805.
- 28 Mannari, V. *Patent Application Publication No.* 13/396988, *Publication No.* 2012/0214938 A1, published on August 23,2012
- 29 Mannari, V.; Rengasamy, S.; Patel, C. *Paint & Coating Industry.* 2012, 28, 28-31.

## **Chapter 6: Hydrophobic and Oil-Resistant Coatings Based on Advanced Green Polyurethane Dispersions**

**Senthilkumar Rengasamy, Vijay Mannari**

*This chapter is published in Journal of Applied Polymer Science, (2013), 130, 3874 - 3884.*

© 2013 Wiley Periodicals, Inc. All rights reserved.

### **6.1 Abstract:**

In recent years, there have been significant interests among scientists around the world to design smart coatings that combine the standard desirable mechanical and chemical resistance properties with additional functionalities such as oil and water repellency, hydrophobicity, self-cleaning and gas barrier properties. In the present research work, advanced aqueous polyurethane dispersions (PUD) systems have been designed and developed using three different types of polyols as soft-segments. These polyols differ in their chemical structure, functionality, polarity and interfacial properties. The effects of soy based polyol, hydroxy-terminated perfluoropolyether and hydroxy-terminated polydimethylsiloxane – on various mechanical properties of their uncross-linked and cross-linked films, and more specifically on their hydrophobicity and oil-resistance (oleophobicity) have been studied. Hydrophobicity of these coatings has been characterized by their Dynamic Contact Angle (DCA) measurements and their oleophobicity by n-octane absorption method. The investigations showed that presence of fluorine and siloxane structures significantly improve the hydrophobicity and oil resistance of these coatings and it is possible to optimize these properties using suitable composition of PUDs.

## 6.2 Introduction:

Environmental legislations, depleting fossil resources and economic burdens have motivated industrial and academic researchers to develop renewable feedstock for sustainable development of environmental friendly coating, adhesive, sealant and elastomers.<sup>1,2</sup> For sustainable development and growth of such advanced material technologies, it is increasingly important to develop a platform of polymer building blocks based on renewable resources.<sup>3,4</sup> Vegetable and plant oils are important agricultural resources that are available at low costs. The unique combination of chemical structure, functionality, reactivity, low toxicity and biodegradability makes vegetable oils excellent resources for deriving sustainable polymers.<sup>3,5-7</sup> Using principles of green chemistry and through chemical transformations, it is possible to derive bio-based materials with significantly lower carbon footprint while meeting the high performance demands of application.<sup>5,8-13</sup>

A variety of soy-polyols, prepared from different synthetic routes, have been reported in the literature.<sup>10-21</sup> Polyurethanes prepared from these soy-polyols, replacing petro-based polyols, show interesting performance properties, besides their high bio-renewable contents.<sup>10,13-22</sup> Soy-polyols for use in polyurethane dispersions (PUD) require unique set of property requirements and hydroxyl functionality. In keeping with this, we developed a soy-polyol with low molecular weight and hydroxyl functionality of  $\sim 2.0$ , from epoxidized soy methyl esters, using a novel process.<sup>25-27</sup>

The polymeric binders for coating applications require customized bulk properties and surface, to meet the challenging demands during end-use applications. The bulk properties contribute to the coating's chemical resistance and mechanical properties, such as film toughness, hardness, flexibility, and thermal properties such as glass transition temperature and

thermal stability. Whereas surface properties control such attributes as water repellency, oil repellency, hydrophilicity, besides many more. Control over surface properties are important, to ensure better performance of materials in many engineering and scientific applications.<sup>28-31</sup> It has been well established that wettability of solid surface is governed by both surface free energy (surface chemical composition) and topographical microstructure of coating surface. Coatings with high water and oil repellency is very important because of myriads of such industrial applications such as oil water separations, anti-reflection, printing, and anti-bio adhesion.<sup>32-38</sup>

In this present research work, we have developed novel hydrophobically modified polyurethane dispersions to study their mechanical properties, water-repellency and oil-resistance. The PUDs have been prepared with bio-based soft-segments (bio-PUD) using a novel hyper-branched soy polyol derived from epoxidized soy fatty acid methyl ester. Soy-polyol was synthesized by following our earlier research work.<sup>25-27</sup> The polyurethane architecture has been modified by the incorporation of perfluoropolyether and/or polydimethyl siloxane (PDMS) moieties as hydrophobizing structures in varying proportions. The effect of these modifications on various mechanical properties, water and oil resistance properties of their cross-linked and un-crosslinked films are reported. The study shows that it is possible to optimize mechanical properties (bulk), water and oil-resistance (surface) using suitable polymer compositions.

## **6.3 Experimental:**

### **6.3.1 Raw materials:**

Soy polyol was derived from epoxidized soy fatty acid methylester (ESFAME) which was procured from Arkema, USA under trade name of Vikoflex 7010, polydimethylsiloxane based polyol (PDMS polyol) was obtained from Siltech Corporation, Canada under the trade name of Silmer OH-Di-10 and perfluoropolyether polyol (Fluoro polyol) was purchased from Solvay

Solexis, Inc, USA as fluorolink D10/H. All three polyols were used to build a soft segment of aqueous PUD. Desmodur I, the trade name of Isophorone diisocyanate (IPDI) was received from Bayer Material Science, USA and dimethylolpropionic acid (DMPA) from Geo Specialty Chemicals, USA were used as procured. All other raw materials such as triethylamine (TEA) as neutralizing agent, ethylene diamine (EDA) as chain extender, N-methylpyrrolidone (NMP), acetone, dibutyltin dilaurate (DBTDL), 1,4 Butane diol, 48% tetrafluoroboric acid in water, were purchased from Sigma Aldrich, USA and used as received. The carbodiimide based crosslinker carbodilite SV-02, a product of Nisshinbo was procured from GSI Exim America. Inc.

### **6.3.2 Standard Testing Methods:**

Intermediates, products and coatings were characterized using ASTM methods where applicable; % oxirane content (ASTM D-165297), Acid number (ASTM D-1639-96), hydroxyl number (ASTM D - 4274-05), Pencil hardness (ASTM D – 3363), impact resistance (ASTM D - 2794-99), Adhesion (cross-cut) test (ASTM D - 3359-02), MEK double rub test (ASTM D - 4752-98). Functional group characterization of Soy-polyol was done recording Fourier Transform Infrared (FTIR) spectra with Bruker Tensor 27 FTIR analyzer in the range of 400 - 4000  $\text{cm}^{-1}$  at room temperature and Brookhaven 90Plus particle size instrument was used to determine the particle size of PUD at 25°C.

### **6.3.3 Synthesis of soy-polyol (SP):**

A novel hyper-branched soy-polyol was derived from epoxidized soy fatty acid methyl ester (ESFAME) using a cationic ring-opening polymerization method developed by our research group earlier.<sup>25-27</sup> Figure 6.1 shows simplified schematic reaction scheme for synthesis of soy-polyol. Epoxy (oxirane) compounds can undergo acid-catalyzed cationic ring-opening polymerization reactions through oxiranium intermediates with the formation of polyether



chains<sup>13,25-27,39</sup> as shown in Figure 6.2. Soy-polyol was characterized for viscosity, Acid number (ASTM D -1639-96) and hydroxyl number (ASTM D 4274-05) and stored in airtight glass jar.

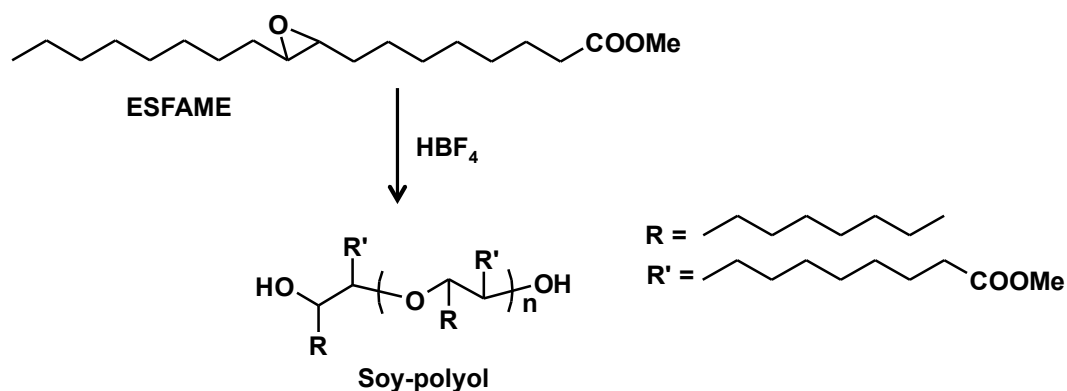


Figure 6.1: Schematic reaction scheme for synthesis of soy-polyol

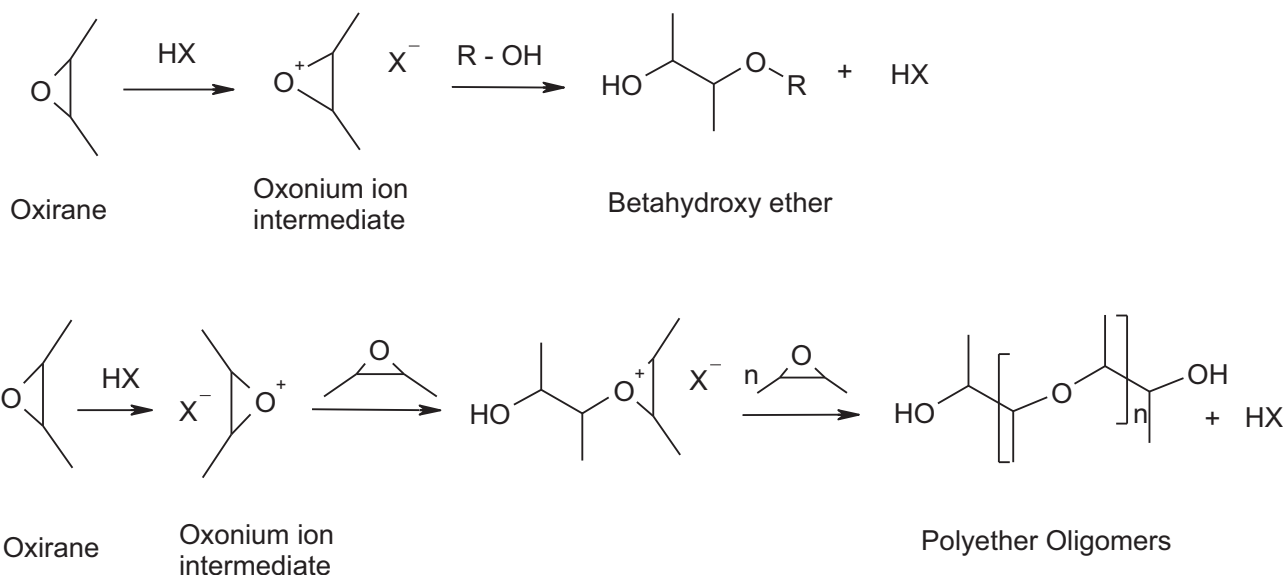


Figure 6.2: Cationic ring-opening polymerization of epoxy compound

#### 6.3.4 Synthesis of Green (bio)- PUD:

Calculated amount of Soy-polyol, NMP, DMPA and 1,4 butane diol were placed in a 3-neck flask connected with mechanical stirrer, water condenser, nitrogen inlet and outlet and heating mantle connected with temperature controller. Reaction was carried out at 100°C until DMPA was completely dissolved in polyol and NMP mixture. Then reaction temperature was cooled down to 80°C at which point IPDI was slowly added in to the reaction mixture in the

presence of DBTDL catalyst. Every 30 minutes a sample of reaction mixture was drawn and tested for % isocyanate content (ASTM D 2572-97). When desired % isocyanate content was reached, reaction mixture was cooled down to 55°C and calculated amount of triethylamine (neutralizer) was added (degree of neutralization ~ 90%) and the mixture was stirred for 30 minutes. Immediately after neutralization, pre-polymer was transferred to high-speed disperser (HSD) to extend the pre-polymer chain with EDA and further dispersed with de-ionized water. Table 6.1 shows composition of PUDs used in present study. Figure 6.3 shows the general reaction scheme for synthesis of bio-PUD.

Table 6.1: Composition of Green PUDs

<b>PUD Composition &amp; Characteristics</b>	<b>Bio PUD 1</b>	<b>Bio PUD 2</b>	<b>Bio PUD 3</b>
Soy-Polyol (moles)	0.018	0.026	0.050
1,4-Butane diol (moles)	0.026	0.010	0.000
DMPA (moles)	0.030	0.038	0.065
IPDI (moles)	0.108	0.111	0.174
EDA (moles)	0.031	0.032	0.050
NMP (% based on final dispersion)	6.0	6.0	6.0
Pre-polymer NCO/OH (Equivalent weight ratio)	1.40	1.40	1.40
% Neutralization	90	90	90
Acid value (mgKOH/g)	30.0	30.0	30.0
Soft Segment (SS) (% by weight)	45.0	55.0	60.0
Hard Segment (HS) (% by weight)	55.0	45.0	40.0

### 6.3.5 Synthesis of Hydrophobically modified Bio-PUDs:

The surface chemistry of the green PUDs (bio-PUDs) were modified by incorporating

silicone and fluorine groups into the backbone of polyurethane soft segment. These PUDs are called as hydrophobic PUDs. For these PUDs, the soft segment content was kept constant at 55% since at this level bio-PUD-2 showed balanced properties. The hydrophobic PUDs were synthesized by using the same procedure that was followed for the bio-PUDs. Table 6.2 shows the compositions and some important parameters of hydrophobic PUDs prepared for this study. Following Figure 6.4 represents schematic reaction of the hydrophobic PUD.

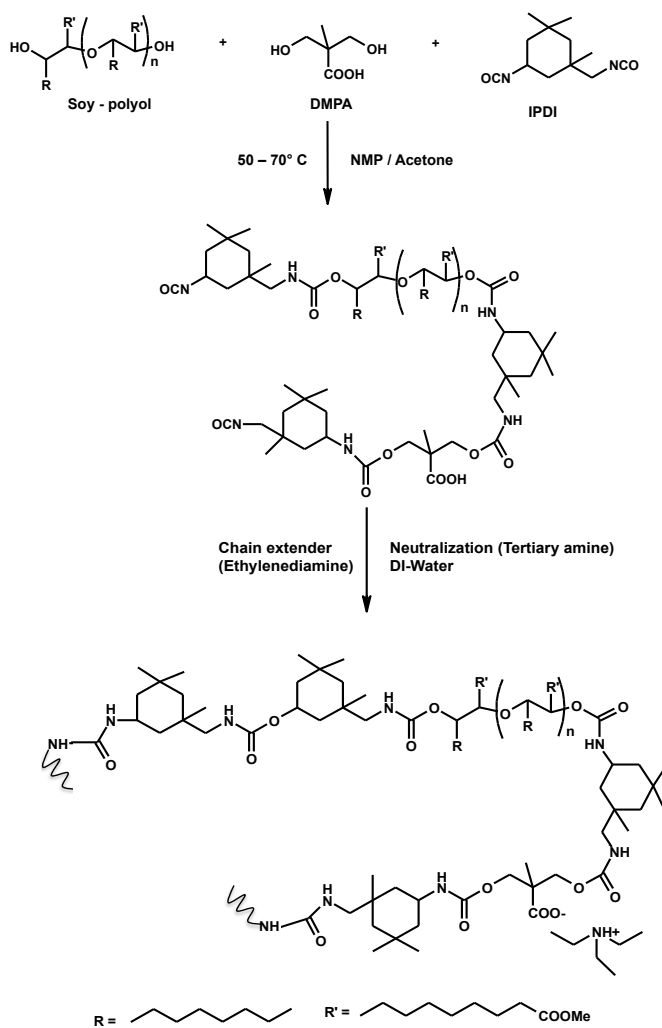


Figure 6.3: Schematic reaction scheme for synthesis of Bio PUD

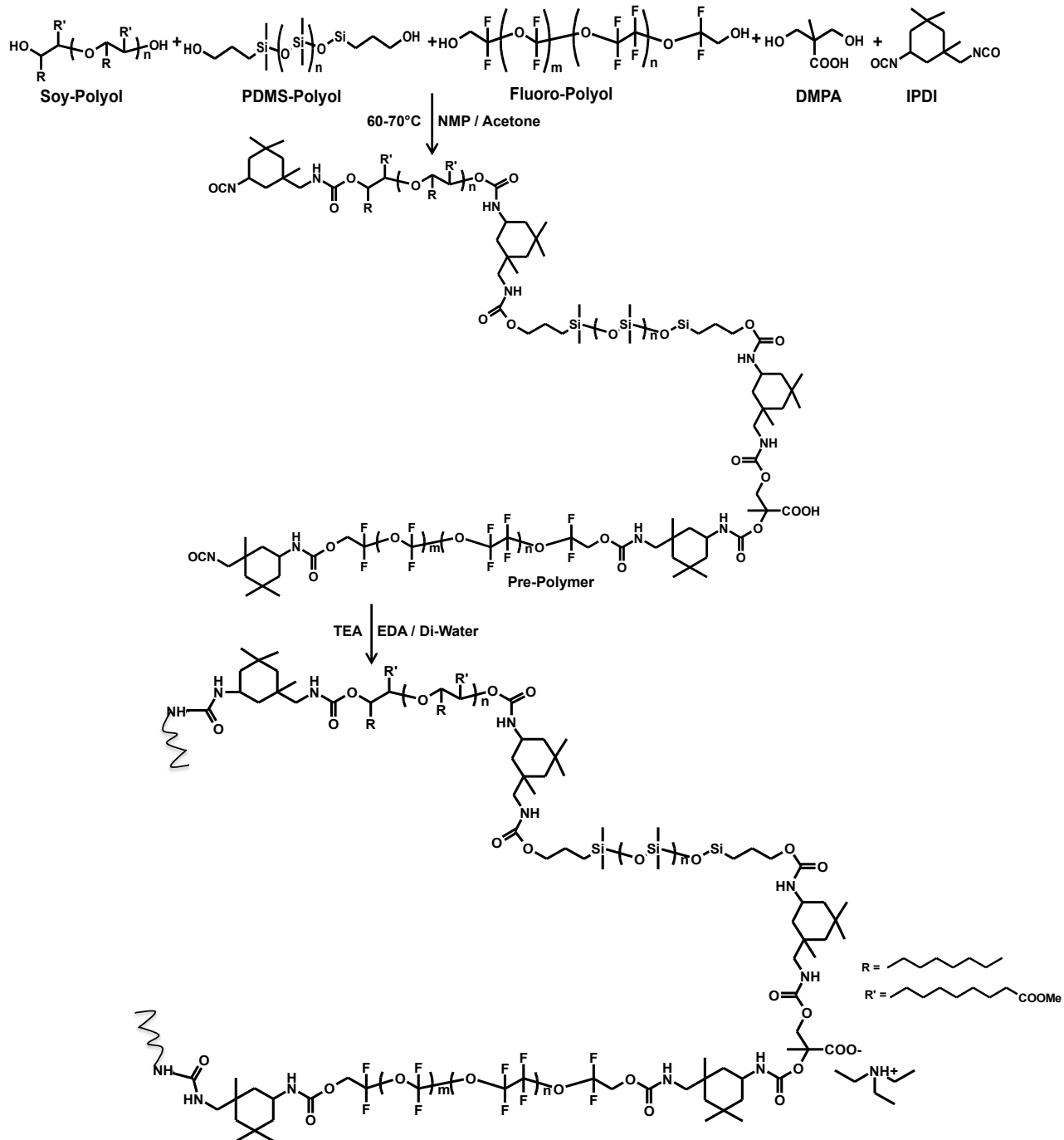


Figure 6.4: Schematic representation of hydrophobic PUDs with three different polyol polymeric chain backbone.

Table 6.2: Compositions of Hydrophobic PUDs

PUD Composition & Characteristics		55B	55Si	55F	Surface Chemical Modified PUD					
					30B 25Si	30B20 Si5F	30B15 Si10F	30B10Si 15F	30B5Si2 0F	30B 25F
Soy-polyol (Mw =1517g/mole)		0.026m	0	0	0.012m	0.012m	0.012m	0.012m	0.012m	0.012m
PDMS polyol (Mw =1000g/mole)		0	0.026m	0	0.016m	0.012m	0.009m	0.006m	0.003m	0
Fluoro polyol (Mw =1539g/mole)		0	0	0.013m	0	0.002m	0.004m	0.012m	0.008m	0.010m
1,4 Butane diol (Mw = 90 g/mole)		0.01m	0.001m	0.009m	0.006m	0.007m	0.008m	0.009m	0.010m	0.011m
DMPA (Mw =134.13g/mole)		0.038m	0.025m	0.019m	0.033m	0.032m	0.031m	0.031m	0.032m	0.031m
IPDI (Mw = 222g/mole)		0.111m	0.076m	0.056m	0.098m	0.095m	0.093m	0.093m	0.094m	0.092m
EDA (Mw =60g/mole)		0.032m	0.020m	0.014m	0.025m	0.024m	0.024m	0.026m	0.024	0.023m
Soft Segment Composition (%)	Soy – Polyol	55	0	0	30	30	30	30	30	30
	PDMS Polyol	0	55	0	25	20	10	15	5	0
	Fluoro Polyol	0	0	55	0	5	15	10	20	25
Pre-polymer NCO/OH (eq.wt)		1.40	1.40	1.40	1.40	1.40	1.40	1.40	1.40	1.40
% Neutralization		90	90	90	90	90	90	90	90	90
Acid value (mgKOH/g)		30	30	30	30	30	30	30	30	30
NMP (% based on final dispersion)		6	6	6	6	6	6	6	6	6
Soft Segment SS (% by weight)		55	55	55	55	55	55	55	55	55
Hard Segment HS (% by weight)		45	45	45	45	45	45	45	45	45

m = moles, eq.wt = equivalent weight ratio

## 6.4 Results and Discussion:

### 6.4.1 Characterization of Soy-polyol:

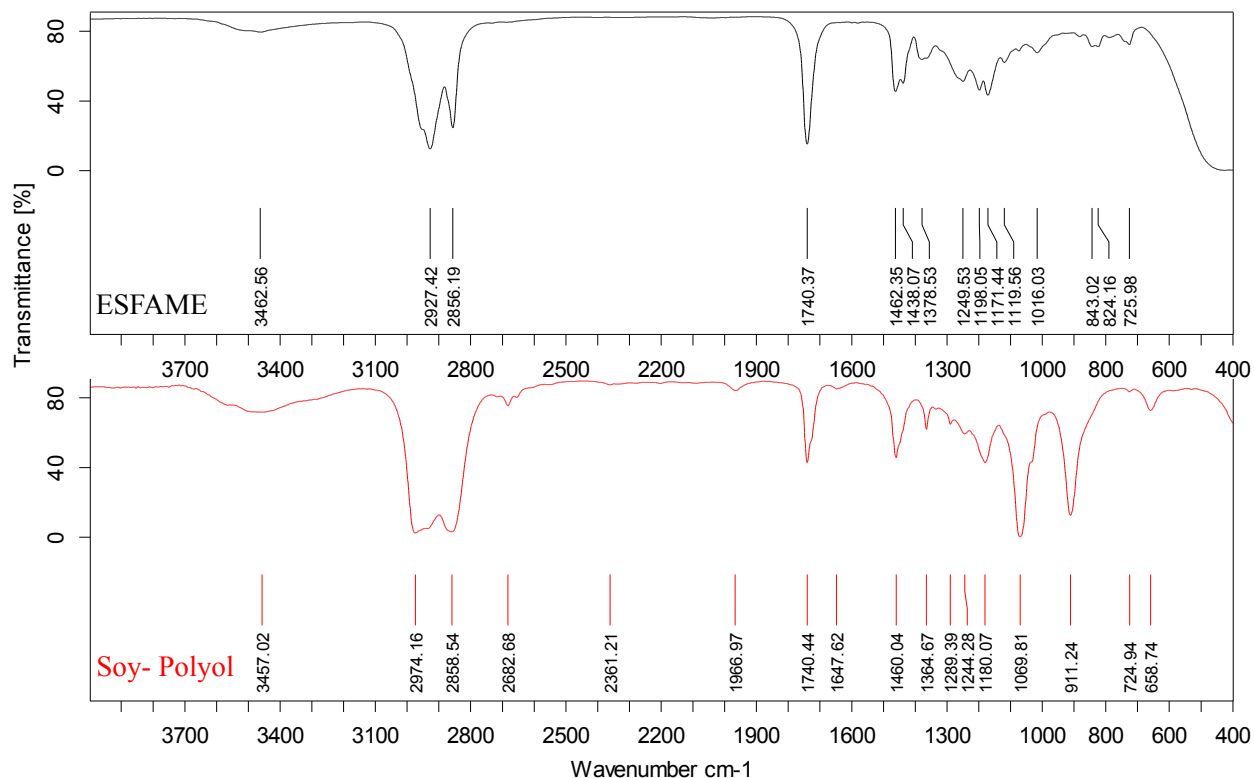


Figure 6.5: FTIR Characterization of ESFAME & Soy – Polyol

The oligomerization reaction was monitored by following % oxirane content as well as by FTIR spectroscopy, which showed a decrease in the absorption peaks of 824 cm<sup>-1</sup> and 843 cm<sup>-1</sup> corresponding to an oxirane ring, and finally disappeared. An increase in the absorption at 1070 cm<sup>-1</sup> (C-O-C ether) and in the broad band around 3400 -3500 cm<sup>-1</sup> (O-H hydroxyl group) was also noticed. This indicated that oxirane ring opening took place to form ether linkages and the formation of hydroxyl groups. Figure 6.5 presents FT-IR spectrum for soy-polyol. The resultant soy-polyol was a clear yellow viscous oil having –OH number 88 (mgs of KOH per g), viscosity 6200 cPs (at 25°C), hydroxyl equivalent weight of 637.5 g. The number average molecular weight of polyol was 1517 g/mole (GPC) with polydispersity index of 6.04.

#### 6.4.2 Characterization of Bio PUDs and their film properties:

Bio-PUDs wet films were applied onto cold-rolled steel panels using automatic drawdown applicator to yield coatings with  $\sim 40\mu$  dry film thickness. All coatings were cured at room temperature for 7-days before testing.

Table 6.3 shows film properties of various Bio-PUD coatings. A comparison of Bio-PUD 1, Bio-PUD 2 and Bio-PUD 3 shows that with increasing Soy-polyol (soft segment) content film hardness (both pencil and pendulum hardness) and glass transition temperature ( $T_g$ ) decreases. This is expected since increasing soy-polyol content would increase free-volume and flexibility. It follows that Bio-PUD 1 and Bio-PUD 2 shows better hardness for most applications while Bio-PUD 3 with 60% soft-segment gives coatings with very poor hardness. Impact resistance of Bio-PUD 1 is slightly lower than other two samples, indicating higher stiffness or brittleness due to higher “hard segment” content. All samples show excellent adhesion on steel substrate - characteristic of PU coatings.

Table 6.3: Characteristics of Bio PUDs and Their Film Properties

Bio - PUD Characteristics and Film Properties		Bio PUD 1	Bio PUD 2	Bio PUD 3
Pencil Hardness		4H	2H	3B
Koenig Hardness (seconds)		120	108	60
Cross Cut Adhesion		5B	5B	5B
Impact Resistance (lbs x inch)	Direct	100	160	160
	Reverse	60	160	160
Contact Angle (degree)		69	73	75
Average Particle Size (nm)		203	146	137
Stability (60 days @ 60°C)		Stable	Stable	Stable

### 6.4.3 Hydrophobic and water resistance characteristics of Bio-PUDs:

One of the outstanding properties of bio-PUD was excellent water-resistance. In order to study hydrophobicity of soy-polyol and its effect on water sensitivity of PUDs as function of their soy-polyol content, water-absorption test was carried out. Free-films of different bio-PUD samples were immersed in water for 24 hours and their water absorption values were recorded. Figure 6.6 shows images of bio-PUD samples before and after water immersion test. As can be seen, the appearance of samples just after water-immersion test has significantly changed; Bio-PUD 1 with lower soy-polyol content was completely opaque with 45% water absorption while Bio-PUD 3 showing fair degree of clarity with only 9% water absorption. This clearly shows remarkable hydrophobicity of coatings with higher soy-polyol content. The water-contact angle data for these PUD samples were consistent with these observations.

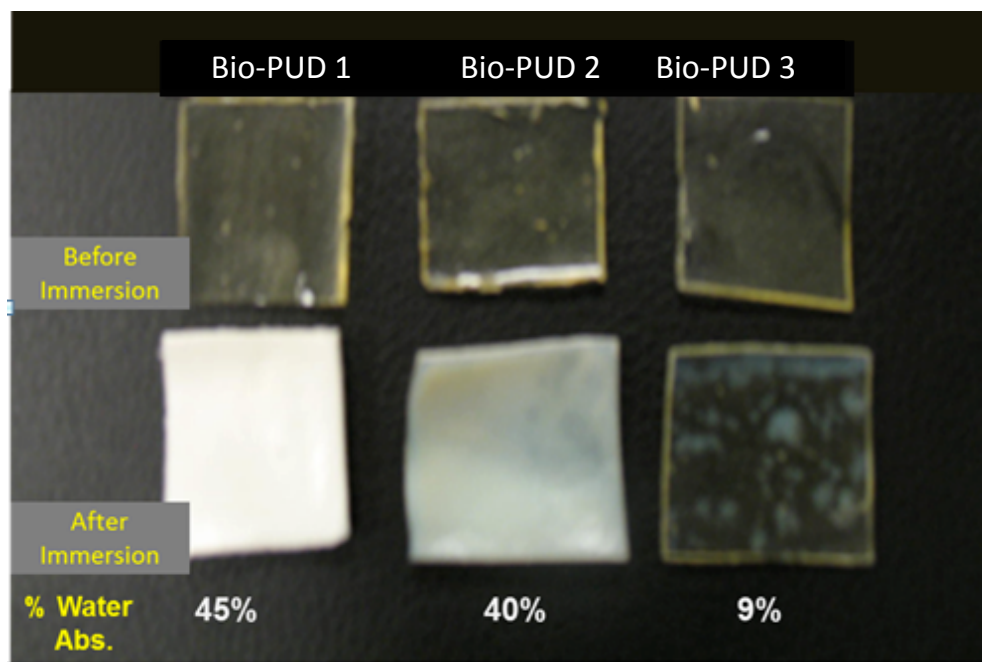


Figure 6.6: Water immersion test of Bio-PUD samples

Water resistance test was performed by immersion of coated steel panels in water at 30°C for 24 hours. Films were then evaluated by visual observation of delamination, rusting, adhesion



failure etc. As can be seen in Figure 6.7, Bio-PUD 2 and Bio-PUD 3 showed good resistance while Bio-PUD 1 showed very poor performance. With increasing soy-polyol content, there is improvement in corrosion resistance performance due to increasing hydrophobicity. We attribute relatively poor water-resistance of Bio-PUD 1 to the presence of more polar groups at the surface of coating. It should also be noted that with increasing soy-polyol content from 45% to 60%, there is corresponding reduction in urethane content and arguably, that may be a probable reason for increasing water resistance.

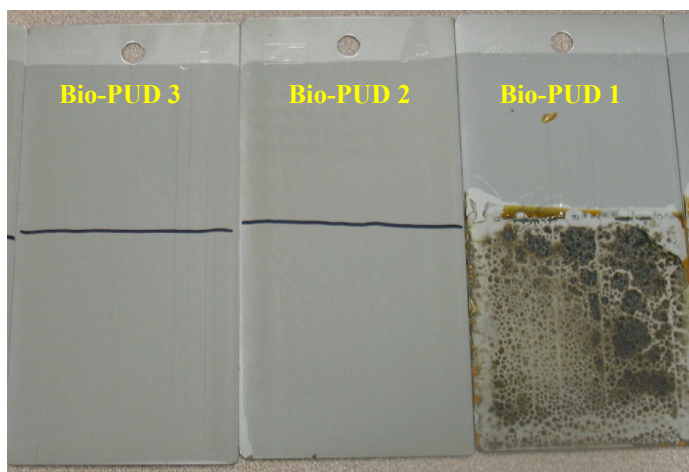


Figure 6.7: Water resistance test of Bio-PUD samples by 24 hours water immersion of steel panels in tap water

#### 6.4.4 Characterization of PUD film properties:

Table 6.4 shows the basic mechanical properties of uncross-linked hydrophobic PUDs prepared for this study. Coatings with dry film thickness of approximately  $35\mu\text{m}$  were applied on cold-roll steel panel and cured at room temperature. Films were tested for mechanical properties after one week of room temperature cure. As can be seen from the Table 6.4, incorporation of PDMS polyol in the soft segment (sample 30B25Si) decreased the pencil hardness from 2H to B. The decrease in pencil hardness, which is related to the modulus of the film, can be attributed to lower modulus of the film due to incorporation of low Tg PDMS.

Interestingly, Koenig hardness, which measures dampening property of coatings, is much higher with samples containing both PDMS polymer chains. We believe that this is due to higher hard-segment content in samples containing PDMS due to its lower molecular weight compared to that of soy-polyol. The resulting higher urethane group content is believed to be the reason for higher Koenig hardness of these films. Introduction of the fluoro-polyol backbone (sample 30B20Si5F) increased both pencil and Koenig hardness. Two factors might be at play here: (a) fluoro-polyols have high modulus (compared to PDMS polyol and soy-polyol) which will tend to increase pencil hardness of the film. (b) Also, in all fluoro-polyol based PUD formulation, it was necessary to use some amount of 1,4-butanediol (hard segment) in order to maintain soft segment / hard segment ratio to 55:45 for all PUD compositions. This resulted in increased hard segment content (1,4 butane diol based hard segment content) in 30B20Si5F, 30B15Si10F, and 30B10Si15F resulting in higher pencil and Koenig hardness.

The reduced impact resistance for both Si and F containing films (samples 30B25Si and 30B20Si5F) can be attributed to the possibility of micro phase separation in the film. It can be seen from Figures 6.8 and 6.9 that increasing amount of fluorinated polyol in polyurethane dispersion increases the nano-structured surface roughness (peaks) and changing the phase morphology respectively. Interestingly such phase contrast morphology was also showed in reference 43 with the help of microscopy images. Number of researchers<sup>40-46</sup> have shown that PDMS polyol and fluoro polyol contributes to phase separation and can affect impact resistance of their films. It is interesting, however, that the cross-cut adhesion was not affected by this possible phase morphology. This indicated minimal perturbation to the underlying coating layer of modified PUD. The increase in solvent resistance (MEK double-rub) for PUDs containing

siloxane and fluorine (compared to bio PUD) is because of the low swelling nature of siloxane and fluorine containing polymers to MEK.

Table 6.4: Mechanical Properties of uncross-linked Film Properties

Film Properties		55B	55Si	55F	Surface Chemical Modified PUD					
					30B2 5Si	30B20 Si5F	30B15 Si10F	30B10 Si15F	30B5 Si20F	30B2 5F
Pencil Hardness		2H	B	Very Poor Film Appearance	B	F	H	2H	Very Poor Film Appearance	Very Poor Film Appearance
MEK Double RUB		0	0		75	70	25	30		
Koenig Hardness (seconds)		49	91		133	136	128	148		
Cross Cut Adhesion		5B	5B		5B	5B	5B	5B		
Impact Resistance (lbs.in)	Direct	160	160		100	160	140	160		
	Reverse	160	160		40	40	80	40		
Average Contact Angle (°)		72	95	127	124	121	111			
Average Particle Size (nm)		146	34	143	88	98	102	110	126	135
Stability (60 days @ 60°C)		Stable	Stable	Settled after 20 days	Stable	Stable	Stable	Stable	Settled after 14 days	Settled after 17 days

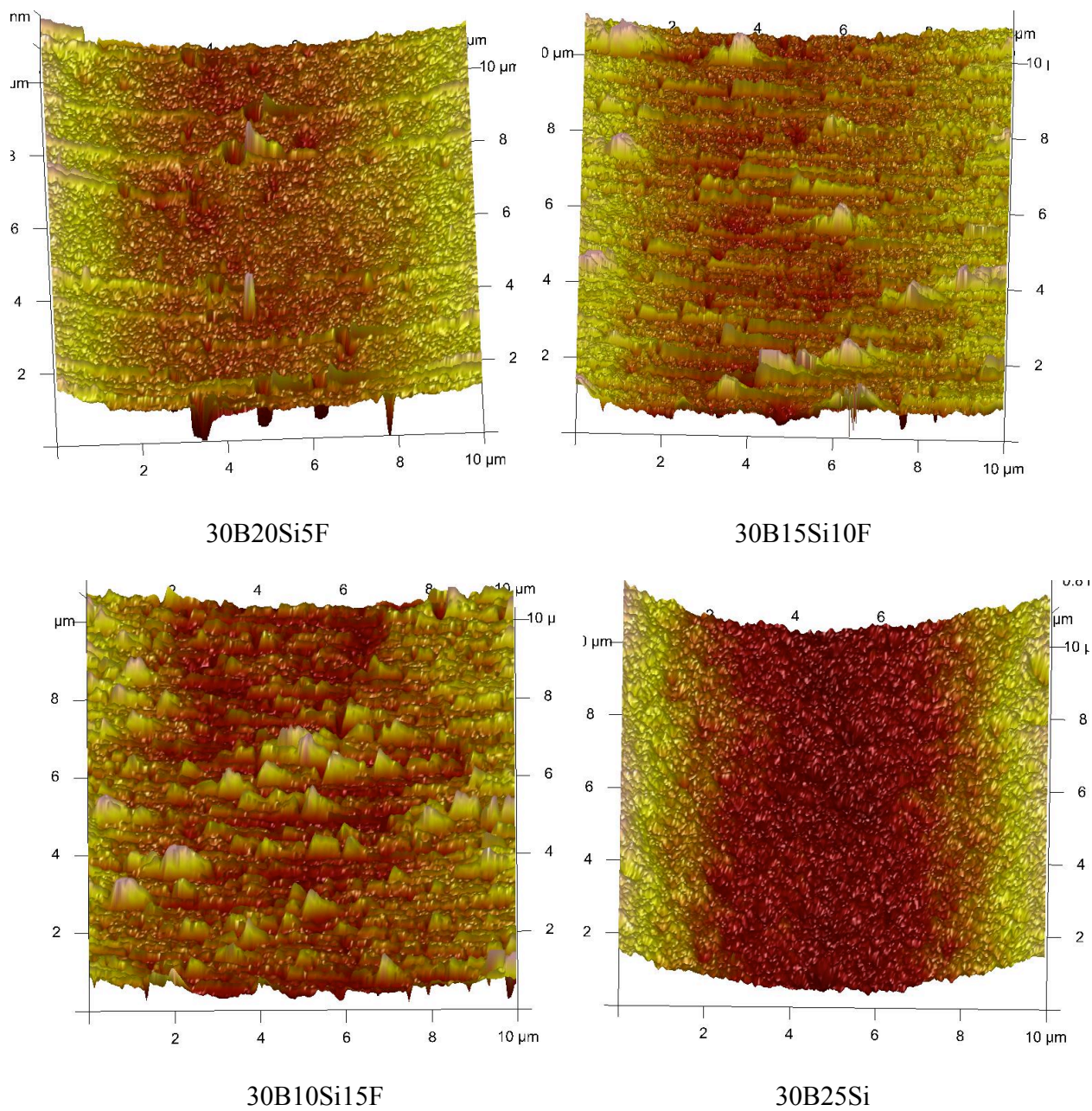
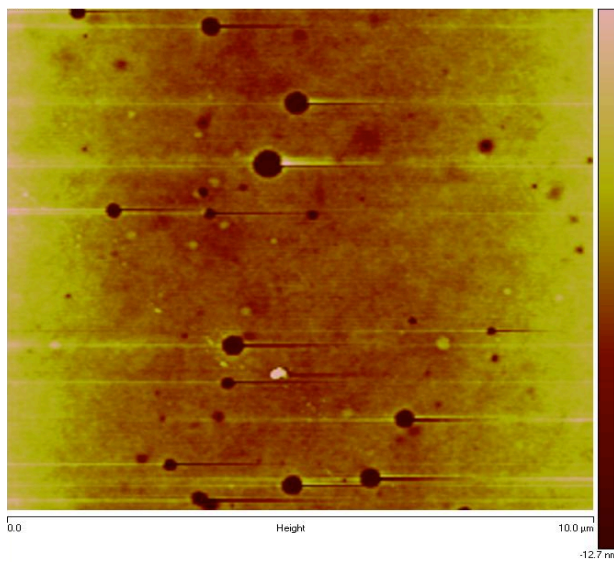
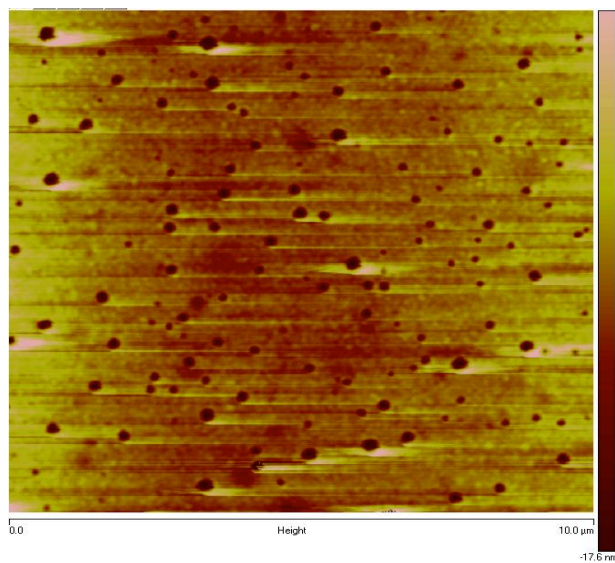


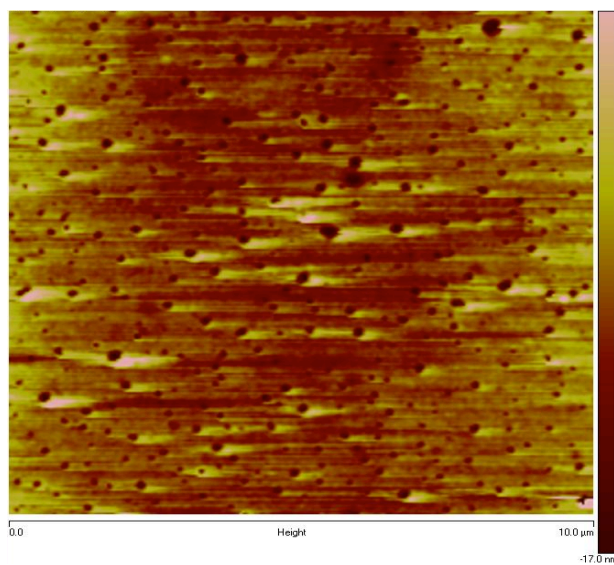
Figure 6.8: Three-dimensional AFM 10 X 10  $\mu\text{m}$  images for hydrophobic PUDs obtained by tapping method.



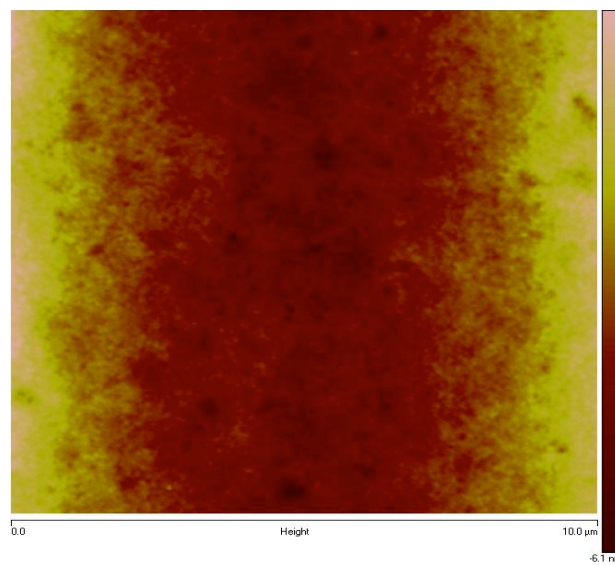
30B20Si5F



30B15Si10F



30B10Si15F



30B25Si

Figure 6.9: Two dimensional AFM 10 X 10 μm changing phase morphology images for hydrophobic PUDs obtained by tapping method.

#### 6.4.5 Self-Crosslinking of PUD:

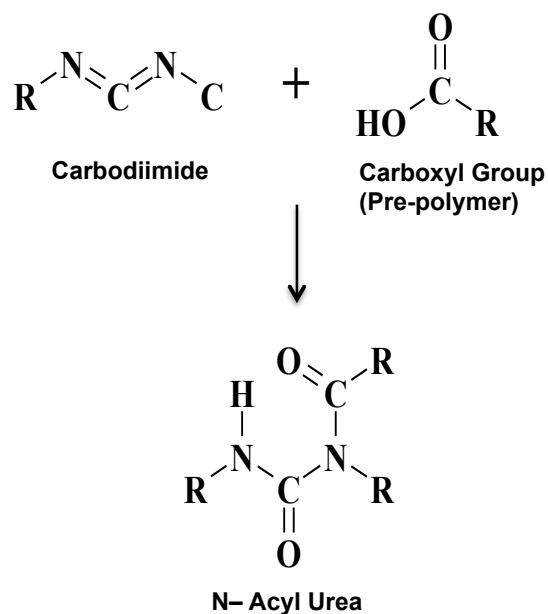


Figure 6.10: Schematic reaction of formation of N-Acyl Urea

With a view to improve mechanical properties of PUDs discussed above, we thought of cross-linking these PUDs. This was achieved by self cross-linking the carboxylic acid groups from PUD backbone with poly-carbodiimide, as shown in Figure 6.10. Compositions were added with poly-carbodiimide (5% by weight based on PUD non-volatiles) were applied (~35 $\mu$ m dry-film thickness) on cold-rolled steel and cured for 7-days at ambient temperature. Upon curing, neutralizing amine will be released from the coating film, leaving the free carboxylic acid groups available for reaction with poly-carbodiimide cross linker. In order to enhance the rate of crosslinking, pH of PUDs was kept slightly acidic. Therefore, all the PUDs (containing carbodiimide cross-linkers) were prepared with degree of neutralization of ~ 90%.

Table 6.5: Mechanical Properties of Self Cross-linked PUD Film Properties

Film Properties	55B	55Si	Surface Chemical Modified PUD			
			30B 25Si	30B 20Si5F	30B 15Si10F	30B 10Si15F
Pencil Hardness	3H	F	F	F	2H	2H
MEK Double RUB	25	25	150	145	50	60
Koenig Hardness (seconds)	67	100	140	140	144	154
Cross Cut Adhesion	5B	5B	5B	5B	5B	5B
Impact Resistance (lbs.in)	Direct	160	160	160	160	160
	Reverse	160	160	160	160	120
Average Contact Angle (°)	68	91	124	120	115	107

As can be seen in Table 6.5, crosslinked PUDs showed good overall improvement in mechanical properties. This clearly indicates appreciable degree of cross-linking by poly carbodiimide under the conditions of curing. Remarkable improvement can be observed in MEK double rub and impact resistance of the coating. MEK double rubs values were almost doubled compared to their non-crosslinked counterparts. The increase in crosslink density and formation of urea groups were believed to have improved the reverse impact resistant by increasing overall toughness of the coating.

#### 6.4.6 Contact Angle Measurements:

As shown in the Figure 6.11, increasing the siloxane content in pre-polymer backbone increased the water contact angle. Since, contact angle measurements characterizes hydrophobicity of coating surface, the increased contact angle could be the result of hydrophobic siloxane groups that are readily available on the surface of the coating. Since, 18.15% siloxane

content formulation (55Si-PUD) exhibits lower contact angle, surface enrichment of siloxane appears to have limited values. It is very interesting to note that contact angle of sample 30B25Si, which contains a blend of soy-polyol and PDMS exhibit much higher contact angle compared to the samples containing pure individual components (samples 55B and 55Si). This clearly shows the synergistic effect of two types of polyols. We believe that the hyper-branched soy-polyol may be facilitating siloxane group orientation at the surface. Comparison between cross-linked and uncross-linked films showed no appreciable difference in contact angle values. This indicates, cross-linking with carbodiimide increases mechanical properties of the films but does not have appreciable effect on their surface properties.

The PUDs 30B10Si15F, 30B15Si10F & 30B20Si5F have 8.55%, 5.70% & 2.85% fluorine content respectively. Unlike siloxane content, increasing the fluorine content decreased the hydrophobicity of the coating. This behavior contradicts the general notion of fluorine groups migrating to the surface and decreasing the surface free energy and hence increasing the water contact angle. As stated in literature (44) to exhibit surface properties, all the fluoroalkyl groups in the coating system should be at the surface rather at bulk. The fluorinated urethane is amphiphobic in nature in which high-energy urethane groups are chemically connected with low energy perfluoropolyether groups. When the fluorocarbon groups segregate at polymer/air interface, the high-energy urethanes could be pulled to the coatings subsurface by low energy moieties. The concentration of urethane groups near subsurface increased as the percent of fluorine content in PUD formulation was increased. When such surface comes in contact with water the urethane groups from subsurface easily migrate to the polymer/water interface and lead the fluorine groups re-orientation towards bulk of the coating film. Thus decreased water contact angle with increased perfluoropolyether polyol content. The aforementioned claim is in



accordance with literature (47,48). Also the achieved pencil hardness from Table 6.4 proves fluorine groups' re-orientation towards bulk of the film. As fluorine content increased the pencil hardness also increased due to more re-orientation of fluorine into bulk. Such phenomenon could be expected in PDMS-urethane part of the PUD, but the alkyl chain length (propyl group) that chemically bonds the urethane with PDMS is longer than the alkyl chain (methyl group) bonding urethane with fluorine. This linker length made the urethanes belong to fluorine closer to surface than the urethanes belong to PDMS. Thus the reduction in contact angle was observed with fluorine moieties. When percent content of fluorine was increased from 8.55 along with other two polyols the appearance of films were hazy. In this case the larger quantity might have possibly phase separated the fluorochemical domains from hydrocarbon of the polymer. As fluorine percent increased, the haze increased and rendered the films (30B5Si20F, 30B25F, 55F) unusable for further analysis. For the aforementioned reason, to improve the appearance and surface property of the film, % of fluorine used in the coating formulation should be optimized.

Table 6.6: Contact angle of uncross-linked PUD and their respective % Content of Siloxane and Fluorine

<b>Types of PUD</b>	<b>Contact Angle (°)</b>	<b>% of Siloxane content</b>	<b>% of Fluorine content</b>
55B	72	0	0
55Si	95	18.15	0
55F	-	0	31.35
30B25Si	127	8.4	0
30b25F	-	0	14.25
30B20Si5F	124	6.72	2.85
30B15Si10F	121	5.04	5.70
30B10Si15F	111	3.36	8.55

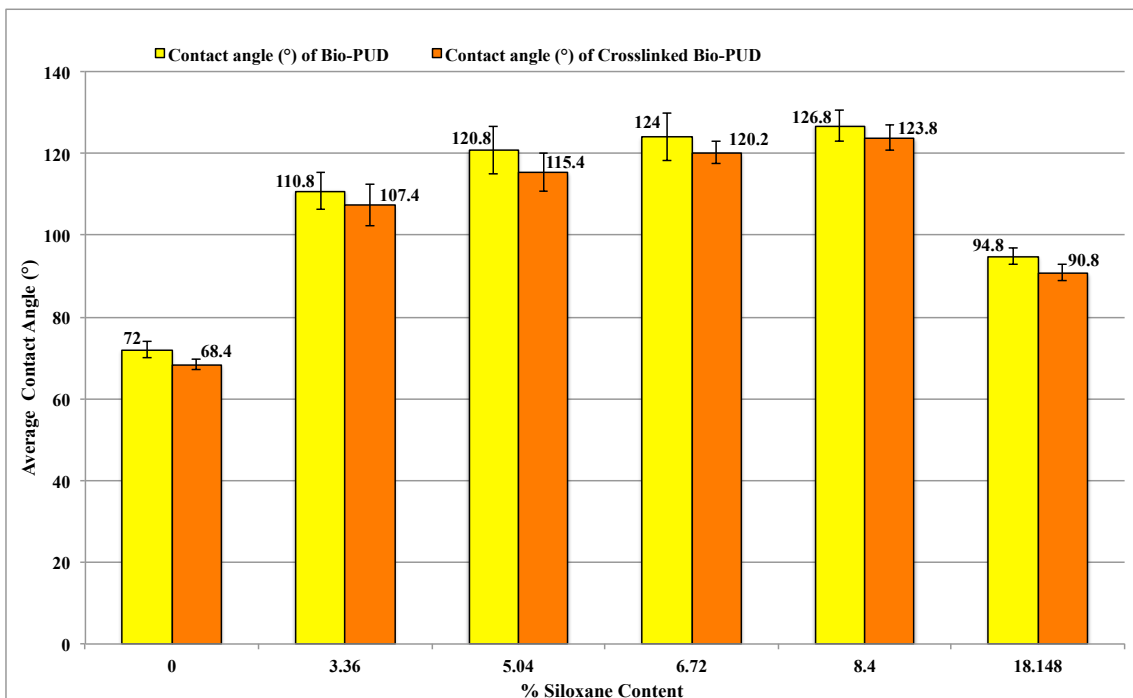


Figure 6.11: Effect of % Siloxane Content on Water Contact Angle

#### 6.4.7 Hydrophobic & Oleophobic Properties:

General solvent absorption technique was used to characterize hydrophobicity and oleophobicity of coating. About 1 square inch of free PUD film was dipped in Di-water (for hydrophobicity) and in n-octane (for oleophobicity) for 24 hours. After 24 hours both hydrophobicity and oleophobicity of coating films were measured based on % absorption (swelling ratio) of solvent (Figure 6.12).

$$\% \text{ Swelling Ratio} = \frac{\text{Final film weight} - \text{Initial Film Weight}}{\text{Final film weight}} \times 100$$

The water resistance of free PUD films is shown in Figures 6.12 and 6.13. Once again, synergistic effect can be observed when more than one polyol type was present in soft segment. PUDs 30B20Si5F, 30B15Si10F and 30I0Si15F have all of the three types of polyols in their soft segments. Water and oil resistance has been studied as a function of % siloxane and % fluorine

content of PUD films. It is evident from Figures 6.11 and 6.13 that increasing the siloxane content increased the hydrophobicity of coating. When siloxane content was increased from 3.36% to 6.72%, the water absorption was decreased from 55.1% to 14.2%. This is 74.23% improvement in water resistance.

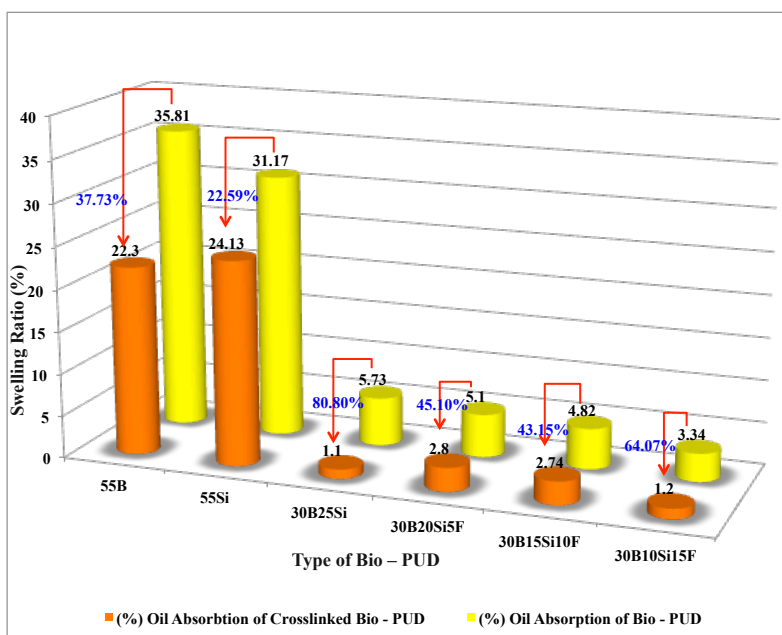
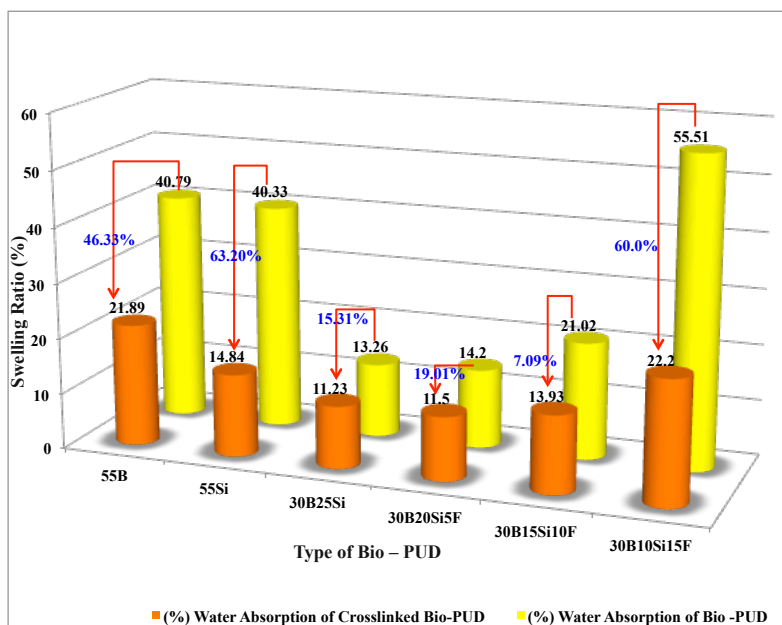


Figure 6.12: Solvent absorption of Bio-PUD and Crosslinked Bio-PUD

% Values represents the % improvement in water and oil resistance after crosslinking

Interestingly, unlike hydrophobicity (water contact angle), oil resistance increased with increasing the amount of fluorine content. Even though % improvement in oil resistance that resulted due to increased fluorine content is considerably small, it is still evident that contribution of fluorine groups to oil resistance is greater than that of siloxane content. In fact, increasing the siloxane content compromised the oil resistance of coating. Attempts were made (30B5Si20F, 30B25F, 55F) to increase the fluorine content more than 8.55%, but due to the poor film integrity and appearance of haze, these samples were excluded from the data pool. A comparison of cross-linked and uncross-linked coatings showed that both water and oil resistance can be improved with self-crosslinking of PUDs. Though newly formed hydrophilic groups (N-acyl urea) in crosslinked PUD slightly lowered the contact angle, the increase in crosslink density appeared to improve the water and oil resistance properties.

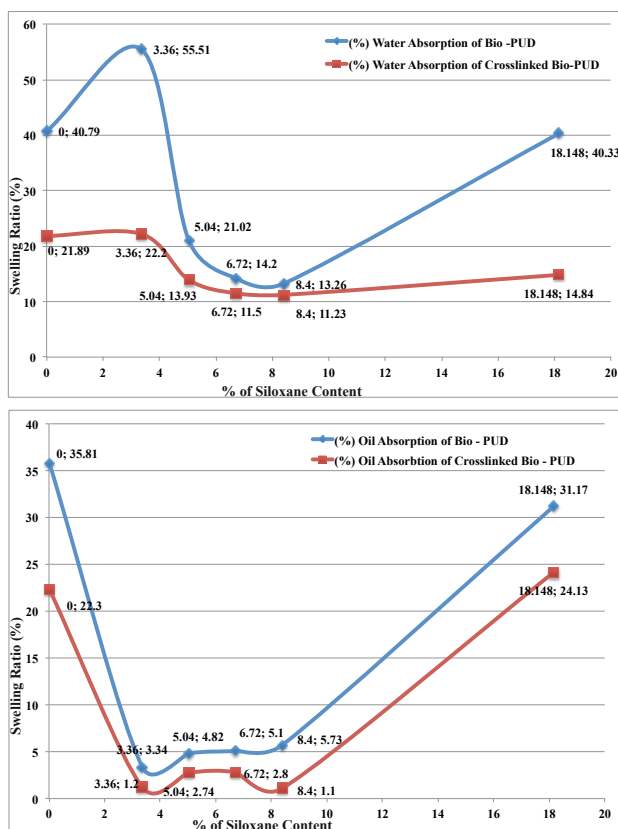


Figure 6.13: Solvent absorption of bio-PUD and crosslinked bio-PUD based on % Siloxane content

## **6.5 Conclusion:**

A range of green PUDs have been synthesized using soy-based polyether polyol (soy-polyol) synthesized from epoxidized soy methyl ester. The synergistic effect on water and oil resistance was observed, when the surface chemical of the soy-polyol based PUD was modified with PDMS and fluoro-polyol. The study of water contact angle, hydrophobicity and oleophobicity showed that surface enrichment of siloxane increased the hydrophobicity (water resistance) whereas fluorine modification improved oil resistance of coatings. Combining siloxane and fluorine content in bio-PUD and changing their ratio in the formulation it is possible to develop a wide variety of coatings for water and oil resistance application. Self-crosslinking the green PUDs with carbodiimide cross linkers further improved the solvent resistance, impact resistance, water and oil resistance of surface chemical modified green PUDs.

## **6.6 Acknowledgement:**

Authors sincerely acknowledge USDA for financial support under Cooperative State Research Education, and extension Services (CSREES) through Grant award no. 2009-38303-05085. We would also like to express the deepest appreciation to Arkema Inc. Bayer MaterialScience LLC, Siltech Corporation, GSI Exim America Inc. and Geo Specialty Chemicals for providing raw materials respectively ESFAME, IPDI, PDMS Polyol, Carbodiimide and DMPA.

## 6.7 Reference:

1. Shah, M.Y.; Ahmad, S. *Prog. Org. Coat.* **2012**, *75*, 248-252.
2. Philipp, C.; Eschig, S. *Prog. Org. Coat.* **2012**, *74*, 705-711.
3. Campanella, A.; La Scala, J.J.; Wool, R.P. *Polymer Engineering and Science.* **2009**, *49*, 2384-2392.
4. Doll, K.M.; Erhan, S.Z. *Journal of Surfactants and Detergents.* **2006**, *9*, 377-383.
5. Bajpai, M.; Shukla, V.; Singh, D.K.; Singh, M.; Shukla, R. *Pigment and Resin Technology.* **2004**, *33*, 160-164.
6. Subramani, J.; Lee, M.; Cheong, I.W.; Kim, J.H. *J. App. Polym. Sci.* **2005**, *98*, 620-631.
7. Patel, J.; Rengasamy, S.; Mannari, V. *Eur. Coat. J.* **2011**, 125-129.
8. Behera, D.; Banthia, A.K. *J. App. Polym. Sci.* **2008**, *109*, 2583-2590.
9. Guo, Y.; Hardesty, J.H.; Mannari, V.M.; Massingill, J.L. *J. Am. Oil. Chem. Soc.* **2007**, *84*, 929-935.
10. Lligadas, G.; Ronda, J.C.; Galia, M.; Biermann, U.; Metzger, J.O. *J. Polym. Sci. Part A: Poly. Chem.* **2006**, *44*, 634-645.
11. Hojabri, L.; Kong, X.; Narine, S.S. *Biomacromolecules.* **2009**, *10*, 884-891.
12. Dumont, M.J.; Kong, X.; Narine, S.S. *J. App. Polym. Sci.* **2010**, *117*, 3196-3203.
13. Rengasamy, S.; Mannari, V. *Prog. Org. Coat.* **2013**, *76*, 78-85.
14. Guo, A., Cho, Y., & Petrovic, Z.S. *J. Polym. Sci.* **2000**, *38*, 3900 – 3910.
15. Petrovic, Z.S., Guo, A., Zhang, W. *J. Polym. Sci. Part A: Polym. Chem.* **2000**, *38*, 4062 – 4069.
16. Lligadas, G.; Ronda, J.C.; Galia, M.; & Cadiz, V. *Biomacromolecules*, **2007**, *8*, 686 – 692.

17. Lligadas, G.; Ronda, J.C.; Galia, M.; & Cadiz, V. *Biomacromolecules*, **2007**, *8*, 1858 – 1864.
18. Lu, Y., & Larock, R.C. *Biomacromolecules*. **2007**, *8*, 3108 – 3114.
19. Lu, Y., & Larock, R.C. *J. Appl. Polym. Sci.* **2008**, *9*, 3332 - 3340.
20. Khot. S.N., Lascalea, J.J., Can, E., Shantaram, S., Williams, G.I., Palmese, G.R., Kusefoglou, S.H., & Wool, R.P. *J. App. Polym. Sci.* **2001**, *82*, 703 – 723.
21. Sharmin, E., Ashraf, S.M., & Ahmad, S. *Eur. J. Lipid. Sci. Technol.* **2007**, *109*, 134 – 146.
22. Kong, X.H., & Narine, S.S. *Biomacromolecules*, **2007**, *8*, 2203 – 2209.
23. Petrovic, Z.S., Guo, A., Javni, I., Cvetkovic, I., & Hong, D.P. *Polym. Int.* **2008**, *57*, 275 – 281.
24. Javni, I., Zhang, W., & Petrovic, Z.S. *J. Appl. Polym. Sci.* **2003**, *88*, 2913 – 2916.
25. Mannari, V. *Patent Application Publication No. 13/396988, Publication No. 2012/0214938 A1*, published on **August 23,2012**
26. Mannari, V.; Rengasamy, S.; Patel, C. *Paint & Coating Industry.* **2012**, *28*, 28-31.
27. Mannari, V.; Rengasamy, S. *Proceedings of the American Coatings Conference*, Charlotte, N.C., April 12-14, **2010**.
28. Bodkhe, R.B.; Stafslie, S.J.; Cilz, N.; Daniels, J.; Thompson, S.E.M.; Callow, M.E.; Callow, J.A.; Webster, D.C. *Prog. Org. Coat.* **2012**, *75*, 38-48.
29. Tang, W.; Huang, Y.; Meng, W.; Qing, F.L. *European Polymer Journal.* **2010**, *46*, 506-518.
30. Feng, X.; Jiang, L. *Adv. Mater.* **2006**, *18*, 3063-3078.

31. Choi, W.; Tuteja, A.; Chhatre, S.; Mabry, J.M.; Cohen, R.E.; Mckinley, G.H. *Adv. Mater.* **2009**, *21*, 2190-2195.
32. Liu, Y.; Chen, X.; Xin, J.H. *Nanotechnology.* **2006**, *17*, 3259-3263.
33. Marmur, A. *Langmuir*, **2004**, *20*, 3517-3519.
34. Barthlott, W.; Neinhuis, C. *Planta.* **1997**, *202*, 1-8.
35. Neinhuis, C.; Barthlott, W. *Ann. Bot.* **1997**, *79*, 667-677.
36. Hurst, S.M.; Farshchian, B.; Choi, J.; Kim, J.; Park, S. *Colloids and Surfaces A: Physicochem. Eng. Aspects.* **2012**, *407*, 85-90.
37. Sheen, Y.C.; Huang, Y.C.; Liao, C.S.; Chou, H.Y.; Chang, F.C. *J. Polym. Sci. Part B: Polym. Phys.* **2008**, *46*, 1984-1990.
38. Howarter, J.A.; Youngblood, J.P. *Macromol. Rapid. Commun.* **2008**, *29*, 455-466.
39. Jabbour, J.; Calas, S.; Gatti, S.; Kribich, R.K.; Myara, M.; Pille, G.; Etienne, P.; Moreau, Y. *Journal of Non-Crystalline Solids.* **2008**, *354*, 651- 658.
40. Lin, Y.H.; Liao, K.H.; Huang, C.H.; Chou, N.K.; Wang, S.S.; Chu, S.H.; Hsieh, K.H. *Polym Int.* **2010**, *59*, 1205-1211.
41. Krol, B.; Krol, P.; Pikus, S.; Chmielarz, P.; Skrzypiec, K. *Colloid Polym Sci.* **2010**, *288*, 1255-1269.
42. Kim, S.R.; Kim, D.J. *J. App. Polym. Sci.* **2008**, *109*, 3439-3446.
43. Levine, F.; Scala, J.L.; Kosik, W. *Prog. Org. Coat.* **2010**, *69*, 63-72.
44. Anton, D. *Adv. Mater.* **1998**, *10*, 1197-1205.
45. Xin, H.; Shen, Y.; Li, X. *Colloids and Surfaces A: Physiochem. Eng. Aspects.* **2011**, *384*, 205-211.
46. Dai, J.B.; Zhang, X.Y.; Chao, J.; Bai, C.Y. *J. Coat. Technol. Res.* **2007**, *4*, 283-288.



47. Vaidya, A.; Chaudhury, M.K. *Journal of Colloid and Interface Science*. **2002**, *249*, 235-245.
48. Thanawala, S.K.; Chaudhury, M.K. *Langmuir*. **2000**, *16*, 1256-1260.

## **Chapter 7: Development of Soy-based UV-curable Acrylate Oligomers and Study of their Film Properties**

**Senthilkumar Rengasamy, Vijay Mannari**

*Part of this chapter is published in Progress in Organic Coatings, (2013), 76, 78-85.*

© 2012 Elsevier B.V. All rights reserved.

### **7.1 Abstract:**

Bio-based coating materials have emerged as an environmentally friendly alternative to petrochemical based ones due to their sustainability, lower carbon footprint and often lower cost. Acrylated vegetable oils and their derivatives are increasingly preferred for advanced photo-curable “green” coatings due to a number of technical and commercial benefits. We report a novel family of acrylate-functional monomers/oligomers derived from epoxidized soybean oil (ESO) and epoxidized soy-methyl ester (EME), using 2-hydroxyethyl acrylate (HEA) as an acrylating agent. Using super-acid catalyzed etherification, acrylated soy-monomers and oligomers with lower viscosity and high acrylate content have been synthesized. Soy-acrylate products are characterized for their chemical structures and functionality using chemical, physical and spectroscopic methods.

In order to investigate their suitability and usefulness, UV-cure coatings have been studied using soy-acrylates as primary components. Compositions containing blend of soy-acrylates and conventional polyester acrylates have also been studied. The results of the study show that these new families of acrylated soy-oligomers are promising candidates for environmentally friendly and sustainable UV-cure coatings for diverse end-use applications.

## 7.2 Introduction:

Radiation-cure technology and more specifically the UV-cure technology is among the rapidly growing and very promising coating technologies due to their low environmental impact, low energy consumption, high efficiency, and contribution towards safe and healthy working environment, combined with acceptable performance of their coatings.<sup>1</sup> Acrylic oligomers and monomers are important components of free-radical type UV-cure coating systems that primarily dictate performance properties and their end-use applications. A majority of raw materials for UV-cure coatings that are available in commercial market is derived from fast depleting petroleum-based fossil resources. For sustainable development, we must reduce our dependence on these fossil resources. Bio-based resources, such as annually renewable vegetable oils, provide an excellent alternative material platform for development of advanced sustainable materials. Through clever chemical transformations, it is possible to derive bio-based materials with significantly lower carbon footprint while meeting high performance demands of their products.<sup>2-4</sup> While petro-based acrylic oligomers and reactive diluents have excellent performance properties, some of their limitations are skin irritancy associated with acrylic monomers and reactive diluents, poor pigment wetting, and film shrinkage resulting often in poor adhesion. Bio-derived, especially vegetable oil derived, materials have potential to minimize or completely overcome these limitations.<sup>5,6</sup>

There has been an increased interest among the researchers in the development of wide range of chemical products by harnessing potential of versatile natural triglyceride oils for polymeric coatings.<sup>7-22</sup> Extensive studies have been done for replacement of petroleum-based raw materials with vegetable oils derived ones from epoxidized soybean oil (ESO) and

epoxidized fatty acid methyl ester of vegetable oils (EME). ESO and EME contain reactive oxirane functionalities, through which numbers of chemical modifications are possible.<sup>22-30</sup> For UV-curing applications, the epoxidized oils can be used in their true form. In the presence of suitable photo latent acid catalyst, these oils can be irradiated by appropriate spectral output of UV-light, to achieve dry film through ring opening cationic polymerization mechanism. However, cationic UV-cure systems suffer from a number of limitations, major being their sensitivity to moisture, making them unpopular for commercial exploitation. Free-radical type UV-cure systems, typically having (meth) acrylate functionality are not sensitive to moisture and therefore have become most popular type of commercial UV-cure systems. The epoxy groups of ESO or EME can also be used to incorporate acrylate functionality by ring-opening esterification with compounds such as acrylic acid.<sup>4,31,32</sup> There are number of commercial products offered that use this chemistry. While such acrylated products are commercially used, there are some inherent limitations of such products. These acrylates have higher viscosities due to certain degree of etherification (through oxirane-oxirane reaction), which is not completely avoidable in presence of acidic reagent such as acrylic acid. Higher viscosities are also contributed by the presence of ester groups through their polar-polar interactions.

Since viscosity of oligomers is of paramount importance in UV-cure coatings, we believe there exist opportunities of deriving low viscosity acrylates by replacing acrylic acid as acrylating agent with a hydroxyl acrylate to produce acrylic ethers rather than esters. In the present work we have focused on synthesis of acrylic functional oligomers / monomers using catalytic ring-opening reaction of ESO and EME using 2-hydroxyethyl acrylate (HEA). It has been found that the acrylic functional products produced by this route show considerably low viscosity and high acrylic contents. The acrylic functional products are characterized to confirm

their chemical structure; functionality and their coating compositions are studied to investigate their suitability for UV-cure coatings.

### **7.3 Experimental:**

#### **7.3.1 Raw Materials:**

Epoxidized Soybean Oil (ESO) (Vikoflex™ 7170) and - Epoxidized Methyl Ester (EME) (Vikoflex™ 7010) were procured from Arkema Inc., USA and used without purification. Darocur™ 1173, a radical type photo-initiator was obtained from BASF, USA. Tetrafluoroboric acid (HBF<sub>4</sub>) 48% in water, 2-Hydroxyethyl acrylate (HEA), Monomethylether of hydroquinone (MEHQ), Diethyl ether and anhydrous magnesium sulfate were purchased from Sigma Aldrich, USA and used as received. Polyester acrylate (CN2282) and the reactive diluents such as SR 306, SR 508 and SR 350 were procured from Sartomer and used as received.

#### **7.3.2 Synthesis of Acrylated ESO (AESO) and Acrylated EME (AEME):**

2-Hydroxyethyl acrylate (150g) was placed into a 500 ml 3-neck flask equipped with a mechanical stirrer, condenser, temperature controller, an inlet for nitrogen and an addition funnel. Flask was placed in a water-bath at room temperature under stirring. MEHQ (1.5% by wt. of HEA) and HBF<sub>4</sub> (0.5g) were added as a catalyst and mixture was heated to 80° C under stirring. ESO (150 g) was then added slowly into the flask from an addition funnel for about 45 min. After addition of ESO was completed, the reaction was allowed to continue at 80° C until desired oxirane oxygen content (less than 0.05%) was obtained. Reaction product was then dissolved in diethyl ether and transferred into a separating funnel. Excess and unreacted HEA was removed by washing the etharal solution several times with DI-water. Etharal layer was separated and dried using anhydrous magnesium sulfate. Ether was then evaporated and product Acrylated ESO (AESO) was transferred in a brown bottle and stored in refrigerator. Acrylated

EME (AEME) was synthesized using identical process using 150 g of EME in the place of ESO.

### **7.3.3 Methods of characterization:**

Acrylated soy-oligomers have been characterized for oxirane oxygen content (ASTM D – 1652-97) acid number (ASTM D - 1639-96), iodine value (ASTM D - 5768-02), and hydroxyl number (ASTM D - 4274-05). Viscosity of the epoxidized vegetable oils and their derivatives were determined at 25°C using the Brookfield viscometer. Proton NMR spectra of acrylated ESO and EME was recorded on a Bruker NMR spectrometer in CDCl<sub>3</sub> at room temperature. A 45° pulse width, 400 MHz field strength, 2.18 seconds acquisition time and 5 seconds pulse delay were used in the spectrum analysis. The FTIR spectra of acrylated products were recorded with Bruker-Tensor 27 FTIR spectrometer using NaCl pellets. Gel permeation chromatography (GPC) was used to determine the molecular weight of oligomers. The UV-cured film properties were characterized using ASTM standards such as pencil hardness (ASTM D – 3363), impact resistance (ASTM D - 2794-99), Adhesion (cross-cut) test (ASTM D - 3359-02), MEK double rub test (ASTM D - 4752-98). BYK film thickness gauge instrument was used to check the dry film thickness. TGA Q-500 and DSC Q-2000 (TA Instruments) were used to characterize respectively decomposition temperature and glass transition temperature (T<sub>g</sub>) of UV cured free films at 10°C/min temperature ramp rate.

### **7.3.4 Coating compositions and testing:**

Various UV-cure coatings have been formulated using AESO, AEME, commercial polyester acrylate (CN 2282) and reactive diluents. Free-radical type photo-initiator Daracure™ 1173 (BASF) has been used. Coating compositions are shown in Table 7.5. Coatings were applied on cold rolled steel panels (6"x4"x0.032") to ~50 micron wet film thickness and cured under UV-irradiation. A UV-cure system (Fusion UV) with a D-bulb was used with the

conveyor belt speed set to 40 feet/min. Using a compact radiometer (UVPS), the energy density measured was ~ 2100 mJ/cm<sup>2</sup>. Properties of cured films were tested and compared after 48 hours.

## **7.4 Results and Discussion:**

### **7.4.1 Synthesis of AESO and AEME**

Acrylated ESO and acrylated EME have been synthesized by reaction of corresponding epoxy (oxirane) soy-derivative with excess of 2-HEA in presence of fluoroboric acid as catalyst. Free-radical inhibitor (MEHQ) has been used to avoid free-radical initiated polymerization through acrylic groups. Figure 7.1a shows a general reaction of oxirane compounds with alcohols in presence of strong acid (HX) catalyst, producing  $\beta$ -hydroxy ether. Under the same reaction conditions, a competing reaction (Figure 7.1b) involving oxirane-oxirane groups is also possible, resulting into formation of polyether oligomers. Thus, it is important that for deriving AESO or AEME in high yields, oxirane-oxirane reaction is appreciably suppressed to minimize formation of undesirable oligomeric species. We have attempted to accomplish this by using stoichiometric excess of 2-HEA over epoxy compounds. Petrovic et al have prepared soy-polyol from ESO using ring-opening reaction by methanol [33]. Using large excess of methanol these researchers could avoid any appreciable polymerization. To estimate the relative extents of acrylation and oligomerization, hydroxyl number of AESO and AEME were determined and compared with the theoretical -OH numbers (assuming no oligomerization). Since acrylation reaction (reaction of 2EHA and epoxide) produces one -OH group per epoxide, while oligomerization reaction does not, OH number can be used to calculate degree of acrylation and oligomerization fairly accurately. Table 7.1 reports results for degree of acrylation and oligomerization. Under the conditions of reactions, degree of acrylation of 86% for AESO and 97% for AEME could be achieved. Comparison of Iodine Number (Table 7.1) for AESO and

AEME also supports the above results. Lower degree of acrylation and higher oligomerization in AESO compared to AEME may be due to higher functionality of ESO and proximity of epoxy-epoxy groups resulting in greater possibility for oligomerization.

Viscosity of acrylated products is of paramount importance, especially for their use in UV-cure coatings. Low viscosity oligomers are preferred due to their reduced demand for reactive diluents besides other technical benefits. Comparison of viscosity of AESO and AEME in Table 7.1, shows, as expected, higher viscosity for AESO. The two major factors affecting viscosity of AESO are molecular weight and H-bonding through –OH groups. Molecular weight is significantly dependent on extent of oligomerization (due to epoxy-epoxy reaction) during acrylation. H-bonding is mainly depends on –OH content within AESO. It should be noted that while viscosity of AESO (~5000 cPs) is higher than AEME (~109 cPs), it is still very much lower than most of the commercially available AESO that were prepared by direct esterification of ESO with acrylic acid. In direct acrylation process (using acrylic acid), in addition to desired esterification, substantial oligomerization (etherification) takes place, due to the additional catalytic effect of acrylic acid for this reaction. In case of acrylation reaction using 2HEA, we have used large excess of 2HEA, which will reduce possibility of oligomerization and hence molecular weight builds up. In addition to this, reaction between ESO and 2HEA results in formation of an ether linkage with the fatty acid chain, while acrylation with acrylic acid would produce ester linkages. Since, ether linkages have relative freedom of rotation compared to ester linkages, they have increased free volume and hence expected to have lower viscosity. Also, in 2HEA based AESO, ester groups are away from fatty acid chains and may have less H-bonding participation with OH groups on the fatty acids. We believe these are the reasons for lower viscosity of AESO derived from 2HEA.



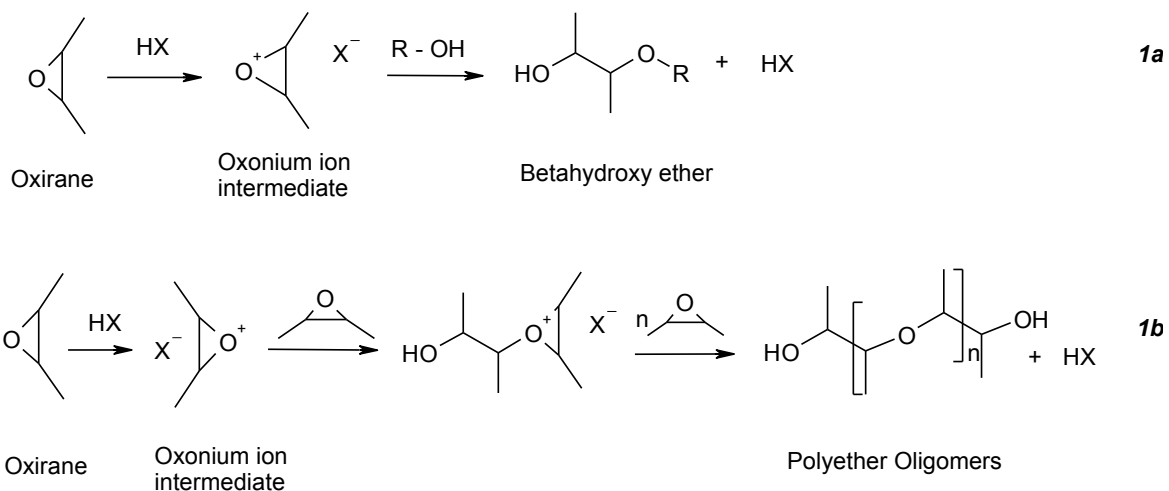


Figure 7.1: Competing reactions of oxirane compounds with alcohol in presence of strong acid yielding (1a) beta hydroxyl ether and (1b) polyether oligomers

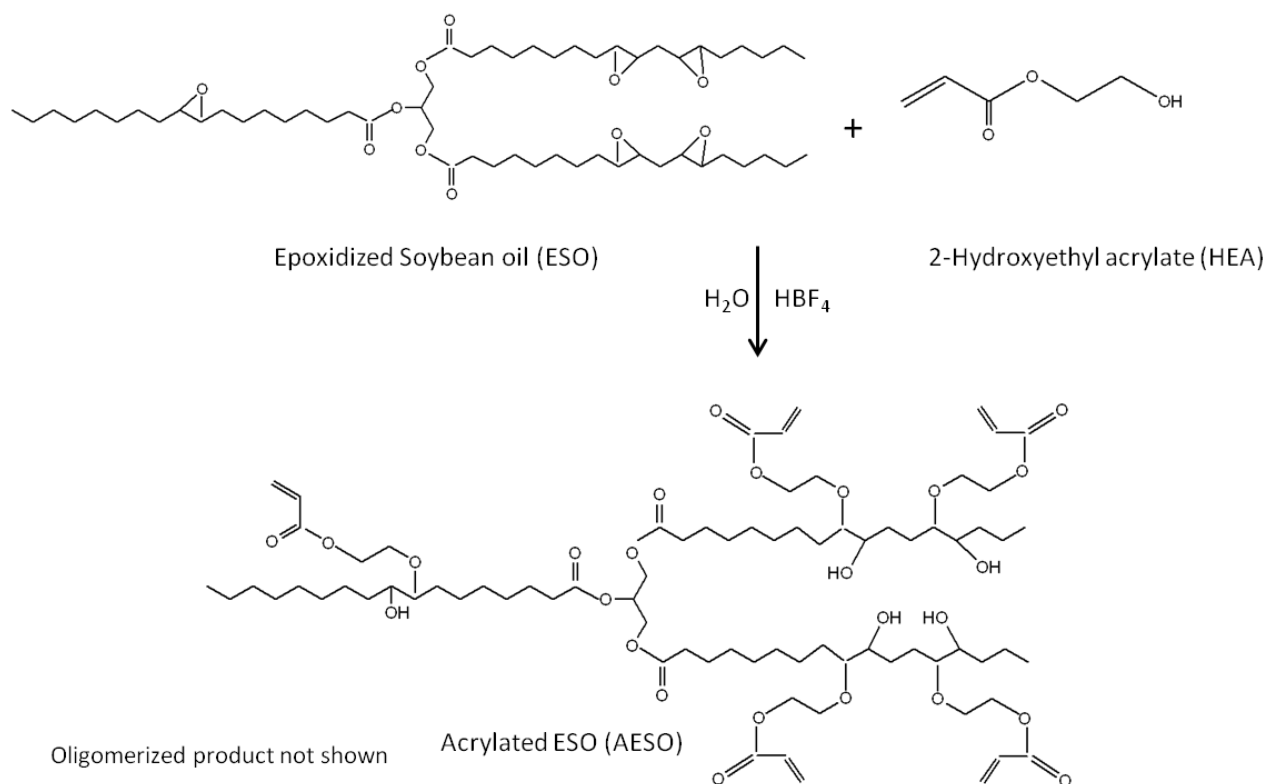


Figure 7.2: Synthetic scheme for acrylated ESO in presence of strong acid catalyst



### 7.4.3 $^1\text{H}$ NMR Characterization of AESO & AEME:

Spectroscopic characterization of AESO and AEME has been carried out using  $^1\text{H}$  NMR and the spectra are shown in Figure 7.4. Also, the characteristic peaks are summarized in Table 7.2.

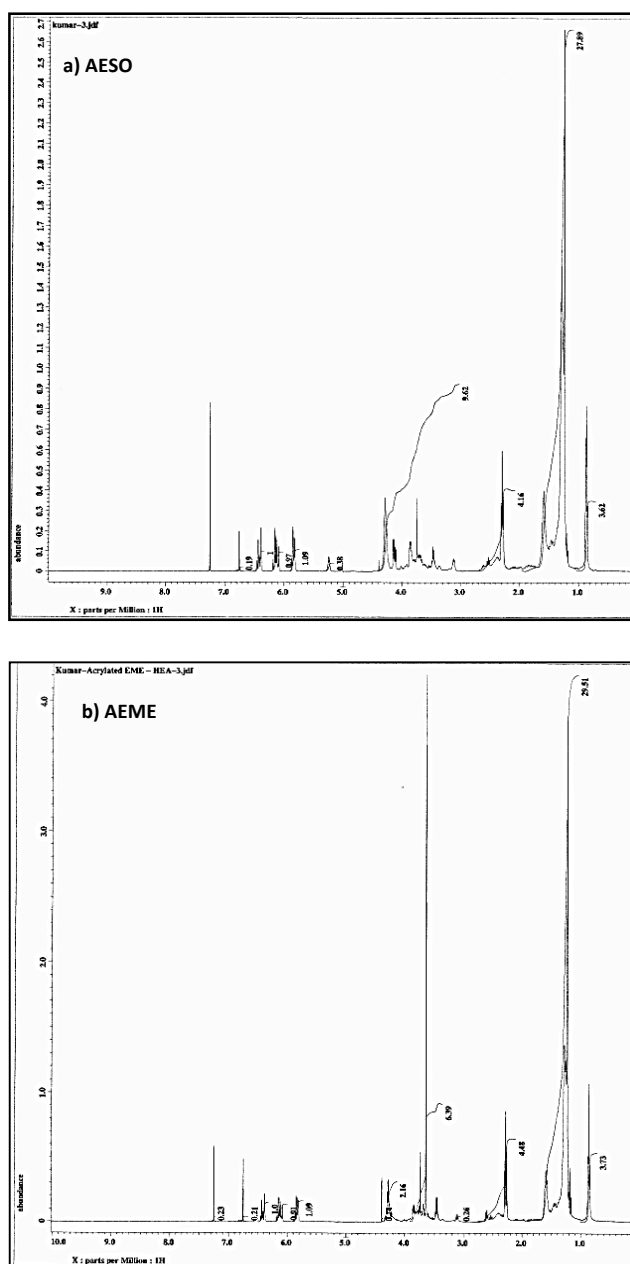


Figure 7.4: Proton NMR Spectra of a) AESO, b) AEME

Table 7.2: <sup>1</sup>H NMR Spectral data of AESO and AEME

<sup>1</sup> H NMR Spectra (Signal Peak - ppm)	AESO**	AEME*
0.8 - 0.9	CH <sub>3</sub> (terminal group)	CH <sub>3</sub> (terminal group)
1.2 - 1.4	CH <sub>2</sub> (aliphatic backbone)	CH <sub>2</sub> (aliphatic backbone)
1.5 - 1.7	β CH <sub>2</sub> -(C=O)-O (methylene proton adjacent to carbonyl group)	β CH <sub>2</sub> -(C=O)-O (methylene proton adjacent to carbonyl group)
*2.2 - 2.3 / **2.2 - 2.	α CH <sub>2</sub> -(C=O)-O (methylene proton adjacent to carbonyl group)	α CH <sub>2</sub> -(C=O)-O (methylene proton adjacent to carbonyl group)
3.4 - 3.5	OH groups	OH groups
3.6 - 3.9	CH <sub>2</sub> -O-CH <sub>2</sub> (polyether backbone)	CH <sub>2</sub> -O-CH <sub>2</sub> (polyether backbone)
4.1	CH <sub>2</sub>	-
4.2 - 4.4	Protons of saturated CH <sub>2</sub> in HEA	Protons of saturated CH <sub>2</sub> in HEA
5.2	CH	-
5.8 - 6.5	CH <sub>2</sub> = CH (acrylic moiety)	CH <sub>2</sub> = CH (acrylic moiety)

For both AEME and AESO, the three olefinic protons of the acrylate functional group correspond to 5.8-6.5ppm peaks. For every acrylate groups generated at epoxy moieties, a hydroxyl groups appears and the corresponding peak appears at 3.4-3.5ppm. The difference between AESO and AEME can be observed from the peaks obtained at 4.1ppm (CH<sub>2</sub>) and 5.2ppm (CH), which is characteristics spectral feature of AESO triglyceride.<sup>29,30</sup>

#### 7.4.4 FTIR Spectra Characterization of Initial and Acrylated Products:

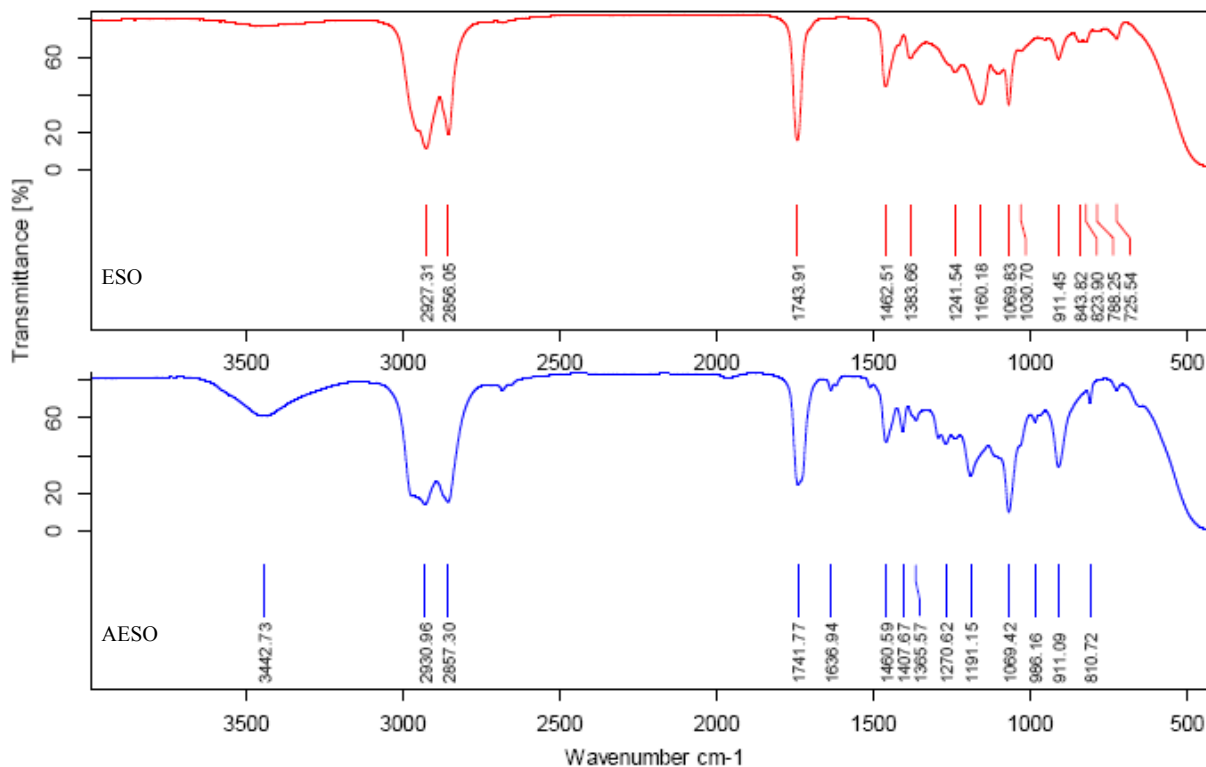


Figure 7.5: FTIR Spectra of ESO and AESO

Table 7.3: FTIR absorption peaks of ESO and AESO

ESO		AESO	
Absorption Peak, $\text{cm}^{-1}$	Functional Group	Absorption Peak, $\text{cm}^{-1}$	Functional Group
2927, 2856	CH stretch	3443	OH (strong)
1744	C=O carbonyl group	2931, 2857	CH
1463	CH scissoring band	1742	C=O carbonyl group
1384	CH symmetric band	1637	$\text{CH}_2=\text{CH}$
1241	C-O	1461	CH scissoring band
1160	C-C-O	1408	$\text{CH}_2=\text{CH}$ scissoring band for terminal alkene
824, 844	C-O-C oxirane group	1366	CH symmetric band
		1271	C-O
		1191, 1069	C-C-O
		911, 811	C-C-O Asymmetric band

ESO, EME and their acrylated derivatives have been fully characterized by FTIR

spectroscopy and spectra are shown in Figures 7.5 and 7.6 and the summary of their characteristic absorption peaks are presented in Tables 7.3 and 7.4. The oxirane (C-O-C) groups in ESO and EME can be clearly observed from the absorption peaks at  $824\text{ cm}^{-1}$  and  $844\text{ cm}^{-1}$ . The disappearance of these peaks for AESO and AEME proves the incorporation of acrylation reaction (or oligomerization) at epoxy moieties. These newly formed acrylic groups are responsible for observed transmittance peaks of  $1408\text{ cm}^{-1}$  and  $1637\text{ cm}^{-1}$ . Formation of  $\text{-OH}$  groups through ring-opening reaction can be confirmed by the enhancement of peak at  $3443\text{ cm}^{-1}$  corresponding to OH stretching [29,30]. The FTIR analysis corroborates very well with chemical characteristics of the products determined (Iodine number, hydroxyl number). This also concludes that the epoxide groups are reacted with HEA in the presence of super acid catalyst, resulting in the formation of an ether group and  $\text{-OH}$  group, as proposed in the reaction scheme in Figures 7.2 and 7.3.

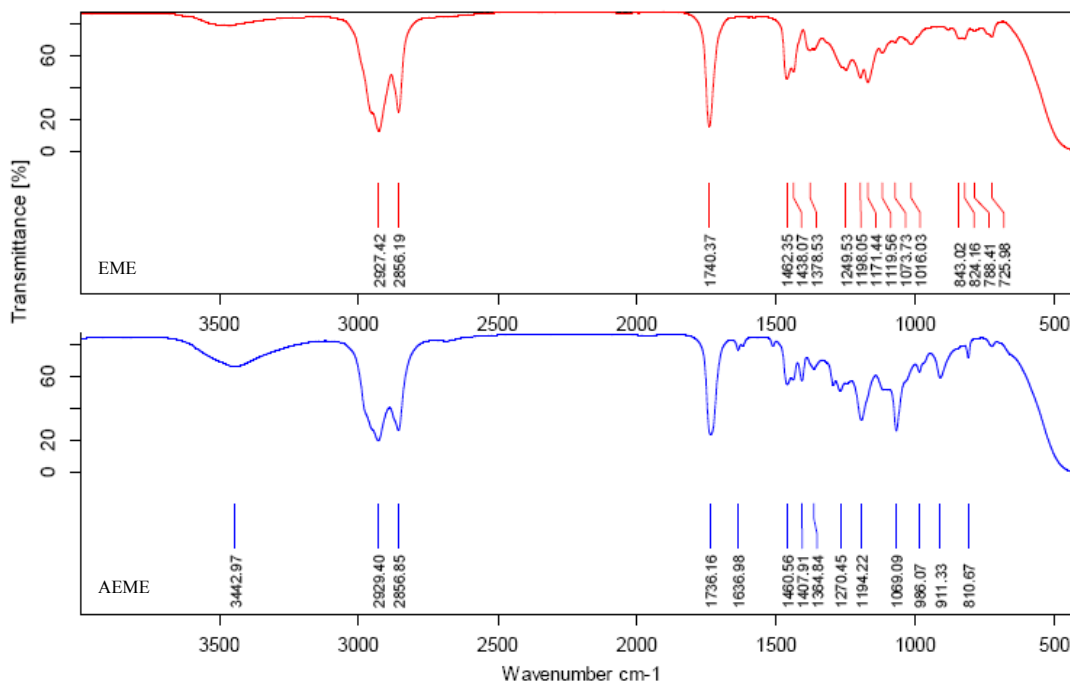


Figure 7.6: FTIR Spectra of EME and AEME

Table 7.4: FTIR Spectra for EME and AEME

EME		AEME	
Absorption Peak, cm <sup>-1</sup>	Functional Group	Absorption Peak, cm <sup>-1</sup>	Functional Group
2927, 2856	CH Stretch	3443	OH (strong)
1740	C=O carbonyl group	2929, 2857	CH
1462	CH scissoring band	1736	C=O carbonyl group
1379	CH symmetric band	1637	CH <sub>2</sub> =CH
1250	C-O	1461	CH scissoring band
1171	C-C-O	1408	CH <sub>2</sub> =CH scissoring band for terminal alkene
824, 843	C-O-C oxirane group	1365	CH symmetric band
		1270	C-O
		1194, 1069	C-C-O
		911, 811	C-C-O Asymmetric band

#### 7.4.5 Thermal Analysis:

Thermal stability of the AESO and AEME based UV-curable coatings were assessed using TGA. The results are shown in Figure 7.7. The main decomposition temperature was observed at 434° C for AESO and at 390° C for AEME. Also the initial decomposition temperature (from the temperature of 3% weight loss) for AESO can be observed at 387° C and for AEME it was at 295° C. It is evident that thermal stability of AESO is higher than AEME. This might be due to the high molecular weight and high functionality of AESO compared to AEME. In general crosslink density can be improved with high functionality materials that directly corresponds to better thermal stability. This pattern also reflected in DSC thermograms (Figure 7.8) in which glass transition temperature (T<sub>g</sub>) of AESO and AEME was reported 32°C and 9°C respectively.

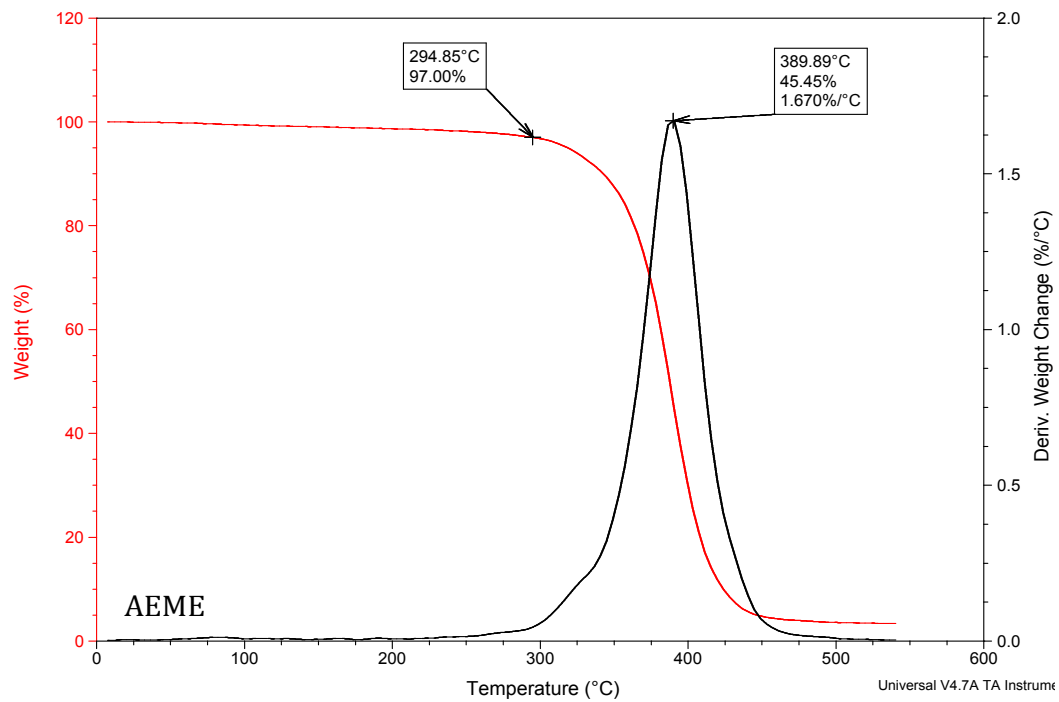
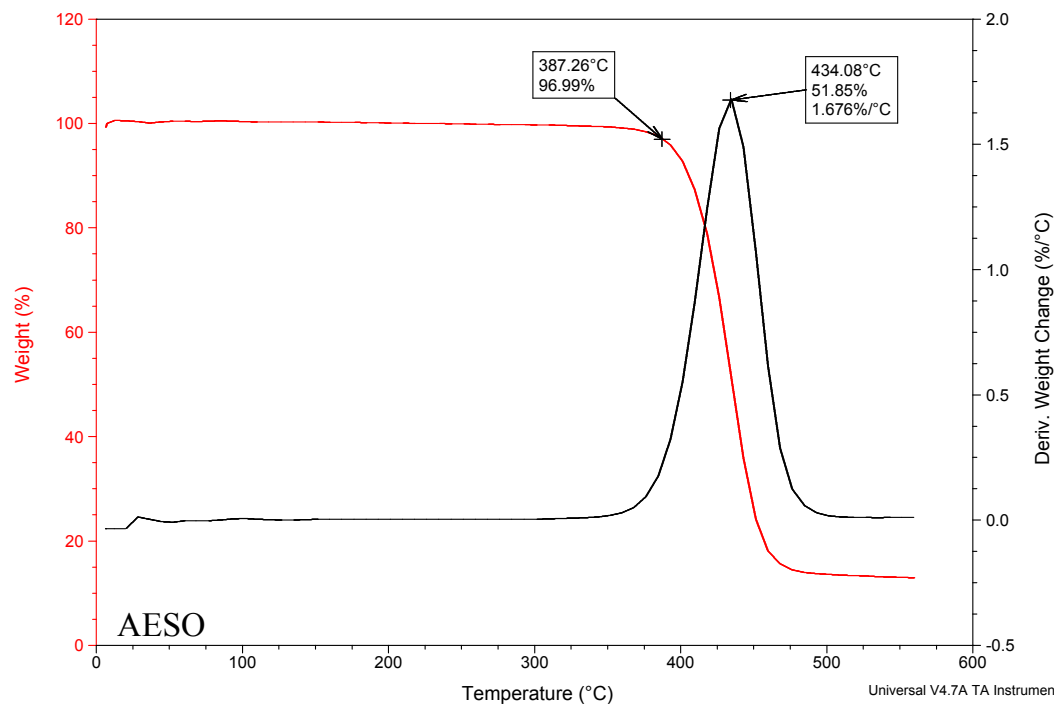


Figure 7.7: TGA thermogram of AESO & AEME



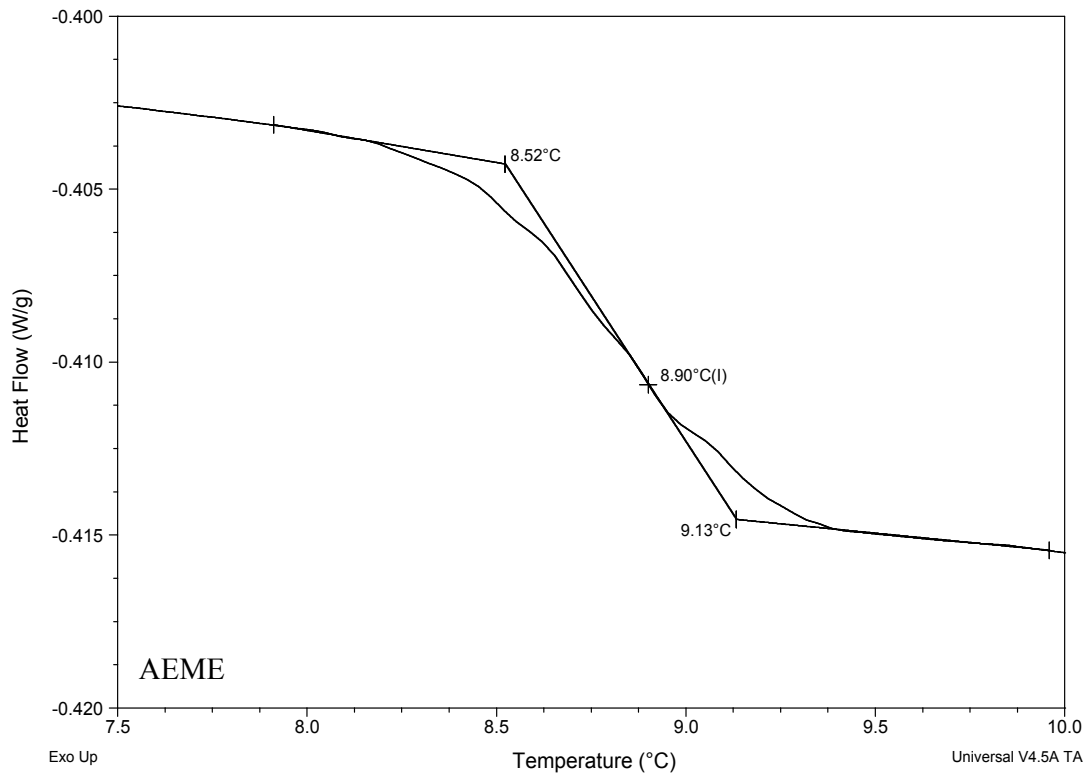
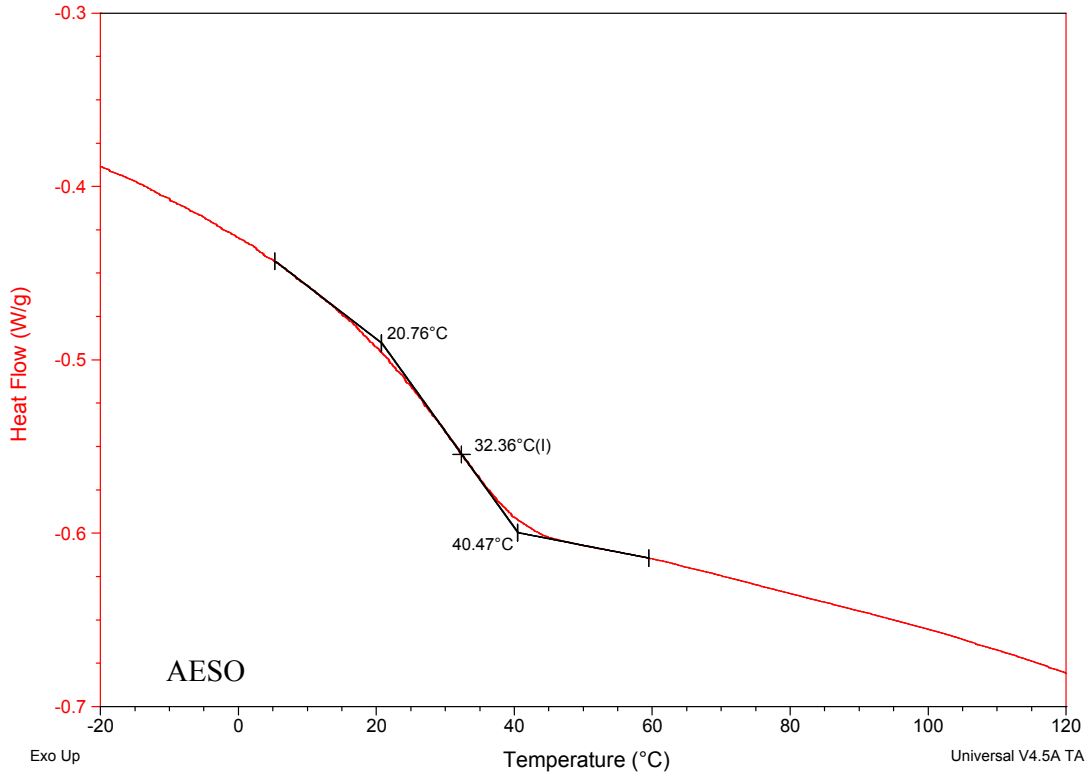


Figure 7.8: DSC thermogram of AESO & AEME

#### 7.4.6 Coating Compositions and Cured Film Properties:

In order to study the potential of AESO and AEME for their usefulness in UV-cure coatings, a series of UV-cure coating compositions were prepared and properties of their UV-cured films were studied (Table 7.5). Film properties of compositions containing straight AESO, AEME have been compared with commercial polyester acrylate (CN 2282, Ex Sartomer). Compositions containing blend of AESO and commercial polyester acrylate (along with reactive diluents) were studied to explore compatibility of polyester acrylate and AESO, and effect of composition on their film properties.

Table 7.5: Composition and coating properties of UV-curable AESO and AEME

Raw Materials	AESO	AEME	PEA	Polyester Acrylate/ AESO Ratio (by wt.)					
				100:00	70:30	60:40	40:60	30:70	
Polyester (CN2282*) (g)			5	5	3.5	3	2	1.5	
AESO (g)	5			-	1.5	2	3	3.5	
AEME (g)		5							
TPGDA(SR306*)	-	-	-	1.5	1.5	1.5	1.5	1.5	
DPGDA (SR508*) (g)	-	-	-	1.5	1.5	1.5	1.5	1.5	
3EoTMPTA(SR350*) (g)	-	-	-	1.5	1.5	1.5	1.5	1.5	
Photo Initiator (Daracure 1173**) (g)	0.25	0.25	0.25	0.5	0.5	0.5	0.5	0.5	
<b>Resin and Cured Film Properties</b>									
Viscosity (cPs) @ 25°C	5406	109	70000	453	310	285	235	222	
Dry Film Thickness (µm)	35	35	35	35	35	35	35	35	
Pencil Hardness	F	6B	F	6H	5H	5H	4H	3H	
Pendulum hardness(Koenig)	42	12	42	160	102	97	88	84	
MEK Double rub	50	0	200	200	200	200	200	200	
Adhesion (Cross-hatch)	B	0B	B	0B	0B	B	2B	4 B	
Impact	Direct	100	10	80	10	25	25	40	120
Resistance(lbs.In)	Reverse	80	10	50	0	4	6	10	15

\* Sartomer \*\* BASF Products

The results of film properties in Table 7.5 show that all compositions studied formed tack-free and dry film under the conditions of UV-curing. The coating based on straight AEME is found to be very soft with poor adhesion and solvent resistance, as compared to that for AESO or commercial polyester acrylate. This can be attributed to low functionality and low molecular weight of AEME compared to AESO or polyester acrylate.

Table 7.5 also shows properties of coatings prepared by blending AESO and polyester acrylate (PEA) in varying proportions, along with constant quantities of reactive diluents. As expected, viscosity of these compositions decreases as AESO content is increased. This indicates that AESO can be used to formulate low viscosity compositions or it can reduce the need for reactive diluents. It is also observed that with increasing AESO content, film hardness (both pencil and pendulum hardness) decreases. However, it should be noted that even at 70% replacement of PEA with AESO (composition 30:70), film hardness remains quite good and acceptable for many commercial end-use applications. The solvent resistance (MEK double-rub test) of all compositions, even at high AESO content, shows excellent performance indicating high cross-link density of films. The most striking benefit of AESO seems to be the improvement of adhesion. With increasing AESO content above 40%, noticeable improvement in crosshatch adhesion and for composition with 70% AESO (composition 30:70), it shows excellent adhesion. In general, UV-curing coatings suffer from adhesion issues due to rapid cure kinetics which does not allow relaxation of polymer segments during curing process, resulting into residual internal stresses in the film that leads to poor adhesion with substrate. AESO, due to its flexible triglyceride structure seems to produce cured films with reduced internal stresses and hence improved adhesion. Improvement of toughness, as observed from impact resistance, can also be attributed to flexible nature of AESO.

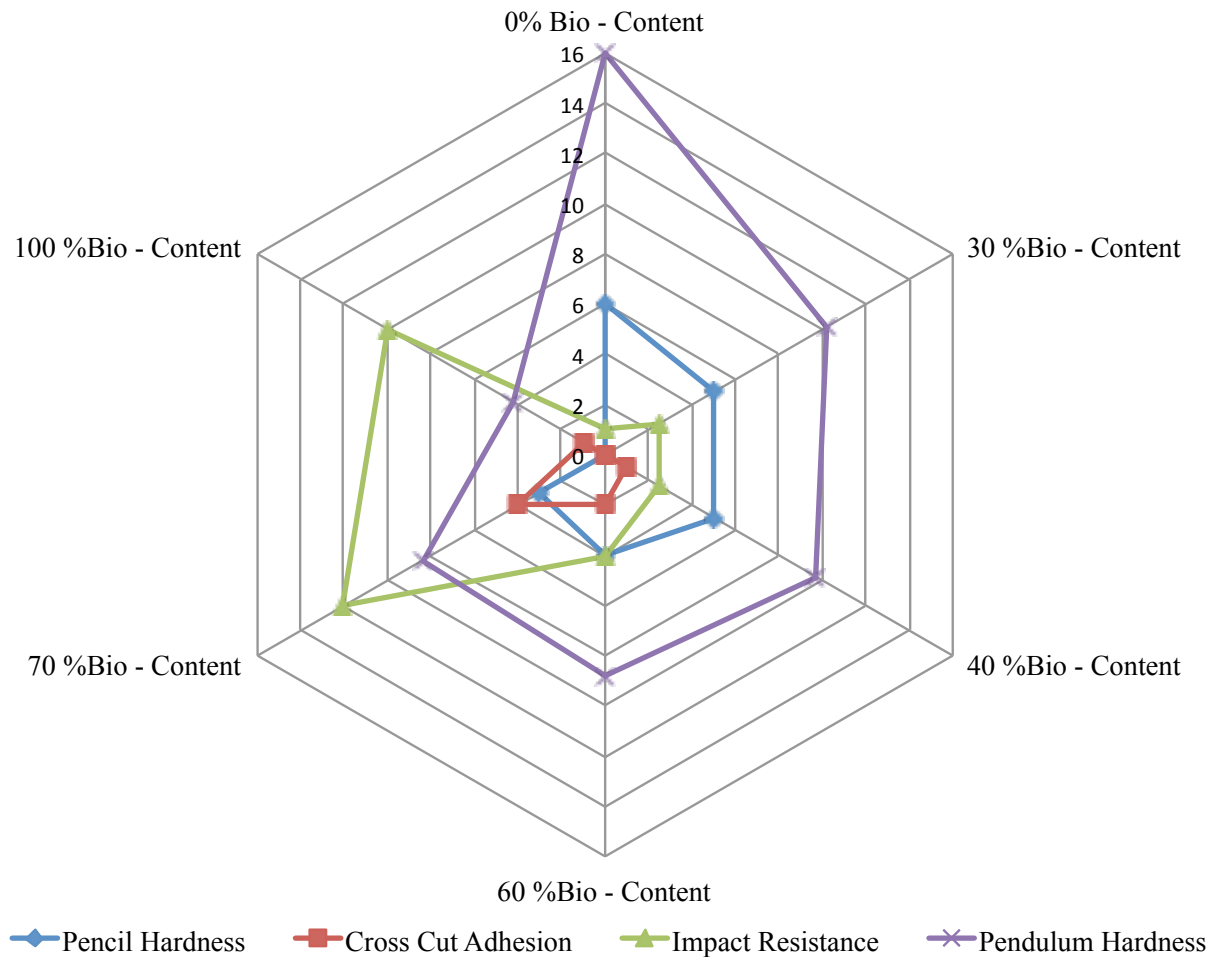


Figure 7.9: Effect of %Bio – Content of UV-Cured Film Properties. Results of all properties normalized to 0-16 scale.

Figure 7.9 demonstrates the effect of % bio-based content on basic film properties such as pencil hardness, pendulum hardness, cross cut adhesion and impact resistance. The data for all the properties were normalized as per following. 0 to 6 scale used for pencil hardness where 0 = F hardness value and 6 = 6H hardness value. For impact resistance (direct) & pendulum hardness 1 unit = 10 units of respective scale. 0 to 5 scale used for cross cut adhesion where 0 = 0B and 5 = 5B of adhesion strength.

### 7.4.7 Dual Cure Acrylic Urethane Coating Film Properties:

As we discussed earlier synthesis of acrylic oligomers using carbonium ion reaction opens the oxirane oxygen ring and produces both hydroxyl and acrylic functional groups (Figure 7.3). These newly formed OH groups can be utilized to achieve the optimum film properties that can be used in applications like automotive OEM and refinish clear coats. At the time of application hydroxyl groups from AESO can be react with isocyanate to obtain acrylic urethane coating system as shown in Figure 7.10.

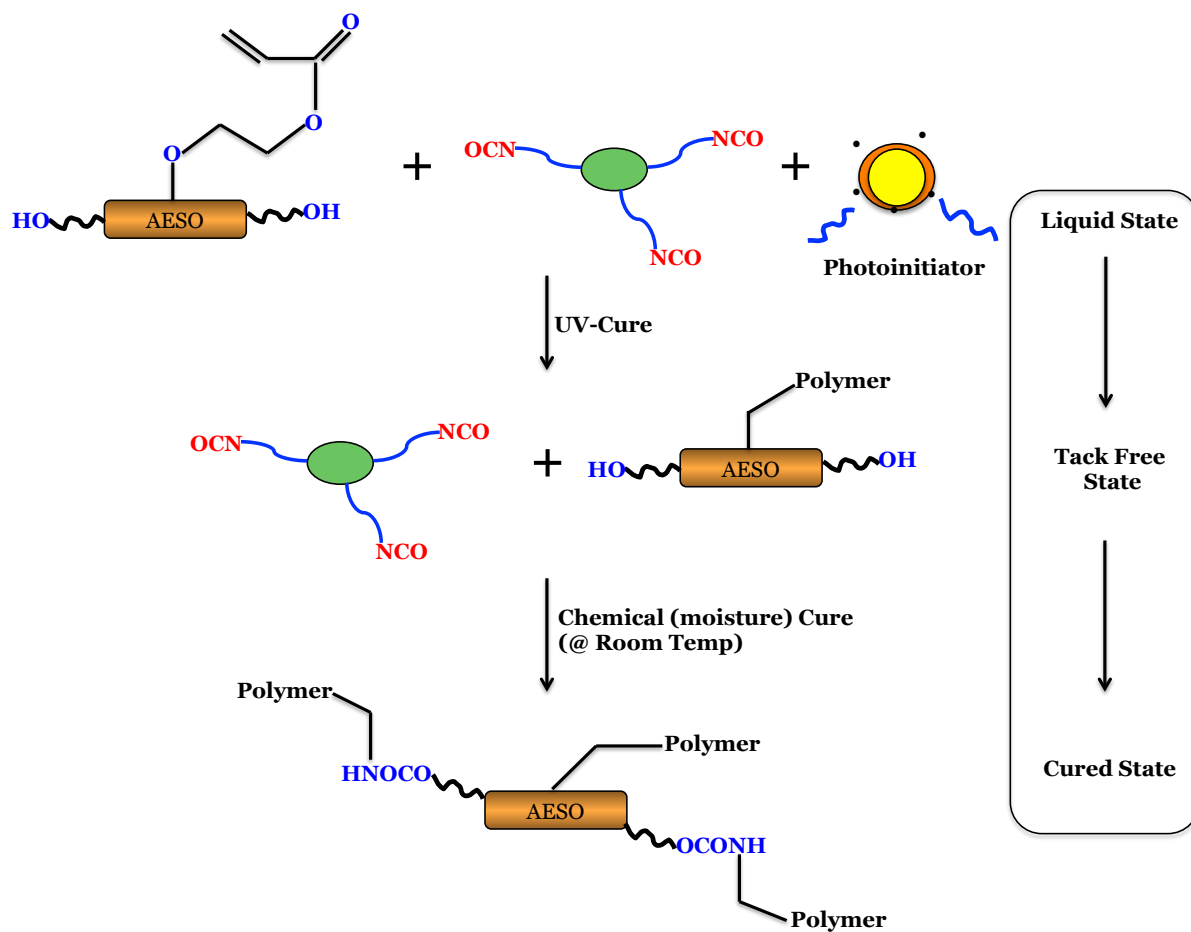


Figure 7.10: Schematic representation of dual cure acrylic polymer

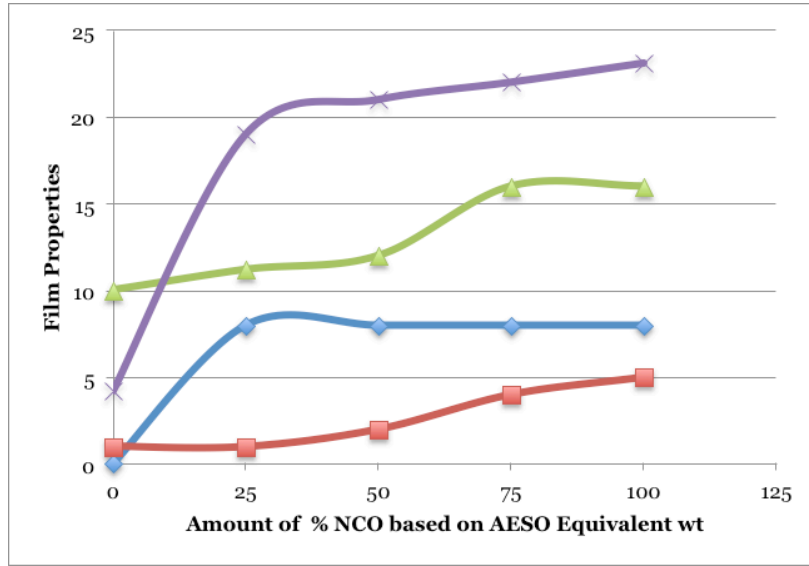
Unlike acrylic acid based AESO, HEA based AESO yields considerably low viscous oligomer, which requires low or no solvent in coating formulation. Table 7.6 represents the acrylic urethane coating formulation and its film properties using HDI trimer. Introduction of urethane groups in acrylic backbone further improved both flexibility and toughness of cured coating film that can be observed from Table 7.6 and Figure 7.11. Even with 25% of HDI, pendulum hardness, pencil hardness and MEK double rub have tremendously improved from respective properties of 0% of HDI formulation. Excellent properties were obtained with formulation-d, where 100% NCO was used in the formulation.

Generally introduction of urethane linkages in the coatings increases the thermal stability of polymeric film by increasing its  $T_g$ . Higher value of  $T_g$  shows higher degree of crosslinking.<sup>21</sup> As shown in Figure 7.12 increasing the urethane groups made the coating structure more compatible that resulted in increased  $T_g$ . Adjoined to reference<sup>20</sup> all acrylic-urethane coating systems behave like homogeneous polymeric networks with respect to storage modulus curves. No phase-separated (single peak mode from Figure 7.12) structures prove rapid curing followed by room temperature curing is not adversely affecting polymeric network. Also in glassy region increasing the urethane groups increases the storage modulus. Increase in intermolecular attraction between  $-NH$  &  $-CO$  through H-bonding and Polar–Polar interaction may be the reason for increase in compact structure.<sup>20,22</sup> Since, chain flexibility of molecules and crosslink density of coating film increased by urethane linkages,<sup>34,35</sup> high performance coatings were obtained with excellent hardness, flexibility, adhesion and MEK double rub value.

Table 7.6: Coating formulation and dual cured film properties of acrylic urethane coatings

COATING FORMULATION		A	B	C	D
AESO		5g	5g	4g	3.5g
Photoinitiator (Darocur 1173)		0.357g	0.463g	0.456g	0.473g
HDI Trimer (Desmodur N3300)		2.13g	4.26g	5.11g	5.96g
Catalyst (DBTDL – 10% in Toluene)		0.1g	0.1g	0.1g	0.1g
Hydroxyl to NCO Equivalent weight ratio		1:0.25	1:0.50	1:0.75	1:1
Amount of HDI used		25%	50%	75%	100%
(Based on OH - equivalent weight of AESO)					
<b>Resin and Cured Film Properties</b>					
Viscosity (cPs) @ 25°C		5080	4760	4280	3898
Dry Film Thickness (µm)		35	35	35	35
Pendulum Hardness (Koenig)		190	210	220	231
Pencil Hardness		8H	8H	8H	8H
Impact Resistance (lbs x inch)	Direct	112	120	160	160
	Reverse	100	100	140	140
MEK Double Rubs		> 400	> 400	> 400	> 400
Crosshatch Adhesion		B	2B	4B	5B

All the ingredients were mixed well and applied on to the untreated steel panel using automatic applicator bar. One-hour flash off was allowed before passing through ultra violet “D” bulb. All the panels were passed 3 times at 40 rpm. Tack free films were obtained immediately after passing through the UV source. Mechanical properties were checked after 7 days of condensation curing at room temperature.



(For Impact Resistance & Pendulum Hardness 1 unit in Y axis = 10 units of respective scale of property)  
0 to 6 scale used for Pencil Hardness where 0 = F and 6 = 6H hardness value)

Figure 7.11: Acrylic Urethane Dual Cure Film Properties

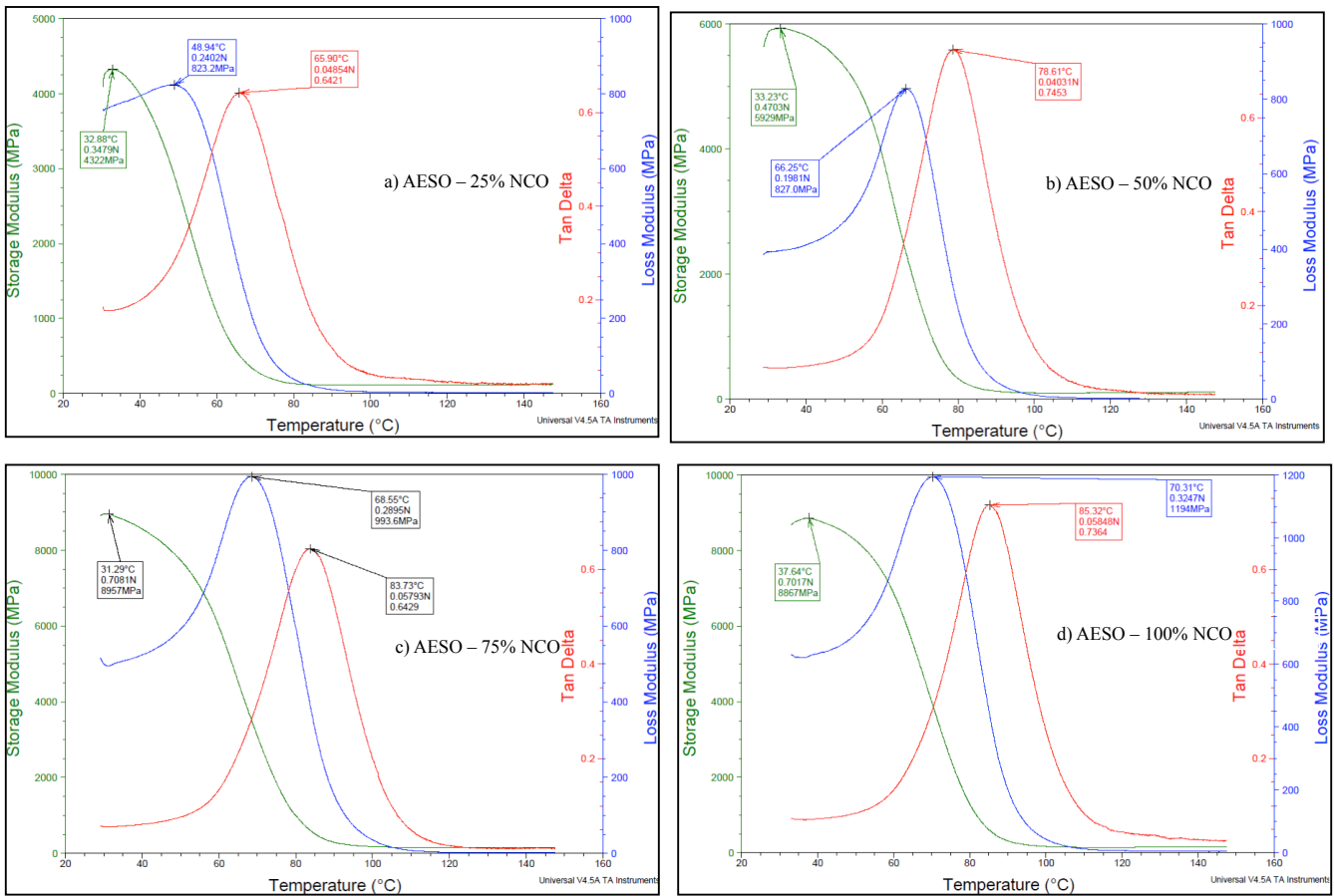


Figure 7.12: Dynamic Mechanical Analysis of Dual Cure Coating Films



Table 7.7: Interpretation of DMA Curve

Sample	Storage Modulus	Loss Modulus	Tg – Based on Tan Delta
a	4322 MPa (@ 32.88°C)	823.2 MPa (@ 48.94°C)	65.9 °C
b	5929 MPa (@ 33.23°C)	827.0 MPa (@ 65.25°C)	78.61 °C
c	8957 MPa (@ 32.88°C)	993.6 MPa (@ 68.55°C)	83.73 °C
d	8867 MPa (@ 37.64°C)	1194 MPa (@ 70.31°C)	85.32 °C

Sample dimension (mm) : 20 x 5.3 x 0.02 and Ramp rate: 3 °C/minute

### 7.5 Conclusion:

Novel bio-based UV-cure oligomers have successfully been synthesized from epoxidized soybean oil derivatives using hydroxyl functional acrylate compound in presence of strong acid catalyst. The process yields low viscosity products with very high degree of acrylation under mild reaction conditions. The results of spectroscopic analysis and chemical analysis confirm acrylation in high yields. The UV-cured and dual cured film properties of compositions studied suggest that AESO and AEME can be used as components of such coatings, and that these bio-based oligomers can significantly control mechanical properties. Thus, these high bio-based content soy-derived oligomers, when used in conjunction with petrochemical based derivative UV-cure coatings; offer systems with significantly reduced environmental impact.

## 7.6 Acknowledgement:

Authors sincerely acknowledge USDA for financial support under Cooperative State Research Education, and extension Services (CSREES) through grant award no. 2009-38303-05085 to Prof. Mannari. We also would like to express the deepest appreciation to Arkema Inc. Philadelphia and BASF, Delaware for providing us Epoxidized vegetable oils and photoinitiators, respectively.

## 7.7 Reference:

1. D.K. Chattopadhyay, S.S. Panda, K.V.S.N. Raju, *Progress in Organic Coatings*. 54 (2005) 10-19.
2. H. Dai, L. Yang, B. Lin, C. Wang, G. Shi, *J.Am. Oil Chem. Soc.* 86 (2009) 261-267.
3. Z. Liu, S.Z. Erhan, *J.Am. Oil Chem. Soc.* (2009).
4. D. Behera, A.K. Banthia, *Journal of Applied Polymer Science*. 109 (2008) 2583-2590.
5. A. Campanella, J.J. La Scala, R.P. Wool, *Polymer Engineering and Science*. (2009) 2384-2392.
6. M. Bajpai, V. Shukla, D.K. Singh, M. Singh, R. Shukla, *Pigment & Resin Tecnology*. 33 (2004) 160-164.
7. Y. Guo, J.H. Hardesty, V.Mannari, J.L. Massingill, *J. Am. Oil Chem Soc.* 84 (2007) 929-935.
8. E. Sharman, S.M. Ashraf, S. Ahmad, *Eur. J. Lipid Sci. Technol.* 109 (2007) 134-146.
9. S. Karatas, Z. Hosgor, Y.M. Menciloglu, N.K. Apohan, A. Gungor, *Journal Applied Polymer Science*. 102 (2006) 1906-1914.
10. A.Paramarta, T. Nelson, X. Pan, D.Webster, Joint 46<sup>th</sup> Midwest and 39<sup>th</sup> Great Lakes Regional Meeting of the American Chemical Society, St.Louis, MO, United States, October 19 – 22 (2011).

11. A. Paramarta, X. Pan, D. Webster, *241<sup>st</sup> ACS National Meeting & Exposition, Anaheim, CA, United States, March 27 – 31, 2011.*
12. A. Campanella, J.J. La Scala, R.P. Wool, *Journal of Applied Polymer Science.* 119 (2010) 1000 – 1010.
13. Z.S. Petrovic, A. Guo, J. Ivan, C. Ivana, D.P. Hong, *Polym. Int.* 57 (2008) 275–281.
14. Z. S. Petrovic, W. Zhang, I. Javni. *Biomacromolecules*, 6 (2005) 713–719.
15. R.L. Quirino, J. Woodford, R.C. Larock, *J. Appl Polym Sci.* (2011).
16. Y. Xia, R.C. Larock, *Macromolecular Materials and Engineering.* 296 (2011) 703 – 709.
17. M. Meier, J.O. Metzger, U.S. Schubert, *Chem. Soc. Rev.* 36 (2007) 1788–1802.
18. M. Meier, U. Biermann, U. Bornscheuer, J.O. Metzger, H.J. Schafer, *Angew. Chem. Int. Ed.* 50 (2011) 3854 – 3871.
19. S. Opera, *J. Mater Sci.* 45 (2010) 1315-1320.
20. G. Lligadas, J.C. Ronda, M. Galia, V. Cadiz, *Biomacromolecules.* 8 (2007) 686-692.
21. G. Lligadas, J.C. Ronda, M. Galia, U. Biermann, J.O. Metzger, *Journal Polymer Science: Part A: Polymer Chemistry.* 44 (2006) 634-645.
22. D. Harikrishna, K. Niranjan, *Prog. Org. Coat.* 66 (2009) 192-198.
23. Z. Alisa, L. Charlene, Z. Wei, P.S. Zoran, *Journal of Polymer Science: Part B: Polymer Physics.* 42 (2004) 809-819.
24. P. Jigarkumar, R. Senthilkumar, M. Vijay, *European Coatings Journal.* (2011) 125-129.
25. K.N. Shrikant, L.J. John, C. Erde, M.S. Shantaram, W.I. George, P.R. Giuseppe, K.H. Selim, W.P. Richard, *Journal of Applied Polymer Science.* 82 (2001) 703-723.
26. S.K. Brajendra, D.M. Kenneth, E.Z. Sevim, *Green Chem.* 9 (2007) 469-474.
27. S. Sinan, C. Gokhan, *Polym Int.* 59 (2010) 1122-1129.

28. Q. Luo, M. Liu, Y.J. Xu, M. Lonescu, Z.S. Petrovic, *Macromolecules*. 44 (2011) 7149-7157.
29. S. Eram, A.M. Syed, A. Sharif, *Eur. J. Lipid Sci. Technol.* 109 (2007) 134-146.
30. F. Liyu, Y. Liting, D. Chunlan, Z. Chengshan, M. Lijun, *Journal of Applied Polymer Science*. 117 (2010) 2220-2225.
31. H. Pelletier, A. Gandini, *Eur. J. Lipid Sci. Technol.* 108 (2006) 411-420.
32. S.S. Cutie, D.E. Henton, C. Powell, R.E. Reim, P.B. Smith, T.L. Staples, *Superabsorbent Gel Preparation*. (1996) 577-589.
33. Petrovic, Z., *Polymer Reviews*. (2008), 48, 1.
34. C.Xilei, H. Yuan, S. Lei, J. Chao, *Polym. Adv. Technol.* 19 (2008) 322-327.
35. R.Schwalm, L. Haeussling, W. Reich, E. Besk, P. Enenkel, K. Menzel, *Prog. Org. Coat.* 2 (1997) 191.

## **Chapter 8: UV-curable PUDs based on sustainable acrylated polyol: Study of their hydrophobic and oleophobic properties**

**Senthilkumar Rengasamy, Vijay Mannari**

*This chapter is published in Progress in Organic Coatings, (2013),*

*<http://dx.doi.org/10.1016/j.porgcoat.2013.11.029>.*

© 2013 Elsevier B.V. All rights reserved.

### **8.1 Abstract:**

UV-curable polyurethane dispersions (UV-PUDs) are fast expanding commercial applications since they combine benefits of both water-borne as well as UV-curing technologies while addressing many technical, environmental and performance benefits. Varying the compositions and cross-link density of UV-PUD polymeric chain backbone can control the film properties of UV-PUDs. There are many design restrictions posed by availability of commercial materials. In the present research work we demonstrate synthesis and application of a multi-functional acrylate polyol derived from soybean oil, as soft-segment of UV-PUDs. A series of UV-PUDs have been designed for high performance coatings that are specifically hydrophobic and oil-resistant. To this end, UV-PUDs based on acrylated soy-polyol have been further modified by siloxane and perfluoro compounds and their films with varying cross-link density have been investigated. The UV-PUD films were characterized for their film properties, particle size, contact angle and solvent swelling ratio. The outcome of this study provides useful insights into design considerations for hydrophobic and oil-resistant UV-curable coatings.

## 8.2 Introduction:

Polyurethanes are established as polymers of choice, due to their versatile structure-property relationship<sup>1-3</sup> in such industrial applications as coatings, sealants, adhesives textiles, foot-wear and rapidly expanding in many others.<sup>4-6</sup> The early development of polyurethanes for coatings was mainly limited to solvent-based or high-solid systems. Due to the environmental reasons and regulatory pressures water-borne polyurethanes (WPU) have emerged as compliant systems and have been offered both as one-component and two-component systems. Polyurethane dispersions (PUDs), a class of water-borne PUDs, are typically aqueous dispersions of high-molecular weight polyurethanes and have become very popular in recent years in coatings and related industries. While PUDs offer many technical and environmental advantages, their predominantly thermoplastic nature and relatively slow drying, limits their applications in many industrial coatings requiring high performance.

UV-cure technology is another environmentally friendly and sustainable technology adopted by coating industry and is fast advancing and expanding in products with myriads of end-use applications. In general, most common UV-cure systems are 100% liquids comprised of acrylate functional oligomers and reactive diluents along with a suitable photo-initiators. Upon UV irradiation these systems rapidly cure through radical-initiated addition polymerization to form cross-linked film structure. A three dimensional (3D) polymeric network formed by this solvent free UV-curable coatings give excellent resistance to chemicals, scratching and weathering.<sup>7,8</sup> Because of these advantages, UV-cure technology can be utilized in fast drying protective coatings,<sup>9,10</sup> printing inks, printing plates,<sup>11</sup> microcircuits and optical disks<sup>12-16</sup> besides many more. Such systems have advantages of low or zero VOC, very high cure speed, low energy consumption and provides coatings with high hardness, solvent resistance and very high

gloss due to their high cross-linked density. Despite these benefits, conventional UV-cure systems have some limitations, such as lack of flexibility, lower adhesion due to substantial film shrinkage, odor and skin irritation issues, and difficulties in handling after application (and before curing) due to their tacky nature.<sup>17</sup> One important shortcoming of such system is their applications for three-dimensional substrates that has shadow areas where the coating material has limited or no exposure to irradiation suffers from poor curing.<sup>18,19</sup> A dual-cure coating system having a ambient dry cure mechanism in addition to UV-curing can address the aforementioned problem.

Thus, a new generation systems called UV-PUD have been introduced to address the above stated limitations of both conventional and 100% solid UV-cure systems. UV-PUDs are essentially aqueous dispersions of polyurethanes containing UV-curable acrylate functionality. In UV-PUDs, PUDs having sufficiently high molecular weight are capped with acrylic functionality<sup>20,21</sup> which upon cure provides excellent solvent resistance and surface and bulk properties depending on their crosslinking density. The crosslink density is controlled by the molecular weight of PUD and functionality of the capping agents. In most commercial UV-PUDs the acrylate functionality is invariably introduced at the end of the polymer chain using end-capping acrylate compound of varying functionality.

The specific benefits of UV-PUDs are low or zero VOC, no need for reactive diluents, much lower shrinkage, reduced oxygen inhibition and ready to handle before UV cure due to their tendency to form dry-to-touch films even before UV-curing, due to their sufficiently high molecular weight.<sup>22</sup> Since water is used as continuous phase, viscosity is not an issue. Absence of reactive diluents makes UV-PUD technology more environmental friendly and free from odor and skin irritation issues. Due to the aforementioned distinct advantages, the UV-PUD

technology steadily extended its branches to many sectors of industrial applications.<sup>23-25</sup> The UV-PUDs exhibits excellent resistant to chemicals,<sup>23,26</sup> water,<sup>23,27</sup> mar<sup>28,29</sup> and weathering.<sup>23,30,31</sup> The conventional UV-cure systems where reactive diluents are used generally suffer from volume shrinkage upon curing. As Mequanint. K et al.<sup>32</sup> explained, the shrinkage is caused by conversion of non-bonding distances between the monomers are converted to shorter bonding distances in polymers. The shrinkage develops internal stresses responsible for delamination of films from underlying substrate over a period of time or even with minimal external forces. Unlike conventional UV-cured system, UV-PUD provides films with better flexibility due to low crosslink density of their films. Since crosslink density is low, the average MW between crosslinks is higher, and due to presence of urethane groups that results in tack-free film before irradiation.<sup>22,33</sup> These characteristics make UV-PUD more suitable for furniture and floor applications where handling of tack-free film become more useful during irradiation process.

In the present work we have designed and developed UV-PUDs with unique set of attributes. We have attempted to prepare “green” UV-PUDs that have high bio-based content (sustainability) and exhibit superior hydrophobicity and oil (hydrocarbon) resistance. In order to accomplish this goal, we have used a soy-based acrylated polyol developed earlier by our research group<sup>34</sup> and used that as a primary soft-segment of UV-PUD. It should be noted that unlike conventional UV-PUDs, these UV-PUDs have acrylate functionality on the soft-segment and thus is evenly distributed along the entire polymer chain. In order to make them hydrophobic and oil resistant, we have also incorporated polysiloxane diol as a component of soft segment. While soy-polyols are known to provide hydrophobicity to the film,<sup>35-38</sup> in order to enhance this property as well as to confer oil resistance of their films, PUDs were modified with perfluoro moiety in varying degree. Further, to study the effect of cross-link density of their UV-cured film



on various properties, polymer chains were end-capped with acrylate groups in varying degree. UV-cured film properties of these PUDs have been studied as function of their composition and cross-link density.

### **8.3 Experimental:**

#### **8.3.1 Raw Materials:**

Acrylic polyol (AESO) was derived from epoxidized soybean oil (ESO) (Arkema, USA, Vikoflex 7170) and polydimethylsiloxane diol (PDMS diol, Silmer OH-Di-10) was procured from Siltech Corporation, Canada. Isophorone diisocyanate (IPDI, Desmodur-I) was received from Bayer Material Science, USA and dimethylolpropionic acid (DMPA) from Geo Specialty Chemicals, USA were used as procured. Darocur<sup>TM</sup> 1173, a radical type photo-initiator was obtained from BASF, USA. All other raw materials such as triethylamine (TEA), N-methyl-2-pyrrolidone (NMP), acetone, dibutyltin dilaurate (DBTDL), 1,4-butanediol, tetrafluoroboric acid (HBF<sub>4</sub>) 48% in water, 2-hydroxyethyl acrylate (HEA), monomethyl ether of hydroquinone (MEHQ), diethyl ether, anhydrous magnesium sulfate, 4,4',5,5',5''-Pentafluoro-1-Pentanol (PFP) and 1-Heptanol (Hept) were purchased from Sigma Aldrich, USA and used as received.

#### **8.3.2 Methods of Characterization:**

Acrylated soy-oligomers have been characterized for oxirane oxygen content (ASTM D – 1652-97), acid number (ASTM D - 1639-96), iodine value (ASTM D - 5768-02) and hydroxyl number (ASTM D - 4274-05). Viscosity of the epoxidized vegetable oils and their derivatives were determined at 25°C using the Brookfield viscometer. Gel permeation chromatography (GPC) was used to determine the molecular weight of oligomers. Various UV-PUDs were mixed with 3% of free-radical type photo-initiator Daracure<sup>TM</sup> 1173 and applied on cold rolled steel panels (6"x4"x0.032") to ~50 micron wet film thickness and cured under UV-irradiation. A

UV-cure system (Fusion UV) with a D-bulb was used with the conveyor belt speed set to 40 feet/min. Using a compact radiometer (UVPS), the energy density measured was~ 2100 mJ/cm<sup>2</sup>. Properties of cured films were tested and compared after 7 days. The UV-cured film properties were characterized for pencil hardness (ASTM D – 3363), impact resistance (ASTM D - 2794-99), Adhesion (cross-cut) test (ASTM D - 3359-02), MEK double-rub test (ASTM D - 4752-98). BYK film thickness gauge was used to measure the dry-film thickness. Dynamic contact angle analyzer (First Ten Angstroms) was used to measure contact angles of cured PUD films. Swelling ratio of solvents (water and n-octane) were measured by immersion of 1 square inch of free films in respective solvent for 24 hours and measurement of % absorption based their weight gain. Swelling ratio was calculated as per the following formula.

$$\% \text{ Swelling Ratio} = \frac{\text{Final film weight} - \text{Initial Film Weight}}{\text{Final film weight}} \times 100$$

The stability of PUDs was monitored as per the following method. In a 20 ml glass vial containing, 10 g of PUD sample was placed in an oven maintained at 60°C. For up to 60 days, samples were observed weekly for their visual homogeneity, phase separation, change in viscosity, settling, and sedimentation. Sample was rated as “passed” if no such appreciable changes are observed. If such changes are observed, sample was rated as “failed”, with remark of days passed at 60°C temperature.

### **8.3.3 Synthesis of Soy-based Acrylic Polyol:**

Acryltated epoxidized soybean oil (AESO) was synthesized as per the procedure described earlier.<sup>34</sup> 2-Hydroxyethyl acrylate (150g) was placed into a 500 ml 3-neck flask equipped with a mechanical stirrer, reflux condenser with temperature controller, an inlet for nitrogen and an addition funnel. Flask was placed in a water-bath at room temperature under

stirring. MEHQ (1.5% by wt. of HEA) and  $\text{HBF}_4$  (0.5g) were added as a catalyst and mixture was heated to  $80^\circ\text{C}$  under stirring. ESO (150 g) was then added slowly into the flask through an addition funnel for about 45 min. After addition of ESO was completed, the reaction was allowed to continue at  $80^\circ\text{C}$  until desired oxirane oxygen content (less than 0.05%) was obtained. Reaction product was then dissolved in diethyl ether and transferred into a separating funnel. Excess and unreacted HEA was removed by washing the ethereal solution several times with DI-water. The ether layer was separated and dried using anhydrous magnesium sulfate. Ether was then evaporated from the final product under reduced pressure. The obtained yellowish acrylated oligomeric polyol was stored in refrigerator in a glass bottle. Figure 8.1 represents the schematic reaction step for synthesis of AESO.

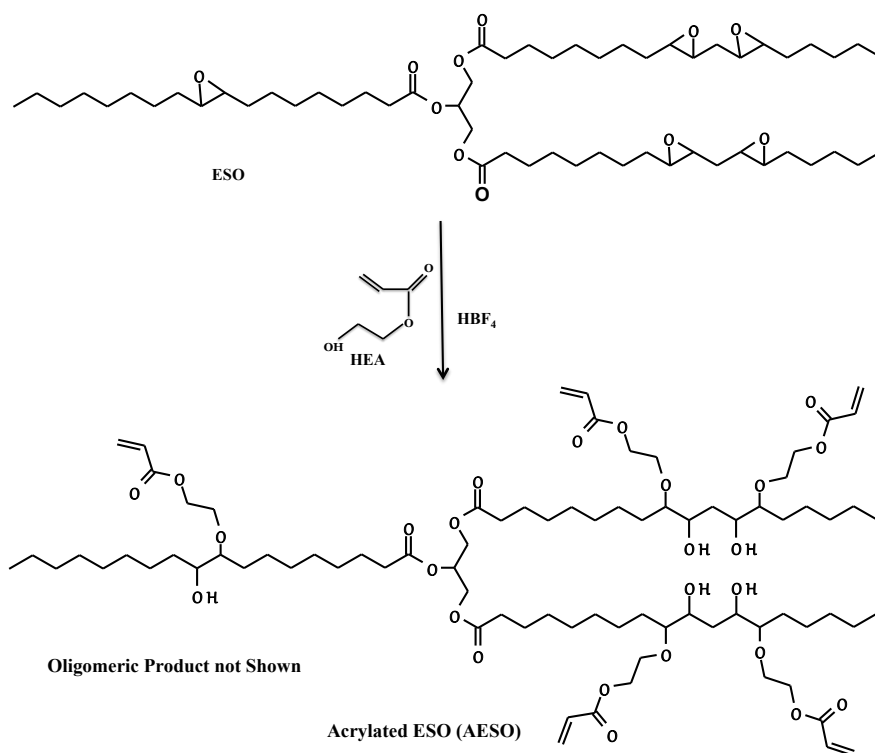


Figure 8.1: A simplified synthetic scheme for acrylated ESO (Oligomeric product not shown)

### 8.3.4 Synthesis of Silylated and Fluorinated UV-PUDs:

Calculated amount of acrylated AESO (Polyol), PDMS diol, NMP, DMPA and 1,4 butane diol were placed in a 3-neck flask connected with mechanical stirrer, water condenser, nitrogen inlet and outlet and heating mantle connected with temperature controller. Reaction was carried out at 80°C until DMPA was completely dissolved in polyol and NMP mixture. DBTL catalyst (0.01% by weight of total reaction mass) was added at this point. Then IPDI was slowly added into the reaction mixture within approximately 45 minutes. A sample of reaction mixture was drawn at every 30 minutes and tested for % isocyanate content (ASTM D 2572-97). When desired % isocyanate content was reached, reaction mixture was cooled down to ~50°C and calculated amount of triethylamine (neutralizer) was added (degree of neutralization ~ 100%) and the mixture was stirred for 30 minutes. Immediately after neutralization, pre-polymer was end-capped with HEA, PFP, Heptanol or their combinations as showed in Table 8.1 and Table 8.2, appropriate component and stirring the reaction mixture at 80°C until %NCO content was close to 0%. Figure 8.2 shows the general reaction scheme for synthesis of silicone and fluorine containing UV-PUDs. As shown in Table 8.1 and Table 8.2, two different series of UV-PUDs were made in this research work. In the first series (F1-F5), with the use of 1-Heptanol as end-capping agent crosslink density was kept constant by varying the amount of pentafluoropentanol (PFP) and n-heptaol as end-capping agents. In the second series (F6-F9), crosslink density of the systems were varied by end-capping the chains with HEA in varying degree. However, it should be noted that for both the series amount of polyols used in soft-segment was kept constant along with their acid value and degree of neutralization.

Table 8.1: UV-PUD Compositions in millimoles

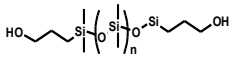
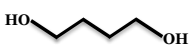
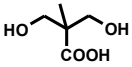
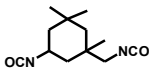
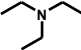
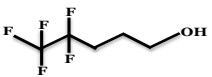
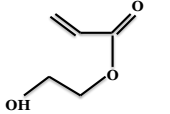

UVPUD - Composition	Chemical Formula	Mw (g/mol)	Constant Crosslink Density				Control	Increasing Crosslink Density			
			F1	F2	F3	F4		F5	F6	F7	F8
AESO - OH	Figure 8.2	1842	3.0	3.0	3.0	3.0	3.0	3.0	3.0	3.0	3.0
PDMS polyol		1000	4.0	4.0	4.0	4.0	4.0	4.0	4.0	4.0	4.0
1,4 Butane diol		90	1.0	1.0	1.0	1.0	1.0	1.0	1.0	1.0	1.0
DMPA		134.13	10.0	10.0	10.0	10.0	10.0	10.0	10.0	10.0	10.0
IPDI		222	31.0	31.0	31.0	31.0	31.0	31.0	31.0	31.0	31.0
TEA		101	9.0	9.0	9.0	9.0	9.0	9.0	9.0	9.0	9.0
PFP		178	13.0	9.0	4.0	0.000	17.0	13.0	9.0	4.0	0.000
2HEA		116.12	-	-	-	-	-	4.0	9.0	13.0	17.0
1-Heptanol		116.2	4.0	9.0	13.0	17.0	0.000	-	-	-	-

Table 8.2: Characteristics of UV-PUD Compositions

UVPUD - Composition		Constant Crosslink Density				Control	Increasing Crosslink Density			
		F1	F2	F3	F4	F5	F6	F7	F8	F9
Soft Segment (% by Wt.)	AESO – Polyol	30	30	30	30	30	30	30	30	30
	PDMS-diol	20	20	20	20	20	20	20	20	20
End-Capping Agents (% by Wt.)	Pentafluoro pentanol (PFP)	75	50	25	0	100	75	50	25	0
	2HEA	0	0	0	0	0	25	50	75	100
	1-Heptanol	25	50	75	100	0	-	-	-	-
DMPA (mgs. KOH/g)	DMPA (mgs KOH/g)	30	30	30	30	30	30	30	30	30
NCO to OH Ratio*	NCO Index	1.4	1.4	1.4	1.4	1.4	1.4	1.4	1.4	1.4
Neutralization	TEA	90	90	90	90	90	90	90	90	90
Weight Per Acrylate	-	1622.0	1622.0	1622.0	1622.0	1622.0	1225.3	975.6	804.1	678.9
* NCO to OH ratio is based on equivalent weight										

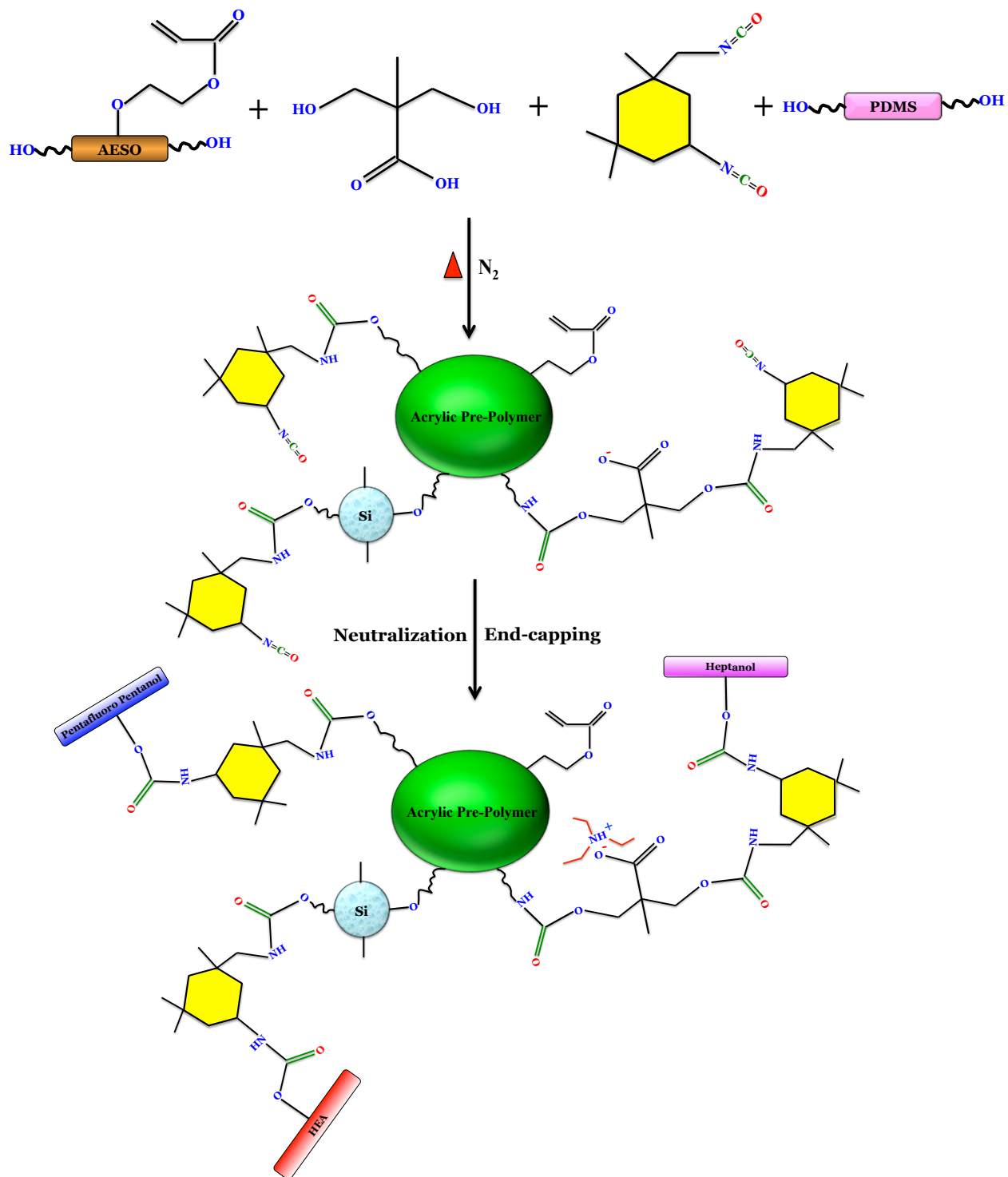


Figure 8.2: General reaction scheme for synthesis of silylated and fluorinated UV-PUDs. (For illustration purpose all three end-capping agents were showed in the Figure 8.2)

## **8.4 Results and Discussion:**

### **8.4.1 Design of UV-PUDs:**

The objective of our research is to develop value-added functionalized polymeric materials from agro-based renewable resources that can be utilized in aqueous UV-curable polyurethane dispersions with high hydrophobic and oil-resistance characteristics. In conventional UV-PUDs, acrylate moieties are introduced on to the polyurethane chain-ends by end-capping the NCO-terminated chains with hydroxy-acrylate compounds. End-capping compounds with varying acrylate functionality are used to vary cross-link density of the cured films. Introduction of acrylate groups throughout polymeric chain backbone (both in soft segment and hard segment) might result in improved crosslink density due to which chemical resistance and mechanical properties of coatings can be further improved. Also, the introduction of acrylate groups at the soft segment gives the flexibility of using other end-capping (or chain extending) compounds that can improve functional performance of coatings. In this study pentafluoro pentanol (PFP) has been used as end-capping agent to improve hydrophobicity and/or oil-resistance. Our earlier research work<sup>35</sup> showed the synergistic effect of soy polyol and PDMS diol in improving hydrophobicity of PUD films. We intend to leverage this observation in UV-PUDs, along with the introduction of dangling hydrophobic perfluoro chain-ends, known to improve oil resistance. Thus, we have designed UV-PUDs with soy-based acrylated polyol and PDMS-diol as soft-segments and acrylate / perfluoro moieties at the chain ends. Cross-link density has been varies by varying the content of acrylate end-capping compound, 2-HEA.



#### 8.4.2 Synthesis of Acrylated Epoxidized Soybean Oil (AESO):

Most commercially available (and also used by many researchers) acrylated epoxidized soybean oil is prepared by direct esterification of ESO with acrylic acid. In such a reactions, in addition to formation of acrylate esters, significant degree of etherification (oligomerization) due to oxirane-oxirane and/or –hydroxyl-oxirane reaction also occurs. This type of reaction yields the final product with high viscosity. In this research work, we have used AESO prepared by reaction between ESO and 2-hydroxyethyl acrylate that has several technical benefits. A comparison of these two types of AESO has been presented in our earlier research paper.<sup>34</sup> As mentioned earlier, AESO has been chosen as one of the soft segment due to the presence of pendent acrylate functionality as well as its unique hyper-branched structure that is thought to afford interesting properties, besides hydrophobicity due to its triglyceride structure containing fatty acid moieties. Table 8.3 shows characteristics of AESO. In the synthesis of AESO, the oxirane oxygen contents of the reaction mixture were monitored throughout the course of reaction to track the progress of reaction. The final product was characterized for acid number, hydroxyl number, iodine number, viscosity and molecular weight. The results in Table 8.3 conclude that cationic ring opening of ESO by HEA in the presence of super acid catalyst is feasible and the product with high acrylation can be obtained. The GPC data ( $M_n = 1842$ ) indicates that there is some degree of oligomerization taking place under the reaction conditions employed. A detailed characterization of AESO can be obtained from our previous publication.<sup>34</sup>

Table 8.3: Characteristics of ESO and AESO

Properties	ESO	Acrylic Polyol (AESO - OH)
Oxirane Oxygen Content (%)	7.0	0.0
Iodine Number (g Iodine/100g)	2.5	52.2
Acid Number (mgKOH/g)	0.5	1.80
Viscosity (cPs) @ 25°C	417	5406
Hydroxyl Number (mgKOH/g)	0	113
Number Average Molecular Weight (Mn) g/mole (GPC)	993	1842

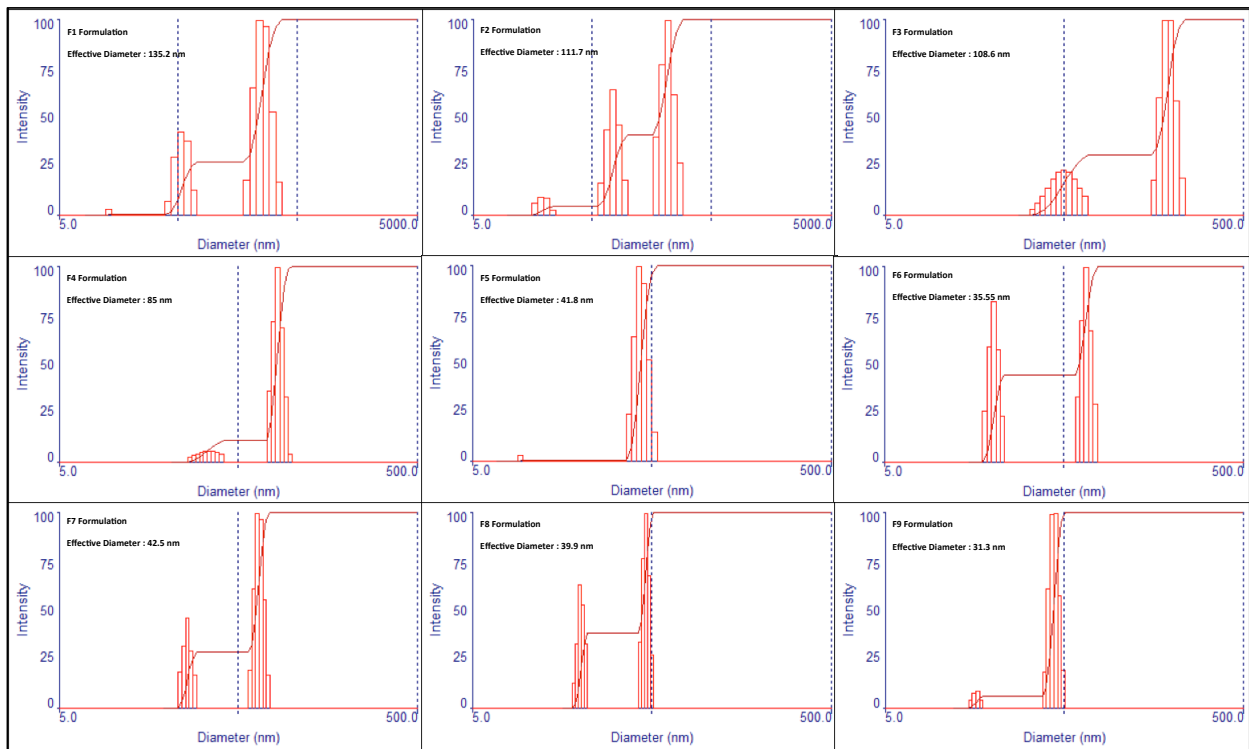


Figure 8.3: Average Particle Size of UV-PUDs

Table 8.4: Characteristics of UV-PUDs and their Cured Film Properties

UV-PUDs and Their Cured film properties		Constant Crosslink Density				Control	Increasing Crosslink Density			
		F1	F2	F3	F4	F5	F6	F7	F8	F9
Average Particle Size (nm)		135.2	111.7	108.6	85	41.8	35.55	42.5	39.9	31.3
Stability (@ 60° C for 60 days) Days passed		48	52	52	60	60	60	60	60	60
Stability in months (@ Room Temperature)		>7	>7	>7	>7	>7	>7	>7	>7	>7
Koenig Hardness (Before UV-Cure)		56	39	36	28	40	42	45	56	59
Koenig Hardness (After UV-Cure)		148	138	118	116	120	125	132	143	151
Pencil Hardness		2H	2H	2H	F	3H	3H	3H	3H	3H
MEK Double Rub		20	20	0	0	30	30	45	45	60
Cross-Cut Adhesion Strength		5B	5B	5B	5B	5B	5B	5B	5B	5B
Impact Resistance (lbs.inches)	Front	>160	100	140	>160	>160	>160	>160	20	20
	Back	>160	100	140	>160	>160	>160	>160	0	0
Film Thickness (mil)		≈1.0	≈1.0	≈1.0	≈1.0	≈1.0	≈1.0	≈1.0	≈1.0	≈1.0

### 8.4.3 Average Particle Size and Stability of UV-PUDs:

As shown in Table 8.4 and Figure 8.3, the mean particle size of the PUDs from constant crosslink density (CCD) series ranges from 85 to 135.2 nm and those for increasing crosslink density (ICD) series, ranges between 31.3 nm to 42.5 nm. The average particle diameter of PUDs particles in CCD series linearly increased with increasing pentafluoro pentanol content for samples F1-F4. This can be attributed to increasing hydrophobicity of pentafluoro pentanol compared to 1-heptanol. In general, with other factors being comparable, hydrophobic polymers tend to produce larger particles during dispersion process compared to hydrophilic polymers.<sup>39</sup> However, it is surprising to note that sample F5 with highest pentafluoropentanol content showed lowest particle size. This could be due to the fact that F5 sample has only one type of hydrophobic end-capper compared to two-types of hydrophobic end-cappers in samples F1-F4. We do not have any good explanation for lower particle size observed for sample F5. Surprisingly, this linear pattern cannot be viewed in ICD series where pentafluoro pentanol/2EHA ratio was varied as shown in Table 8.2. However, it is important to mention that ICD series exhibit particles with much smaller hydrodynamic diameter than CCD series. The particle size of the PUD can be influenced by concentration of IPDI, processing temperature, amount of DMPA, degree of neutralization, molecular weight of PUD particle, type and amount of chain extenders or end-capping agents and hydrogen bonding.<sup>39</sup> In the present study for both CCD and ICD series, all the aforementioned parameters have been kept constant except the type and ratio of end-cappers used. It is, therefore, very clear that particle size is significantly influenced by the nature of end-capping group. In CCD series the variable end-capper used is 1-heptanol whereas that for ICD series is 2-HEA. 1-heptanol with its aliphatic straight chain structure is much more non-polar and hydrophobic while 2-HEA with ester group makes it much more polar

and hence hydrophilic. Therefore UV-PUDs containing 1-heptanol end-capper along with PFP show larger particle size than ICD series. The lower average particle size for PUDs of ICD series is mainly due to contribution of hydrophilic 2-HEA, increasing 2-HEA content does not show significant reduction in particle size.

#### **8.4.4 Cured Film Properties:**

In general, PUDs are segmented polymeric chain that consists of soft segment and hard segment. These segments are thermodynamically incompatible in nature that results in increased phase separation between segmented domains.<sup>35</sup> All 9 formulations have 30% AESO and 20% PDMS as soft segment. The hard segments are comprised of urethane groups from IPDI and DMPA moieties or IPDI and hydroxyl groups of end cappers. These hard and soft segments play a significant role in controlling mechanical properties of cured films. In thermoplastic urethanes, in general, cured film's flexibility (impact resistance) can be explained by soft segments whereas strong hydrogen bonding of urethane groups from hard segments that play a key role in film hardness, modulus and chemical resistance.<sup>27</sup> In case of cross-linked polyurethanes, in addition to above, cross-link density plays a significant role in governing their physical, mechanical and chemical resistance properties.<sup>35</sup>

The UV-PUDs developed in this study uses acrylic polyol derived from vegetable oil. While this is essentially a soft segment, it also contains cross-linkable acrylate functional groups, which serve as cross-linking site. Also note that these are the only cross-linking sites in CCD series samples. In case of ICD series, the PU chains are end-capped with acrylate groups through HEA. These crosslinked structures can increase the coating performance to certain extent.<sup>22</sup> In this research work, we have investigated the effect of both composition and cross-link density on various film properties discussed in below paragraph.

As mentioned earlier, crosslink density of the CCD series was kept constant by maintaining acrylic moieties only at soft-segment and keeping the amount of AESO equal from F1 to F5 formulation. So, the only possible explanation for differences in mechanical and chemical resistance would be the type and amount of end-capping agents used in the formulation. It can be viewed from Table 8.4, though there are no significant differences in pencil hardness, the effect of pentafluoro pentanol (PFP) content on cured films hardness can be clearly explained from Koenig hardness values. It is clear as PFP content increased the hardness of the film also increased linearly. Interestingly, the F5 formulation in which 100% of excess NCO from pre-polymer was end-capped with PFP yielded lower Koenig hardness value than the F1 and F2 formulations, where only 75% and 50% of excess NCO from pre-polymer was respectively end-capped with PFP. This phenomenon is the result of bimodal particle size observed in F1 and F2 formulations. Approximately 45 to 50% of the particle size intensity observed in both F1 and F2 formulation is less than their original effective particles size diameter. This smaller and bigger particle arrangement can aid effective coalescence of film, which resulted in improved film hardness. Even though, it is minimal the effect of PFP content in MEK double rub can be still recognized from CCD series. The low swelling nature of fluorine containing polymers to MEK resulted in increased chemical resistance for fluorine rich PUDs.

As can be seen from Table 8.4, the overall impact resistance of cured UV-PUD films is better for CCD series than ICD series. This is due to the available crosslink density via acrylate moieties, which are less for CCD series than ICD series. The reduced crosslink density of CCD series gives flexibility to the overall polymeric chain that resulted in improved impact resistance. In UV-PUD (ICD series), crosslink density with respect to acrylate functionality changes molecular structure and molecular weight of the cured polymeric chain. This can be viewed

from F8 and F9 UV-PUD where the end-capping group HEA was used as 75% and 100% respectively. The increased acrylate functionality increased the crosslink density so as the flexibility of entire film decreased. In other words, crosslink density influences the hardness of the acrylic PU film. Since, there are no significant differences in pencil hardness, the crosslink density effect can be determined from Koenig hardness values. As the acrylate functionality of the hard segment gradually increased in ICD series, the pendulum hardness of the film increased linearly. The increase in crosslink density also increases the cross-linked polymer molecular weight. Since, the molecular weight of the polymeric chain between each cross-linked network increased, the restriction of molecular mobility also increased. Thus increased hardness and reduced impact strength for ICD series. The increase in crosslink density is also reflected in chemical resistance (MEK double rub) of cured films. The ICD series MEK double rub values ranges from 30 to 60 than its respective counter PUDs in CCD series. The MEK double rub values obtained in F1 and F2 can be correlated with presence of fluorine molecule. The increase in fluorine content improved the chemical resistance. The chemical resistance value obtained from F1 to F5 proves the aforementioned theory. The F5 formulation was made to see the fluorine content effect alone in hard segment and corresponding mechanical properties cured film. Normally UV curable coatings suffer from shrinkage that results in poor adhesion. It seems one of the striking benefit of the developed bio-based UV-PUDs are excellent adhesion strength. The flexible triglyceride chain from AESO polyol might have helped to reduce shrinkage and the strong hydrogen bonding from urethane groups might have also aided in adhesion strength.

#### 8.4.5 Contact Angle:

The Table 8.5 and Figure 8.4 was utilized to investigate the effect of constant crosslink density (F1 to F5), increasing crosslink density (F5 to F9) and % perfluoro content on water and oil (hexadecane) contact angle on cured surface of the films.

In F1-F5 series, PFP content was varied from 0% to 100%, with corresponding changes in hydrocarbon (1-heptanol) content. The results show that water-contact angles of samples increases appreciably with increasing perfluoro content. Since perfluoro moieties are known to confer hydrophobicity to the surfaces, this observation is consistent with literature results.<sup>34,39-40</sup> However, the hexadecane contact angles, which used as measure of oleophobicity of these films, are nearly constant indicating that perfluoro content has no significant effect on oleophobicity of the films. In other words, the polyurethane chains end-capped with hydrocarbon chains or perfluoro chains of comparable size have no significant effect on oleophobicity of the developed UV-PUD surfaces. The coating surfaces of ICD series (F5-F9) exhibit very similar behavior to those in CCD series (F1-F5) with respect to their hydrophobicity and oleophobicity.

It is interesting to compare results of contact-angles of counterpart samples across the CCD and ICD series. Comparison of counter-part samples (F1 and F6, F2 and F7 and so on...) with identical perfluoro content but varying cross-link density shows that the samples of CCD series have slightly higher water contact-angles compared to their ICD counterparts. We attribute this small difference in water-contact angles to the presence of liner aliphatic heptane group at the chain ends in CCD series that are more hydrophobic in nature compared to polar acrylate ester groups at the chain end in ICD series samples.

Based on these observations it can be concluded that polyurethanes containing perfluoro end-groups have significant impact on hydrophobicity of their film surfaces and such effect



increases with increasing perfluoro content. Further, hydrophobicity of such surfaces does not seem to be substantially affected by degree of crosslinking of the films.

Table 8.5: Average Contact Angle UV-PUDs

UV-PUD Type & Formulation Number		End-Capping Groups (%)	Average Contact Angle (°)	
			Water	Hexadecane
<b>Constant Cross-link Density</b>	F1	25Hept:75PFP	107±5	34.2±4
	F2	50Hept:50PFP	104±2.5	32±2
	F3	75Hept:25PFP	98±2.5	32±3
	F4	100Hept:0PFP	96±3	28±4
<b>(100% PFP end-capping)</b>	F5	100 PFP	104±2	35±2
<b>Increasing Cross-link Density</b>	F6	25HEA:75PFP	103±4.5	34±3
	F7	50HEA:50PFP	101±4	32±4
	F8	75HEA:25PFP	95±4	34±3
	F9	100HEA:0PFP	91±3	26±2.5

#### 8.4.6 Hydrophobic and Oleophobic Properties based on Swelling Ratio of Solvents:

The Table 8.6 and Figure 8.5 represent the water and oil absorption of constant crosslink density, increased crosslink density and control UV-PUDs. The control UV-PUD (F5) in which 100% excess NCO was terminated with fluorine compound showed 17.21% weight increase in water and 2.92% weight increase in oil after immersing 1 square inch free films in respective solvents for 24 hours. As mentioned earlier, in a view to further study the hydrophobic and oleophobic properties, stoichiometric amount of fluorine compound was replaced with 2-HEA and 1-heptanol as shown in Table 8.6. Effect of constant crosslink density (F1 to F5) and

increased crosslink density (F5 to F9) was compared with control sample (F5). It can be clearly viewed from Figure 8.5 that increasing the crosslink density significantly improved the water and oil resistance properties, especially at higher crosslink density. Figure 8.6, represents the percent increment or decrement of various UV-PUDs compared to control UV-PUD (F5). Although 1-heptanol shows some hydrophobic effect in coating's surface, as in bulk property, replacing PFP with 1-heptanol increased the water absorption when amount of 1-heptanol exceeds the amount of PFP in the end-capping unit. This can be viewed from F3 and F4 formulation where water absorption by weight increased respectively 5.17% and 6.68% with respect to control F5. This could be explained based on a C-F bond characteristic. Compared to F3 and F4, better water resistance with fluorine rich F5 formulation was achieved due to the strength of carbon-fluorine bond and the steric hindrance arising from strong forces between hydrogen and fluorine atoms.<sup>41</sup> Thus, replacing fluorine moiety with 75% (F3) and 100% (F4) 1-heptanol resulted in less steric hindrance due to which more water was absorbed in the final cured film. This steric hindrance was not adversely affected, when only 25% (F1) and 50% (F2) PFP was replaced with 1-heptanol. Besides the combination of 1-heptanol and PFP in F1 and F2 resulted in higher water resistance compared to control F5 formulation. This could be the result of optimum formulation (F1 & F2), where the end-capping ratio of 1-heptanol and PFP were perfectly aligned in order to benefit from both long carbon chain of 1-heptanol and strong electronegativity of fluorine. Where as for oil absorption replacing the PFP with 1-heptanol adversely affected the oil resistance, which can be viewed from CCD section of Figure 8.5.

Interestingly replacing the PFP with HEA increased the overall water resistance of coatings. It can be seen from Figure 8.5 that 100% replacement of PFP with HEA improved 24.75% water resistance of coatings. Overall ICD series improved both water and oil resistance

of crosslinked UV-PUDs compared to control and CCD series. Increasing the crosslink density reduces the free volume of the cured film matrix, resulting in reduced diffusion of water / solvent in the matrix and hence improves water/solvent resistance. As noted in water resistance values of ICD series, crosslink density governs the swelling of polymer in water. The crosslink density achieved with 25% HEA (F6) and 50% HEA (F7) UV-PUDs were not high enough to achieve excellent oil resistance properties. Since tremendous crosslink density can be achieved with higher amount of HEA, the UV-PUDs with 75% (F8) and 100% (F9) HEA in end-capping groups achieved excellent oil resistance than control UV-PUD. The UV-PUD (F9) end-capped with 100% HEA absorbed 70.548% less oil than control UV-PUD.

Table 8.6: Water and n-Octane Absorption (%) of UV-PUDs

UV-PUD Type & Sample Identity		End-Capping Groups (%)	Absorption (% by wt.)	
			Water	n-Octane
<b>Constant Cross-link Density</b>	F1	25Hept:75PFP	14.56	3.36
	F2	50Hept:50PFP	15.59	4.06
	F3	75Hept:25PFP	18.10	5.68
	F4	100Hept:0PFP	18.36	5.74
<b>(100% PFP end-capping)</b>	F5	100 PFP	17.21	2.92
<b>Increasing Cross-link Density</b>	F6	25HEA:75PFP	16.88	3.33
	F7	50HEA:50PFP	14	3.17
	F8	75HEA:25PFP	13.04	1.69
	F9	100HEA:0PFP	12.95	0.86

Comparing both CCD and ICD series from Figure 8.5 and Figure 8.6 clearly show that

effect of cross-link on both water and oil absorption is much more profound as compared to that of their PFP content. For example, comparison of sample F3 and its counterpart F8 (both have 25% PFP) shows that sample F3 absorbed 28% more water and 70% more oil than sample F8. This effect is relatively lower at lower cross-link density (F2 absorbed 10% more water and 22% more oil than F7) but much higher as crosslink density increases (F4 absorbed 29.5% more water and 94% more oil than F9). This clearly shows that while PFP content has influence on water and oil resistance, their cross-link density is a much stronger factor. Thus it is possible to tailor these properties into PU coatings by controlling both cross-link density and polymer composition.

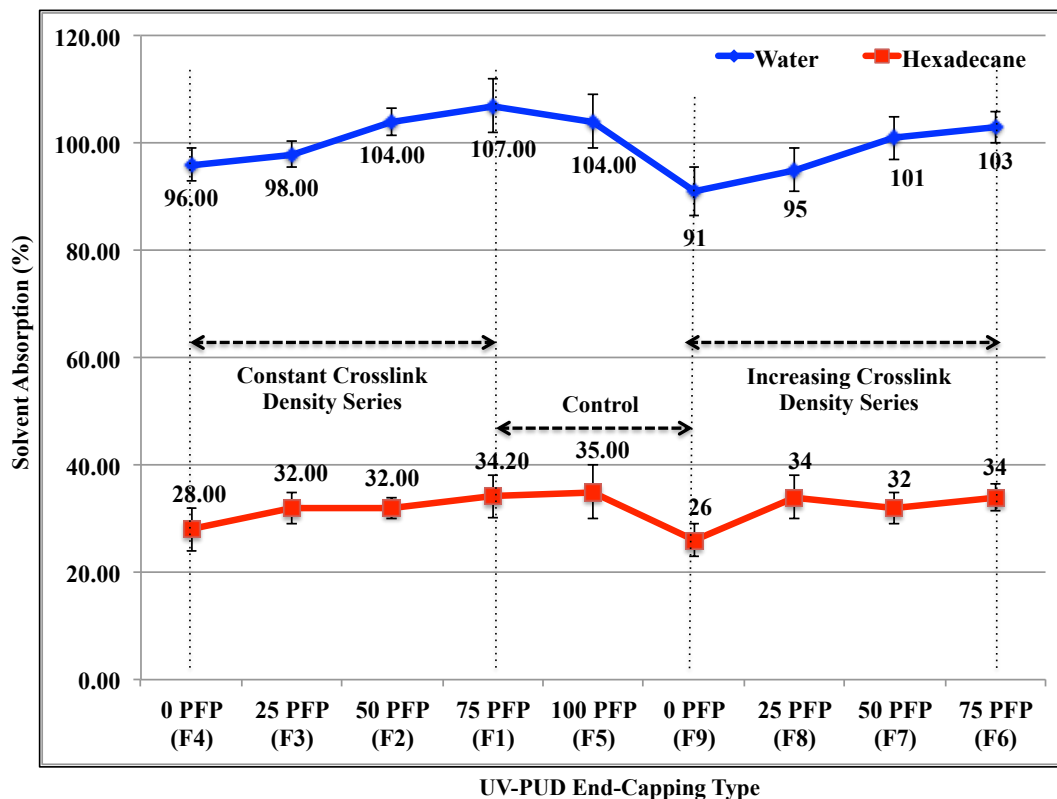


Figure 8.4: Water and Hexadecane Contact Angle of UV-PUDs

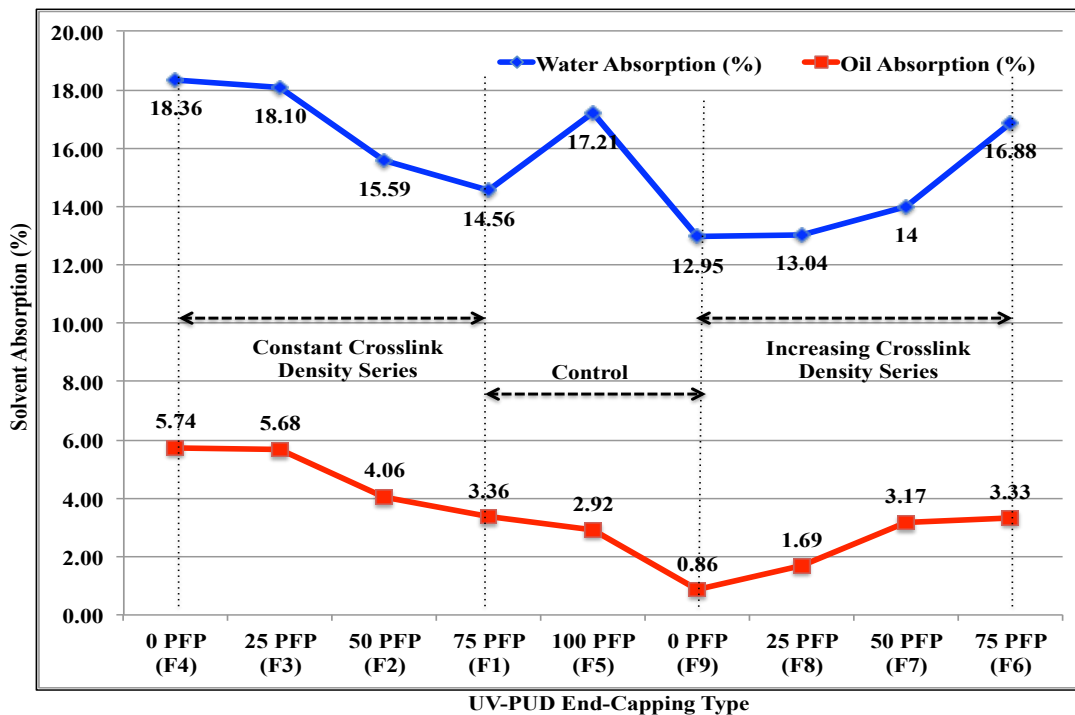


Figure 8.5: Solvent absorption of UV-PUDs

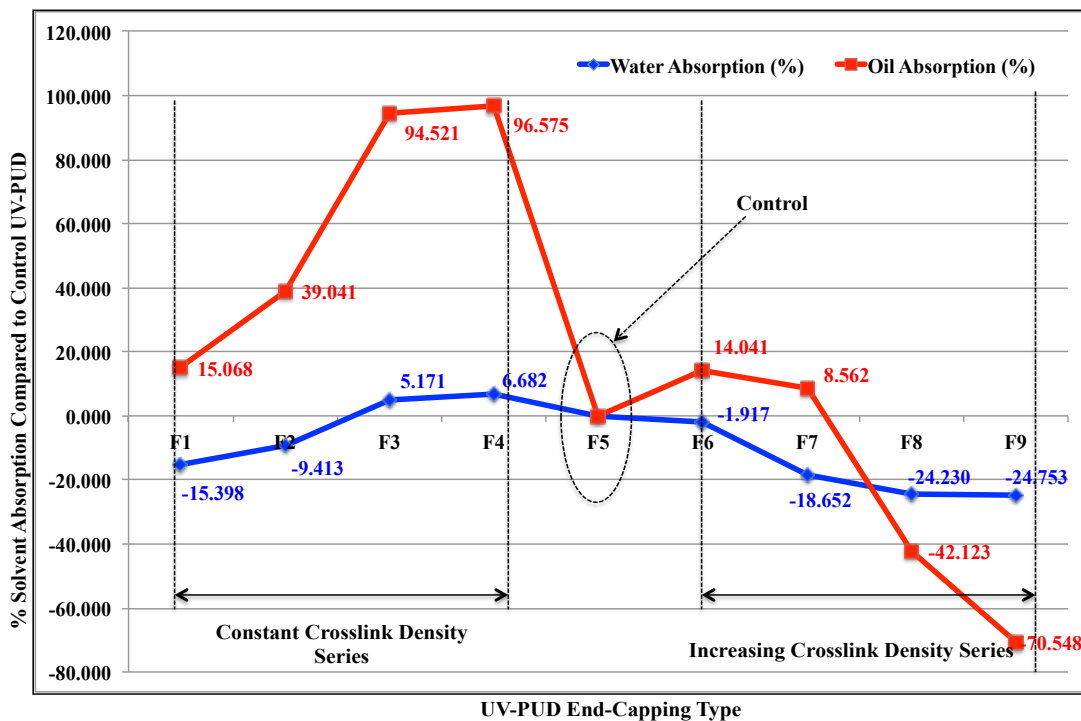


Figure 8.6: % Solvent absorption compared to control UV-PUD (For illustration purpose F5 was started with 0% value)

## 8.5 Conclusion:

UV-PUDs based on the PFP, 2-HEA and 1-heptanol have been designed and synthesized with different ratio of PFP to 2-HEA and PFP to 1-heptanol as end-capping agents in order to get ICD and CCD series of UV-PUDs respectively. The soft-segment of UV-PUDs were designed with indigenous hydroxylated AESO and commercial hydroxylated PDMS.

Regarding the effect of end-capping agents, CCD series resulted in bigger particles size than ICD series due to more hydrophobic seven carbons (1-heptanol) polymeric chain in UV-PUD backbone. The coatings obtained with CCD series were more flexible than ICD series which can be observed from impact resistance of coatings. Whereas, both film hardness and MEK chemical resistance improved with increasing the crosslink density of UV-PUD.

In CCD series alone increasing the PFP content proven to be the reason for higher water and oil resistance properties. Whereas in ICD series increasing the cross-link density resulted in higher water and oil resistance. Comparing the CCD series with ICD series suggested that crosslink density is the overriding factor to achieve optimum water and oil resistance properties. Excellent water resistance and oil resistance coatings were achieved with the UV-PUDs end-capped with 100% HEA with no fluorine compound in polymeric chain backbone. Compared to 100% pentafluoro pentanol end-capped UV-PUD, 100% HEA end-capped UV-PUD showed 24.75% more water resistance and 70.54% more oil resistance in solvent absorption values.

## 8.6 Acknowledgement:

Authors sincerely acknowledge USDA for financial support under Cooperative State Research Education, and extension Services (CSREES) through Grant award no. 2009-38303-05085. We would also like to express the deepest appreciation to Arkema Inc. Bayer MaterialScience LLC, Siltech Corporation, GSI Exim America Inc. and Geo Specialty Chemicals for providing raw materials respectively ESFAME, IPDI, PDMS Polyol, Carbodiimide and DMPA.

## 8.7 References:

1. Furukawa, M., Hamada, Y., & Kojio, K. *J. Polym. Sci., Polym. Phys.*, *41*, (2003), 2355–2364.
2. Kim, B.S., & Park, S.H. *Colloid Polym. Sci.*, *284*, (2006), 1067–1072.
3. Jeong, H.Y., Lee, M.H., & Kim, B.K. *Colloid Surf. A: Physicochem. Eng. Aspects*, *290*, (2006), 178–185.
4. Madbouly, S.A., & Otaigbe, J.U. *Macromolecules*, *39*, (2006), 4144–4151.
5. Nanda, A.K., & Wicks, D.A. *Polymer*, *47*, (2006), 1805–1811.
6. Yen, M.S., P.Y. Tsai, P.Y., & Hong, P.D. *Colloid Surf. A: Physicochem. Eng. Aspects*, *279*, (2006), 1–9.
7. Decker, C., Moussa, K., & Bendaikha, T. *J. Polym. Sci., Polym. Chem. Ed.* *29*, (1991), 739.
8. Decker, C., & Zahouily, K. *Polym. Degrad. Stab.* *64*, (1999), 293.
9. Blanchard, V., & Blanchet, P. *Bioresources*. *6*, (2011), 1219 – 1229.
10. Chang, D., Yoon, D., Ro, M.D., Hwang, I., Park, I & Shin, D. *Japanese Journal of Applied Physics Part 1 – Regular Papers Short Notes & Review Papers*. *42*, (2003), 754 – 758.
11. Sun, F., & Jiang, S.L. *Nuclear Instruments & Methods in Physics Research Section B: Beam Interactions with Materials and Atoms*. *254*, (2007), 125 – 130.
12. Decker, C. *Macromol. Rapid. Commun.* *23*, (2002), 1067.

13. Decker, C. *Materials Science and Technology*. 18, (1997), 615.
14. Moon, J.H., Han, H.S., Shul, Y.G., Jang, D.H., Ro, M.D., & Yun, D.S. *Prog. Org. Coat.* 59, (2007), 106 – 114.
15. Kim, J.H. *European Physical Journal – Applied Physics*. 37, (2007), 175 – 180.
16. Chang, D., Yoon, D., Ro, M.D., Park, I & Shin, D. *Korean Polymer Journal*. 9, (2001), 313 – 318.
17. Ahn, B.U., Lee, S.K., Lee, S.K., Park, J.H., & Kim, B.K. *Prog. Org. Coat.* 62, (2008), 258-264.
18. Park, S.H., Lim, T.W., Yang, D.Y., Jeong, J.H., Kim, K.D., Lee, K.S., & Kong, H.J. *Applied Physics Letters*. 88, (2006), 1-3.
19. Gilberts, J., Tinnemans, A.H.A., Hogerheide, M.P., & Koster, T.P.M. *Journal of Sol-gel Science and Technology*. 11, (1998), 153 – 159.
20. Bontick, D. *Eur. Coat. J.* 6, (2002), 708–710.
21. Hsu, S.L., Xiao, H.X., Szmant, H.H., & Frisch, K.C. *J. Appl. Polym. Sci.*, 29, (1984), 2467–2479.
22. Rengasamy, S., Patel, J., & Mannari, V. *European Coating Journal*. 4, (2011), 125 – 129.
23. Williams, T.C., Callen, K., Gambino, C.A & Dvorchak, M. 39<sup>th</sup> *Waterborne Symposium, Sponsored by the School of Polymers and High Performance Materials, The University of Southern Mississippi, February 13- 17, 2012 in New Orleans, L.A.*
24. Ahn, B.U., Lee, S.K., Lee, S.K., Park, J.H., & Kim, B.K. *Prog. Org. Coat.* 62, (2008), 258 – 264.
25. Decker, C., Masson, F., & Schwalm, R. *Macromol. Mater. Eng.* 288, (2003), 17 – 28.
26. Bai, C., Zhang, X., & Dai, J. *Prog. Org. Coat.* 60, (2007), 63 – 68.
27. Zhang, T., Wu, W., Wang, X., & Mu, Y. *Prog. Org. Coat.* 201, (2010), 201-207.
28. Hwang, H., Moon, J., Choi, J.H., Kim, H.J., Kim, S.D., & Park, J.C. *Journal of Industrial and Engineering Chemistry*. 15, (2009), 381 – 387.
29. Lee, S.H., & Kim, D.S. *Polym. Adv. Technol.* 23, (2012), 414 – 417.



30. Decker, C., & Lorinczova, I. *JCT. Research. I*, (2004), 247 – 256.
31. Wang, X., Hu, Y., Song, L., Xing, W., Lu, H., Lv. P., & Jie, G. *J. Polym. Res. 18*, (2011), 721 – 729.
32. Mequanint, K., & Sanderson, R.D. *Macromol. Symp. 193*, (2003), 169 – 185.
33. Liu, T., Pan, X., Wu, Y., Zhang, T., Zheng, Z., Ding, X., & Peng, Y. *J. Polym. Res. 19*, (2012), 9741 – 9748.
34. Rengasamy, S., & Mannari, V. *Prog. Org. Coat. 76*, (2013), 78 – 85.
35. Rengasamy, S., & Mannari, V. *J. Appl. Polym. Sci. 130*, (2013) 3874 - 3884.
36. Mannari, V., & Rengasamy, S.; Patel, C. *Paint & Coating Industry. 28*, (2012), 28-31.
37. Mannari, V., & Rengasamy, S. *Proceedings of the American Coatings Conference*, Charlotte, N.C., (2010), April 12-14.
38. Mannari, V., & Rengasamy, S. *European Coating Journal. 03*, (2013), 80-85.
39. Anton, D. *Adv. Mater. (1998) 10*, 1197-1205.
40. Dai, J.B.; Zhang, X.Y.; Chao, J.; Bai, C.Y. *J. Coat. Technol. Res. (2007) 4*, 283-288.
41. Chattopadhyay, D.K., & Raju, K.V.S.N. *Prog. Polym. Sci. 32*, (2007), 352 – 418.

## **Chapter 9: Overall Conclusion and Recommendation**

This dissertation discusses the synthesis and characterization of bio-renewable oil based polyols and their application in the development of thermoplastic and thermoset types of aqueous polyurethane dispersions (PUD). Both the PUD families display wide range of mechanical properties, chemical resistance, water resistance, and solvent resistance. The obtained coating properties prove the possibility of using bio-renewable oil as an alternative for petrochemical based coating materials.

In Chapter 3, bio-renewable polyols (bio-polyols) having phosphate ester & phthalic ester polymeric chain backbone have been successfully synthesized from epoxidized soybean oil (ESO) and its derivative epoxidized monoglyceride (EMG). The spectroscopic analysis of bio-polyols prove, the cationic ring opening polymerization has been successfully carried out by nucleophilic compounds attack on acid protonated electrophilic sites of oxirane oxygen groups. Also, it has been determined that the hydroxyl numbers of developed bio-polyols range from 165 to 389 mgKOH/g. Attempts have been made to develop PUDs from the bio-polyols, but due to high functionality and phosphate ester polymeric chain backbone, the PUD batches either resulted as gelled product or poor hydrolytic stability. So, in order to determine the applications, the hydroxyl groups of bio-polyols have been crosslinked with isocyanate or melamine to develop high solids of urethane and melamine based coatings respectively. These conventional urethane and melamine based coating films have been exhibited excellent physicochemical properties with adhesion strength value 5B, direct and reverse impact resistance values >160 lbs.inches and MEK double rub values >200. The obtained coating properties prove the possibility of using bio-polyols as an alternative for petrochemical based high solids coatings.

In Chapter 4, the factors affecting the yield of the PUD has been identified and the alternate processing parameters have been successfully developed. A systematic approach of Six Sigma methodology based design of experiment has been revealed that 63.1% of the change in yield is due to addition time of chain extenders in to pre-polymer solution and the exposure time of pre-polymer to surrounding environment. These factors have been optimized by regression analysis through which the waste has been minimized by increasing the yield from 78.9% to 98.05%. The optimized processing parameters have been used in bio-renewable polyol based PUDs synthesized in Chapter 5, Chapter 6 and Chapter 8.

In Chapter 5, the bio-renewable soy polyol (polyether backbone) from epoxidized soy fatty acid methyl ester (ESFAME) has been successfully synthesized, characterized and applied in the development of environmentally friendly agro-based PUDs having soft segment content of 45% - 60%. The high polar groups of 45% soft-segmented bio-PUD have been resulted in poor water resistance properties and the 60% soft-segmented bio-PUD turned out to be too soft coating due to low hard segment content. Due to the optimum polar urethane groups and hard segment, the 55% soft-segmented bio-PUD (55% bio-PUD) has been resulted with excellent water resistance properties and reasonable physicochemical properties.

In Chapter 6, the 55% bio-PUD has been incorporated with siloxane and fluorine compounds and the water resistance; oil resistance and water contact angle have been further increased. The study of the aforementioned film properties have been showed that surface enrichment of siloxane increased hydrophobicity where as fluorine enrichment increased oil resistance of coatings. The self crosslinking of the siloxane and fluorine incorporated bio-PUD further improved the water resistance, oil resistance, MEK double rub values, and impact resistance of PUD film. Depending on the % siloxane and % fluorine content in bio-PUD

backbone the uncrosslinked version of bio-PUDs resulted in 54.17% to 76.39% more hydrophobicity (contact angle); 2.44% to 48.78% less water absorption and 83.33% to 91.67% less oil absorption than the uncrosslinked 55% bio-PUD. Whereas the self-crosslinked version yielded 57.35% to 82.35% more hydrophobicity; 31.82% to 47.73% less water absorption and 86.36% to 95.45% less oil absorption than their self-crosslinked 55% bio-PUD. Less solvent absorption means more solvent resistance.

In Chapter 7, UV-cure vegetable oil based polyols have been successfully synthesized from ESO and ESFAME using 2-hydroxyethyl acrylate (HEA) in presence of strong acid catalyst. The acrylic functional groups and the triglyceride polymeric chain backbone of developed UV-curable polyols have been connected through ether linkages. These ether linkages enhance the molecular mobility due to which acrylated polyols with low viscosity have been obtained. The high molecular weight of ESO based acrylated polyol exhibit excellent physicochemical properties than acrylated polyols derived from ESFAME. The  $T_g$ s of the dual cured (UV & moisture cured) films increase with an increase in the amount of isocyanate (crosslinker). Depending on the crosslinker amount the  $T_g$  of the dual cured coating films varied from 66°C to 85°C and also the physicochemical properties have been dramatically improved. Thus, this high bio-based content acrylated polyol derived from vegetable oil feedstock can be used either individually or in conjunction with fossil feedstock to offer UV-cure coatings with significantly reduced environmental impact.

In Chapter 8, siloxane and fluorine incorporated soybean oil based UV-PUDs have been successfully synthesized and their crosslink density have also been varied with HEA and 1-heptanol. The evaluation of UV-cured coating film proved, the crosslink density is important to achieve better mechanical properties, whereas both crosslink density and surface enrichment of

siloxane / fluorine is required to achieve excellent water and oil resistance properties. Due to the additional crosslink density, the UV-PUDs with HEA exhibited better performance properties than their counterpart UV-PUDs with 1-heptanol with exact amount of fluorine and siloxane content in their polymeric chain backbone. Depending on the % crosslink density the UV-PUD with HEA yielded up to 29.5% more water resistance and 94% more oil resistance than their counterpart UV-PUD with 1-heptanol.

It is apparent that the developed vegetable oil based coatings in this dissertation can be used as an alternative for fast depleting fossil feed stock based coatings. However, the raw materials and the coatings developed in this research work have to be further investigated, in order to address and reduce / eliminate existing challenges and their suitability in industrial production process. For instance, bio-based PUDs with high solid content (50% solids) are still challenging due to the high hydrophobic nature of vegetable oil based raw materials. Furthermore the research design that can utilize the high functional polyols in PUD development has to be investigated further. One of the exciting finding of this dissertation is synthesis of acrylated soy based polyol with low viscosity; but due to the excess HEA used in the acrylation process and the usage of ethereal solution and water to remove the unreacted HEA may create an obstacles in industrial production process. The aforementioned problems have to be addressed and solved in future research work.

Moreover, the agro-based PUDs can also be explored further in smart coating area. The antimicrobial, anticorrosive, and self-healing polymeric materials can be encapsulated as nano sized polymeric particles and can be introduced in the PUD formulation. The bio-PUDs with the aforementioned encapsulated particles can find applications in medical and automotive sectors. Also, the petrochemical based polyols and PUDs in automotive trim adhesives, pressure sensitive

adhesives and hot melt adhesives can be replaced with renewable oil based polyols and PUDs to extend their application area.

In conclusion, the performance and environmental benefits of the agro-based polyols and the bio-PUDs can facilitate the paradigm shift from fossil to bio-renewable coatings. This could reduce the demand for fossil related raw materials and could substantially reduce the production of carbon dioxide - “green house gas” to fend off global warming.